Reliability and Availability Analysis of Mining Systems with Human-Error

By

Nadheer Alqudsi

Thesis submitted to the Faculty of Graduate and Postdoctoral Studies
in partial fulfilments of the requirement for the degree of

MASTER OF APPLIED SCIENCE

in Mechanical Engineering

Mechanical Engineering Department
Faculty of Engineering
University of Ottawa

Abstract

This study presents reliability and availability analysis of mining systems with hardware and human-error failures. The failures of proposed models representing the mining systems could be safe or unsafe. To understand model reliability and availability behaviours, different values of failure and repair rates were used at different number of parallel units and different repair policies. Also, a model with partial and complete failures was analysed beside two miscellaneous models representing systems used in mining sector. The failure and repair rates are assumed constant. Markov method was used to perform analysis of the models and Laplace transforms were used to solve associated equations.

Acknowledgments

First and foremost, thank you God for giving me the strength to believe in myself to follow and achieve my dreams.

I would like to thank my wife Kloud for her continuous support, encouragement and love. Also, I would like to extend my thanks to my kids Yara and Hatim who give me the inspiration to be the best. Equally, I thank my parents for their support throughout my life without which this work would not be possible. Also, I thank my closest friend Faisal for his friendship and support ever since.

I would like to convey my sincere gratitude to my supervisor Professor B. S. Dhillon for his support, encouragement and motivation since the first day. It is an honor for me to have his supervision during my Master's degree. Also, I express my gratitude to University of Ottawa and Department of Mechanical Engineering for supporting this work.

I would like to convey my gratitude to my employer, Saudi Aramco for awarding me the scholarship to pursue my higher education.

Table of Contents

List of Figures

Chapter 1 : Introduction

1.1 Background

Global economy is the driving force behind continuous improvement of mining equipment reliability to meet the global demand and competitions. Thus, mining equipment is becoming more complex, sophisticated and costly [1]. Over global economy challenges, humans play a role in any system reliability because humans are the link between all phases of system life cycle. Human involvement may be as simple as hand tool or as complex as programing a monitoring system. Studies show that human error accounts 60% to 80% of complex system failures while 96% of simple system failures [2]. In 1958, H. L. Williams was the first to point out that the realistic reliability prediction of systems must consider human-element [5]. Since that time, a large number of publications on human factors and errors have appeared [1]. These publications studied the reliability of human-machine systems that can be classified according to their orientations into three phases. Each phase focuses and discusses certain type of potential human errors [14].

If human-machine systems are defined as systems that have direct or indirect interaction between people and other system components [12], we can realise the potential human-error in all systems. Therefore, human-error was given the attention in this study beside hardware failure. In the United States, a study found that almost 85% of all accidents in mining can be attributed to at least one human error [111]. In Australia, two-third of occupational accidents can be attributed to human error [148].

Also, this study analyses models that consider safe and unsafe failure modes of mining systems because unsafe failures might be catastrophic failures or involve environment concerns. Historical data for the United States mining industries shows that the annual mining death was as high as over 3000 per year in 1910 [60]. After authorizing the Federal Coal Mine Safety Act to conduct annual inspections of underground coal mines , the yearly fatality number was dropped to around 500 in the late 1950s [102]. Over 25% of underground coal mining accidents occurred during maintenance activities [108]. Continuous improvement efforts focused on the mining safety

dropped that number to 41 fatalities in 2013. Figure 1-1 shows fatalities number for period between 2004 and 2013, in the United States mining sector [107, 109].

Figure 1-1 Number of mining fatalities by year 2004 -2013, in the United States.

The mathematical modelling in this report uses Markov method to perform analysis of the models and Laplace transforms to solve associated equations. The results were used to develop the plots of the reliability parameters, i.e. system reliability, mean time to failure (MTTF), availability. These parameters were investigated to observe the influence of different values of failure and repair rates, number of units in parallel configuration, and the different repair policies.

1.2 Literature Review

1.2.1 **Human Factor Engineering**

International Organisation of Standardisation (ISO) [70] definition of human factors (or ergonomics) is "scientific discipline concerned with the understanding of interactions among humans and other elements of a system, and the profession that applies theory, principles, data, and other methods to design in order to optimize human well-being and overall system performance". Sanders and Haight [13, 18] identified the main objective of human factor to be a study aims to maximizing systems reliability, safety, health, comfort and quality of life.

Horberry et al [62, 88, 96] presented two broad critical reasons of human factor engineering in mining systems: First reason is related to safety and health and second one is related to productivity and work efficiency. Freiheit and Hu [103] stated that estimating system productivity typically starts by determining subsystem reliabilities. In 2005, Barabady [98], indicated that although the unplanned failure of mining equipment will result in significantly higher repair cost, the production losses associated with the failure is the critical concern. By improving the mining equipment reliability, the impact of failure will be mitigated. Basically, reliability is a performance indicator of overall equipment condition.

Human Factor engineering has wide applications, i.e.design engineers apply it to improve system reliability when investigating the system reliability through applying some methods such as hazardous operation (HazOp), simulation and modelling, fault-tree analysis (FTA), failure mode and effects analysis (FMEA) and other methods that were explained by Stapelberg [33]. Unfortunately, most of the methods are either misunderstood or misused, stated by Lee and Hillman [49]. Therefore, Krarti [50], in 2003, pointed out that artificial intelligence-based model was developed to help in determining the integrity of engineering design. However, it has been not properly appreciated and its implementation needs more evaluation. In 2012, Zhao [75], pointed that artificial intelligence is developing rapidly and there are potential for more powerful technologies. Even though human factor engineering aims to optimize the overall system performance, the current engineered systems could be investigated for further optimization. For example Li et al [133] investigated a current status of operation control room to highlight several common shortcomings in the integration of people and technology.

Sharidan [14], classified human factor studies into three phases according to the studies orientations: First phase focused on crafts with limited applications in the automotive and communication industries. After World War II, there were more appreciations and needs to continue developing human factors. As a result, second phase involved and dominated a wider applications of factors engineering. During the 1960s, human factors engineers began to use modelling techniques. Latest phase refers to the era of human-computer interaction.

In area of mining, in 1924, Haldane [104] discussed the coal mining industries in UK to clarify the relationship among miners comradeship and also between employees and employer. In

1971, Sanders and Hitchcock [105] conducted the first formal study that was concerned with identifying human-factor related problem in underground coal mines. In 1988, Sanders and Peay [106] summarized the application of human-factor to improve miners' safety, productivity, and the general physical and psychological. In the same year, Dhillon and Rayapati [99] presented a model of human performance when subjected an external factor. The results show that the critical effect of external factors should be recovered by factor engineering.

1.2.2 **Modelling**

Shooman [9], presented a general approach to study any system probabilities and reliability related measures that has three phases: (1) Transition of the physical problem into a mathematical statement, which is called modelling. (2) Application of probabilities theories and laws to solve the model. (3) Interpretation of mathematical results in term of engineering principles. Chaturvedi [21] argued that reliability analysis of complex systems is almost impossible when treat systems in full details. Therefore, he proposed a logical approach to simplify the analysis of system, subsystems and components.

Over the years many methods have been developed to perform reliability analysis of engineering systems [20]. Buzacott [28] argued that Markov model is an appropriate and most frequent method to describe systems with discrete-state continuous-time. Therefore, Markov process was the only modelling method was considered in this study. Markov [26, 27] defined the simple chain as an infinite sequence of independent variables connected in such a way they are memoryless and next variable depends only at the current one. In fact, mining process has a stochastic nature that makes simulation the only reliable method for manipulating such systems [87].

In 1996, Lisnianski and Levitin [44] presented universal algorithm proposes an optimal configuration that minimizes the investment cost according to reliability constrains. In 1999, Basu and Baafi [84], reviewed common practices in Australia that have been used in simulating mining system reliability where they discussed the limitation of each practice. In 2000, Kuo and Prasad [45] presented an overview of the system reliability optimization that discusses the limitation of commonly used methods. In 2001, Levitin and Lisnianski [134] presented a technique for solving a family of multi-state systems reliability optimization problems that took into account many

criteria that combined a universal generating function method and a generic algorithm. In 2003, Hall and Daneshmend [85], discussed the reliability modelling of mobile mining equipment to enhance decision making for maintenance planning and reliability simulating to enable the evaluation of more rigorous production planning scenarios. In 2008, Yuriy and Vayenas [82] developed a methodology involving the combination of reliability assessment model based on generic algorithms with discrete-event simulation model of mine equipment systems. In 2008, Fioroni [97] presented models of mining system simulation and optimization to achieve a feasible, reliable and accurate short-term planning schedules. In the same year, Dhillon [1], pointed out that due to costly equipment in mining systems, standby units configuration is an effective method to increase system reliability. In 2014, Peng and Vayenas [83] published a paper dealt with reliability analysis and prediction for mining machinery where a software simulates failure rate during a time period of interest based on generic algorithms combined with several statistical procedures.

This study was inspired by previous models to obtain reliability related measures. In 1982, Dhillon [113] presented two models to predict human reliability of time continuous operation tasks under two levels of stress that was also analysed by Dhillon and Rayapati [114], in 1985, under three levels of stress. Later, Kumar and Garg [116] analysed it when the item is repairable. In 1985, Goel et al [120], studied the model of a two units system under two different weather conditions. In 1986, Kumar et al [117] analysed a model of operation performance under two levels of stress when the model has a critical human error. Cao in 1989 and Singh in 1993 [127, 131] published papers analysed human reliability of continuous operation tasks under four type of operating conditions that specify the repair possibility. In 1991, Chung [118, 119, 152] analysed human reliability under N-level of stress that an item failure is repairable when it fails due to non-human-error and unrepairable when it fails due human-error. In 1990, Agarwal and Templeton [128] analysed a model of single unit under three operating condition with non-exponential repair rate. In 1992, Guo and Cao [121] studied a multistate repairable system that has changing environment. In 1993, Singh [131] investigated a model of two identical units in cold standby configuration model in which operation is affected by the weather conditions while repair does not. In 1993, Deng and Song [122] developed a general model that has m-identical units with k-levels of stress with one repair facility. In 1993, Song and Deng [125] analysed the same model but with three units. In 1997, Mokaddis et al [130] proposed a model dealt with some characteristics of a single unit of a human-machine system operating under different weather

conditions when failure, repair and changing weather conditions are stochastically independent random variables, each having an arbitrary distribution. In 1998, Li et al [126] analysed a similar model with three units and two repair facilities. In the same year, Goel, and Shrivastava [129] analysed a model has two failure modes (hardware failure and human-error) under two environment conditions and two repairman conditions. In 2002, Chaudhuri and Agarwal [124] obtained the steady state of an N-unit parallel system with R-repair facility under three types of environment. In 2015, Savita [123] analysed a model with m-identical units and k-levels of stress when it has non-identical units.

In 1963, Gaver [100] analysed a model with two identical units where repair is instantly after a unit failure. In 1984, Dhillon [115] analysed four models for two identical units in standby configuration when each unit may fail due to hardware failure or human-error. In 1985, Dhillon and Rayapati [47] analysed a non-maintained models in parallel configuration with hardware failure and human-error. In 1987, Chung presented a model with M-parallel and N-standby identical units in which system can be repaired only when system failed. In 1986, Gupta and Kumar [154] analysed the reliability and MTTF of a two-state complex non-repairable system, consisting of two sub-systems A and B arranged in series in which sub-system may fail due to hardware or human failure. Later, Manna [155] argued a simpler concept to obtain the same model reliability and MTTF. In 1991, Chung [150], presented the reliability and availability of a series repairable system with multiple failures in which system fails when any unit fail. In 1991, Chao and Fu [101] investigated a more general series model and determined the limiting reliability of the system when the repaired unit is as good as new. In 1993, Dhillon and Yang [90] analysed the availability of a model with two parallel units and one standby unit in which unit may fail due to non-human-error, non-critical human-error and critical human-error. In 1994, Chung [151] analysed the reliability and availability of repairable systems having k-active, N-cold standby identical units with repair facilities and multiple non-critical and critical failures i.e. the system in failure state when any of critical errors occurred or all (N+1) units failed. In 1996, Mahmoud and Esmail [153] analysed the reliability of a two-unit warm standby redundant system under hardware and human error failures where failure and repair rate are arbitrary. In 1996, Lam and Zhang [102] investigated general series system reliability considering the deterioration of repaired units. In 2010, Dhillon [60], presented several models that predicting the mining system reliability when there are two repair facilities.

1.2.3 **Human-Machine Interaction**

Salvendy [12] defined human-machine systems as any system that has direct or indirect interaction between people and other system components. Basically, human-machine interaction has four different stages of activities: intention, selection, execution, and evaluation. Donald [52] analysed the four stages to have insight into potential human-errors under each stage. Rouse [54] proposed a general approach to human-error classification that identify possible causes contribute to human-error occurrence. Human-machine interaction can be at any form such as operation, assembly, design, inspection, installation and maintenance. Maintenance can be defined according to Dhillon and Liu [52] as any activity required to keep a facility in "as-built" condition and therefore continuing to have its original productive capacity. Consequently, maintenance has three types: corrective, predictive and preventive maintenance. Clark [11] studies show that approximately 10% of production time is lost by corrective maintenance in the Australian underground coal mining industry. According to Lewis and Steinberg [24], the maintenance related cost is approximately 30 to 50 % of the overall mining costs.

The majority of human-machine models consider human as a system component that has no constrain in performing assigned tasks, stated by Rothrock et al [29, 30]. Therefore, modelling human-machine systems must consider human capability. Under ideal conditions, a human can affect both physical and logical aspects of the system when allowed to control manipulable components. Therefore, human contribution should be limited by the system environment and the judgment demand.

According to the increase in global competitions, companies are continuously improving their control system toward automation which has wide applications. However, it does not actually displace the human role rather than adds more challenges to the human factors engineers and designers as well as more load on operation and maintenance personnel [14, 15, 16]. Sarter et al [35] clarified some hidden issues with automation such as the workload will actually be unevenly distributed rather than reduced. Also, new knowledge, more attention, coordination and training will be demanded. In addition, a point raised by Endsley [36] that more opportunities for error to occur and loss of situation awareness due to manual skill decay. Parasuraman et al [15], summarized three factors are commonly cited in automated systems: (1) inadequate interface

between the operator and information about the configuration of the machine; (2) intricate and confusing interactions among complex machine components; (3) the operator has an insufficient model and experience of the machine's behaviour. These factors may limit the operator's ability to anticipate the future behaviour of the machine. Likewise, Young and Neville [73] pointed that automation raises the issue of mental underload, which can be at least as detrimental to performance as overload. Endsley and Kaber [25] presented that human operational skills and awareness are enhanced though the involvement in operation assignments. This in turn will enable human to takeover automated control in case of unanticipated conditions. Therefore, Lynas and Horberry [34] argued that the level of automation approach seeks to optimize the system control assignments between human and automation.

In area of mining systems, Lynas and Horberry [89], in 2011, introduced the impact of automation degree over the human factors. They also discussed the importance of considering operators and maintainers when designing and deploying mining automation. In 2012, Horberry and Lynas [139] pointed out that human element implications in recent mining technologies have not yet been explored in any detail. Therefore, the operator interaction with automated mining equipment was discussed to develop a database to capture the emerging technology trends associated with such equipment. In the same year, Horberry and Cooke [138] discussed the application of both safe and inclusive design of equipment used by operational and maintenance personnel in mining in which the study applied a newly developed task-orientated risk assessment and design process. In 2013, Horberry et al [95] argued that although automation has the benefit of production sustainability to the minerals industry, many human-element concerns would still exist, and new ones could certainly be created. As a result, determining the optimal level of automation is needed beside automated equipment breakdown procedures. In 2014, Horberry [135] discussed the need to a better integration among human factors considerations within safe design by systematically involving end-users and decision makers in the full life cycle of the designed product or system. In 2014, Boudreau et al [140, 141] examined the impact of new equipment on productivity and injury rate in underground mining according to certain criteria which show that the introduction of new equipment with technological innovations does not necessarily improve productivity nor injury rate. This is due to human factor deficiencies that required identification of mechanisms and conditions that determine their effectiveness. Therefore, Boudreau et al [142] studied the key factors and measures that quantify the success level of new equipment in

underground mines. In 2015, Horberry and Burgess-Limerick [136] published a paper dealt with redesign, rather than original design in which a human-centred safe redesign method is presented. Later, Pazell et al and [137] described human-centred design and its application in mining.

1.2.4 **Human-Error**

Watson and Oakes [62] argued that the term "human-error" is ambiguous and generally carries negative attribution because it covers many different situations and events. Therefore, Ref [67] suggested a human-error definition that is widely used which is "the failure to perform a specified task (or the performance of a forbidden action) that could result in disruption of scheduled operations or damage to equipment and property". In contrast, human reliability definition is the probability of accomplishing a specified task successfully by humans at any required stage in system operation within a defined minimum time limit (if the time requirement is specified). Human-error has many classification proposals. Buchanan [55] categorised human-error into two categories: catastrophic and insidious problem. The former refers to events may occur with warning and result in considerable damages or loss of life. While the latter is the problems those whose effects are only noticed over a long period of time. Reason and Rasmussen [51, 58] emerged two classifications of human-error which have become the most widely accepted and use. First one is skill-based, rule-based and knowledge-based. Second one is slips/lapses, mistake and violations. Reason [59] added two more general classifications that are often used: errors of commission and omission, and input, decision and output. HSE [65] schemed human errors into five types or forms, i.e. misperception, mistaken priorities, attention lapse, mistaken action and wilfulness, violations, sabotage.

Reason [63, 64] suggested that the root causes in all cases appeared to be 'latent' which help in understanding the interaction between organization, design and management of systems. Rasmussen and Meister [65, 66] argued that the reliability of specific systems need the classification of errors and explanation in the context of work process. Ref [56] states that human-error is unavoidable in the long term, but improving the tolerance offers the opportunity to reduce the level of harm.

Over years, there were many studies related to mining system maintenance activities [33]. Patterson [145] argue that skilled-based errors are the most common unsafe act based on the data

analysis of mining accident in Australia and the United States. Heinrich [57] was the first to distinguish between human unsafe acts and unsafe conditions. In 2007, Ruckart and Burgess [144] analysed data of human-error contribution in mining and manufacturing hazardous substances emergency events for 1996- 2003, which resulted in four times as many events with victims and almost three times as many events with evacuations when comparing human-error events with non-human-error events. They provided human factor engineering design to systematise human interaction which potentially minimize the human error in workplace. In 2011, Ruff et al [146] argued that machine-related accidents accounted for 41% of all severe accidents in the mining industry during 2000-2007 in which most of them were related to machines operation and maintenance. Several recommendations were proposed to decrease accidents further. In 2014, Oliveira et al [143] argued that 13-17% of accidents are related to maintenance due to the conflict between the procedural and dynamic maintenance actions.

1.2.5 **Safety**

Everett and Honiden [79] defined safety as the probability that conditions which can lead to an accident (hazards) do not occur whether the intended function is performed or not. Verma et al [77] pointed out that the link between reliability and safety, i.e. reliability deals with the failure concept whereas the safety deals with the consequences after the failure. However, the first to link reliability and safety is Shewart [80] when he inspired the rise of statistical quality control at Bell labs in 1920s. In fact, the establishment of the United States Congress passed the Occupational Safety and Health Act (OSHA) in 1970 is a milestone in the history of safety management tool [59]. In 2003, Hobbs and Williamson [147] studied the link between the contributing factors and safety occurrence. In 2010, Verma et al [77] stated that reliability and safety are the core issues to be addressed during the design, operation, and maintenance of engineering systems. Cavallaro and Walker [78] emphasised the need of applying the reliability standards, particularly in hazardous environment, and fault tolerance, whenever the repair is difficult and failures potentially catastrophic.

In 2009, Dhillon [110] reviewed various important aspect of mining equipment safety and discussed number of methods with strategies to perform mining systems analysis and increase their safety. In 2009, Mirmohammadi et. Al [91] broke down the environment affect into thirteen

components with a scale of each to quantify the impact of mining activities on the environment. McPhee [92] highlighted that mining industries managers have the ability to prevent work-related illness and injuries. In 2012, Elías [93], stated that ergonomics studies and decisions should involve workers. In 2014, Jianhua and Xiaoyan published a paper that emphasises the need of understanding human unsafe behaviour in mining accidents. Thus, the behaviour-based safety management method was introduced to accumulate all potential factors may contribute in mining accident.

1.3 Objectives

Mining systems are complex and sophisticated systems that involve interaction between human and equipment. The level of interaction has wide variation more than any other system [38]. Also, mining is renowned to be one of the more dangerous occupations and there have been many serious accidents worldwide over the years in mining [43]. There have however been various number of studies in recent years to improve the working conditions for miners, and to create a safer, healthier work environment.

The main objective of this study was to perform effective reliability and availability analysis of mining systems. This study one of the first attempts to analyse the effect of safe and unsafe failures of mining systems when the system may fail due to hardware or human-error. Also, this study consolidated the desired analysis that provide insight into mining systems and their maintenance and operation.

In this study, Markov method was used to perform analysis of the proposed models presenting mining systems and Laplace transforms were used to solve the associated equations. Reliability, mean time to failure (MTTF) and availability plots of each model were developed to illustrate the influences of different value of failure and repair rates, number of units in parallel configurations, and different repair policies. Based on the results, general models and equations were developed.

This report focused on mining systems and deviated from previous researches at several points that can be summarized as follows:

- The models of previous researchers considered hardware failure and human-error of different model configurations. This study was extended to investigate the reliability measures when each failure mode might be a safe or unsafe failure.
- This study investigated and compared the reliability and availability of same models at different values of failure and repair rates, number of parallel units and repair policies.
- General equations for proposed models were developed to obtain the state probabilities.

1.4 Organization of Study

This study is presented in six chapters.

Chapter 1 provides a brief introduction to mining systems reliability and safety and a detailed literature review of related publications.

Chapter 2 presents the reliability and availability analysis of mining systems having n-parallel units with hardware failure and human-error. Also, presents and compares the analysis of four different repair policies.

Chapter 3 presents an extension of Chapter 2 models that considers the safety of each failure. Also, this chapter comperes the results in Chapter 2 with Chapter 3 when same failure and repair rates were used.

Chapter 4 investigates a mining system model with possible partial and complete failures.

Chapter 5 presents the reliability and availability of miscellaneous models concerning worker performance and system operation condition.

Chapter 6 discusses the result of study and gives observations and recommendations.

Chapter 2 : Reliability and Availability Analysis of Mining Systems with Hardware Failure and Human-Error

2.1 Introduction

The reliability has been a major concern in recent mining studies [88]. The concept of parallel configuration is widely used to increase the reliability and safety of mining system because standby is ineffective method when units are costly [1]. The block diagram in Figure 2-1 shows a mining system with n identical units in parallel configuration. If each unit has the capability to sustain the operation demand, the system is at full capacity as long as at least one unit in normal operation. Thus, the system fails when all units fail. If first unit failed due to any failure mode the second unit may fail due to any failure mode as well, and so forth.

This chapter discusses the mathematical models of mining systems at different configurations, namely single, dual and triple units. Each configuration was analysed at different values of failure and repair rates of hardware and human-error. Reliability parameters i.e. state probabilities, system reliability, mean time to failure (MTTF) and availability were obtained and plots were developed. General equations were developed for state probabilities, reliability and availability. Also, this chapter investigates the effect of different repair policies on the reliability parameters. Markov process and Laplace transform were used to obtain the expressions of time dependent reliability parameters. Associated equations were solved by using Maplesoft software.

The values of failure and repair rates were assumed in reference to a certain value. Specifically, each rate was multiplied by 5, 2, 1, 1/2 and 1/5. Then, the results were used to develop reliability parameters. This provided a reference plot and resulted plots that help in understanding the reliability parameters behaviour. This approach was used because of limited data resources and database accesses.

All models in this chapter underlay one of the four repair policies as follows:

Without repair: This case assumed that system and units are unrepairable whether they failed due to hardware failure or human-error.

Type I repair policy: This case assumed that the units are unrepairable while the system repair is possible after total system failure.

Type II repair policy: This case assumed that the units are repairable while system is not.

Type III repair policy: This case assumed that the units and system repairs are possible.

Assumptions:

The following assumptions are associated with this model:

i) All units are identical.
ii) All units are in new condition at initial state.
iii) All failures are statistically independent.
iv) All units' failure and repair rates are constant.
v) Any repaired units and systems are as good as new.
vi) There is only one repair facility.
vii) Each unit can fail due to hardware failure or human-error.

Notation

n	Number of parallel units
t	Time in hours
s	Laplace transform variable
λ_0	Constant unit hardware failure rate
λ_H	Constant human-error rate
μ_1, μ_3	Constant repair rate of hardware failures
μ_2, μ_4	Constant repair rate of human-error
AV(t)	System availability at time (t)
$P_i(t)$	The probability that the system is in state i at time (t), for i= 1, 2, 3, …,n

$P_i(s)$ The Laplace transform of state probability, for i= 1, 2, 3, …,n

R(t) System reliability at time (t)

MTTF System mean time to failure

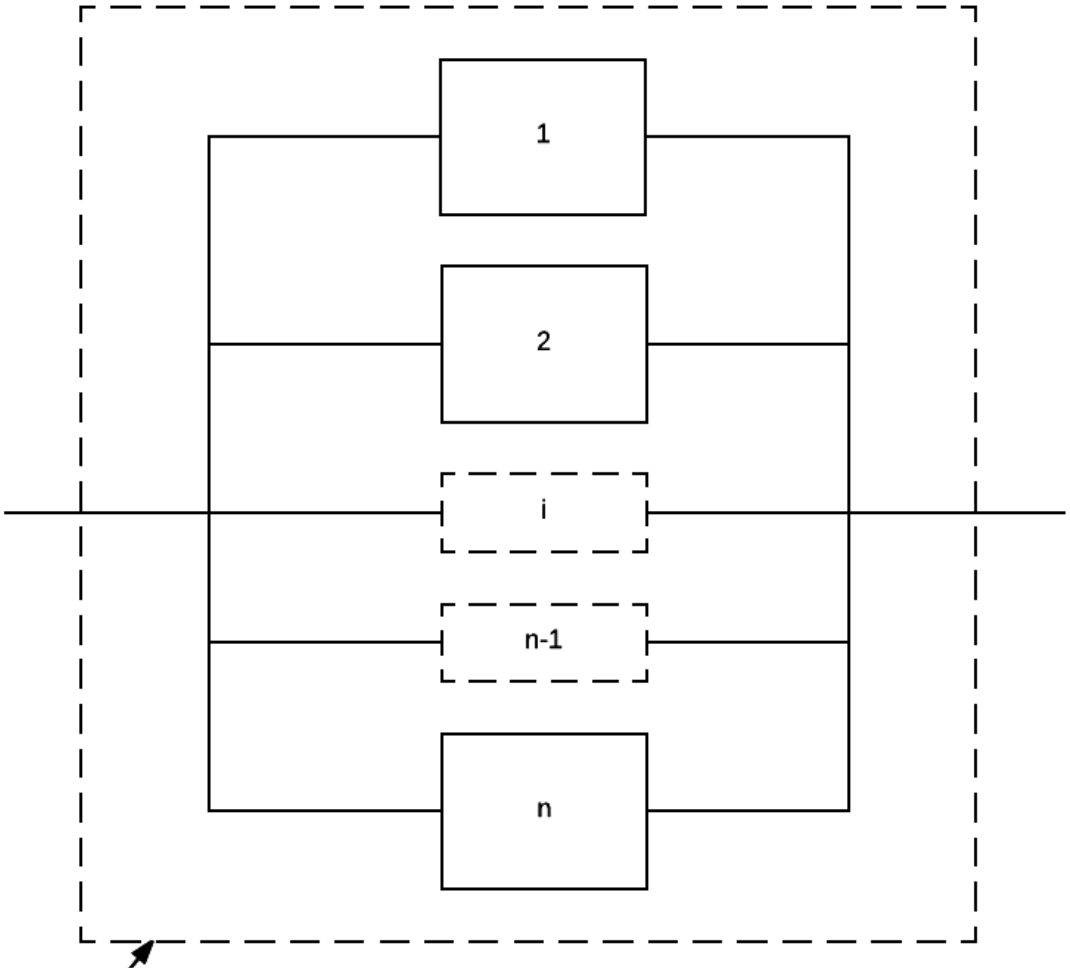

Figure 2-1 Block diagram of mining system with n units in parallel configuration.

2.2 Human-Error and Hardware Failures without Repair

2.2.1 **General n-Units System without Repair**

In this model, units and system are unrepairable as shown in Figure 2-2 in which units might fail due to hardware failure or human-error. The symbolic representation of general model

is that, (n) is the number of units in the system, (j) is the failure mode that can either be 1 or 2 where j=1 for hardware failure and j=2 for human-error. Likewise, λ_j refers to unit failure rates where λ_1 refers to hardware failure rate and λ_2 refers to human-error. (i) is the number of failed units at time (t).

At the initial state, all n parallel units are in normal operation. So, the failure rates are $n\lambda_1$ and $n\lambda_2$ represent all units. After first unit failure, the failure rate is $(n-1)\lambda_1$ and $(n-1)\lambda_2$ because (n-1) units in normal operation, and so forth $(n-i)\lambda_1$ and $(n-i)\lambda_2$. When there is only one unit in normal operation, the failure rates are λ_0 and λ_H. Based on proposed models when n=1, n=2 and n=3, the general differential equations describing the system using the Markov method were obtained as follows:

$$\frac{dP_0(t)}{dt} + nP_0(t) \cdot \sum_{v=1}^{2} \lambda_j = 0 \tag{2.1}$$

$$\frac{dP_{1-j}(t)}{dt} + P_{1-j}(t)\,(n-1) \sum_{v=1}^{2} \lambda_v = P_0(t)\, n\, \lambda_j \tag{2.2}$$

$$\frac{dP_{i-j}(t)}{dt} + P_{i-j}(t)\,(n-1) \cdot \sum_{v=1}^{2} \lambda_v = (n-(i-1))\, \lambda_j \cdot \sum_{v=1}^{2} P_{(i-1)-v}(t) \tag{2.3}$$

At time t= 0, $P_0(0)= 1$, and all other initial state probabilities are equal to zero. By using equations (2.1) - (2.3), the following general s-domain equations were developed:

$$P_0(s) = \frac{1}{s+nF} \tag{2.4}$$

$$P_{i-j}(s) = \frac{F^{(i-1)}\, \lambda_j \prod_{q=1}^{i} (n-q+1)}{\prod_{v=n-i}^{n} (s+vF)} \tag{2.5}$$

Where

$$F = \sum_{q=1}^{2} \lambda_q$$

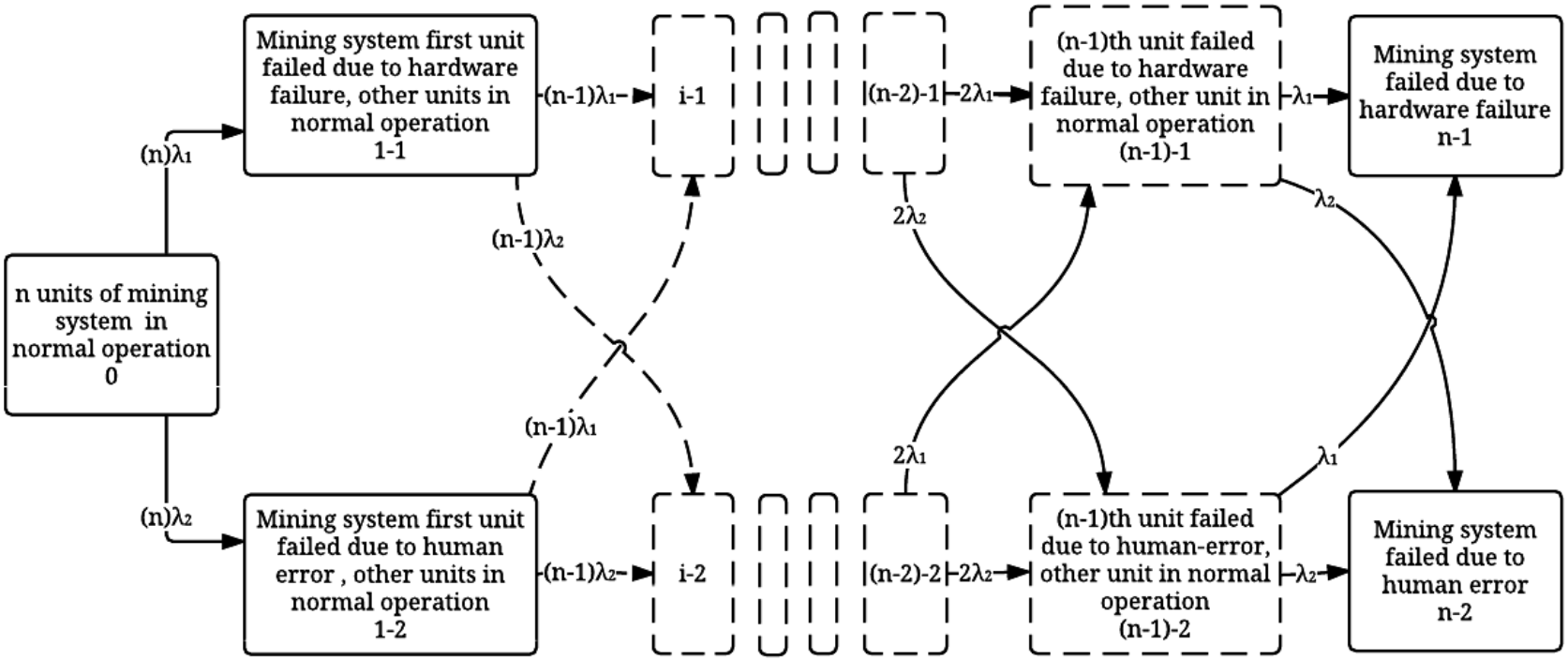

Figure 2-2 State space diagram of n-units system with two failure modes without repair

The time-dependent equations of state probabilities can be obtained by taking the inverse Laplace transform of equations (2.4) and (2.5) as follows:

$$P_0(t) = \mathrm{e}^{-n \cdot \left(\sum_{j=1}^{2} \lambda_j \right) t} \tag{2.6}$$

$$\mathrm{P}_{i-j}(t) = \sum_{K=0}^{i} \left(\frac{\prod_{L=0}^{i-1} (n-L)\,\lambda_j}{\left(\prod_{\mathrm{P}=0}^{K-1} (K-P) \right) \left(\prod_{\mathrm{P}=\mathrm{K}+1}^{i} (K-P) \right) F} \cdot \mathrm{e}^{-(n-K)\,F\,t} \right) \tag{2.7}$$

In this particular model configurations, units and system are unrepairable. Thus, the reliability is the total probabilities of operating states as follows:

$$R(t) = \sum_{j=1}^{2} \left(\sum_{i=0}^{n-1} P_{i-j}(t) \right) \tag{2.8}$$

By integrating Equation (2.8) over the time interval [0 -∞], the following general equation of MTTF is obtained:

$$MTTF = \frac{1}{\sum_{j=1}^{2} \lambda_j} \cdot \sum_{i=0}^{n-1} \left(\frac{1}{n-i} \right) \tag{2.9}$$

2.2.2 **Special Case: One-Unit System without Repair**

The transition state diagram in Figure 2-3 shows a single unit model of mining system that has two failure modes. If this unit failed, the system fails and cannot be repaired. By using the Markov method, the differential equations associated with Figure 2-3 are as follows.

$$\frac{dP_0(t)}{dt} + P_0(t) \left(\lambda_{\mathrm{O}} + \lambda_H \right) = 0 \tag{2.10}$$

$$\frac{dP_1(t)}{dt} = P_0(t)\,\lambda_{\mathrm{O}} \tag{2.11}$$

$$\frac{dP_2(t)}{dt} = P_0(t)\,\lambda_H \tag{2.12}$$

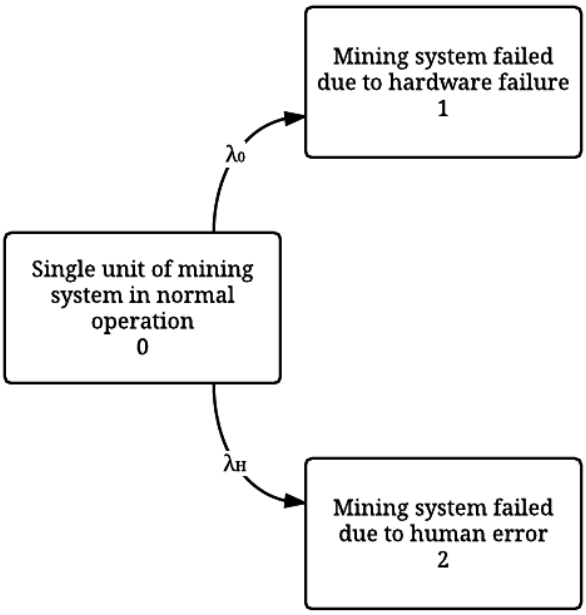

Figure 2-3 State space diagram of one-unit system with two failure modes without repair

At time t= 0, $P_0(0)$= 1 and all other initial state probabilities are equal to zero. By taking the Laplace transforms of equations (2.10) - (2.12), we get the following equations:

$$P_0(s) = \frac{1}{s + \lambda_O + \lambda_H} \tag{2.13}$$

$$P_1(s) = \frac{\lambda_O P_0(s)}{s} \tag{2.14}$$

$$P_2(s) = \frac{\lambda_H P_0(s)}{s} \tag{2.15}$$

By using equations (2.13) – (2.15), we get the following equations:

$$P_0(s) = \frac{1}{s + \lambda_O + \lambda_H} \tag{2.16}$$

$$P_1(s) = \frac{\lambda_O}{\left(s + \lambda_O + \lambda_H\right) s} \tag{2.17}$$

$$P_2(s) = \frac{\lambda_H}{\left(s + \lambda_O + \lambda_H\right) s} \tag{2.18}$$

By taking the inverse Laplace transform of equations (2.16) – (2.18), the following equations were obtained:

$$P_0(t) = e^{-\left(\lambda_O + \lambda_H\right) t} \tag{2.19}$$

$$P_1(t) = \frac{\lambda_O \left(1 - e^{-1.\left(\lambda_O + \lambda_H\right) t}\right)}{\lambda_O + \lambda_H} \tag{2.20}$$

$$P_2(t) = \frac{\lambda_H \left(1 - e^{-1.\left(\lambda_O + \lambda_H\right) t}\right)}{\lambda_O + \lambda_H} \tag{2.21}$$

System Reliability and MTTF

When system cannot be repaired, the reliability can be obtained by finding the probability of operating state.

$$R(t) = P_0(t) \tag{2.22}$$

MTTF is obtained by using $\lim_{s \to 0} R(s)$. the following equation of MTTF was obtained:

$$\text{MTTF} = \lim_{s \to 0} R(s) = \frac{1}{\lambda_0 + \lambda_H} \tag{2.23}$$

To analyse the model reliability parameters, specific values of hardware failure and human-error rates were assumed. Accordingly, the state probability equations (2.19) - (2.21) were used to develop the plots in Figure 2-4, and the reliability equation (2.22) was used to develop the plots in Figure 2-5. Detailed plots are presented in Appendix B.1.

$$\lambda_0 = 0.00125 \left(\frac{failure}{hour}\right)$$
$$\lambda_H = 0.005 \left(\frac{failure}{hour}\right)$$

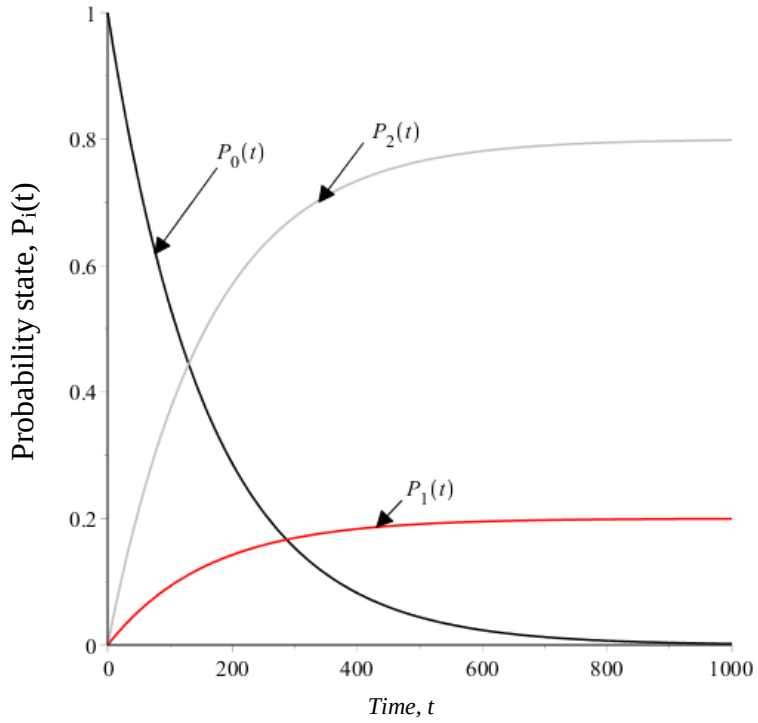

Figure 2-4 State probabilities of one-unit system with two failure modes without repair

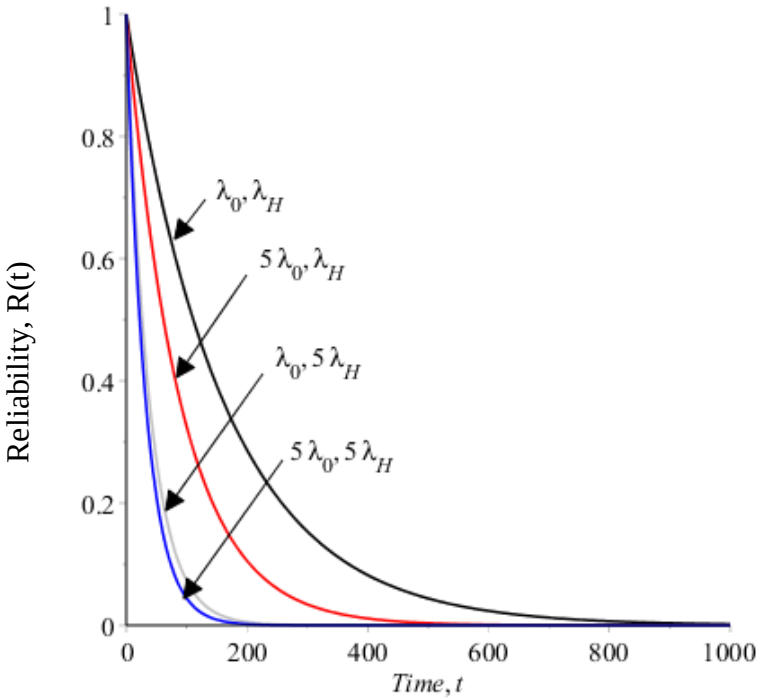

Figure 2-5 Reliability plots of one-unit system with two failure modes without repair at different failure rates

2.2.3 **Special Case: Two-Units System without Repair**

The transition state diagram in Figure 2-6 shows a two identical units of mining system in parallel configuration in which each unit has two failure modes. By using the Markov method to analyse Figure 2-6, the associated differential equations are as follows:

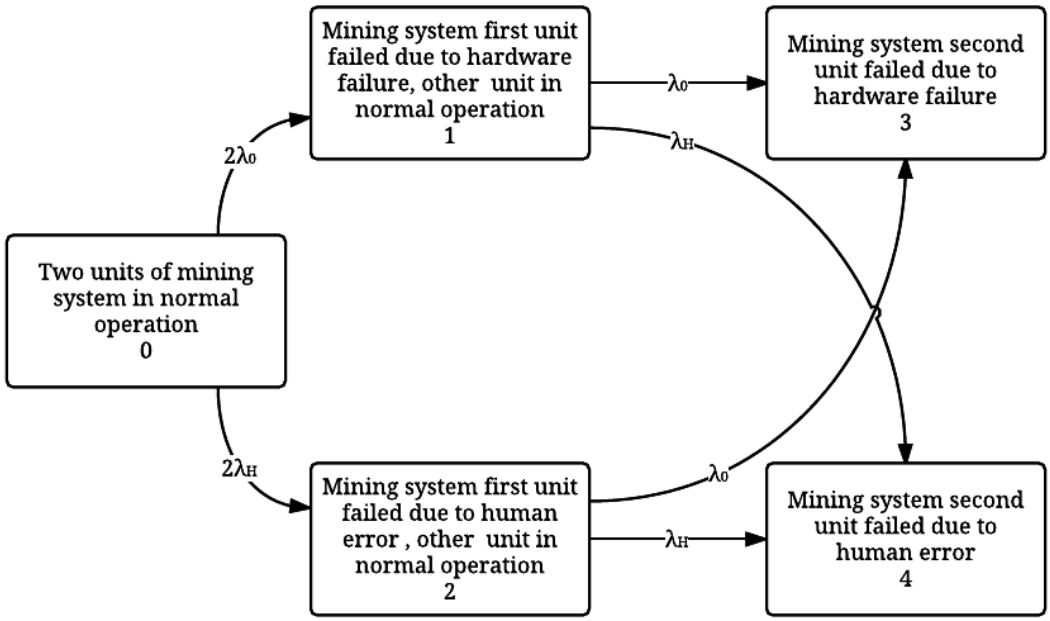

Figure 2-6 State space diagram of two-units with two failure modes without repair

$$\frac{dP_0(t)}{dt} + P_0(t)\left(2\cdot\lambda_0 + 2\lambda_H\right) = 0 \tag{2.24}$$

$$\frac{dP_1(t)}{dt} + P_1(t)\left(\lambda_0 + \lambda_H\right) = 2\lambda_0 P_0(t) \tag{2.25}$$

$$\frac{dP_2(t)}{dt} + P_2(t)\left(\lambda_0 + \lambda_H\right) = 2\lambda_H P_0(t) \tag{2.26}$$

$$\frac{dP_3(t)}{dt} = \lambda_0\left(P_1(t) + P_2(t)\right) \tag{2.27}$$

$$\frac{dP_4(t)}{dt} = \lambda_H\left(P_1(t) + P_2(t)\right) \tag{2.28}$$

At time t= 0, $P_0(0)$= 1 and all other initial state probabilities are equal to zero. By taking the Laplace transforms of equations (2.24) – (2.28), we get the following equations:

$$P_0(s) = \frac{1}{s + 2\lambda_0 + 2\lambda_H} \tag{2.29}$$

$$P_1(s) = \frac{P_0(s) \cdot 2 \cdot \lambda_0}{s + \lambda_0 + \lambda_H} \tag{2.30}$$

$$P_2(s) = \frac{P_0(s) \cdot 2 \cdot \lambda_H}{s + \lambda_0 + \lambda_H} \tag{2.31}$$

$$P_3(s) = \frac{\lambda_0 \cdot \left(P_1(s) + P_2(s)\right)}{s} \tag{2.32}$$

$$P_4(s) = \frac{\lambda_H \cdot \left(P_1(s) + P_2(s)\right)}{s} \tag{2.33}$$

By using equations (2.29) - (2.33), we get the following:

$$P_0(s) = \frac{1}{s + 2\lambda_0 + 2\lambda_H} \tag{2.34}$$

$$P_1(s) = \frac{2\lambda_0}{\left(s + \lambda_0 + \lambda_H\right)\left(s + 2\lambda_0 + 2\lambda_H\right)} \tag{2.35}$$

$$P_2(s) = \frac{2\lambda_H}{\left(s + \lambda_0 + \lambda_H\right)\left(s + 2\lambda_0 + 2\lambda_H\right)} \tag{2.36}$$

$$P_3(s) = \frac{\lambda_0\left(2\lambda_0 + 2\lambda_H\right)}{s\left(s + \lambda_0 + \lambda_H\right)\left(s + 2\lambda_0 + 2\lambda_H\right)} \tag{2.37}$$

$$P_4(s) = \frac{\lambda_H\left(2\lambda_0 + 2\lambda_H\right)}{s\left(s + \lambda_0 + \lambda_H\right)\left(s + 2\lambda_0 + 2\lambda_H\right)} \tag{2.38}$$

By taking the inverse Laplace transform of equations (2.34) – (2.38), we get the equations of time dependent state probabilities as follows:

$$P_0(t) = \mathrm{e}^{-2\left(\lambda_0 + \lambda_H\right)t} \tag{2.39}$$

$$P_1(t) = \frac{2 \cdot \lambda_0}{\lambda_0 + \lambda_H}\left(\mathrm{e}^{\left(-\left(\lambda_0 + \lambda_H\right)t\right)} - \mathrm{e}^{\left(-2 \cdot \left(\lambda_0 + \lambda_H\right)t\right)}\right) \tag{2.40}$$

$$P_2(t) = \frac{2 \cdot \lambda_H}{\lambda_0 + \lambda_H}\left(\mathrm{e}^{\left(-\left(\lambda_0 + \lambda_H\right)t\right)} - \mathrm{e}^{\left(-2 \cdot \left(\lambda_0 + \lambda_H\right)t\right)}\right) \tag{2.41}$$

$$P_3(t) = \frac{\lambda_0}{\left(\lambda_0 + \lambda_H\right)}\left(1 - 2\cdot e^{\left(-\left(\lambda_0 + \lambda_H\right)\cdot t\right)} + e^{\left(-2\cdot\left(\lambda_0 + \lambda_H\right)\cdot t\right)}\right) \tag{2.42}$$

$$P_4(t) = \frac{\lambda_H}{\left(\lambda_0 + \lambda_H\right)}\left(1 - 2\cdot e^{\left(-\left(\lambda_0 + \lambda_H\right)\cdot t\right)} + e^{\left(-2\cdot\left(\lambda_0 + \lambda_H\right)\cdot t\right)}\right) \tag{2.43}$$

System Reliability and MTTF

When system failure cannot be repaired, the reliability can be obtained by finding the probabilities of all operating states.

$$R(t) = P_0(t) + P_1(t) + P_2(t) \tag{2.44}$$

MTTF is obtained by using $\lim_{s \to 0} R(s)$. The following equation of MTTF was obtained:

$$MTTF = \lim_{s \to 0}(R(s)) = \lim_{s \to 0}\left(P_0(s) + P_1(s) + P_2(s)\right) = \frac{3}{2\left(\lambda_0 + \lambda_H\right)} \tag{2.45}$$

To analyse the model reliability parameters, specific values of hardware failure rate and human-error rate were assumed. Accordingly, the state probability equations (2.39) to (2.43) were used to develop the plots in Figure 2-7, and the reliability equation (2.44) was used to the plots in Figure 2-8. Detailed plots are presented in Appendix B.2.

$$\lambda_0 = 0.00125\left(\frac{failure}{hour}\right) \qquad \lambda_H = 0.005\left(\frac{failure}{hour}\right)$$

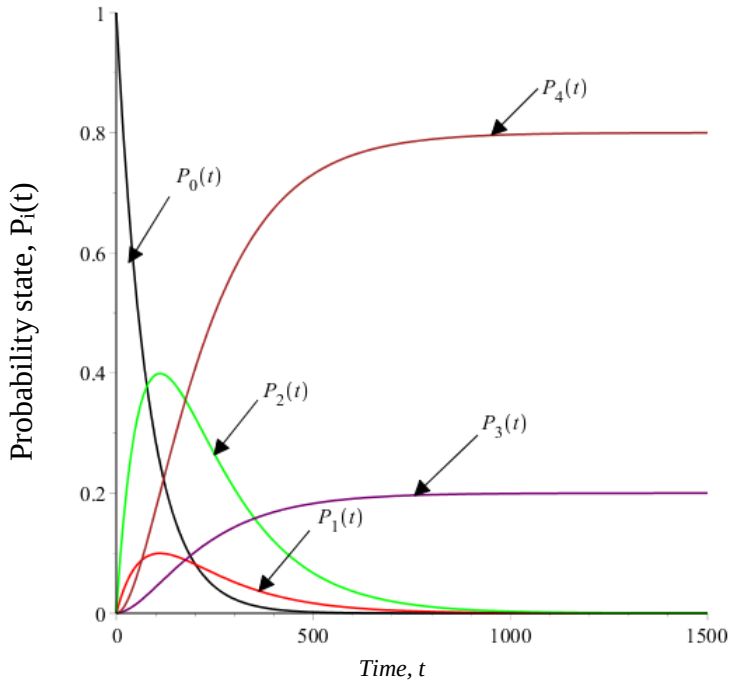

Figure 2-7 State probabilities of two-units system with two failure modes without repair

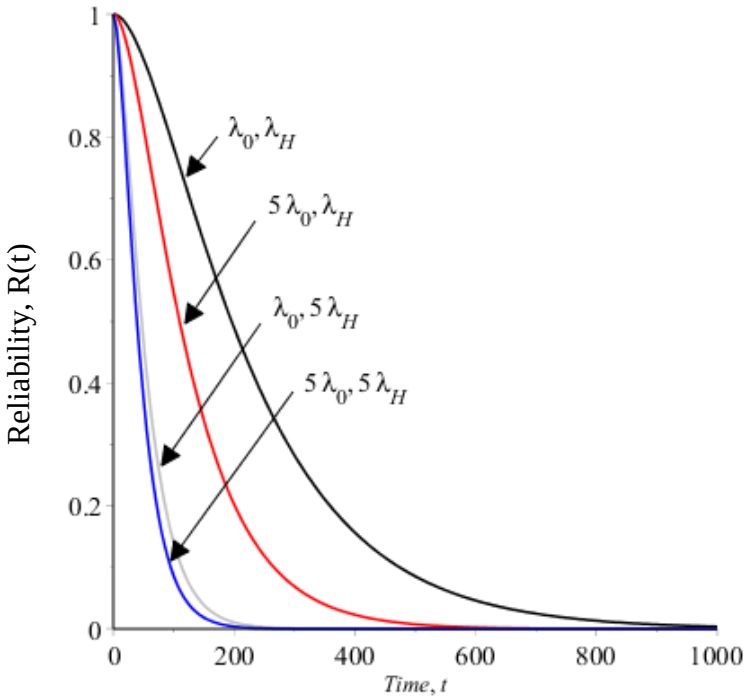

Figure 2-8 Reliability plots of two-units system with two failure modes without repair at different values of failure rates.

2.2.4 **Special Case: Three-Units System without Repair**

The transition state diagram in Figure 2-9 shows a three identical units model of mining system in parallel configuration in which each has two failure modes. By using the Markov method to analyse Figure 2-9, the following differential equations are obtained.

$$\frac{dP_0(t)}{dt} + P_0(t)\cdot\left(3\cdot\lambda_0 + 3\cdot\lambda_H\right) = 0 \tag{2.46}$$

$$\frac{dP_1(t)}{dt} + P_1(t)\left(2\cdot\lambda_0 + 2\cdot\lambda_H\right) = P_0(t)\cdot 3\cdot\lambda_0 \tag{2.47}$$

$$\frac{dP_2(t)}{dt} + P_2(t)\left(2\cdot\lambda_0 + 2\cdot\lambda_H\right) = P_0(t)\cdot 3\cdot\lambda_H \tag{2.48}$$

$$\frac{dP_3(t)}{dt} + P_3(t)\left(\lambda_0 + \lambda_H\right) = 2\cdot\lambda_0\cdot\left(P_1(t) + P_2(t)\right) \tag{2.49}$$

$$\frac{dP_4(t)}{dt} + P_4(t)\left(\lambda_0 + \lambda_H\right) = 2\cdot\lambda_H\left(P_1(t) + P_2(t)\right) \tag{2.50}$$

$$\frac{dP_6(t)}{dt} = \lambda_H\left(P_3(t) + P_4(t)\right) \tag{2.51}$$

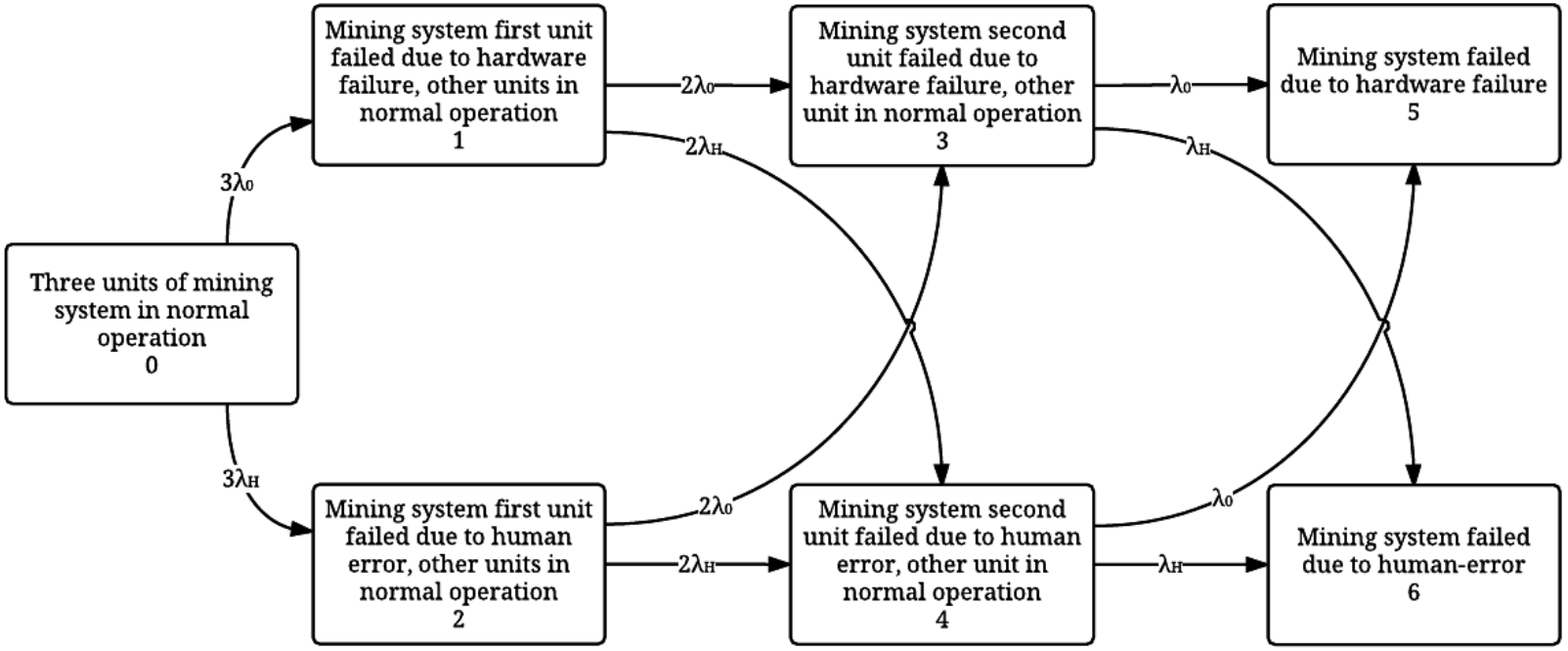

Figure 2-9 State space diagram of three-units system with two failure modes without repair

At time t= 0, $P_0(0)$= 1 and all other initial state probabilities are equal to zero. By taking the Laplace transforms of equations (2.46) – (2.51), we get the following equations:

$$P_0(s) = \frac{1}{s + 3\cdot\lambda_0 + 3\cdot\lambda_H} \tag{2.52}$$

$$P_1(s) = \frac{P_0(s)\cdot 3\cdot\lambda_0}{s + 2\cdot\lambda_0 + 2\cdot\lambda_H} \tag{2.53}$$

$$P_2(s) = \frac{P_0(s)\cdot 3\cdot\lambda_H}{s + 2\cdot\lambda_0 + 2\cdot\lambda_H} \tag{2.54}$$

$$P_3(s) = \frac{2\cdot\lambda_0\cdot\left(P_1(s) + P_2(s)\right)}{s + \lambda_0 + \lambda_H} \tag{2.55}$$

$$P_4(s) = \frac{2\cdot\lambda_H\cdot\left(P_1(s) + P_2(s)\right)}{s + \lambda_0 + \lambda_H} \tag{2.56}$$

$$P_5(s) = \frac{\lambda_0\cdot\left(P_3(s) + P_4(s)\right)}{s} \tag{2.57}$$

$$P_6(s) = \frac{\lambda_H\cdot\left(P_3(s) + P_4(s)\right)}{s} \tag{2.58}$$

By using equations (2.52) to (2.58), we get the following equations:

$$P_0(s) = \frac{1}{s + 3\cdot\lambda_0 + 3\cdot\lambda_H} \tag{2.59}$$

$$P_1(s) = \frac{3\,\lambda_0}{\left(s + 2\,\lambda_0 + 2\,\lambda_H\right)\left(s + 3\,\lambda_0 + 3\,\lambda_H\right)} \tag{2.60}$$

$$P_2(s) = \frac{3\,\lambda_H}{\left(s + 2\,\lambda_0 + 2\,\lambda_H\right)\left(s + 3\,\lambda_0 + 3\,\lambda_H\right)} \tag{2.61}$$

$$P_3(s) = \frac{6\,\lambda_0\left(\lambda_0 + \lambda_H\right)}{\left(s + \lambda_0 + \lambda_H\right)\left(s + 2\,\lambda_0 + 2\,\lambda_H\right)\left(s + 3\,\lambda_0 + 3\,\lambda_H\right)} \tag{2.62}$$

$$P_4(s) = \frac{6\,\lambda_H\left(\lambda_0 + \lambda_H\right)}{\left(s + \lambda_0 + \lambda_H\right)\left(s + 2\,\lambda_0 + 2\,\lambda_H\right)\left(s + 3\,\lambda_0 + 3\,\lambda_H\right)} \tag{2.63}$$

$$P_5(s) = \frac{6\,\lambda_0\left(\lambda_0 + \lambda_H\right)^2}{s\left(s + \lambda_0 + \lambda_H\right)\left(s + 2\,\lambda_0 + 2\,\lambda_H\right)\left(s + 3\,\lambda_0 + 3\,\lambda_H\right)} \tag{2.64}$$

$$P_6(s) = \frac{\lambda_H \left(\lambda_0 + \lambda_H \right)^2}{s\left(s + \lambda_0 + \lambda_H\right)\left(s + 2\lambda_0 + 2\lambda_H\right)\left(s + 3\lambda_0 + 3\lambda_H\right)} \tag{2.65}$$

By taking the inverse Laplace transform of equations (2.59) to (2.65), the time dependent state probabilities are obtained as follows:

$$P_0(t) = \mathrm{e}^{-3\left(\lambda_0 + \lambda_H\right)t} \tag{2.66}$$

$$P_1(t) = \frac{3\cdot\lambda}{\lambda+\sigma}\cdot\left(\mathrm{e}^{-\left(2\cdot\lambda+2\cdot\sigma\right)\cdot t} - \mathrm{e}^{-\left(3\cdot\lambda+3\cdot\sigma\right)\cdot t}\right) \tag{2.67}$$

$$P_2(t) = \frac{3\cdot\sigma}{\lambda+\sigma}\cdot\left(\mathrm{e}^{-\left(2\cdot\lambda+2\cdot\sigma\right)\cdot t} - \mathrm{e}^{-\left(3\cdot\lambda+3\cdot\sigma\right)\cdot t}\right) \tag{2.68}$$

$$P_3(t) = \frac{3\cdot\lambda}{\left(\lambda+\sigma\right)}\cdot\left(\mathrm{e}^{-3\cdot\left(\lambda+\sigma\right)\cdot t} - 2\cdot\mathrm{e}^{-2\cdot\left(\lambda+\sigma\right)\cdot t} + \mathrm{e}^{-\left(\lambda+\sigma\right)\cdot t}\right) \tag{2.69}$$

$$P_4(t) = \frac{3\cdot\sigma}{\left(\lambda+\sigma\right)}\cdot\left(\mathrm{e}^{-3\cdot\left(\lambda+\sigma\right)\cdot t} - 2\cdot\mathrm{e}^{-2\cdot\left(\lambda+\sigma\right)\cdot t} + \mathrm{e}^{-\left(\lambda+\sigma\right)\cdot t}\right) \tag{2.70}$$

$$P_5(t) = \frac{\lambda}{\lambda+\sigma}\cdot\left(-\mathrm{e}^{-3\cdot\left(\lambda+\sigma\right)\cdot t} + 3\cdot\mathrm{e}^{-2\cdot\left(\lambda+\sigma\right)\cdot t} - 3\cdot\mathrm{e}^{-\left(\lambda+\sigma\right)\cdot t} + 1\right) \tag{2.71}$$

$$P_6(t) = \frac{\sigma}{\lambda+\sigma}\cdot\left(-\mathrm{e}^{-3\cdot\left(\lambda+\sigma\right)\cdot t} + 3\cdot\mathrm{e}^{-2\cdot\left(\lambda+\sigma\right)\cdot t} - 3\cdot\mathrm{e}^{-\left(\lambda+\sigma\right)\cdot t} + 1\right) \tag{2.72}$$

System Reliability and MTTF

In this model, the reliability can be obtained by finding the probabilities of all operating states.

$$R(t) = \sum_{i=0}^{4} P_i(t) \tag{2.73}$$

MTTF is obtained by using $\lim_{s\to 0} R(s)$. The following equation of MTTF was obtained:

$$MTTF = \lim_{s\to 0} R(s) = \lim_{s\to 0} \sum_{i=0}^{4} P_i(s) = \frac{11}{6\left(\lambda+\sigma\right)} \tag{2.74}$$

To analyse the model reliability parameters, specific values of hardware failure rate and human-error rate were assumed. Accordingly, the state probabilities equations (2.66) – (2.72) were used to develop the plots in Figure 2-10, and the reliability equation (2.73) was used to develop the plots in Figure 2-11. Detailed plots are presented in Appendix B.3.

$$\lambda_0 = 0.00125 \left(\frac{failure}{hour} \right)$$
$$\lambda_H = 0.005 \left(\frac{failure}{hour} \right)$$

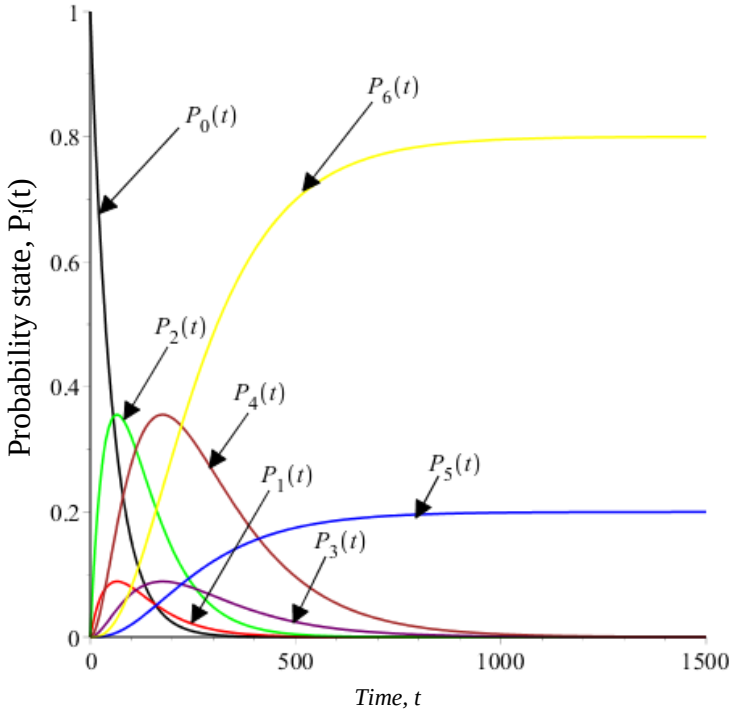

Figure 2-10 State probabilities of three-units system with two failure modes without repair

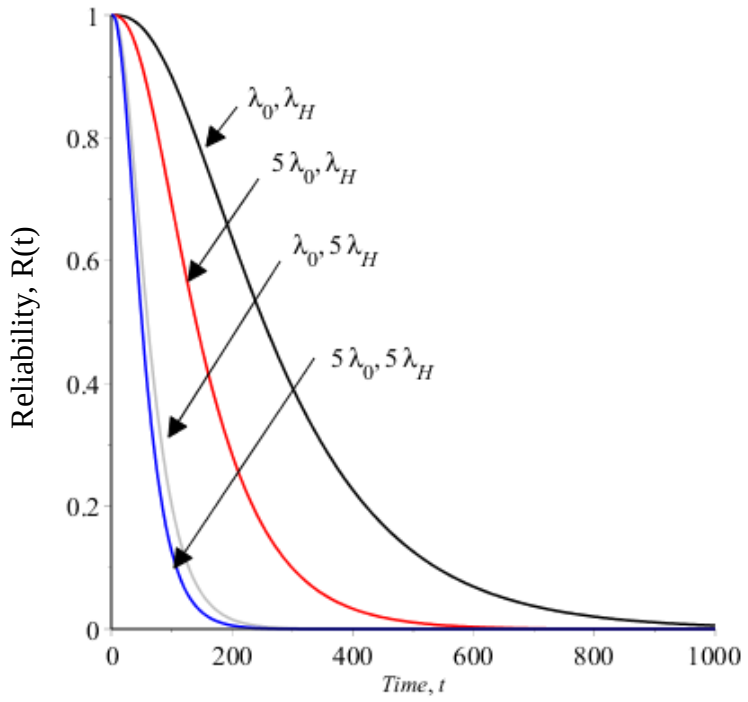

Figure 2-11 Reliability plots of three-units system with two failure modes without repair at different values of failure rates.

2.3 Human-Error and Hardware Failure with Type-I Repair

2.3.1 General n-Units System with Type-I Repair

In this model, units are unrepairable while system failure can be repaired and restored to its initial state according to Type-I repair policy. Also, each unit might fail due to hardware failure or human error. The symbolic representation of general model is that (n) is the number of units in the system, (j) is the failure mode that can either be 1 or 2 where j=1 refers to hardware failure mode and j=2 refers to human-error mode. Likewise, λ_j refers to unit failure rate, i.e. λ_1 refers to hardware failure rate, λ_2 refers to human-error rate. Also μ_j refer to repair rate where μ_1 refers to repair rate of failures due to hardware, μ_2 refers to repair rate of failures due to human-error, and (i) is the number of failed unit at time (t).

At the initial state, all n parallel units are in normal operation. So the failure rates are $n\lambda_1$ and $n\lambda_2$ to represent the failure rate of all units. After first unit failure, the failure rate is $(n-1)\lambda_1$ and $(n-1)\lambda_2$ because (n-1) units in normal operation, and so forth $(n-i)\lambda_1$ and $(n-i)\lambda_2$. When there is

only one unit in normal operation, the failure rates are λ_0 and λ_H. Based on special cases when n=1, n=2 and n=3, with Type-I repair policy, the following general differential equations describing the system using the Markov method were obtained:

$$\frac{dP_0(t)}{dt} + n \cdot P_0(t) \cdot \left(\lambda_1 + \lambda_2\right) = \sum_{j=1}^{2} P_{n-j}(t) \cdot \mu_j \tag{2.75}$$

$$\frac{dP_{1-j}(t)}{dt} + (n-1)\ P_{1-j}(t) \cdot \sum_{v=1}^{2} \left(\lambda_v\right) = (n-i+1)\,\lambda_j P_0(t) \tag{2.76}$$

$$\frac{dP_{i-j}(t)}{dt} + (n-i)\ P_{i-j}(t) \cdot \sum_{v=1}^{2} \left(\lambda_v\right) = (n-i+1)\,\lambda_j \cdot \sum_{v=1}^{2} P_{(i-1)-v}(t) \tag{2.77}$$

$$\frac{dP_{n-j}(t)}{dt} + P_{n-j}(t) \cdot \mu_j = \lambda_j \cdot \sum_{v=1}^{2} P_{(n-1)-v}(t) \tag{2.78}$$

At time t= 0, $P_0(0)$= 1 and all other initial state probabilities are equal to zero. By taking the Laplace transforms of equations (2.75) – (2.78), the following general s-domain equations (2.79) – (2.81) were developed:

$$P_0(s) = \frac{\left(\prod_{v=2}^{n} (s + (v+1)\cdot F)\right)\left(\prod_{i=1}^{2} \mu_i\right)}{\left(\prod_{i=1}^{n} (s + iF)\right) \cdot \prod_{i=1}^{2} \left(s + \mu_i\right) - n!\, F^{n-1} \cdot \left(\sum_{q=1}^{2} \left(\frac{\mu_q \lambda_q \left(\prod_{k=1}^{2} \left(s + \mu_k\right)\right)}{s + \mu_q}\right)\right)} \tag{2.79}$$

$$P_{i-j}(s) = \frac{P_0(s)\,\lambda_j F^{(i-1)} \left(\prod_{v=1}^{i} (n - v + 1)\right)}{\left(\prod_{q=n-i}^{n-1} (s + qF)\right)} \tag{2.80}$$

$$P_{n-j}(s) = \frac{P_0(s)\,\lambda_j F^{(n-1)} \left(\prod_{v=1}^{n} (n - v + 1)\right)}{\left(s + \lambda_j\right) \cdot \left(\prod_{q=2}^{n} (s + (q-1)F)\right)} \tag{2.81}$$

Where

$$F = \sum_{q=1}^{2} \lambda_q$$

The equations of time-dependent state probabilities can be obtained by taking the inverse Laplace transforms of s-domain equations (2.79) – (2.81). However, the resulted equations were complicated and the common pattern was undistinguishable. Instead, the steady state probabilities were obtained by using the final-value theorem as follows:

$$P_0 = \frac{\left(\prod_{i=2}^{n}((i-1))\right)\prod_{i=1}^{2}\mu_i}{\mathrm{n}\cdot\left(\sum_{i=1}^{n}\frac{(n-1)}{i}\right)\cdot\left(\prod_{i=1}^{2}\mu_i\right)+\mathrm{n}!\cdot\left(\sum_{q=1}^{2}\left(\frac{\lambda_q\left(\prod_{k=1}^{2}(\mu_k)\right)}{\mu_q}\right)\right)} \tag{2.82}$$

$$P_{i-j} = \frac{P_0\lambda_j\left(\prod_{v=1}^{i}(n-v+1)\right)}{\sum_{q=1}^{z}(\lambda_q)} \tag{2.83}$$

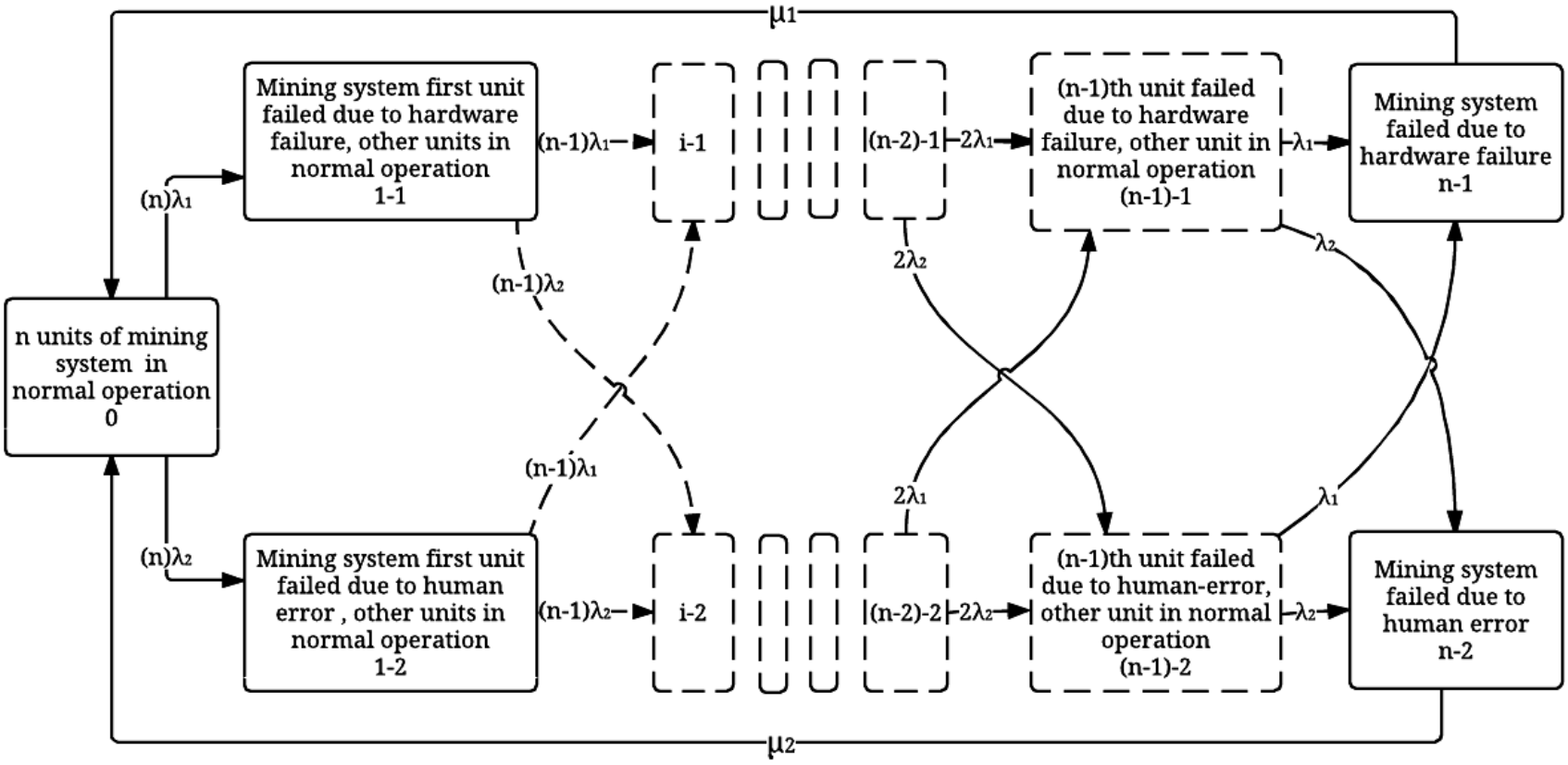

Figure 2-12 State space diagram of n-units system with two failure modes and Type-I repair

$$P_{n-j} = \frac{P_0 \lambda_j \left(\prod_{v=1}^{i} (n - v + 1) \right)}{\mu_j} \tag{2.84}$$

In these model with Type-I repair, the steady state availability can be obtained by adding the probabilities of all operating states as follows:

$$AV_{SS} = \sum_{i=1}^{n-1} \left(\sum_{j=1}^{2} P_{i-j} \right) \tag{2.85}$$

Then, we get the following:

$$MTTF = \lim_{s \to 0} R(s) = \lim_{s \to 0} \sum_{i=0}^{n-2} P_i(s) = \frac{1}{\sum_{j=1}^{2} \lambda_j} \cdot \sum_{i=0}^{n-1} \left(\frac{1}{n-i} \right) \tag{2.86}$$

2.3.2 **Special Case: One-Unit System with Type-I Repair**

The transition state diagram in Figure 2-13 shows a single unit model of mining system that has two failure modes. If this unit fails, the system fails and can be restored back to initial state. By using the Markov method to analyse Figure 2-13, the differential equations were obtained as follows:

$$\frac{dP_0(t)}{dt} + P_0(t) \left(\lambda_O + \lambda_H \right) = P_1(t) \cdot \mu_1 + P_2(t) \cdot \mu_2 \tag{2.87}$$

$$\frac{dP_1(t)}{dt} + P_1(t) \cdot \mu_1 = P_0(t) \cdot \lambda_O \tag{2.88}$$

$$\frac{dP_2(t)}{dt} + P_2(t) \cdot \mu_2 = P_0(t) \cdot \lambda_H \tag{2.89}$$

At time t= 0, $P_0(0)$= 1 and all other initial state probabilities are equal to zero. By taking the Laplace transforms for equations 2.87 to 2.89, the following equations are obtained.

$$P_0(s) = \frac{\left(P_1(s) \cdot \mu_1 + P_2(s) \cdot \mu_2 + 1 \right)}{s + \lambda_O + \lambda_H} \tag{2.90}$$

$$P_1(s) = \frac{\lambda_O \cdot P_0(s)}{s + \mu_1} \tag{2.91}$$

$$P_2(s) = \frac{\lambda_H \cdot P_0(s)}{s + \mu_2} \tag{2.92}$$

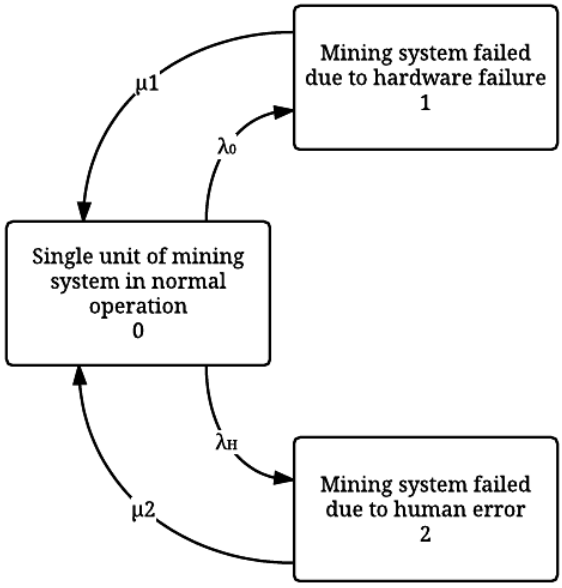

Figure 2-13 State space diagram of one-unit with two failure modes and Type-I repair

By using equations 2.90 to 2.92, we get the following equations:

$$P_0(s) = \frac{\left(s + \mu_1\right)\left(s + \mu_2\right)}{s\left(s^2 + s\left(\lambda_H + \lambda_O + \mu_1 + \mu_2\right) + \left(\lambda_H \mu_1 + \lambda_O \mu_2 + \mu_1 \mu_2\right)\right)} \tag{2.93}$$

$$P_1(s) = \frac{\left(\lambda_O\right)\left(s + \mu_2\right)}{s\left(s^2 + \left(\mu_1 + \mu_2 + \lambda_H + \lambda_O\right)s + \lambda_H \mu_1 + \lambda_O \mu_2 + \mu_1 \mu_2\right)} \tag{2.94}$$

$$P_2(s) = \frac{\left(\lambda_H\right)\left(s + \mu_1\right)}{s\left(s^2 + \left(\mu_1 + \mu_2 + \lambda_H + \lambda_O\right)s + \lambda_H \mu_1 + \lambda_O \mu_2 + \mu_1 \mu_2\right)} \tag{2.95}$$

By taking the inverse Laplace transform of equations (2.93) – (2.95), the following equations are obtained:

$$P_0(t) = \frac{\mu_1 \mu_2}{n_1 n_2} + \frac{\left(n_1 + \mu_1\right)\left(n_1 + \mu_2\right)}{n_1\left(n_1 - n_2\right)} \cdot e^{-n_1 t} + \frac{\left(n_2 + \mu_1\right)\left(n_2 + \mu_2\right)}{n_2\left(n_2 - n_1\right)} \cdot e^{-n_2 t} \tag{2.96}$$

$$P_1(t) = \frac{\lambda_O \mu_2}{n_1 n_2} + \frac{\left(\lambda_O\right)\left(n_1 + \mu_2\right)}{n_1\left(n_1 - n_2\right)} \cdot e^{-n_1 t} + \frac{\left(\lambda_O\right)\left(n_2 + \mu_2\right)}{n_2\left(n_2 - n_1\right)} \cdot e^{-n_2 t} \tag{2.97}$$

$$P_2(t) = \frac{\lambda_H \mu_1}{n_1 n_2} + \frac{(\lambda_H)(n_1 + \mu_2)}{n_1 (n_1 - n_2)} \cdot e^{-n_1 t} + \frac{(\lambda_H)(n_2 + \mu_2)}{n_2 (n_2 - n_1)} \cdot e^{-n_2 t} \quad (2.98)$$

Where n_1 and n_2 are the root of square equation and were determined as follows:

$$n_1, n_2 = \frac{-(\mu_1 + \mu_2 + \lambda_H + \lambda_O) \pm \left((\mu_1 + \mu_2 + \lambda_H + \lambda_O)^2 - 4(\lambda_H \mu_1 + \lambda_O \mu_2 + \mu_1 \mu_2)\right)^{\frac{1}{2}}}{2}$$

System Reliability and MTTF

In Type-I repair policy, the system can be restored after complete failure. To obtain the reliability, μ_1 and μ_2 should be equal zero because they are the repair rate of total system failure. The resulted equations are similar to Special Case: One-Unit System without Repair. The reliability equation is (2.22) and MTTF equation is (2.23). The plots are shown in Figure 2-5 and Appendix B.1.

Availability and Steady State Probabilities

The availability is the probabilities of system operational states.

$$AV(t) = P_0(t) \quad (2.99)$$

The system steady state probabilities can be obtained by applying final-value theorem on each states probability at s-domain as follows:

$$P_0 = \frac{(\mu_1)(\mu_2)}{(\lambda_H \mu_1 + \lambda_O \mu_2 + \mu_1 \mu_2)} \quad (2.100)$$

$$P_1 = \frac{(\lambda_O)(\mu_2)}{(\lambda_H \mu_1 + \lambda_O \mu_2 + \mu_1 \mu_2)} \quad (2.101)$$

$$P_2 = \frac{(\lambda_H)(\mu_1)}{(\lambda_H \mu_1 + \lambda_O \mu_2 + \mu_1 \mu_2)} \quad (2.102)$$

To analyse the model reliability parameters, specific values of hardware failure rate, human-error rate and repair rate were assumed. Accordingly, state probability equations (2.96) – (2.98) were used to develop the plots in Figure 2-14 and availability equation (2.99) was used to develop the plots in Figure 2-15. Detailed plots are presented in Appendix B.4.

$\lambda_O = 0.00125 \left(\frac{failure}{hour} \right)$ $\mu_1 = 0.005 \left(\frac{repair}{hour} \right)$ $\lambda_H = 0.005 \left(\frac{failure}{hour} \right)$ $\mu_2 = 0.007 \left(\frac{repair}{hour} \right)$

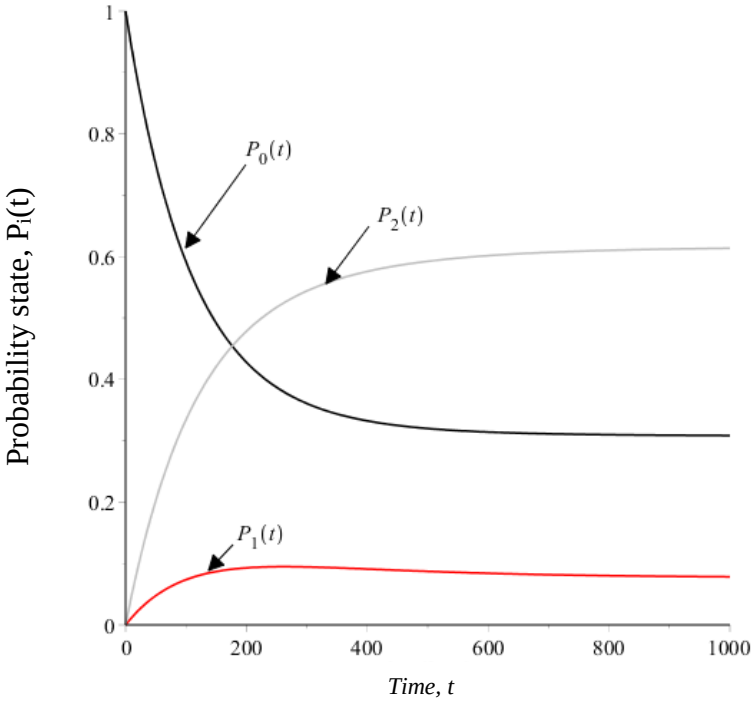

Figure 2-14 State probabilities of one-unit system with two failure modes and Type-I repair

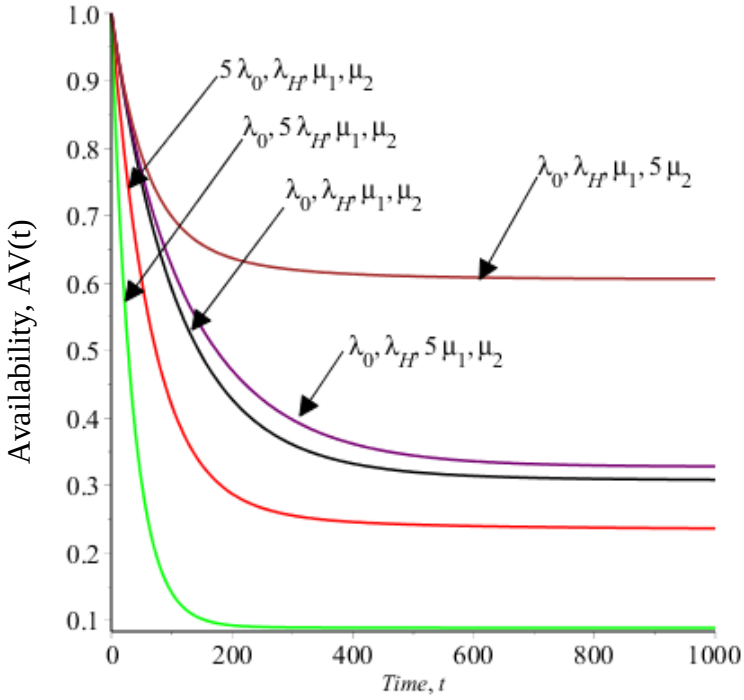

Figure 2-15 Availability plots of one-unit system with two failure modes and Type-I repair at different values of reliability parameters.

2.3.3 **Special Case: Two-Units System with Type-I Repair**

The transition state diagram in Figure 2-16 shows a two identical units model of mining system in parallel configuration in which they have two failure modes. By Using the Markov method to analyse Figure 2-16, the differential equations are obtained as follows:

$$\frac{dP_0(t)}{dt} + P_0(t)\left(2\cdot\lambda_0 + 2\lambda_H\right) = P_3(t)\cdot\mu_1 + P_4(t)\cdot\mu_2 \quad (2.103)$$

$$\frac{dP_1(t)}{dt} + P_1(t)\left(\lambda_0 + \lambda_H\right) = P_0(t)\cdot 2\lambda_0 \quad (2.104)$$

$$\frac{dP_2(t)}{dt} + P_2(t)\left(\lambda_0 + \lambda_H\right) = P_0(t)\cdot 2\lambda_H \quad (2.105)$$

$$\frac{dP_3(t)}{dt} + P_3(t)\cdot\mu_1 = \lambda_0\left(P_1(t) + P_2(t)\right) \quad (2.106)$$

$$\frac{dP_4(t)}{dt} + P_4(t)\cdot\mu_2 = \lambda_H\left(P_1(t) + P_2(t)\right) \quad (2.107)$$

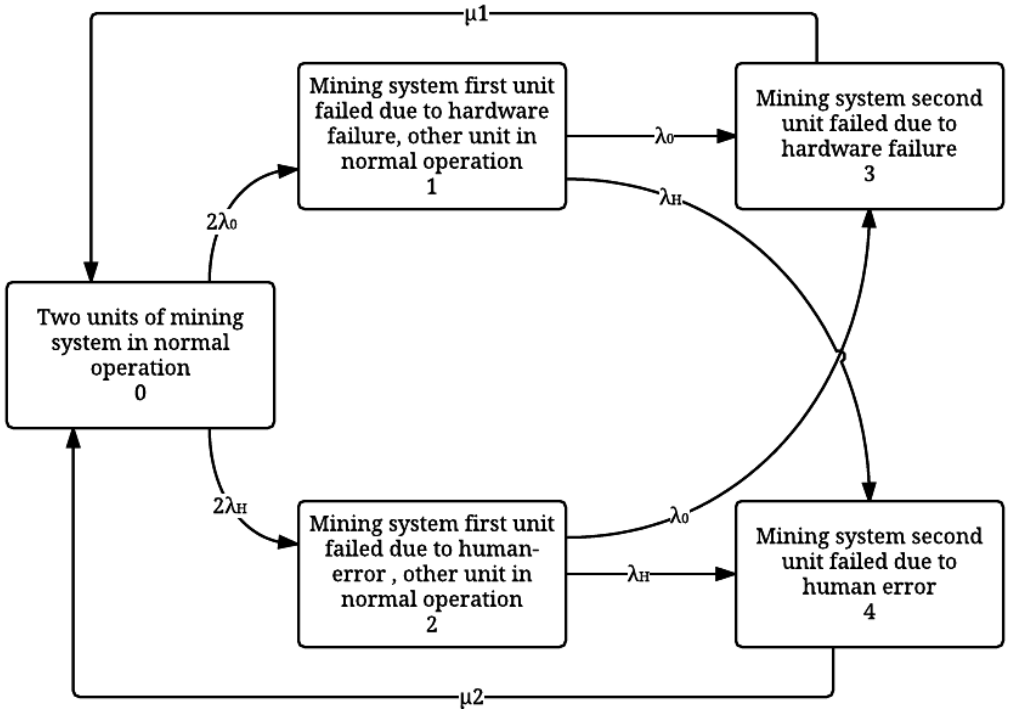

Figure 2-16 State space diagram of two-units system with two failure modes and Type-I repair

At time t= 0, $P_0(0)$= 1 and all other initial state probabilities are equal to zero. By taking the Laplace transforms of equations 2.103 to 2.107, the following equations are obtained:

$$P_0(s) = \frac{P_3(s)\cdot\mu_1 + P_4(s)\cdot\mu_2 + 1}{s + 2\lambda_0 + 2\lambda_H} \tag{2.108}$$

$$P_1(s) = \frac{P_0(s)\cdot 2\cdot\lambda_0}{s + \lambda + \lambda_H} \tag{2.109}$$

$$P_2(s) = \frac{P_0(s)\cdot 2\cdot\lambda_H}{s + \lambda_0 + \lambda_H} \tag{2.110}$$

$$P_3(s) = \frac{\lambda_0\cdot\left(P_1(s) + P_2(s)\right)}{s + \mu_1} \tag{2.111}$$

$$P_4(s) = \frac{\lambda_H\cdot\left(P_1(s) + P_2(s)\right)}{s + \mu_2} \tag{2.112}$$

By using equations 2.108 to 2.112, we get the following equations:

$$P_0(s) = \frac{\left(s+\mu_1\right)\left(s+\mu_2\right)\cdot\left(s+\lambda_0+\lambda_H\right)}{s\cdot\left(s^3 + s^2\beta + s\gamma + \delta\right)} \tag{2.113}$$

$$P_1(s) = \frac{2\lambda_0\left(s+\mu_1\right)\left(s+\mu_2\right)}{s\cdot\left(s^3 + s^2\beta + s\gamma + \delta\right)} \tag{2.114}$$

$$P_2(s) = \frac{2\lambda_H\left(s+\mu_1\right)\left(s+\mu_2\right)}{s\cdot\left(s^3 + s^2\beta + s\gamma + \delta\right)} \tag{2.115}$$

$$P_3(s) = \frac{2\lambda_0\left(s+\mu_2\right)\left(\lambda+\sigma\right)}{s\cdot\left(s^3 + s^2\beta + s\gamma + \delta\right)} \tag{2.116}$$

$$P_4(s) = \frac{2\lambda_H\left(s+\mu_2\right)\left(\lambda+\sigma\right)}{s\cdot\left(s^3 + s^2\beta + s\gamma + \delta\right)} \tag{2.117}$$

Where;

$$\beta = 3\lambda_H + \mu_1 + \mu_2 + 3\lambda_0$$

$$\gamma = 2\lambda_0^2 + 4\lambda_0\lambda_H + 3\lambda_0\mu_1 + 3\lambda_0\mu_2 + 2\lambda_H^2 + 3\lambda_H\mu_1 + 3\lambda_H\mu_2 + \mu_1\mu_2$$

$$\delta = 2\lambda_0^2 + 4\lambda_0\lambda_H + 3\lambda_0\mu_1 + 3\lambda_0\mu_2 + 2\lambda_H^2 + 3\lambda_H\mu_1 + 3\lambda_H\mu_2 + \mu_1\mu_2$$

By taking the inverse Laplace transform of equations 2.113 to 2.117, the time dependent equations of state probabilities are obtained. The steps to obtain time dependent equations are shown in Appendix A.2.

System Reliability and MTTF

In Type-I repair policy, the system can be repaired after complete failure. To obtain the reliability, μ_1 and μ_2 should be equal zero because they are the repair rate of system failure. The resulted equations are similar to Special Case: Two-Units System without Repair. The reliability equation 2.44 and MTTF equation 2.45 were used to develop the plots in Figure 2-8 and Appendix B.2.

Availability and Steady state Probabilities

The availability is the total probabilities of system operational states.

$$AV(t) = P_0(t) + P_1(t) + P_2(t) \tag{2.118}$$

The system steady state probabilities can be obtained by using final-value theorem on each states probability at s-domain which resulted in the following equations:

$$P_0 = \frac{(\mu_1)(\mu_2)\cdot(\lambda_0 + \lambda_H)}{\left(2\lambda_H{}^2\mu_1 + 2\lambda_0{}^2\mu_2 + 3\lambda_H\mu_1\mu_2 + 2\lambda_0\lambda_H\mu_2 + 3\lambda_0\mu_1\mu_2 + 2\lambda_0\lambda_H\mu_1\right)} \tag{2.119}$$

$$P_1 = \frac{2\cdot\lambda_0(\mu_1)(\mu_2)}{\left(2\lambda_H{}^2\mu_1 + 2\lambda_0{}^2\mu_2 + 3\lambda_H\mu_1\mu_2 + 2\lambda_0\lambda_H\mu_2 + 3\lambda_0\mu_1\mu_2 + 2\lambda_0\lambda_H\mu_1\right)} \tag{2.120}$$

$$P_2 = \frac{2\cdot\lambda_H(\mu_1)(\mu_2)}{\left(2\lambda_H{}^2\mu_1 + 2\lambda_0{}^2\mu_2 + 3\lambda_H\mu_1\mu_2 + 2\lambda_0\lambda_H\mu_2 + 3\lambda_0\mu_1\mu_2 + 2\lambda_0\lambda_H\mu_1\right)} \tag{2.121}$$

$$P_3 = \frac{2\lambda_0(\mu_2)(\lambda + \lambda_H)}{\left(2\lambda_H{}^2\mu_1 + 2\lambda_0{}^2\mu_2 + 3\lambda_H\mu_1\mu_2 + 2\lambda_0\lambda_H\mu_2 + 3\lambda_0\mu_1\mu_2 + 2\lambda_0\lambda_H\mu_1\right)} \tag{2.122}$$

$$P_4 = \frac{2\lambda_H(\mu_2)(\lambda + \lambda_H)}{\left(2\lambda_H{}^2\mu_1 + 2\lambda^2\mu_2 + 3\lambda_H\mu_1\mu_2 + 2\lambda\lambda_H\mu_2 + 3\lambda\mu_1\mu_2 + 2\lambda\lambda_H\mu_1\right)} \tag{2.123}$$

To analyse the model reliability parameters, specific values of hardware failure, human-error rates and repair rates were assumed. Accordingly, the inverse Laplace transforms of equations (2.113) – (2.117) were used to develop the state probabilities plots in Figure 2-17, and

the availability equation (2.118) was used to develop the plots in Figure 2-18. Detailed plots were presented in Appendix B.5.

$$\lambda_O = 0.00125 \left(\frac{failure}{hour} \right) \quad \mu_1 = 0.005 \left(\frac{repair}{hour} \right) \quad \lambda_H = 0.005 \left(\frac{failure}{hour} \right) \quad \mu_2 = 0.007 \left(\frac{repair}{hour} \right)$$

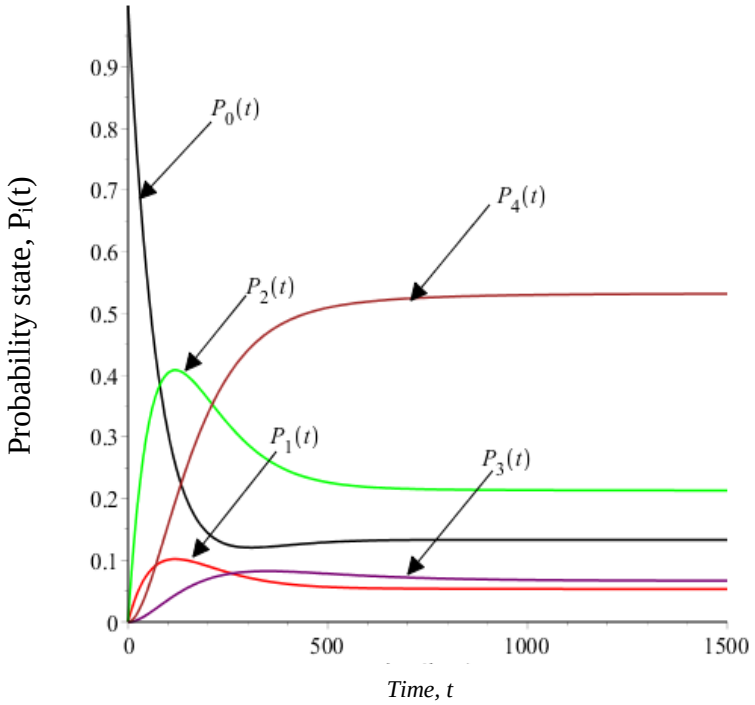

Figure 2-17 State probabilities of two-units system with two failure modes and with Type-I repair

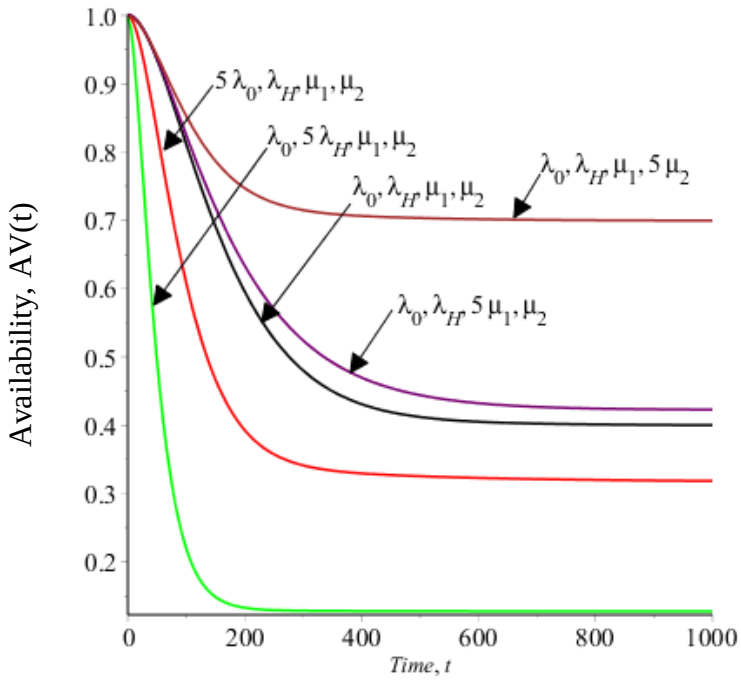

Figure 2-18 Availability plots of two-units system with two failure modes and Type-I repair at different values of reliability parameters.

2.3.4 **Special Case: Three-Units System with Type-I Repair Policy**

The transition state diagram in Figure 2-19 shows a three identical units model of mining system in parallel configuration in which each has two failure modes. By using the Markov method to analyse Figure 2-19, the following differential equations are obtained:

$$\frac{dP_0(t)}{dt} + 3P_0(t)\left(\lambda_0 + \lambda_H\right) = \mu_1 P_5(t) + \mu_2 P_6(t) \tag{2.124}$$

$$\frac{dP_1(t)}{dt} + 2P_1(t)\left(\lambda_0 + \lambda_H\right) = 3\lambda_0 P_0(t) \tag{2.125}$$

$$\frac{dP_2(t)}{dt} + 2P_2(t)\left(\lambda_0 + \lambda_H\right) = 3\cdot\lambda_H \cdot P_0(t) \tag{2.126}$$

$$\frac{dP_3(t)}{dt} + P_3(t)\left(\lambda_0 + \lambda_H\right) = 2\cdot\lambda_0 \cdot \left(P_1(t) + P_2(t)\right) \tag{2.127}$$

$$\frac{dP_4(t)}{dt} + P_4(t)\left(\lambda_0 + \lambda_H\right) = 2\cdot\lambda_H \left(P_1(t) + P_2(t)\right) \tag{2.128}$$

$$\frac{dP_5(t)}{dt} + \mu_1 P_5(t) = \lambda_0 \left(P_3(t) + P_4(t)\right) \tag{2.129}$$

$$\frac{dP_6(t)}{dt} + \mu_2 P_6(t) = \lambda_H\left(P_3(t) + P_4(t)\right) \tag{2.130}$$

At time t= 0, $P_0(0)$= 1 and all other initial state probabilities are equal to zero. By taking the Laplace transforms of equations (2.124) - (2.130), the following equations are obtained:

$$P_0(s) = \frac{\mu_1 P_5(s) + \mu_2 P_6(s) + 1}{s + 3\lambda_0 + 3\lambda_H} \tag{2.131}$$

$$P_1(s) = \frac{P_0(s)\cdot 3\cdot\lambda_0}{s + 2\cdot\left(\lambda_0 + \lambda_H\right)} \tag{2.132}$$

$$P_2(s) = \frac{P_0(s)\cdot 3\cdot\lambda_H}{s + 2\left(\lambda_0 + \lambda_H\right)} \tag{2.133}$$

$$P_3(s) = \frac{2\cdot\lambda_0\cdot\left(P_1(s) + P_2(s)\right)}{s + \lambda_0 + \lambda_H} \tag{2.134}$$

$$P_4(s) = \frac{2\cdot\lambda_H\cdot\left(P_1(s) + P_2(s)\right)}{s + \lambda_0 + \lambda_H} \tag{2.135}$$

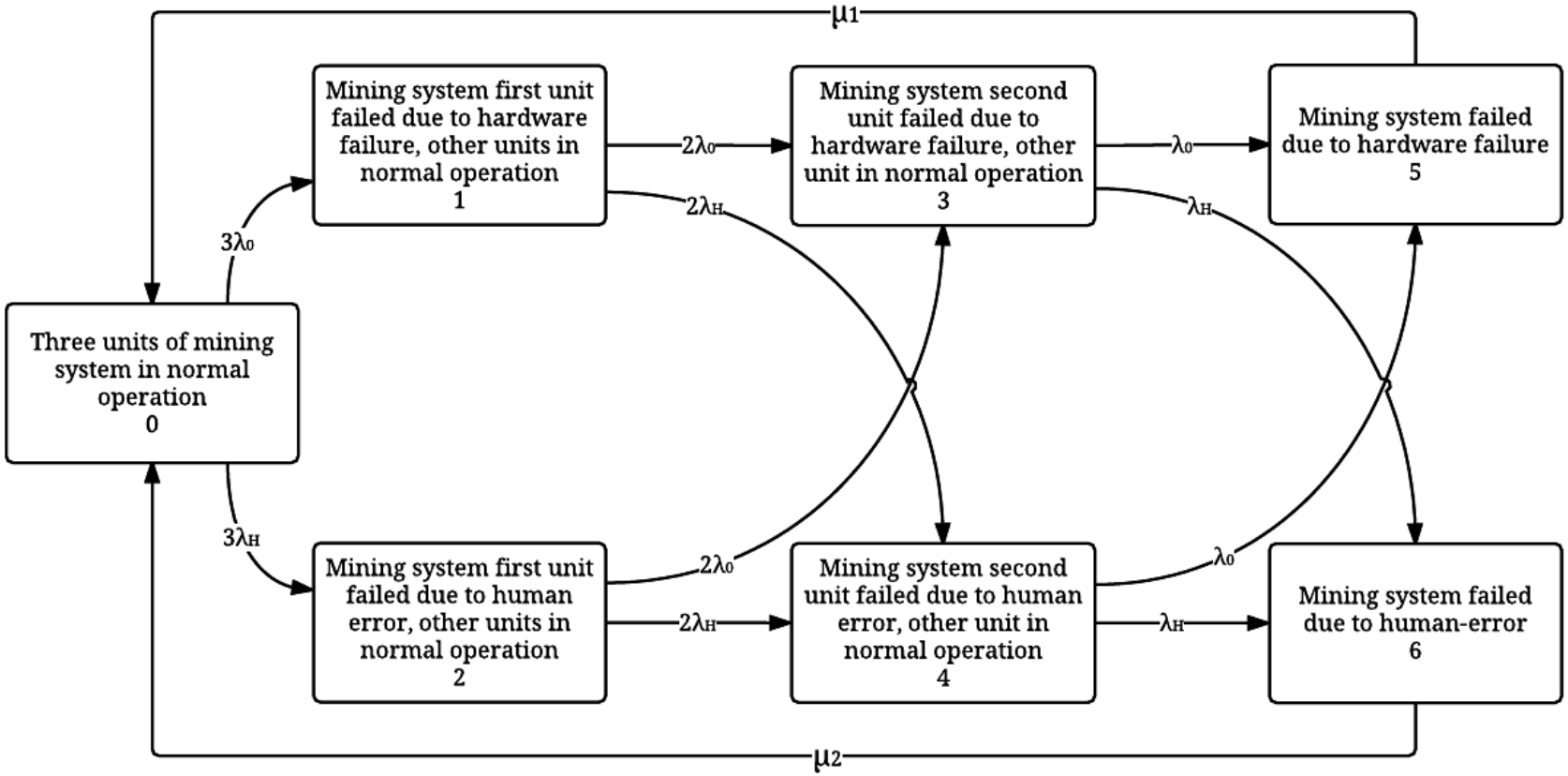

Figure 2-19 State transition diagram of three-units system with two failure modes and Type-I repair

$$P_5(s) = \frac{\lambda_0 \cdot \left(P_3(s) + P_4(s)\right)}{s + \mu_1} \tag{2.136}$$

$$P_6(s) = \frac{\lambda_H \cdot \left(P_3(s) + P_4(s)\right)}{s + \mu_2} \tag{2.137}$$

By using equations (2.131) - (2.139), we get the following equations:

$$P_0(s) = \frac{1}{\left(s + 3 \cdot F - F^2 W\right)} \tag{2.138}$$

$$P_1(s) = \frac{3 \cdot \lambda_0}{(s + 2 \cdot F)\left(s + 3 \cdot F - F^2 W\right)} \tag{2.139}$$

$$P_2(s) = \frac{3 \cdot \lambda_H}{(s + 2 \cdot F)\left(s + 3 \cdot F - F^2 W\right)} \tag{2.140}$$

$$P_3(s) = \frac{6 \lambda_0 F}{(s + F)(s + 2F)\left(s + 3F - F^2 W\right)} \tag{2.141}$$

$$P_4(s) = \frac{6 \lambda_H F}{(s + F)(s + 2F)\left(s + 3F - F^2 W\right)} \tag{2.142}$$

$$P_5(s) = \frac{6 \lambda_0 F^2}{\left(s + \mu_1\right)(s + F)(s + 2F)\left(s + 3F - F^2 W\right)} \tag{2.143}$$

$$P_6(s) = \frac{6 \lambda_H F^2}{\left(s + \mu_1\right)(s + F)(s + 2F)\left(s + 3F - F^2 W\right)} \tag{2.144}$$

Where;

$$F = \lambda_0 + \lambda_H$$

$$W = \left(\frac{6 \lambda_0 \mu_1}{\left(s + \mu_1\right)(s + F)(s + 2F)} + \frac{6 \lambda_H \mu_2}{\left(s + \mu_2\right)(s + F)(s + 2F)} \right)$$

By taking the inverse Laplace transform of equations (2.138) to (2.144), we obtain the time dependent equations of state probabilities.

System Reliability and MTTF

In Type-I repair policy, the system can be restored after complete failure. To obtain the reliability, μ_1 and μ_2 should be equal zero because they are the repair rate of system failure. The resulted equations are similar to Special Case: Three-Units System without Repair. The reliability

equation (2.73) and MTTF equation (2.74) were used to develop the plots in Figure 2-11 and Appendix B.3.

Availability and Steady state Probabilities

Availability is the total probabilities of system operational states as follows:

$$AV(t) = P_0(t) + P_1(t) + P_2(t) + P_3(t) + P_4(t) \tag{2.145}$$

The system steady state probabilities can be obtained by using final-value theorem on equations (2.138) – (2.144). The following equations are obtained:

$$P_0 = \frac{2\mu_1\mu_2}{6\lambda_0\mu_2 + 6\lambda_H\mu_1 + 11\mu_1\mu_2} \tag{2.146}$$

$$P_1 = \frac{3\lambda_0\mu_1\mu_2}{6\lambda_0^2\mu_2 + 6\lambda_0\lambda_H\mu_1 + 6\lambda_0\lambda_H\mu_2 + 11\lambda_0\mu_1\mu_2 + 6\lambda_H^2\mu_1 + 11\lambda_H\mu_1\mu_2} \tag{2.147}$$

$$P_2 = \frac{3\lambda_H\mu_1\mu_2}{6\lambda_0^2\mu_2 + 6\lambda_0\lambda_H\mu_1 + 6\lambda_0\lambda_H\mu_2 + 11\lambda_0\mu_1\mu_2 + 6\lambda_H^2\mu_1 + 11\lambda_H\mu_1\mu_2} \tag{2.148}$$

$$P_3 = \frac{6\lambda_0\mu_1\mu_2}{6\lambda_0^2\mu_2 + 6\lambda_0\lambda_H\mu_1 + 6\lambda_0\lambda_H\mu_2 + 11\lambda_0\mu_1\mu_2 + 6\lambda_H^2\mu_1 + 11\lambda_H\mu_1\mu_2} \tag{2.149}$$

$$P_4 = \frac{6\lambda_H\mu_1\mu_2}{6\lambda_0^2\mu_2 + 6\lambda_0\lambda_H\mu_1 + 6\lambda_0\lambda_H\mu_2 + 11\lambda_0\mu_1\mu_2 + 6\lambda_H^2\mu_1 + 11\lambda_H\mu_1\mu_2} \tag{2.150}$$

$$P_5 = \frac{6\mu_2\lambda_0}{6\lambda_0\mu_2 + 6\lambda_H\mu_1 + 11\mu_1\mu_2} \tag{2.151}$$

$$P_6 = \frac{6\mu_1\lambda_H}{6\lambda_0\mu_2 + 6\lambda_H\mu_1 + 11\mu_1\mu_2} \tag{2.152}$$

To analyse the model reliability parameters, specific values of hardware failure, human-error and repair rates were assumed. Accordingly, the inverse Laplace transform of equation (2.138) – (2.144) were used to develop the plots of state probabilities in Figure 2-20, and availability equation (2.145) was used to develop plots in Figure 2-21. Detailed plots are presented in Appendix B.6.

$\lambda_O = 0.00125 \left(\frac{failure}{hour} \right)$ $\mu_1 = 0.005 \left(\frac{repair}{hour} \right)$ $\lambda_H = 0.005 \left(\frac{failure}{hour} \right)$ $\mu_2 = 0.007 \left(\frac{repair}{hour} \right)$

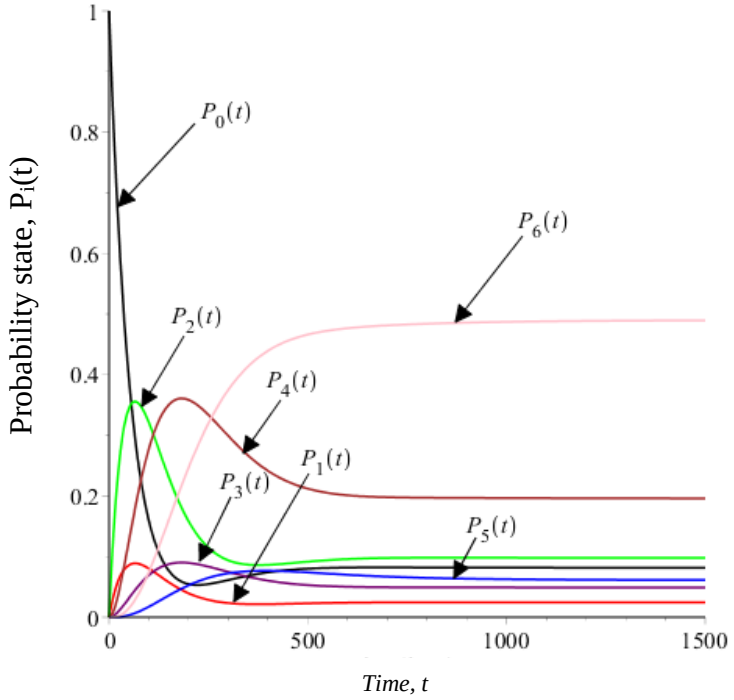

Figure 2-20 State probabilities of three-units system with two failure modes and Type-I repair

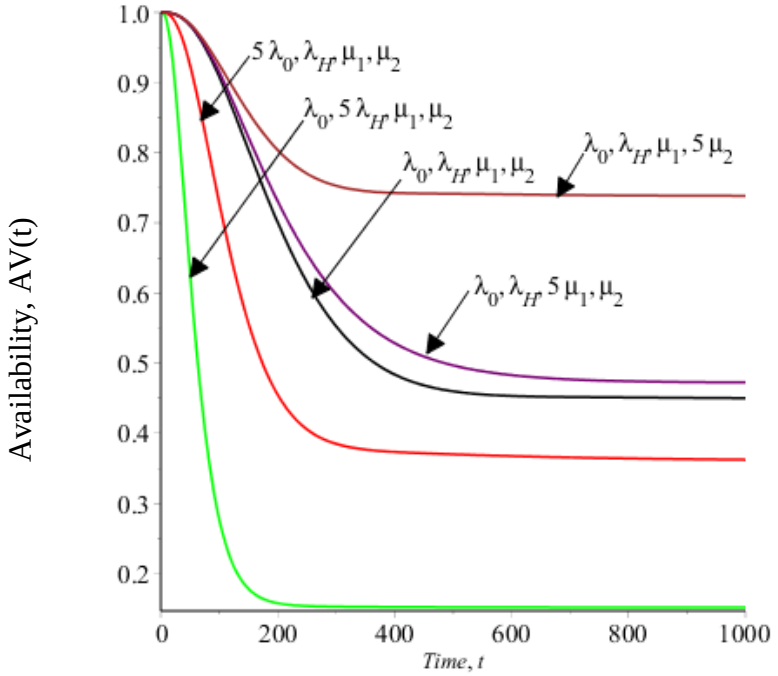

Figure 2-21 Availability plots of three-units system with two failure modes and Type-I policy at different values of model parameters.

2.4 Special Case Two-Units System with Type-II and Type-III Repair

This section discusses the effect of different repair policies on the model reliability and availability. To demonstrate the effect of repair policy, the special case two-units system was investigated when the four repair policies were used: without, Type-I, Type-II and Type-III. The hardware failure rate and human error failure rate were assumed the same for all cases.

The reliability and availability of models without repair and Type-I repair were analysed in "Special Case: Two-Units System without Repair" and "Special Case: Two-Units System with Type-I Repair", respectively.

By using the same assumptions, Type-II and Type-III mathematical models representing mining systems were analysed by using Markov method.

2.4.1 **Special Case: Two-Units System with Type-II Repair**

The transition state diagram in Figure 2-22 shows two identical units model of mining system in parallel configuration in which each has two failure modes. The model has Type-II repair policy, which means the unit failure is instantly identified and the repair action is taken accordingly to return back the unit to the initial state. However, system failed cannot be restored. By using the Markov method, the associated differential equations are obtained as follows:

$$\frac{dP_0(t)}{dt} + P_0(t)\left(2\cdot\lambda_0 + 2\lambda_H\right) = P_1(t)\cdot\mu_1 + P_2(t)\cdot\mu_2 \tag{2.153}$$

$$\frac{dP_1(t)}{dt} + P_1(t)\left(\lambda_0 + \lambda_H + \mu_1\right) = P_0(t)\cdot 2\lambda_0 \tag{2.154}$$

$$\frac{dP_2(t)}{dt} + P_2(t)\left(\lambda_0 + \lambda_H + \mu_2\right) = P_0(t)\cdot 2\lambda_H \tag{2.155}$$

$$\frac{dP_3(t)}{dt} = \lambda_0\left(P_1(t) + P_2(t)\right) \tag{2.156}$$

$$\frac{dP_4(t)}{dt} = \lambda_H\left(P_1(t) + P_2(t)\right) \tag{2.157}$$

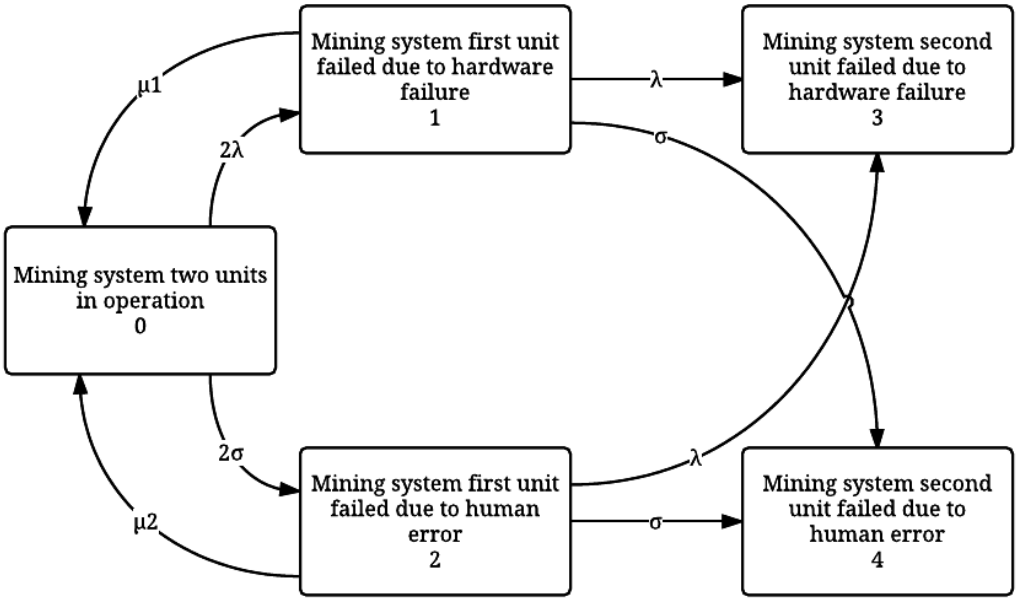

Figure 2-22 State space diagram of two-unit with Type-II repair

At time t= 0, $P_0(0)= 1$ and all other initial state probabilities are equal to zero. By taking the Laplace transforms of equations (2.153) to (2.157), the following equations are obtained:

$$P_0(s) = \frac{P_1(s)\cdot\mu_1 + P_2(s)\cdot\mu_2 + 1}{s + 2\lambda_0 + 2\lambda_H} \tag{2.158}$$

$$P_1(s) = \frac{P_0(s)\cdot 2\cdot\lambda_0}{s + \lambda_0 + \lambda_H + \mu_1} \tag{2.159}$$

$$P_2(s) = \frac{P_0(s)\cdot 2\cdot\lambda_H}{s + \lambda_0 + \lambda_H + \mu_2} \tag{2.160}$$

$$P_3(s) = \frac{\lambda_0\cdot\left(P_1(s) + P_2(s)\right)}{s} \tag{2.161}$$

$$P_4(s) = \frac{\lambda_H\cdot\left(P_1(s) + P_2(s)\right)}{s} \tag{2.162}$$

By using equations (2.158) to (2.164), we get the following equations:

$$P_0(s) = \frac{\left(s + \lambda_0 + \lambda_H + \mu_1\right)\left(s + \lambda_0 + \lambda_H + \mu_2\right)}{\left(s^3 + s^2\beta + s\gamma + \delta\right)} \tag{2.163}$$

$$P_1(s) = \frac{2\lambda_0\left(s+\lambda_0+\lambda_H+\mu_2\right)}{\left(s^3+s^2\beta+s\gamma+\delta\right)} \tag{2.164}$$

$$P_2(s) = \frac{2\lambda_H\left(s+\lambda_0+\lambda_H+\mu_1\right)}{\left(s^3+s^2\beta+s\gamma+\delta\right)} \tag{2.165}$$

$$P_3(s) = \frac{2\lambda_0\left(\lambda_0\left(s+\lambda_0+\lambda_H+\mu_1\right)+\lambda_H\left(s+\lambda_0+\lambda_H+\mu_2\right)\right)}{s\cdot\left(s^3+s^2\beta+s\gamma+\delta\right)} \tag{2.166}$$

$$P_4(s) = \frac{2\lambda_H\left(\lambda_0\left(s+\lambda_0+\lambda_H+\mu_1\right)+\lambda_H\left(s+\lambda_0+\lambda_H+\mu_2\right)\right)}{s\cdot\left(s^3+s^2\beta+s\gamma+\delta\right)} \tag{2.167}$$

Where;

$$\beta = 4\lambda_H+\mu_1+\mu_2+4\lambda_0$$

$$\gamma = 5\lambda_0^2+10\lambda_0\lambda_H+\lambda_0\mu_1+3\lambda_0\mu_2+5\lambda_H^2+3\lambda_H\mu_1+\lambda_H\mu_2+\mu_1\mu_2$$

$$\delta = 2\lambda_0^3+6\lambda_0^2\lambda_H+2\lambda_0^2\mu_2+6\lambda_0\lambda_H^2+2\lambda_0\lambda_H\mu_1+2\lambda_0\lambda_H\mu_2+2\lambda_H^3+2\lambda_H^2\mu_1$$

The steps of finding inverse Laplace transform to obtain time dependent probabilities are presented in Appendix-A.2

System Reliability and MTTF

In Type-II repair policy, the system cannot be restored after complete failure which means the model reliability can be obtained as follows:

$$R(t) = P_0(t) + P_1(t) + P_2(t) \tag{2.168}$$

MTTF is obtained by using $\lim_{s\to 0} R(s)$. The following equation of MTTF is obtained:

$$MTTF = \frac{\left(\lambda_0+\lambda_H+\mu_1\right)\left(\lambda_0+\lambda_H+\mu_2\right)+2\lambda_0\left(\lambda_0+\lambda_H+\mu_2\right)+2\lambda_H\left(\lambda_0+\lambda_H+\mu_1\right)}{2\left(\lambda_0^3+3\lambda_0^2\lambda_H+\lambda_0^2\mu_2+3\lambda_0\lambda_H^2+\lambda_0\lambda_H\mu_1+\lambda_0\lambda_H\mu_2+\lambda_H^3+\lambda_H^2\mu_1\right)} \tag{2.169}$$

To analyse the model reliability parameters, specific values of hardware failure, human-error and repair rates were assumed. Accordingly, the state probability equations (2.163) – (2.166) were used to develop the plots in Figure 2-23, and reliability equation (2.168) was used to develop the plots in Figure 2-24. Detailed plots are presented in Appendix B.7.

$\lambda_O = 0.00125 \left(\frac{failure}{hour} \right)$ $\mu_1 = 0.005 \left(\frac{repair}{hour} \right)$ $\lambda_H = 0.005 \left(\frac{failure}{hour} \right)$ $\mu_2 = 0.007 \left(\frac{repair}{hour} \right)$

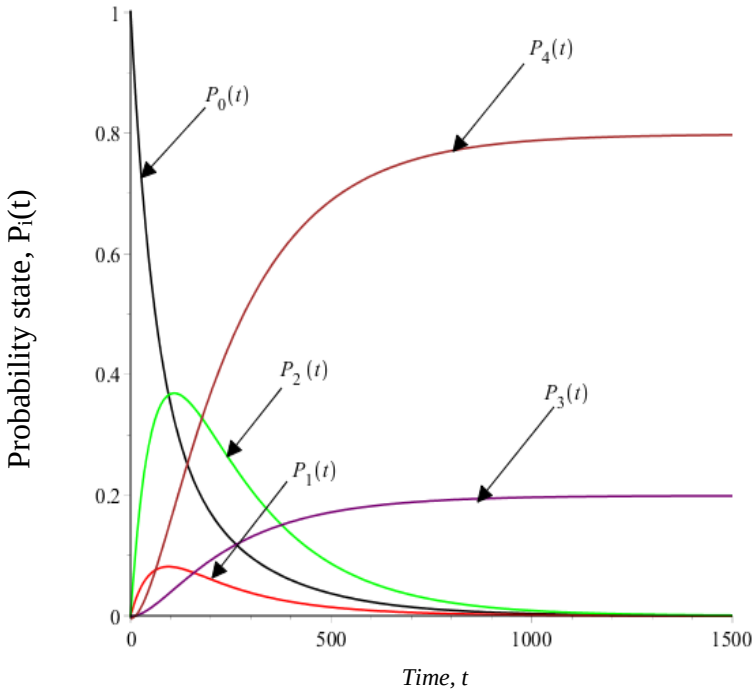

Figure 2-23 State probabilities of two-units system with two failure modes and Type-II repair

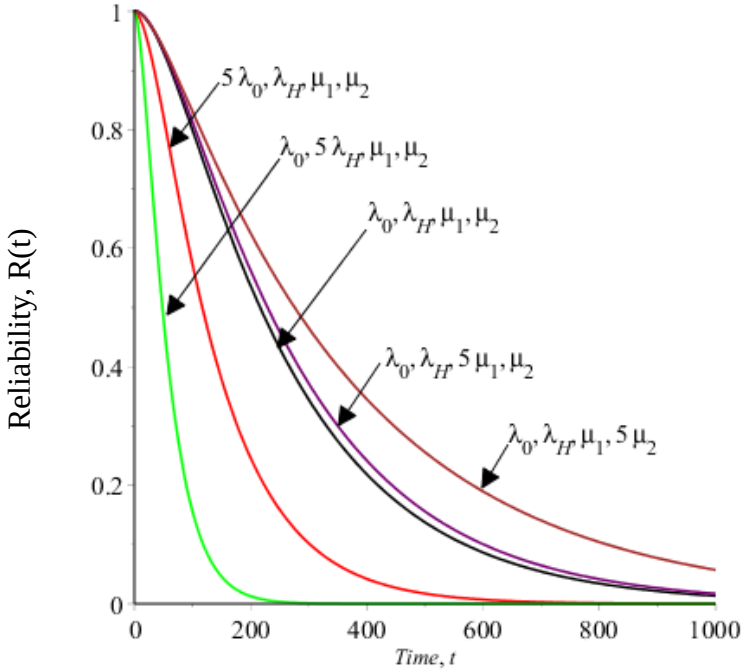

Figure 2-24 Reliability plots of two-units system with two failure modes and Type-II repair at different values of model parameters.

2.4.2 **Special Case: Two-Units System with Type-III Repair**

The transition state diagram in Figure 2-25 shows two identical units model of mining system in parallel configuration in which each has two failure modes. The model is under Type-III repair policy, which means the unit failure is instantly identified and the repair action is taken accordingly to return back the model to its initial state as well as the system failure can be repaired to restore the system failure to initial state.

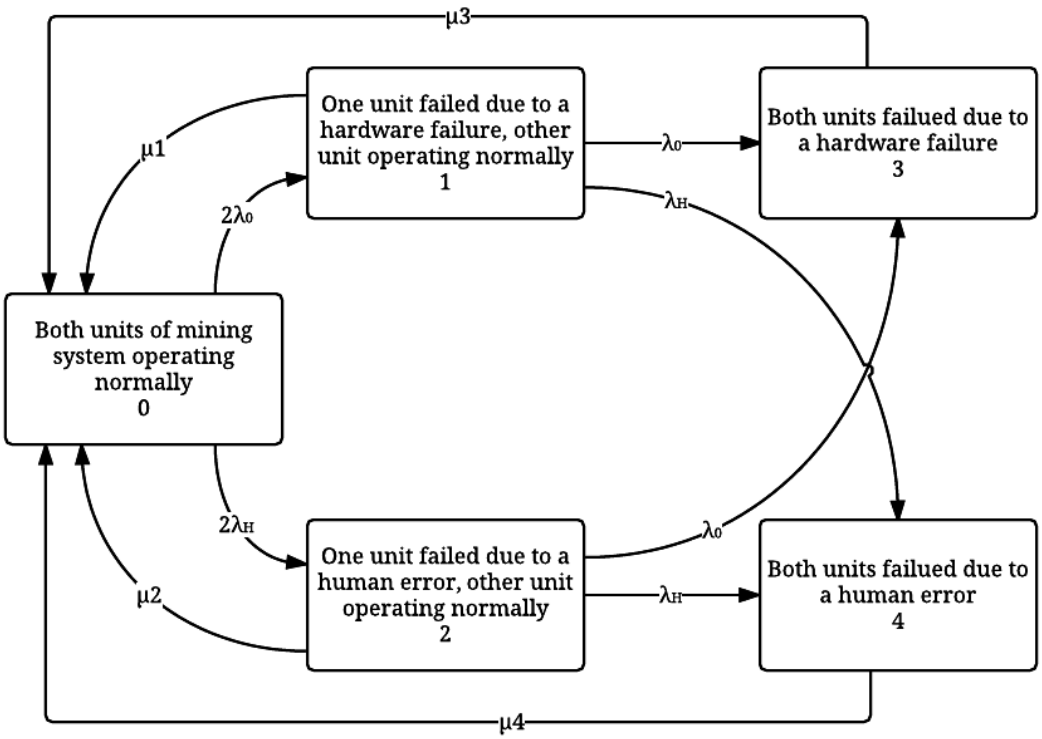

Figure 2-25 State space diagram for two-unit systemwith Type-III repair

With aid of the Markov method, we get the following differential equations for Figure 2-25:

$$\frac{dP_0(t)}{dt} + P_0(t)\left(2\lambda_0 + 2\lambda_H\right) = P_1(t)\,\mu_1 + P_2(t)\,\mu_2 + P_3(t)\,\mu_3 + P_4(t)\,\mu_4 \tag{2.170}$$

$$\frac{dP_1(t)}{dt} + P_1(t)\left(\lambda_0 + \lambda_H + \mu_1\right) = P_0(t)\cdot 2\lambda_0 \tag{2.171}$$

$$\frac{dP_2(t)}{dt} + P_2(t)\left(\lambda_0 + \lambda_H + \mu_2\right) = + P_0(t)\cdot 2\lambda_H \tag{2.172}$$

$$\frac{dP_3(t)}{dt} + P_3(t)\cdot\mu_3 = P_1(t)\cdot\lambda_0 + P_2(t)\cdot\lambda_0 \tag{2.173}$$

$$\frac{dP_4(t)}{dt} + P_4(t)\cdot\mu_4 = P_1(t)\cdot\lambda_H + P_2(t)\cdot\lambda_H \tag{2.174}$$

At time t= 0, $P_0(0)$= 1 and all other initial state probabilities are equal to zero. By taking the Laplace transforms of equations (2.170) – (2.174), the following equations are obtained:

$$P_0(s) = \frac{P_1(s)\cdot\mu_1 + P_2(s)\cdot\mu_2 + P_3(s)\cdot\mu_3 + P_4(s)\cdot\mu_4 + 1}{s + 2\cdot\lambda_0 + 2\cdot\lambda_H} \tag{2.175}$$

$$P_1(s) = \frac{2\cdot\lambda_0\cdot P_0(s)}{s + \lambda_0 + \lambda_H + \mu_1} \tag{2.176}$$

$$P_2(s) = \frac{2\cdot\lambda_H\cdot P_0(s)}{s + \lambda_0 + \lambda_H + \mu_2} \tag{2.177}$$

$$P_3(s) = \frac{\lambda_0\cdot\left(P_1(s) + P_2(s)\right)}{s + \mu_3} \tag{2.178}$$

$$P_4(s) = \frac{\lambda_H\cdot\left(P_1(s) + P_2(s)\right)}{s + \mu_4} \tag{2.179}$$

By using equations (2.175) – (2.179), we get the following equations:

$$P_0(s) = \frac{\left(s+\mu_3\right)\left(s+\mu_4\right)\left(s+\lambda_0+\lambda_H+\mu_1\right)\left(s+\lambda_0+\lambda_H+\mu_2\right)}{s\left(s^4 + s^3\beta + s^2\gamma + s\delta + \epsilon\right)} \tag{2.180}$$

$$P_1(s) = \frac{2\lambda\left(s+\mu_3\right)\left(s+\mu_4\right)\left(s+\lambda+\sigma+\mu_2\right)}{s\left(\beta s^3 + s^4 + \gamma s^2 + \delta s + \epsilon\right)} \tag{2.181}$$

$$P_2(s) = \frac{2\sigma\left(s+\mu_3\right)\left(s+\mu_4\right)\left(s+\lambda+\sigma+\mu_1\right)}{s\left(\beta s^3 + s^4 + \gamma s^2 + \delta s + \epsilon\right)} \tag{2.182}$$

$$P_3(s) = \frac{2\lambda\left(\left(s+\lambda+\sigma+\mu_2\right)\lambda + \left(s+\lambda+\sigma+\mu_1\right)\sigma\right)\left(s+\mu_3\right)}{s\left(s^4 + s^3\beta + s^2\gamma + s\delta + \epsilon\right)} \tag{2.183}$$

$$P_4(s) = \frac{2\sigma\left(\left(s+\lambda+\sigma+\mu_2\right)\lambda + \left(s+\lambda+\sigma+\mu_1\right)\sigma\right)\left(s+\mu_3\right)}{s\left(s^4 + s^3\beta + s^2\gamma + s\delta + \epsilon\right)} \tag{2.184}$$

Where;

$$\beta = 4\lambda + 4\lambda_H + \mu_1 + \mu_2 + \mu_3 + \mu_4$$

$$\gamma = 5\lambda_0^2 + 10\lambda_0\lambda_H + \lambda_0\mu_1 + 3\lambda_0\mu_2 + 4\lambda_0\mu_3 + 4\lambda_0\mu_4 + 5\lambda_H^2 + 3\lambda_H\mu_1 + \lambda_H\mu_2 + 4\lambda_H\mu_3 + 4\lambda_H\mu_4 + \mu_1\mu_2 + \mu_1\mu_3 + \mu_1\mu_4 + \mu_2\mu_3 + \mu_2\mu_4 + \mu_3\mu_4$$

$$\delta = 2\lambda_0^3 + 6\lambda_0^2\lambda_H + 2\lambda_0^2\mu_2 + 3\lambda_0^2\mu_3 + 5\lambda_0^2\mu_4 + 6\lambda_0\lambda_H^2 + 2\lambda_0\lambda_H\mu_1 + 2\lambda_0\lambda_H\mu_2 + 8\lambda_0\lambda_H\mu_3 + 8\lambda_0\lambda_H\mu_4 + \lambda_0\mu_1\mu_3 + \lambda_0\mu_1\mu_4 + 3\lambda_0\mu_2\mu_3 + 3\lambda_0\mu_2\mu_4 + 4\lambda_0\mu_3\mu_4 + 2\lambda_H^3 + 2\lambda_H^2\mu_1 + 5\lambda_H^2\mu_3 + 3\lambda_H^2\mu_4 + 3\lambda_H\mu_1\mu_3 + 3\lambda_H\mu_1\mu_4 + \lambda_H\mu_2\mu_3 + \lambda_H\mu_2\mu_4 + 4\lambda_H\mu_3\mu_4 + \mu_1\mu_2\mu_3 + \mu_1\mu_2\mu_4 + \mu_1\mu_3\mu_4 + \mu_2\mu_3\mu_4$$

$$\epsilon = 2\lambda_0^3\mu_4 + 2\lambda_0^2\lambda_H\mu_3 + 4\lambda_0^2\lambda_H\mu_4 + 2\lambda_0^2\mu_2\mu_4 + 3\lambda_0^2\mu_3\mu_4 + 4\lambda_0\lambda_H^2\mu_3 + 2\lambda_0\lambda_H^2\mu_4 + 2\lambda_0\lambda_H\mu_1\mu_4 + 2\lambda_0\lambda_H\mu_2\mu_3 + 6\lambda_0\lambda_H\mu_3\mu_4 + \lambda_0\mu_1\mu_3\mu_4 + 3\lambda_0\mu_2\mu_3\mu_4 + 2\lambda_H^3\mu_3 + 2\lambda_H^2\mu_1\mu_3 + 3\lambda_H^2\mu_3\mu_4 + 3\lambda_H\mu_1\mu_3\mu_4 + \lambda_H\mu_2\mu_3\mu_4 + \mu_1\mu_2\mu_3\mu_4$$

The steps of finding inverse Laplace transform to obtain time dependent probabilities are presented in Appendix-A.3.

System Reliability and MTTF

In Type-III repair policy, the units and system failures are repairable. Thus, to obtain the reliability, μ_3 and μ_4 should be equal zero because they are the repair rate of system failure. The resulted equations are similar to "Special Case: Two-Units System with Type-II Repair". The reliability equation (2.168) and MTTF equation (2.169) were used to develop the plots in Figure 2-24 and Appendix B.7.

Availability and Steady State Probabilities

The availability is the total probabilities of all operational states.

$$AV(t) = P_0(t) + P_1(t) + P_2(t) \quad (2.185)$$

The system steady state probabilities can be obtained by applying final-value theorem on equations (2.180) – (2.184) as follows:

$$P_0 = \frac{\mu_3\ \mu_4 \left(\lambda_0 + \lambda_H + \mu_1\right)\left(\lambda_0 + \lambda_H + \mu_2\right)}{\epsilon} \tag{2.186}$$

$$P_1 = \frac{2\,\lambda_0 \cdot \mu_3 \cdot \mu_4 \cdot \left(\lambda_0 + \lambda_H + \mu_2\right)}{\epsilon} \tag{2.187}$$

$$P_2 = \frac{2\,\lambda_H \cdot \left(s + \mu_3\right) \cdot \left(s + \mu_4\right) \cdot \left(s + \lambda_0 + \lambda_H + \mu_2\right)}{\epsilon} \tag{2.188}$$

$$P_3 = \frac{2\,\lambda_0\,\mu_3\left(\left(\lambda_0 + \lambda_H + \mu_2\right)\lambda_0 + \left(\lambda_0 + \lambda_H + \mu_1\right)\lambda_H\right)}{\epsilon} \tag{2.189}$$

$$P_4 = \frac{2\,\lambda_H\,\mu_3\left(\left(\lambda_0 + \lambda_H + \mu_2\right)\lambda_0 + \left(\lambda_0 + \lambda_H + \mu_1\right)\lambda_H\right)}{\epsilon} \tag{2.190}$$

To analyse the model reliability parameters, specific values of hardware failure, human-error and repair rates were assumed. Accordingly, the inverse Laplace transforms of equation (2.180) – (2.184) were used to develop the plots of state probabilities in Figure 2-26, and the availability equation (2.185) was used to develop the plots in Figure 2-27 and Figure 2-28. Detailed plots are presented in Appendix B.8.

$$\lambda_0 = 0.00125\left(\frac{failure}{hour}\right)\quad \mu_1 = 0.005\ \left(\frac{repair}{hour}\right)\quad \mu_3 = 0.003\ \left(\frac{repair}{hour}\right)$$
$$\lambda_H = 0.005\ \left(\frac{failure}{hour}\right)\quad \mu_2 = 0.0025\left(\frac{repair}{hour}\right)\quad \mu_4 = 0.0015\ \left(\frac{repair}{hour}\right)$$

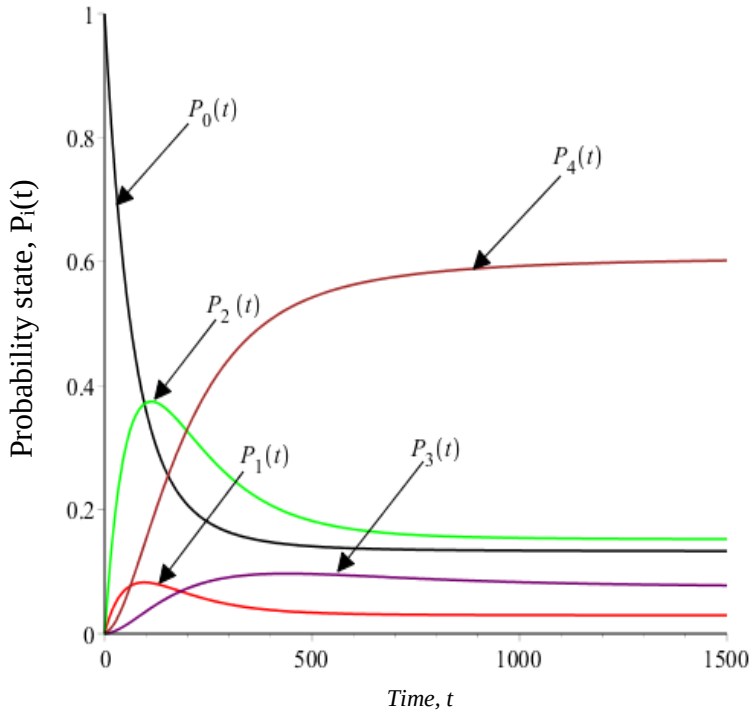

Figure 2-26 State probabilities of two-units system with two failure modes and Type-III repair

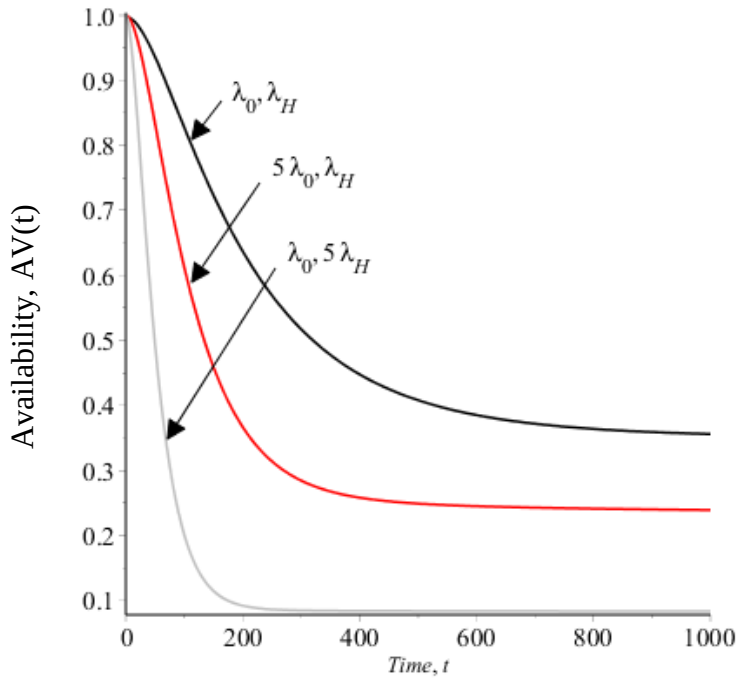

Figure 2-27 Availability plots of two-units system with two failure modes and Type-III repair at different values of failure rates.

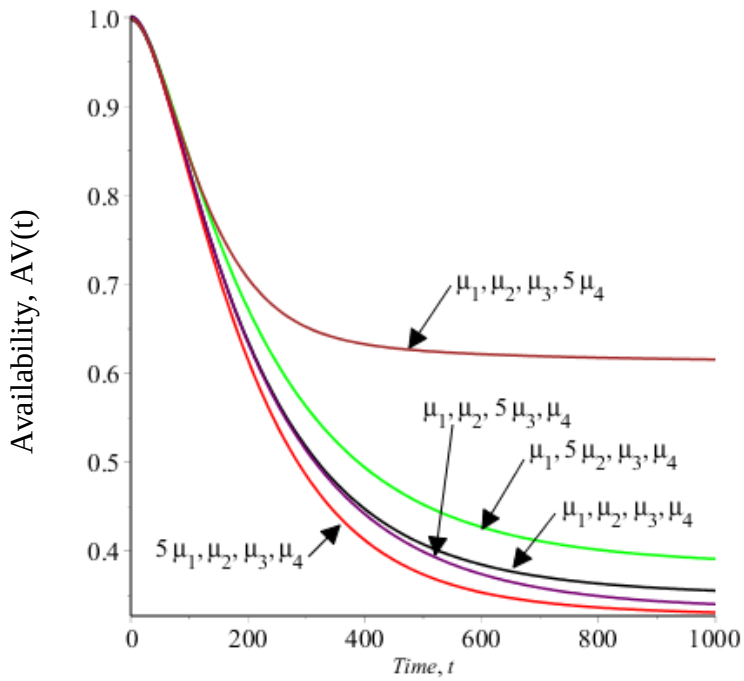

Figure 2-28 Availability plots of two-units system with two failure modes and Type-III repair at different values of repair rates.

2.5 Discussion

This chapter compared and investigated the reliability of mining system models at different number of units in parallel configurations at different values of failure and repair rates. Also, it demonstrates the influence of different repair policies.

According to the reliability plots Figure 2-29 to Figure 2-32 (sold lines), reliability increases as the number of units increase. Also, the reliability increases as the failure rates decrease and vice versa. Also, it is obvious that the model reliability goes to zero at large time (t) because in these particular models under without repair and Type-I repair, the units are unrepairable.

When same failure rates are assumed for different number of units, the reliability plots Figure 2-29 and Figure 2-31 were developed. Figure 2-29 shows the reliability when hardware failure increases. According to assumed failure rates, the reliability for one-unit at failure rate λ_0 is higher than two-units at 5 λ_0 when time (t) is more than 100 hours while it is also higher than

three-units at 5 λ_0 when time (t) is more than 200 hours. Likewise, Figure 2-30 shows the influence of decreasing the hardware failure rate. It was noted that the reliability became almost the same for one-unit at $\lambda_0/5$ and two-units at λ_0 when time (t) equals 600 hours. Also, two-units reliability at $\lambda_0/5$ is higher than three-units at λ_0 at that time.

To investigate the influence of varying human-error rates, Figure 2-31 and Figure 2-32 were developed. Figure 2-31 shows that at a small value of time (t), specifically t= 30 hour, the reliability of one-unit at λ_H is higher than the reliability of two and three units at 5 λ_H. If human-error rate was decreased as in Figure 2-32, the reliability of one-unit at $\lambda_H/5$ is higher than two-units at λ_H when time (t) is 100 hour and higher than three-units at λ_H when time (t) is 200 hours.

To illustrate the influence of different repair policies on model availability, special case two-units system was used with four repair policies: without, Type-I, Type-II and Type-III. The failure rates are assumed the same as well as the repair rates, except Type-III repair where system repair is different than unit repair rates. Figure 2-33 illustrates that Type-II repair increases the availability slightly over without repair policy. However, they go to zero at large time (t). In contrast, Type III repair increases the system availability when it was compared with other policies even at large time (t).

Accordingly, it is not always optimism to increase the number of units in parallel configuration if the failure rates will be increase. Also, it could be optimism to control and reduce the failure rates or human-error rather than increase the number of parallel units.

The availability equations 2.44, 2.119, 2.172 and 2.188 were used to develop availability plots Figure 2-33 based on assumed value of model parameters as follows:

$$\lambda_0 = 0.00125 \left(\frac{failure}{hour}\right) \quad \mu_1 = 0.005 \left(\frac{repair}{hour}\right) \quad \mu_3 = 0.003 \left(\frac{repair}{hour}\right)$$

$$\lambda_H = 0.005 \left(\frac{failure}{hour}\right) \quad \mu_2 = 0.007 \left(\frac{repair}{hour}\right) \quad \mu_4 = 0.0015 \left(\frac{repair}{hour}\right)$$

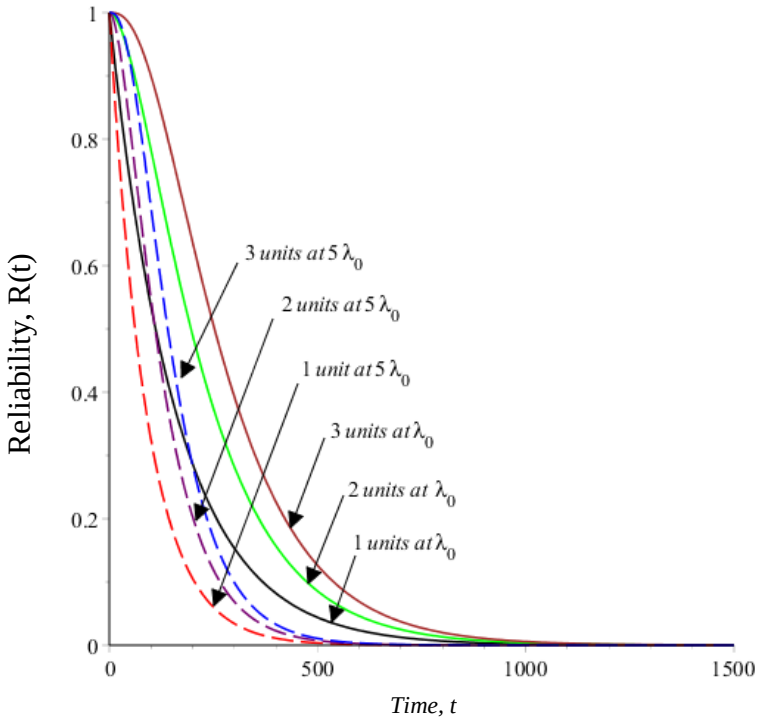

Figure 2-29 All special cases reliability at increased rates of hardware failures

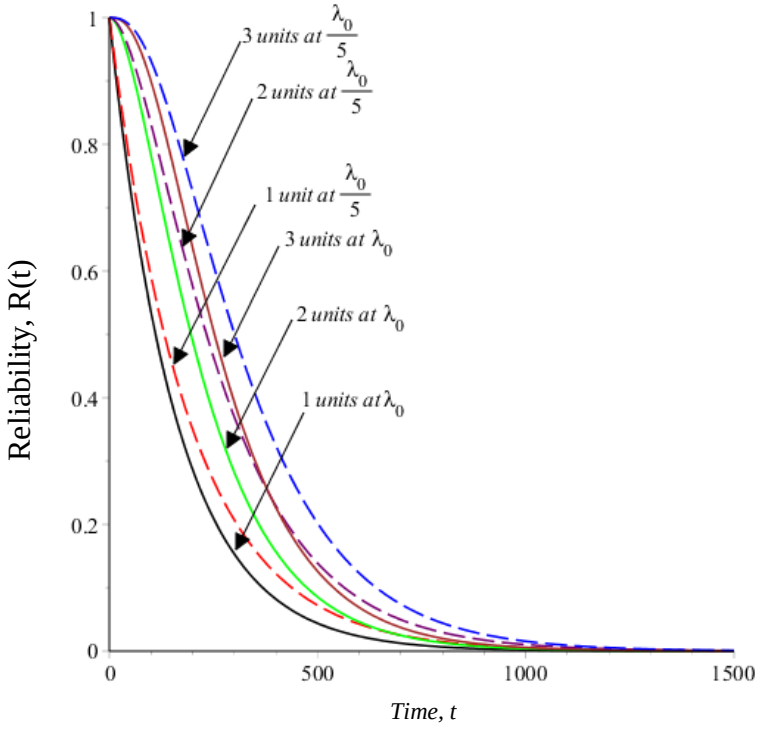

Figure 2-30 All special cases reliability at decreased rates of hardware failures

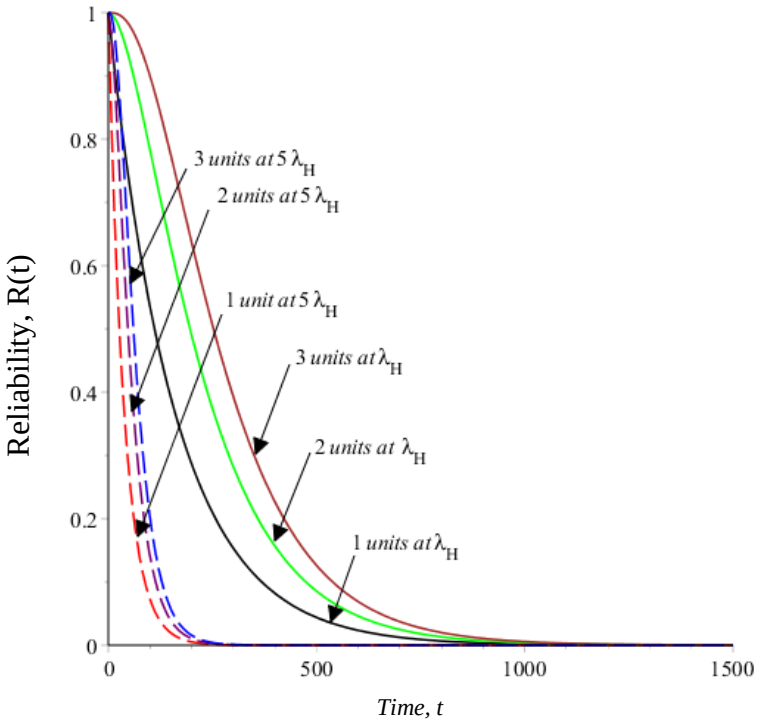

Figure 2-31 All special cases reliability at increased rates of human-errors

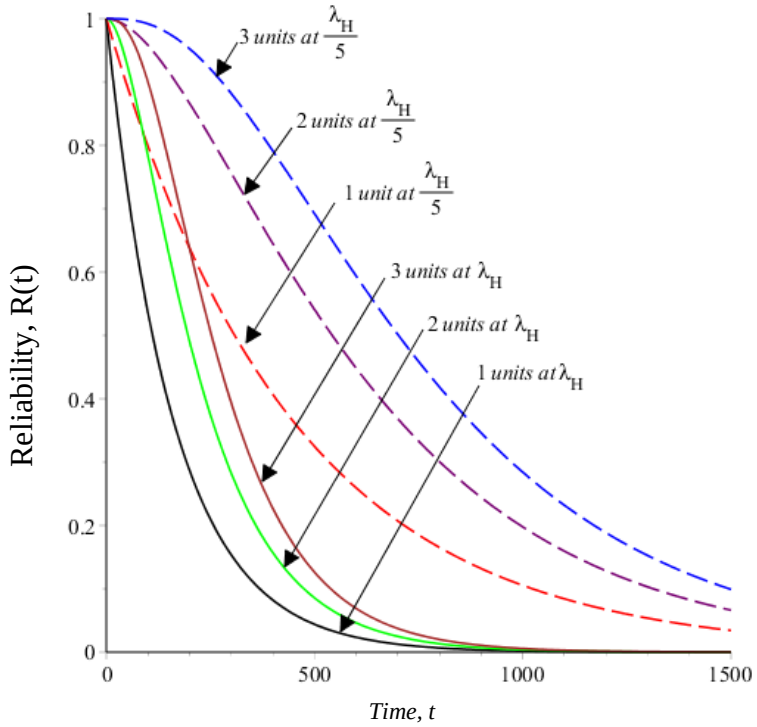

Figure 2-32 All special cases reliability at decreased rates of human-errors

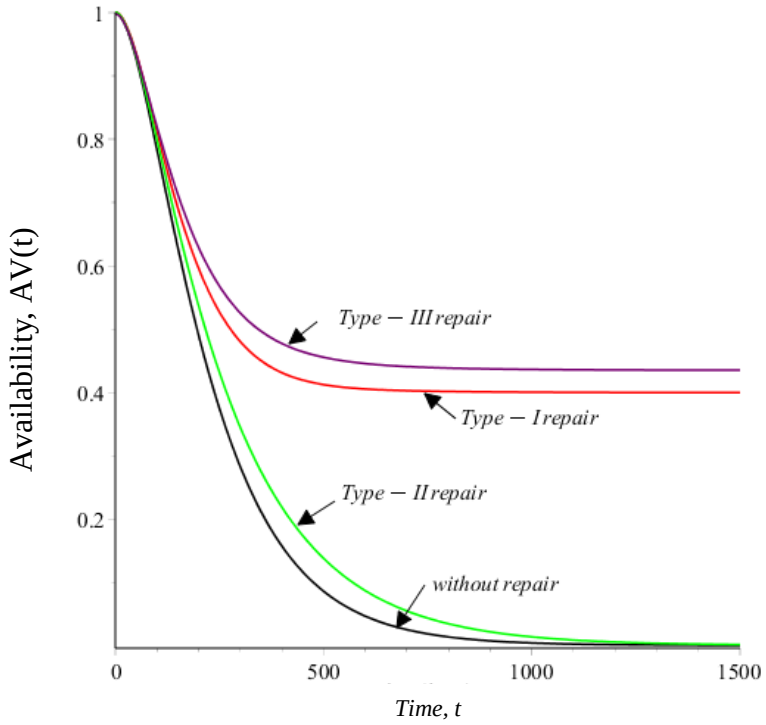

Figure 2-33 Special case two-units system availability with different repair policies

Chapter 3 Reliability and Availability Analysis of Mining Systems with Safe and Unsafe Failure Modes of Hardware and Human-Error

3.1 Introduction

This chapter is almost similar to last one, but it takes into consideration the safety of each failure mode i.e. hardware failure might be safe or unsafe and human-error might be safe or unsafe. Similar assumption are applied on all models underlying this chapter, which block diagram in Figure 2-1 shows. If each unit has the capability to sustain the operation demand, the system is in full operational capacity as long as at least one unit in normal operation. Thus, the system fails when all units failed. If first unit failed due to any failure mode the second unit could fail due to any failure modes as well, and so forth.

This chapter discusses the mathematical models of mining systems at different configurations, namely, single, dual and triple units. Each configuration was analysed at different values of failure and repair rates. The failure and repair rates are assumed to investigate the model reliability parameters i.e. state probabilities, system reliability, mean time to failure (MTTF) and availability. Also, to investigate the effect of considering the safety of failures, the hardware failure λ_0 is equal the summation of safe and unsafe hardware failure rates, λ_{0s} and λ_{0u} respectively. Also, the human-error λ_H is equal the summation of safe and unsafe human-error rates, λ_{Hs} and λ_{Hu} respectively. Markov method and Laplace transforms were used to obtain the expressions of time dependent reliability parameters. Associated equations were solved by using Maplesoft software.

The values of failure and repair rates were assumed in reference to a certain value. Specifically, each parameter was multiplied by 5, 2, 1, 1/2 and 1/5. Then, the results were used to develop reliability parameters which provided a reference plot and resulted plots that help in understanding the reliability measures behaviour.

All models in this chapter underlay one of the two repair policies as follows:

Without repair: This case assumed that system and units are unrepairable.

Type I repair policy: This case assumed that the units are unrepairable while the system repair is possible after total system failure.

Assumptions:

The following assumptions are associated with this model:

i) All units are identical.
ii) All units are in new condition at initial state.
iii) All failures are statistically independent.
iv) All failure and repair rates are constant.
v) The repaired units and systems are as good as new.
vi) There is only one repair facility.
vii) Each unit can fail due to hardware failure or human-error.

Notation

n	Number of parallel units
t	Time in hours
s	Laplace transform variable
λ_{0s}	Constant unit failure rate of safe hardware
λ_{0u}	Constant unit failure rate of unsafe hardware
λ_{Hs}	Constant safe human-error rate
λ_{Hu}	Constant unsafe human-error rate
μ_1	Constant repair rate of safe hardware failures
μ_2	Constant repair rate of unsafe hardware failures
μ_3	Constant repair rate of safe human-error
μ_4	Constant repair rate of unsafe human-error
AV(t)	System availability at time (t)
$P_i(t)$	The probability that the system will be in state i at time (t), for i= 1, 2, 3, …,n
$P_i(s)$	The Laplace transform of state probability, for i= 1, 2, 3, …,n
P_i	Steady state probability for i= 1, 2, 3, …,n
R(t)	System reliability at time (t)

MTTF System mean time to failure

3.2 Hardware Failure and Human-Error with Safe or Unsafe Modes without Repair

3.2.1 General n-Units System without Repair

In this model, units and system are unrepairable as shown in Figure 3-1 in which units might fail safely or unsafely due to hardware failure or human-error. The symbolic representation of general model is that (n) is the number of units in system, (j) is the failure mode that can be 1 to 4 where j=1 refers to safe hardware failure, j=2 refers to unsafe hardware failure, j= 3 refers to safe human-error and j= 4 refers to unsafe human-error. Likewise, λ_j refers to failure rate i.e. λ_1 refers to safe hardware failure rate, λ_2 refers to unsafe hardware failure rate, λ_3 refers to safe human-error rate and λ_4 refers to unsafe human-error rate, and (i) is the number of failed unit at time (t). The states are named as (i-j) based on (i) number of units failed at time (t) and on (j) last unit failure mode.

At the initial state, all n parallel units are in normal operation. So the failure rates are $n\lambda_i$ to represent the failure rate of all units. After first unit failure, the failure rate is $(n-1)\lambda_i$ because (n-1) units in normal operation, and so forth $(n-i)\lambda_i$. Based on special cases when n=1, n=2 and n=3, the general differential equations describing the model according to the Markov method were obtained as follows:

$$\frac{dP_0(t)}{dt} + nP_0(t) \cdot \sum_{v=1}^{4} \lambda_j = 0 \tag{3.1}$$

$$\frac{dP_{1-j}(t)}{dt} + P_{1-j}(t)\,(n-1) \cdot \sum_{v=1}^{4} \lambda_v = P_0(t)\, n\, \lambda_j \tag{3.2}$$

$$\frac{dP_{i-j}(t)}{dt} + P_{i-j}(t)\,(n-1) \cdot \sum_{v=1}^{4} \lambda_v = (n-(i-1))\ \lambda_j \sum_{v=1}^{4} P_v(t)\,(i-1) \quad \text{for all i= 1 to n} \tag{3.3}$$

At $P_0(0)$= 1 at time t= 0 and all other initial state probabilities are equal to zero. By taking the Laplace transform of equations (3.1) – (3.3), the s-domain equations are obtained as follows:

$$P_0(s) = \frac{1}{s + nF} \tag{3.4}$$

$$P_{i-j}(s) = \frac{F^{(i-1)} \lambda_j \prod_{q=1}^{i} (n - q + 1)}{\prod_{v=n-i}^{n} (s + vF)} \tag{3.5}$$

Where

$$F = \sum_{q=1}^{4} \lambda_q$$

The equation of time-dependent state probabilities can be obtained by taking the inverse Laplace transform of equations (3.4) and (3.5). Accordingly, the general time depended equations are developed as follows:

$$P_0(t) = e^{-nFt} \tag{3.6}$$

$$P_{i-j}(t) = \sum_{K=0}^{i} \left(\frac{\prod_{L=0}^{i-1} (n - L) \lambda_j}{\left(\prod_{P=0}^{K-1} (K - P) \right) \left(\prod_{P=K+1}^{i} (K - P) \right) F} \cdot e^{-(n-K)Ft} \right) \quad \text{for all i= 1 to n} \tag{3.7}$$

Where

$$F = \sum_{q=1}^{4} \lambda_q$$

When units and system are unrepairable, the probabilities summation of all operative states will give the model reliability:

$$R(t) = \sum_{j=1}^{4} \left(\sum_{i=0}^{n-1} P_{j-i}(t) \right) \tag{3.8}$$

MTTF is obtained by using $\lim_{s \to 0} R(s)$. The following general equation is obtained:

$$MTTF = \frac{1}{\sum_{j=1}^{4} \lambda_j} \cdot \sum_{i=0}^{n-1} \left(\frac{1}{n - i} \right) \tag{3.9}$$

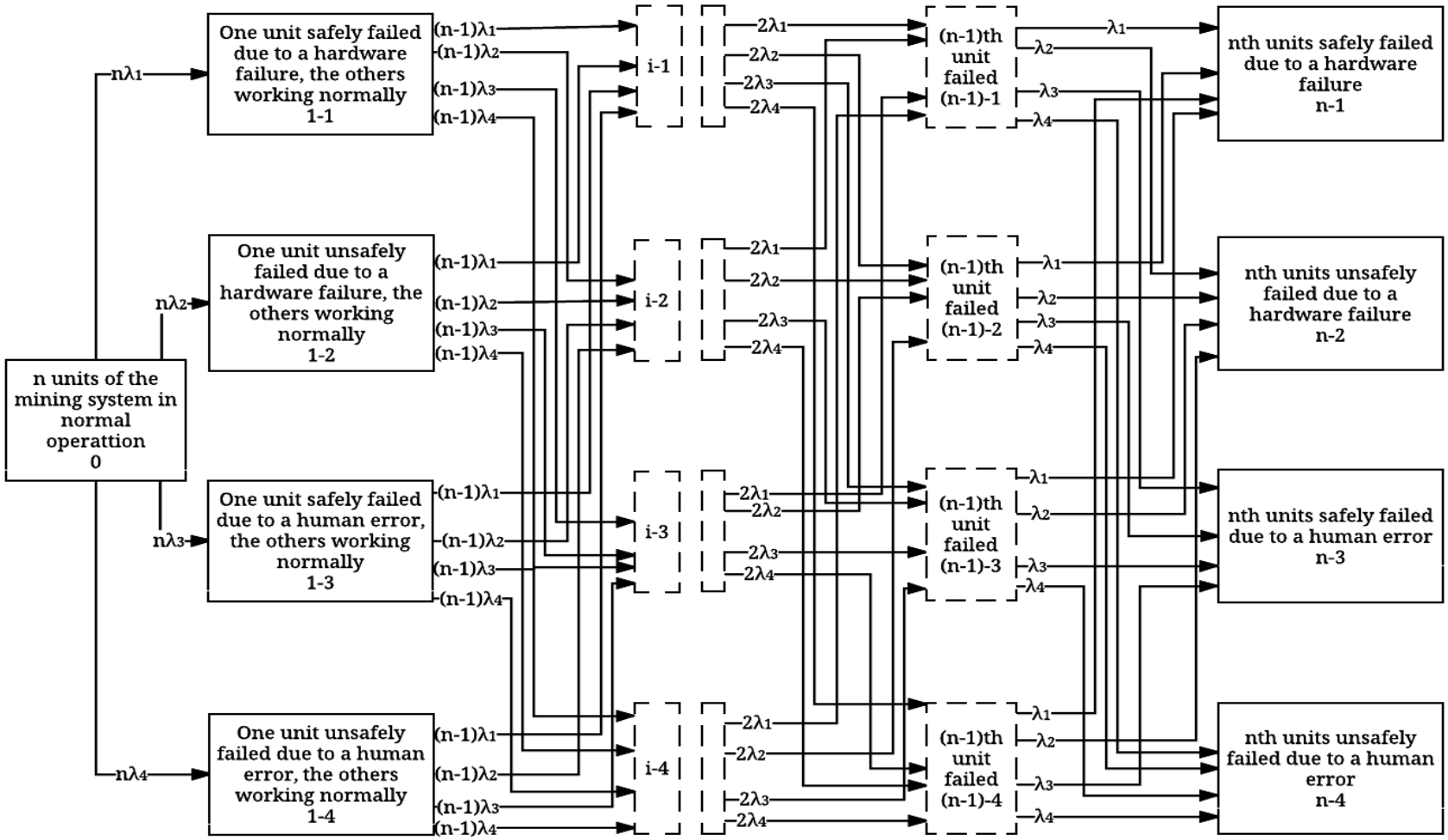

Figure 3-1 State space diagram of n-units with four failure modes without repair

3.2.2 **Special Case: One-Unit System without Repair**

The transition state diagram in Figure 3-2 shows a single unit model of mining system that has four failure modes. If this unit failed, the system fails and cannot be restored back. By using the Markov method, we get the associated equations as follows:

$$\frac{dP_0(t)}{dt} + P_0(t)\left(\lambda_{Os} + \lambda_{Ou} + \lambda_{Hs} + \lambda_{Hu}\right) = 0 \tag{3.10}$$

$$\frac{dP_1(t)}{dt} = P_0(t)\,\lambda_{Os} \tag{3.11}$$

$$\frac{dP_2(t)}{dt} = P_0(t)\,\lambda_{Ou} \tag{3.12}$$

$$\frac{dP_3(t)}{dt} = P_0(t)\,\lambda_{Hs} \tag{3.13}$$

$$\frac{dP_4(t)}{dt} = P_0(t)\,\lambda_{Hu} \tag{3.14}$$

At time t= 0, $P_0(0)$= 1 and all other initial state probabilities are equal to zero. By taking the Laplace transforms of equations (3.10) - (3.14) the following equations are obtained:

$$P_0(s) = \frac{1}{s + \lambda_{Os} + \lambda_{Ou} + \lambda_{Hs} + \lambda_{Hu}} \tag{3.15}$$

$$P_1(s) = \frac{P_0(s)\,\lambda_{Os}}{s} \tag{3.16}$$

$$P_2(s) = \frac{P_0(s)\,\lambda_{Ou}}{s} \tag{3.17}$$

$$P_3(s) = \frac{P_0(s)\,\lambda_{Hs}}{s} \tag{3.18}$$

$$P_4(s) = \frac{P_0(s)\,\lambda_{Hu}}{s} \tag{3.19}$$

By using equations 3.15 to 3.19, the following equations are obtained:

$$P_0(s) = \frac{1}{s + \lambda_{Os} + \lambda_{Ou} + \lambda_{Hs} + \lambda_{Hu}} \tag{3.20}$$

$$P_1(s) = \frac{\lambda_{Os}}{s\left(s + \lambda_{Os} + \lambda_{Ou} + \lambda_{Hs} + \lambda_{Hu}\right)} \tag{3.21}$$

$$P_2(s) = \frac{\lambda_{Ou}}{s\left(s + \lambda_{Os} + \lambda_{Ou} + \lambda_{Hs} + \lambda_{Hu}\right)} \tag{3.22}$$

$$P_3(s) = \frac{\lambda_{Hs}}{s\left(s + \lambda_{Os} + \lambda_{Ou} + \lambda_{Hs} + \lambda_{Hu}\right)} \tag{3.23}$$

$$P_4(s) = \frac{\lambda_{Hu}}{s\left(s + \lambda_{Os} + \lambda_{Ou} + \lambda_{Hs} + \lambda_{Hu}\right)} \tag{3.24}$$

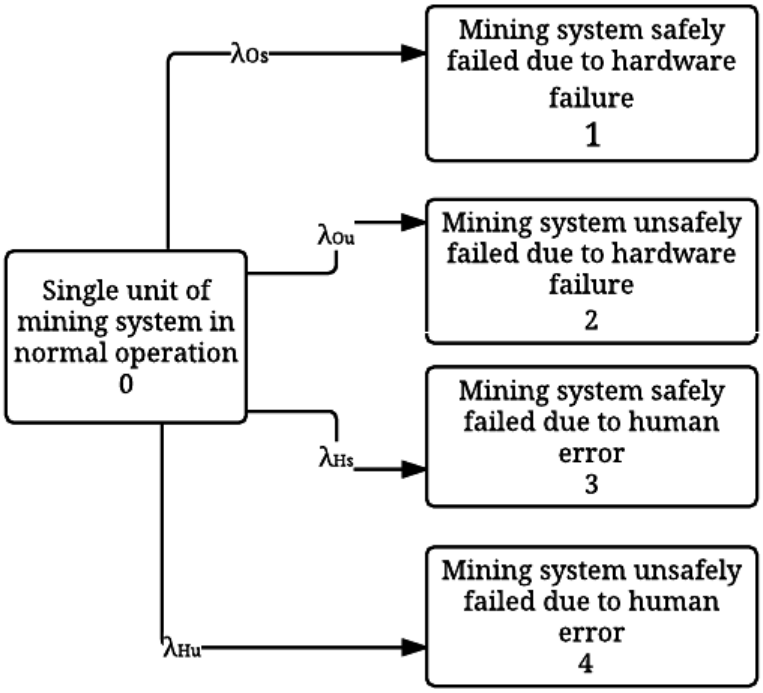

Figure 3-2 State space diagram of one-unit system with four failure modes without repair

By taking the inverse Laplace transform of equations (3.20) – (3.24), time-dependent equations of state probabilities are obtained as follows:

$$P_0(t) = \mathrm{e}^{-\left(\lambda_O + \lambda_H\right) t} \tag{3.25}$$

$$P_1(t) = \frac{\lambda_O\left(1 - \mathrm{e}^{-1.\left(\lambda_O + \lambda_H\right) t}\right)}{\lambda_O + \lambda_H} \tag{3.26}$$

$$P_2(t) = \frac{\lambda_H\left(1 - \mathrm{e}^{-1.\left(\lambda_O + \lambda_H\right) t}\right)}{\lambda_O + \lambda_H} \tag{3.27}$$

System Reliability and MTTF

When system failure cannot be repaired, the reliability can be obtained by finding the probabilities of all operating states.

$$R(t) = P_0(t) \tag{3.28}$$

MTTF is obtained as follows:

$$MTTF = \lim_{s \to 0} R(s) = \frac{1}{\lambda_{Os} + \lambda_{Ou} + \lambda_{Hs} + \lambda_{Hu}} \tag{3.29}$$

To analyse the model reliability parameters, specific values of failure rates are assumed. If the values of model parameters were set as listed below, then state probability equations (3.25) – (3.27) were used to develop the plots in Figure 3-3 and reliability equation 3.28 was used to develop the plots in Figure 3-4. Detailed plots are presented in Appendix C.1.

$$\lambda_{Os} = 0.0008 \left(\frac{failure}{hour} \right) \quad \lambda_{Ou} = 0.00045 \left(\frac{failure}{hour} \right) \quad \lambda_{Hs} = 0.003 \left(\frac{failure}{hour} \right) \quad \lambda_{Hu} = 0.002 \left(\frac{failure}{hour} \right)$$

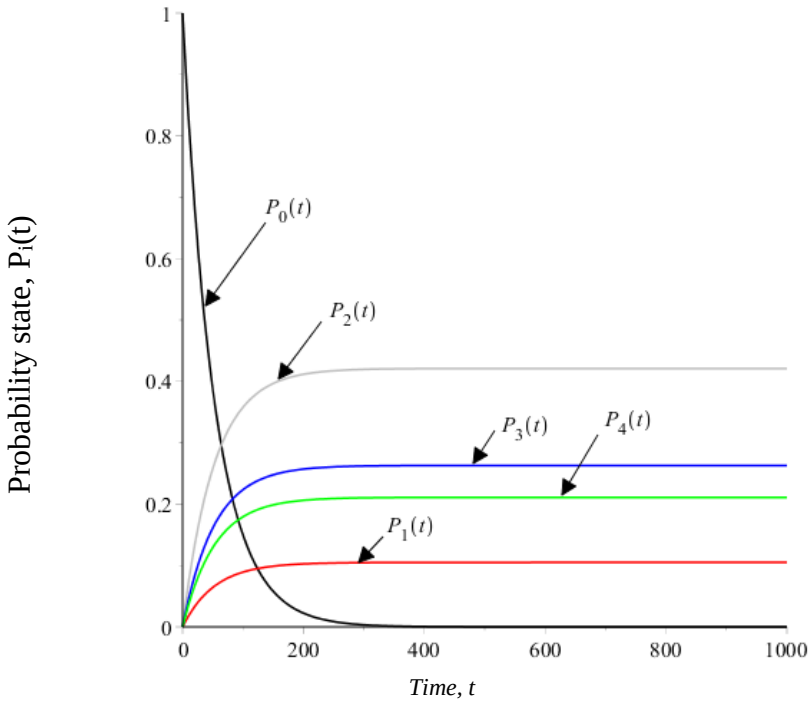

Figure 3-3 State probabilities of one-unit system with four failure modes without repair

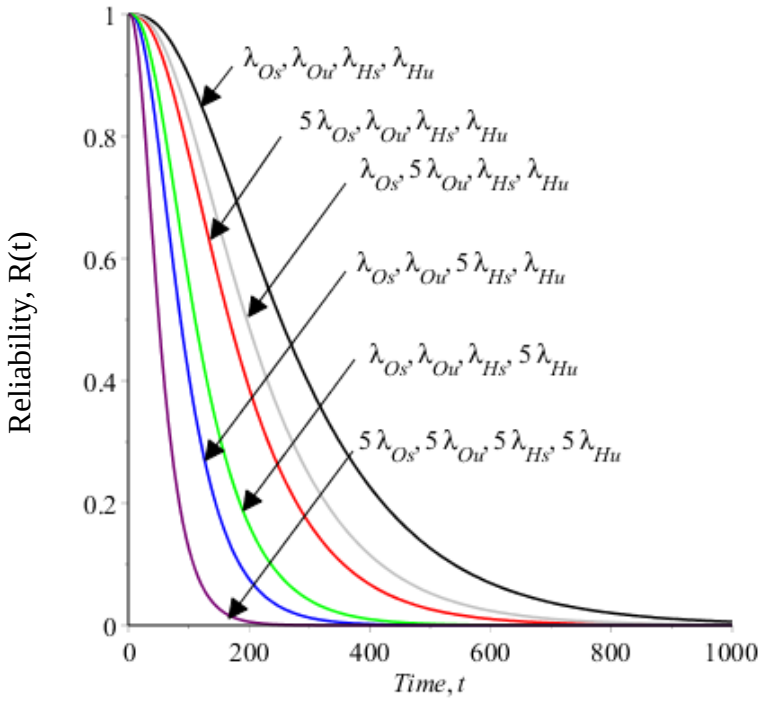

Figure 3-4 Reliability plots of one-unit system with four failure modes without repair at different values of failure rates

3.2.3 **Special Case: Two-Units System without Repair**

The transition state diagram in Figure 3-5 shows a two identical units model of mining system in parallel configuration in which each has four failure modes. By using the Markov method, the associated equations describes the model are obtained as follows:

$$\frac{dP_0(t)}{dt} + P_0(t)\left(2\lambda_{Os} + 2\lambda_{Ou} + 2\lambda_{Hs} + 2\lambda_{Hu}\right) = 0 \tag{3.30}$$

$$\frac{dP_1(t)}{dt} + P_1(t)\left(\lambda_{Os} + \lambda_{Ou} + \lambda_{Hs} + \lambda_{Hu}\right) = 2\lambda_{Os} P_0(t) \tag{3.31}$$

$$\frac{dP_2(t)}{dt} + P_2(t)\left(\lambda_{Os} + \lambda_{Ou} + \lambda_{Hs} + \lambda_{Hu}\right) = 2\lambda_{Ou} P_0(t) \tag{3.32}$$

$$\frac{dP_3(t)}{dt} + P_3(t)\left(\lambda_{Os} + \lambda_{Ou} + \lambda_{Hs} + \lambda_{Hu}\right) = 2\lambda_{Hs} P_0(t) \tag{3.33}$$

$$\frac{dP_4(t)}{dt} + P_4(t)\left(\lambda_{Os} + \lambda_{Ou} + \lambda_{Hs} + \lambda_{Hu}\right) = 2\lambda_{Hu} P_0(t) \tag{3.34}$$

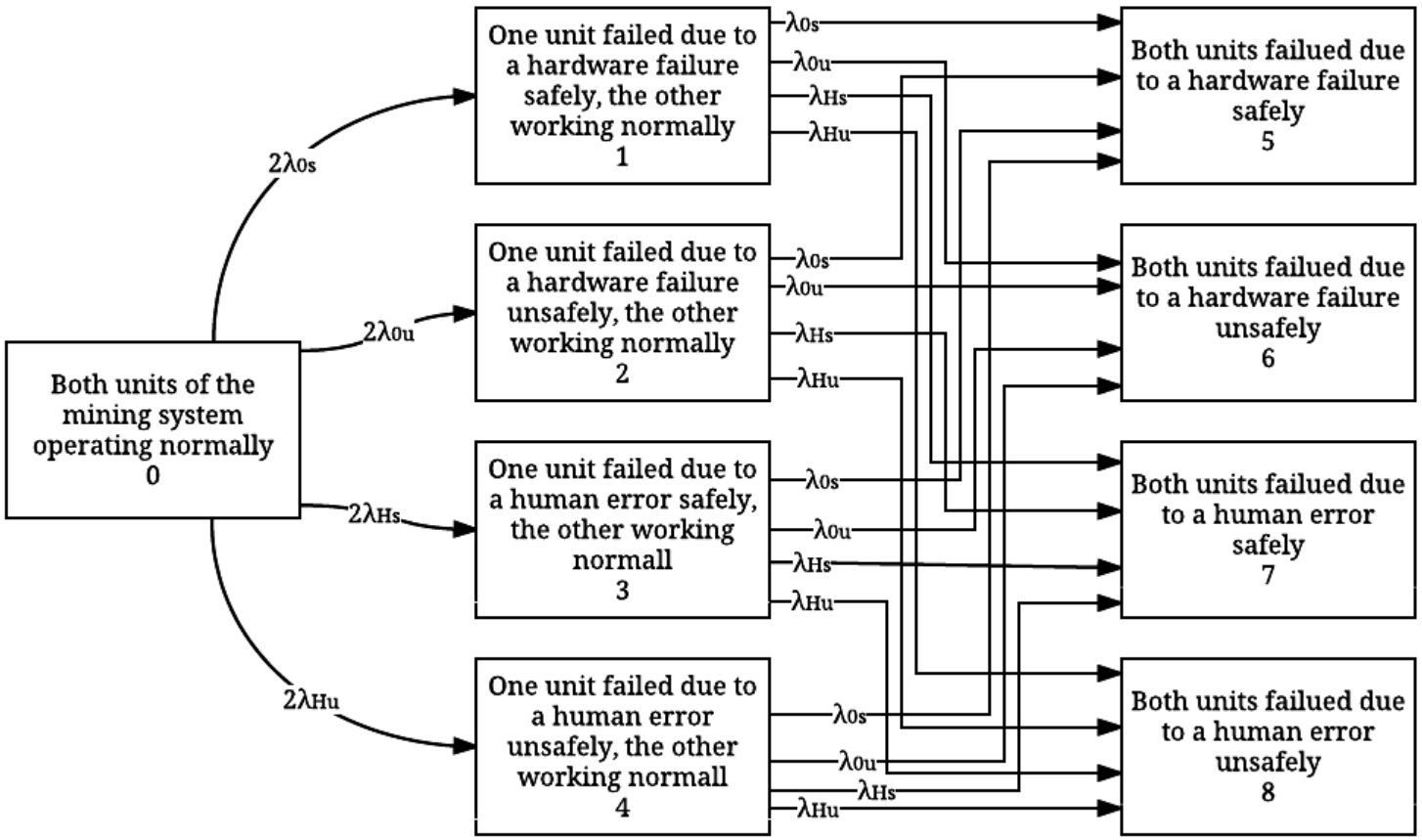

Figure 3-5 State space diagram of two-units with four failure modes without repair

$$\frac{dP_5(t)}{dt} = \lambda_{Os}\left(P_1(t) + P_2(t) + P_3(t) + P_4(t)\right) \tag{3.35}$$

$$\frac{dP_6(t)}{dt} = \lambda_{Ou}\left(P_1(s) + P_2(s) + P_3(s) + P_4(s)\right) \tag{3.36}$$

$$\frac{dP_7(t)}{dt} = \lambda_{Hs}\left(P_1(s) + P_2(s) + P_3(s) + P_4(s)\right) \tag{3.37}$$

$$\frac{dP_8(t)}{dt} = \lambda_{Hu}\left(P_1(s) + P_2(s) + P_3(s) + P_4(s)\right) \tag{3.38}$$

At time t= 0, $P_0(0)$= 1 and all other initial state probabilities are equal to zero. By taking the Laplace transforms of equations (3.30) – (3.38), the following equations are obtained:

$$P_0(s) = \frac{1}{s + 2\lambda_{Os} + 2\lambda_{Ou} + 2\lambda_{Hs} + 2\lambda_{Hu}} \tag{3.39}$$

$$P_1(s) = \frac{2\lambda_{Os}P_0(s)}{s + \lambda_{Os} + \lambda_{Ou} + \lambda_{Hs} + \lambda_{Hu}} \tag{3.40}$$

$$P_2(s) = \frac{2\lambda_{Ou}P_0(s)}{s + \lambda_{Os} + \lambda_{Ou} + \lambda_{Hs} + \lambda_{Hu}} \tag{3.41}$$

$$P_3(s) = \frac{2\lambda_{Hs}P_0(s)}{s + \lambda_{Os} + \lambda_{Ou} + \lambda_{Hs} + \lambda_{Hu}} \tag{3.42}$$

$$P_4(s) = \frac{2\lambda_{Hu}P_0(s)}{s + \lambda_{Os} + \lambda_{Ou} + \lambda_{Hs} + \lambda_{Hu}} \tag{3.43}$$

$$P_5(s) = \frac{\lambda_{Os}\left(P_1(s) + P_2(s) + P_3(s) + P_4(s)\right)}{s} \tag{3.44}$$

$$P_6(s) = \frac{\lambda_{Ou}\left(P_1(s) + P_2(s) + P_3(s) + P_4(s)\right)}{s} \tag{3.45}$$

$$P_7(s) = \frac{\lambda_{Hs}\left(P_1(s) + P_2(s) + P_3(s) + P_4(s)\right)}{s} \tag{3.46}$$

$$P_8(s) = \frac{\lambda_{Hu}\left(P_1(s) + P_2(s) + P_3(s) + P_4(s)\right)}{s} \tag{3.47}$$

By using equations (3.39) – (3.47), we get the following equations:

$$P_0(s) = \frac{1}{s + 2\lambda_{Os} + 2\lambda_{Ou} + 2\lambda_{Hs} + 2\lambda_{Hu}} \tag{3.48}$$

$$P_1(s) = \frac{2\lambda_{Os}}{\left(s+\lambda_{Os}+\lambda_{Ou}+\lambda_{Hs}+\lambda_{Hu}\right)\left(s+2\lambda_{Os}+2\lambda_{Ou}+2\lambda_{Hs}+2\lambda_{Hu}\right)} \tag{3.49}$$

$$P_2(s) = \frac{2\lambda_{Ou}}{\left(s+\lambda_{Os}+\lambda_{Ou}+\lambda_{Hs}+\lambda_{Hu}\right)\left(s+2\lambda_{Os}+2\lambda_{Ou}+2\lambda_{Hs}+2\lambda_{Hu}\right)} \tag{3.50}$$

$$P_3(s) = \frac{2\lambda_{Hs}}{\left(s+\lambda_{Os}+\lambda_{Ou}+\lambda_{Hs}+\lambda_{Hu}\right)\left(s+2\lambda_{Os}+2\lambda_{Ou}+2\lambda_{Hs}+2\lambda_{Hu}\right)} \tag{3.51}$$

$$P_4(s) = \frac{2\lambda_{Hu}}{\left(s+\lambda_{Os}+\lambda_{Ou}+\lambda_{Hs}+\lambda_{Hu}\right)\left(s+2\lambda_{Os}+2\lambda_{Ou}+2\lambda_{Hs}+2\lambda_{Hu}\right)} \tag{3.52}$$

$$P_5(s) = \frac{\lambda_{Os}\left(2\lambda_{Os}+2\lambda_{Ou}+2\lambda_{Hs}+2\lambda_{Hu}\right)}{s\left(s+\lambda_{Os}+\lambda_{Ou}+\lambda_{Hs}+\lambda_{Hu}\right)\left(s+2\lambda_{Os}+2\lambda_{Ou}+2\lambda_{Hs}+2\lambda_{Hu}\right)} \tag{3.53}$$

$$P_6(s) = \frac{\lambda_{Ou}\left(2\lambda_{Os}+2\lambda_{Ou}+2\lambda_{Hs}+2\lambda_{Hu}\right)}{s\left(s+\lambda_{Os}+\lambda_{Ou}+\lambda_{Hs}+\lambda_{Hu}\right)\left(s+2\lambda_{Os}+2\lambda_{Ou}+2\lambda_{Hs}+2\lambda_{Hu}\right)} \tag{3.54}$$

$$P_7(s) = \frac{\lambda_{Hs}\left(2\lambda_{Os}+2\lambda_{Ou}+2\lambda_{Hs}+2\lambda_{Hu}\right)}{s\left(s+\lambda_{Os}+\lambda_{Ou}+\lambda_{Hs}+\lambda_{Hu}\right)\left(s+2\lambda_{Os}+2\lambda_{Ou}+2\lambda_{Hs}+2\lambda_{Hu}\right)} \tag{3.55}$$

$$P_8(s) = \frac{\lambda_{Hu}\left(2\lambda_{Os}+2\lambda_{Ou}+2\lambda_{Hs}+2\lambda_{Hu}\right)}{s\left(s+\lambda_{Os}+\lambda_{Ou}+\lambda_{Hs}+\lambda_{Hu}\right)\left(s+2\lambda_{Os}+2\lambda_{Ou}+2\lambda_{Hs}+2\lambda_{Hu}\right)} \tag{3.56}$$

By taking the inverse Laplace transform of equations (3.48) – (3.56), the following equations are obtained:

$$P_0(t) = \mathrm{e}^{-2\left(\lambda_{Os}+\lambda_{Ou}+\lambda_{Hs}+\lambda_{Hu}\right)t} \tag{3.57}$$

$$P_1(t) = \frac{2\lambda_{Os}\left(\mathrm{e}^{-\left(\lambda_{Os}+\lambda_{Ou}+\lambda_{Hs}+\lambda_{Hu}\right)t} - \mathrm{e}^{-2\left(\lambda_{Os}+\lambda_{Ou}+\lambda_{Hs}+\lambda_{Hu}\right)t}\right)}{\lambda_{Os}+\lambda_{Ou}+\lambda_{Hs}+\lambda_{Hu}} \tag{3.58}$$

$$P_2(t) = \frac{2\lambda_{Ou}\left(\mathrm{e}^{-\left(\lambda_{Os}+\lambda_{Ou}+\lambda_{Hs}+\lambda_{Hu}\right)t} - \mathrm{e}^{-2\left(\lambda_{Os}+\lambda_{Ou}+\lambda_{Hs}+\lambda_{Hu}\right)t}\right)}{\lambda_{Os}+\lambda_{Ou}+\lambda_{Hs}+\lambda_{Hu}} \tag{3.59}$$

$$P_3(t) = \frac{2\lambda_{Hs}\left(\mathrm{e}^{-\left(\lambda_{Os}+\lambda_{Ou}+\lambda_{Hs}+\lambda_{Hu}\right)t} - \mathrm{e}^{-2\left(\lambda_{Os}+\lambda_{Ou}+\lambda_{Hs}+\lambda_{Hu}\right)t}\right)}{\lambda_{Os}+\lambda_{Ou}+\lambda_{Hs}+\lambda_{Hu}} \tag{3.60}$$

$$P_4(t) = \frac{2\lambda_{Hu}\left(\mathrm{e}^{-\left(\lambda_{Os}+\lambda_{Ou}+\lambda_{Hs}+\lambda_{Hu}\right)t} - \mathrm{e}^{-2\left(\lambda_{Os}+\lambda_{Ou}+\lambda_{Hs}+\lambda_{Hu}\right)t}\right)}{\lambda_{Os}+\lambda_{Ou}+\lambda_{Hs}+\lambda_{Hu}} \tag{3.61}$$

$$P_5(t) = \frac{\lambda_{Os}\left(1 - 2\,e^{-\left(\lambda_{Os}+\lambda_{Ou}+\lambda_{Hs}+\lambda_{Hu}\right)t} + e^{\left(\lambda_{Os}+\lambda_{Ou}+\lambda_{Hs}+\lambda_{Hu}\right)t}\right)}{\left(\lambda_{Os}+\lambda_{Ou}+\lambda_{Hs}+\lambda_{Hu}\right)^2} \tag{3.62}$$

$$P_6(t) = \frac{\lambda_{Ou}\left(1 - 2\,e^{-\left(\lambda_{Os}+\lambda_{Ou}+\lambda_{Hs}+\lambda_{Hu}\right)t} + e^{\left(\lambda_{Os}+\lambda_{Ou}+\lambda_{Hs}+\lambda_{Hu}\right)t}\right)}{\left(\lambda_{Os}+\lambda_{Ou}+\lambda_{Hs}+\lambda_{Hu}\right)^2} \tag{3.63}$$

$$P_7(t) = \frac{\lambda_{Hs}\left(1 - 2\,e^{-\left(\lambda_{Os}+\lambda_{Ou}+\lambda_{Hs}+\lambda_{Hu}\right)t} + e^{\left(\lambda_{Os}+\lambda_{Ou}+\lambda_{Hs}+\lambda_{Hu}\right)t}\right)}{\left(\lambda_{Os}+\lambda_{Ou}+\lambda_{Hs}+\lambda_{Hu}\right)^2} \tag{3.64}$$

$$P_8(t) = \frac{\lambda_{Hu}\left(1 - 2\,e^{-\left(\lambda_{Os}+\lambda_{Ou}+\lambda_{Hs}+\lambda_{Hu}\right)t} + e^{\left(\lambda_{Os}+\lambda_{Ou}+\lambda_{Hs}+\lambda_{Hu}\right)t}\right)}{\left(\lambda_{Os}+\lambda_{Ou}+\lambda_{Hs}+\lambda_{Hu}\right)^2} \tag{3.65}$$

System Reliability and MTTF

When system failure cannot be repaired, the reliability can be obtained by finding the total probabilities of all operating states.

$$R(t) = P_0(t) + P_1(t) + P_2(t) + P_3(t) + P_4(t) \tag{3.66}$$

MTTF is obtained as follows:

$$MTTF = \lim_{s \to 0} R(t) = \frac{1}{\lambda_{Os}+\lambda_{Ou}+\lambda_{Hs}+\lambda_{Hu}} \tag{3.67}$$

To analyse the model reliability parameters, specific values of failure rates are assumed. If the values of system parameters were set as listed below, then the state probabilities equations (3.57) – (3.65) were used to develop the plots in Figure 3-6 and reliability equation (3.66) was used to develop the plots in Figure 3-7. Detailed plots are presented in Appendix C.2.

$$\lambda_{Os} = 0.0008\left(\frac{failure}{hour}\right) \quad \lambda_{Ou} = 0.00045\left(\frac{failure}{hour}\right)$$
$$\lambda_{Hs} = 0.003\left(\frac{failure}{hour}\right) \quad \lambda_{Hu} = 0.002\left(\frac{failure}{hour}\right)$$

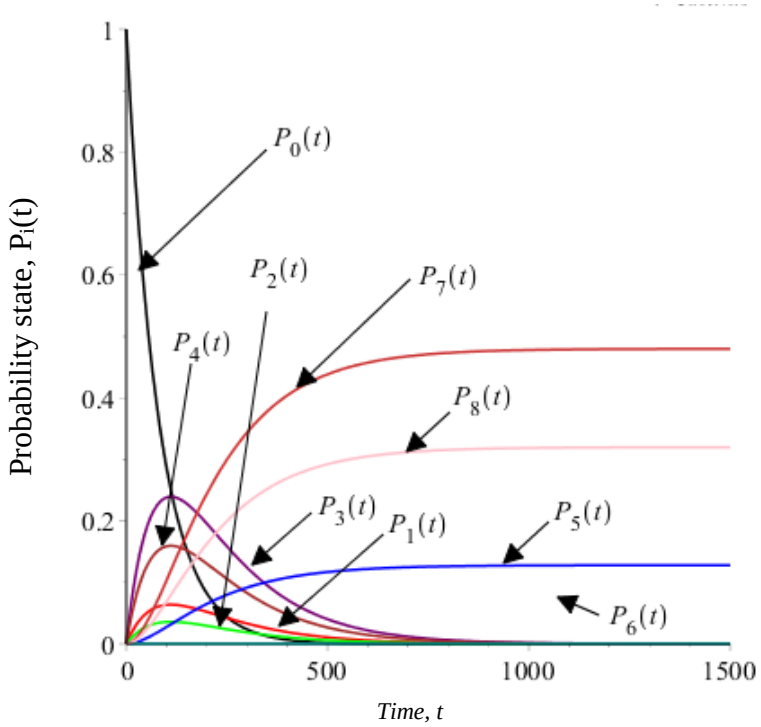

Figure 3-6 State probabilities of two-units system with four failure modes without repair

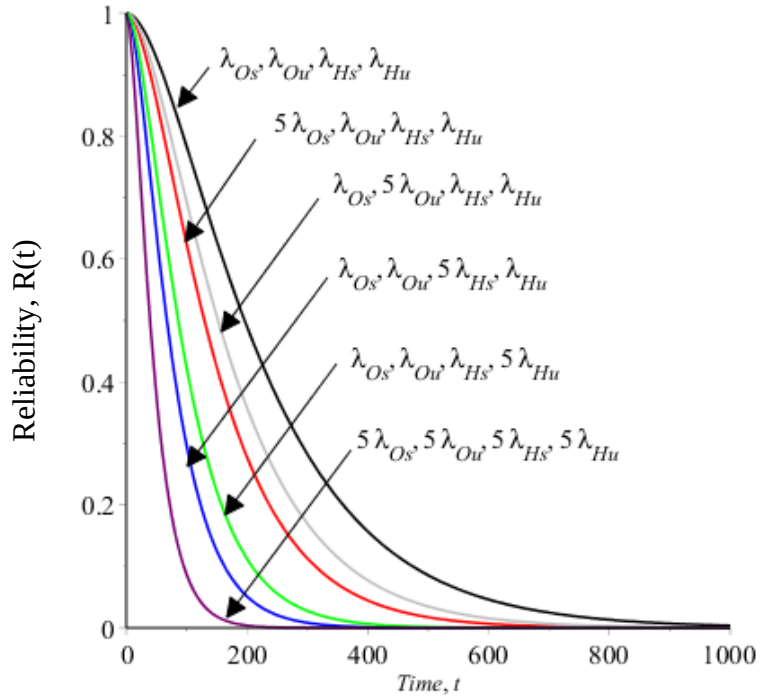

Figure 3-7 Reliability plots of two-units system with four failure modes without repair at different values of failure rates

3.2.4 **Special Case Three-Units without Repair**

The transition state diagram in Figure 3-8 shows a three identical units model of mining system in parallel configuration in which each has four failure modes. At the initial state, three parallel units are in normal operation, so the failure rates are $3\lambda_{0s}$, $3\lambda_{0u}$, $3\lambda_{Hs}$, and $3\lambda_{Hu}$. After first unit failure, the failure rate is $2\lambda_{0s}$, $2\lambda_{0u}$, $2\lambda_{Hs}$, and $2\lambda_{Hu}$, and so forth. By using the Markov method to describe the state space in Figure 3-8, the following equations are obtained:

$$\frac{dP_0(t)}{dt} + 3\,P_0(t)\left(\lambda_{Os} + \lambda_{Ou} + \lambda_{Hs} + \lambda_{Hu}\right) = 0 \tag{3.68}$$

$$\frac{dP_1(t)}{dt} + 2\,P_1(t)\left(\lambda_{Os} + \lambda_{Ou} + \lambda_{Hs} + \lambda_{Hu}\right) = 3\lambda_{Os}P_0(t) \tag{3.69}$$

$$\frac{dP_2(t)}{dt} + 2\,P_2(t)\left(\lambda_{Os} + \lambda_{Ou} + \lambda_{Hs} + \lambda_{Hu}\right) = 3\lambda_{Ou}P_0(t) \tag{3.70}$$

$$\frac{dP_3(t)}{dt} + 2\,P_3(t)\left(\lambda_{Os} + \lambda_{Ou} + \lambda_{Hs} + \lambda_{Hu}\right) = 3\lambda_{Hs}P_0(t) \tag{3.71}$$

$$\frac{dP_4(t)}{dt} + 2\,P_3(t)\left(\lambda_{Os} + \lambda_{Ou} + \lambda_{Hs} + \lambda_{Hu}\right) = 3\lambda_{Hu}P_0(t) \tag{3.72}$$

$$\frac{dP_5(t)}{dt} + P_5(t)\left(\lambda_{Os} + \lambda_{Ou} + \lambda_{Hs} + \lambda_{Hu}\right) = 2\,\lambda_{Os}\cdot\sum_{i=1}^{4}P_i(t) \tag{3.73}$$

$$\frac{dP_6(t)}{dt} + P_6(t)\left(\lambda_{Os} + \lambda_{Ou} + \lambda_{Hs} + \lambda_{Hu}\right) = 2\lambda_{Ou}\cdot\sum_{i=1}^{4}P_i(t) \tag{3.74}$$

$$\frac{dP_7(t)}{dt} + P_7(t)\left(\lambda_{Os} + \lambda_{Ou} + \lambda_{Hs} + \lambda_{Hu}\right) = 2\,\lambda_{Hs}\cdot\sum_{i=1}^{4}P_i(t) \tag{3.75}$$

$$\frac{dP_8(t)}{dt} + P_8(t)\left(\lambda_{Os} + \lambda_{Ou} + \lambda_{Hs} + \lambda_{Hu}\right) = 2\lambda_{Hu}\cdot\sum_{i=1}^{4}P_i(t) \tag{3.76}$$

$$\frac{dP_9(t)}{dt} = \lambda_{Os}\cdot\sum_{i=5}^{8}P_i(t) \tag{3.77}$$

$$\frac{dP_{10}(t)}{dt} = \lambda_{Ou}\cdot\sum_{i=5}^{8}P_i(t) \tag{3.78}$$

$$\frac{dP_{11}(t)}{dt} = \lambda_{Hs}\cdot\sum_{i=5}^{8}P_i(t) \tag{3.79}$$

$$\frac{dP_{12}(t)}{dt} = \lambda_{Hu}\cdot\sum_{i=5}^{8}P_i(t) \tag{3.80}$$

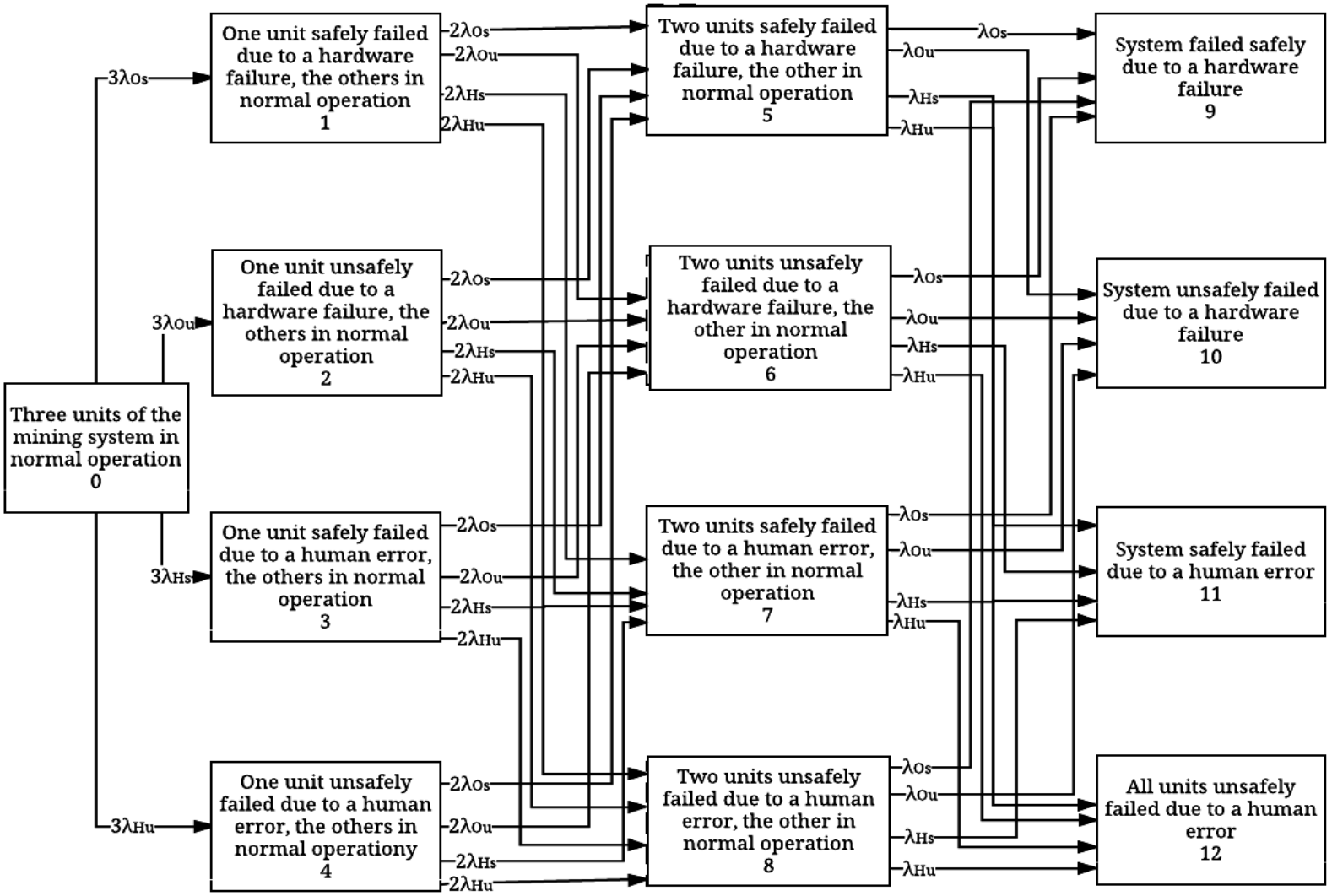

Figure 3-8 State space diagram of three-units with four failure modes without repair

At time t=0, $P_0(0)=1$ and all other initial state probabilities are equal to zero. By taking the Laplace transforms of equations (3.68) – (3.80), the following equations are obtained:

$$P_0(s) = \frac{1}{s + 3\left(\lambda_{Os} + \lambda_{Ou} + \lambda_{Hs} + \lambda_{Hu}\right)} \tag{3.81}$$

$$P_1(s) = \frac{3\lambda_{Os} P_0(s)}{s + 2\left(\lambda_{Os} + \lambda_{Ou} + \lambda_{Hs} + \lambda_{Hu}\right)} \tag{3.82}$$

$$P_2(s) = \frac{3\lambda_{Ou} P_0(s)}{s + 2\left(\lambda_{Os} + \lambda_{Ou} + \lambda_{Hs} + \lambda_{Hu}\right)} \tag{3.83}$$

$$P_3(s) = \frac{3\lambda_{Hs} P_0(s)}{s + 2\left(\lambda_{Os} + \lambda_{Ou} + \lambda_{Hs} + \lambda_{Hu}\right)} \tag{3.84}$$

$$P_4(s) = \frac{3\lambda_{Hu} P_0(s)}{s + 2\left(\lambda_{Os} + \lambda_{Ou} + \lambda_{Hs} + \lambda_{Hu}\right)} \tag{3.85}$$

$$P_5(s) = \frac{2\lambda_{Os}\left(P_1(s) + P_2(s) + P_3(s) + P_4(s)\right)}{s + \left(\lambda_{Os} + \lambda_{Ou} + \lambda_{Hs} + \lambda_{Hu}\right)} \tag{3.86}$$

$$P_6(s) = \frac{2\lambda_{Ou}\left(P_1(s) + P_2(s) + P_3(s) + P_4(s)\right)}{s + \left(\lambda_{Os} + \lambda_{Ou} + \lambda_{Hs} + \lambda_{Hu}\right)} \tag{3.87}$$

$$P_7(s) = \frac{2\lambda_{Hs}\left(P_1(s) + P_2(s) + P_3(s) + P_4(s)\right)}{s + \left(\lambda_{Os} + \lambda_{Ou} + \lambda_{Hs} + \lambda_{Hu}\right)} \tag{3.88}$$

$$P_8(s) = \frac{2\lambda_{Hu}\left(P_1(s) + P_2(s) + P_3(s) + P_4(s)\right)}{s + \left(\lambda_{Os} + \lambda_{Ou} + \lambda_{Hs} + \lambda_{Hu}\right)} \tag{3.89}$$

$$P_9(s) = \frac{\lambda_{Os}\left(P_5(s) + P_6(s) + P_7(s) + P_8(s)\right)}{s} \tag{3.90}$$

$$P_{10}(s) = \frac{\lambda_{Ou}\left(P_5(s) + P_6(s) + P_7(s) + P_8(s)\right)}{s} \tag{3.91}$$

$$P_{11}(s) = \frac{\lambda_{Hs}\left(P_5(s) + P_6(s) + P_7(s) + P_8(s)\right)}{s} \tag{3.92}$$

$$P_{12}(s) = \frac{\lambda_{Hu}\left(P_5(s) + P_6(s) + P_7(s) + P_8(s)\right)}{s} \tag{3.93}$$

By using equations (3.81) – (3.93), we get the following equations:

$$P_0(s) = \frac{1}{s+3F} \tag{3.94}$$

$$P_1(s) = \frac{3\lambda_{Os}}{(s+2F)\,(s+3F)} \tag{3.95}$$

$$P_2(s) = \frac{3\lambda_{Ou}}{(s+2\mathrm{F})\,(s+3\mathrm{F})} \tag{3.96}$$

$$P_3(s) = \frac{3\lambda_{Hs}}{(s+2\mathrm{F})\,(s+3\mathrm{F})} \tag{3.97}$$

$$P_4(s) = \frac{3\lambda_{Hu}}{(s+2\mathrm{F})\,(s+3\mathrm{F})} \tag{3.98}$$

$$P_5(s) = \frac{6\lambda_{Os}\mathrm{F}}{(s+\mathrm{F})\,(s+2\mathrm{F})\,(s+3\mathrm{F})} \tag{3.99}$$

$$P_6(s) = \frac{6\lambda_{Ou}\mathrm{F}}{(s+\mathrm{F})\,(s+2\mathrm{F})\,(s+3\mathrm{F})} \tag{3.100}$$

$$P_7(s) = \frac{6\lambda_{Hs}\mathrm{F}}{(s+\mathrm{F})(s+2\mathrm{F})\,(s+3\mathrm{F})} \tag{3.101}$$

$$P_8(s) = \frac{6\lambda_{Hu}\mathrm{F}}{(s+\mathrm{F})(s+2\mathrm{F})\,(s+3\mathrm{F})} \tag{3.102}$$

$$P_9(s) = \frac{6\lambda_{Os}\mathrm{F}^2}{s\,(s+\mathrm{F})(s+2\mathrm{F})\,(s+3\mathrm{F})} \tag{3.103}$$

$$P_{10}(s) = \frac{6\lambda_{Ou}\mathrm{F}^2}{s\,(s+\mathrm{F})(s+2\mathrm{F})\,(s+3\mathrm{F})} \tag{3.104}$$

$$P_{11}(s) = \frac{6\lambda_{Hs}\mathrm{F}^2}{s\,(s+\mathrm{F})(s+2\mathrm{F})\,(s+3\mathrm{F})} \tag{3.105}$$

$$P_{12}(s) = \frac{6\lambda_{Hu}\mathrm{F}^2}{s\,(s+\mathrm{F})(s+2\mathrm{F})\,(s+3\mathrm{F})} \tag{3.106}$$

Where;

$$F = \lambda_{Os} + \lambda_{Ou} + \lambda_{Hs} + \lambda_{Hu}$$

System Reliability and MTTF

The reliability can be obtained by finding the total probabilities of operating states as follows:

$$R(t) = \sum_{i=1}^{8} P_i(t) \tag{3.107}$$

MTTF is obtained as follows:

$$MTTF = \lim_{s \to 0} R(s) = \lim_{s \to 0} \left(\sum_{i=1}^{8} P_i(s) \right) = \frac{11}{6\left(\lambda_{Os} + \lambda_{Ou} + \lambda_{Hs} + \lambda_{Hu}\right)} \tag{3.108}$$

To investigate the model reliability parameters, their plot should be developed. Thus, specific values of failure rates were assumed. Accordingly, the inverse Laplace transforms of equations (3.94) – (3.106) were used to develop state probability plots in Figure 3-9 and reliability equation (3.107) was used to develop the plots in Figure 3-10. Detailed plots are presented in Appendix C.3.

$$\lambda_{Os} = 0.0008 \left(\frac{failure}{hour} \right) \quad \lambda_{Ou} = 0.00045 \left(\frac{failure}{hour} \right)$$
$$\lambda_{Hs} = 0.003 \left(\frac{failure}{hour} \right) \quad \lambda_{Hu} = 0.002 \left(\frac{failure}{hour} \right)$$

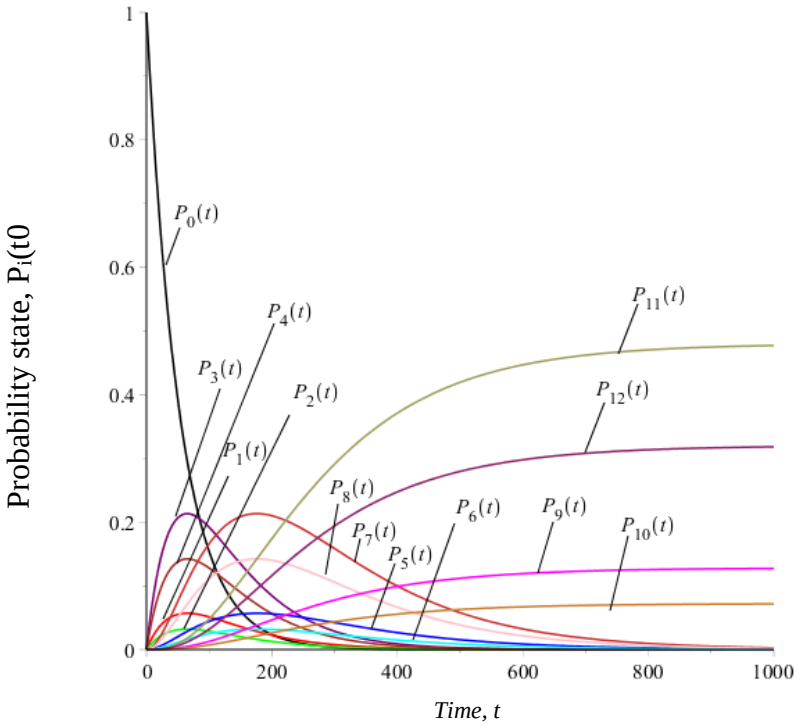

Figure 3-9 State probabilities of three-units system with four failure modes without repair

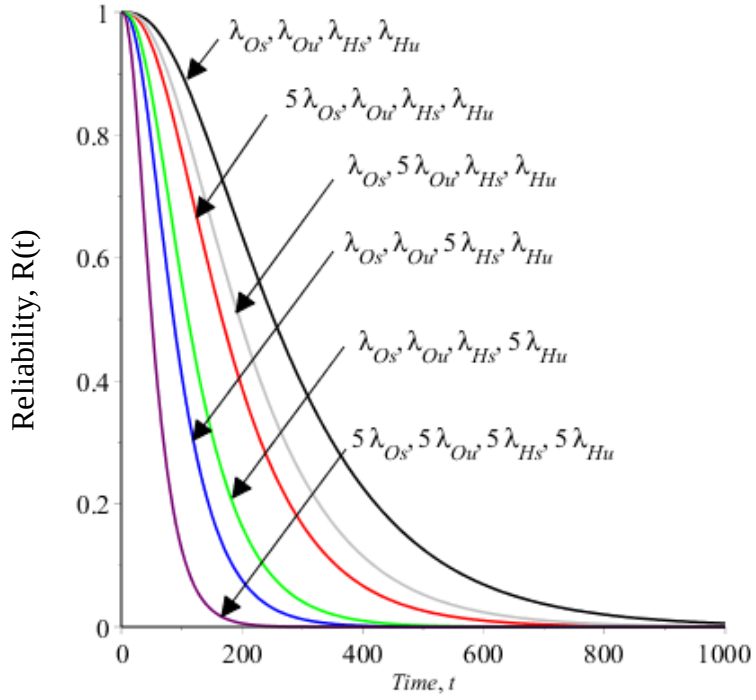

Figure 3-10 Reliability plots of three-units system with four failure modes without repair at different values of failure rates

3.3 Hardware Failure and Human-Error with Safe or Unsafe Modes with Type-I Repair

3.3.1 General n-Units System Type-I Repair

In this model, Figure 3-11, units are unrepairable but system repair is possible to restore the system to its initial state according to Type-I repair policy. Also, each unit might fail safely or unsafely due to hardware failure or human-error. The symbolic representation of general model is that (n) is the number of units in system, (j) is the failure mode that can be 1 to 4, where j=1 refers to safe hardware failure, j=2 refers to unsafe hardware failure, j=3 refers to safe human-error and j=4 refers to unsafe human-error. In same manner, λ_j refers to units failure rates where λ_1 refers to safe hardware failure rate, λ_2 refers to unsafe hardware failure rate, λ_3 refers to safe human-error rate and λ_4 refers to unsafe human-error rate. Also, μ_1 to μ_4 is repair rate based on the system failure mode i.e. μ_1 refers to repair rate when system had safely hardware failure, μ_2 refers to repair rate when system had unsafely hardware failure, μ_3 refers to repair rate when system had safely human-

error, μ_4 refers to repair rate when system had unsafely human-error. In general model, (i) is the number of failed unit at time (t).

At the initial state, all n parallel units are in normal operation, so the failure rates are $n\lambda j$, to represent the failure rate for n number of units in normal operation. At time (t), the failure rate is $(n\text{-}i)\lambda_j$ where (i) is the number of failed unit at that time. The general differential equations describing the system according to the Markov method are obtained as follows:

$$\frac{dP_0(t)}{dt} + n\, P_0(t) \cdot \sum_{v=1}^{4} \left(\lambda_v\right) = \sum_{j=1}^{4} P_{j-n}(t) \cdot \mu_j \tag{3.109}$$

$$\frac{dP_{1-j}(t)}{dt} + (n-i)\; P_{i-j}(t) \cdot \sum_{v=1}^{4} \left(\lambda_v\right) = (n-i+1)\,\lambda_j P_0(t) \tag{3.110}$$

$$\frac{dP_{i-j}(t)}{dt} + (n-i)\; P_{i-j}(t) \cdot \sum_{v=1}^{4} \left(\lambda_v\right) = (n-i+1)\,\lambda_j \cdot \sum_{v=1}^{4} P_{(i-1)-v}(t) \tag{3.111}$$

$$\frac{dP_{n-j}(t)}{dt} + P_{n-j}(t) \cdot \mu_j = \lambda_j \cdot \sum_{v=1}^{4} P_{(n-1)-v}(t) \tag{3.112}$$

At time t= 0, $P_0(0)= 1$ and all other initial state probabilities are equal to zero. By taking the Laplace transforms of equations (3.109) – (3.112), we obtain the following equations:

$$P_0(s) = \frac{\left(\prod_{v=2}^{n} (s + (v+1)\cdot F)\right)\left(\prod_{i=1}^{4} \mu_i\right)}{\left(\prod_{i=1}^{n} (s + iF)\right) \cdot \prod_{i=1}^{4} \left(s + \mu_i\right) - n!\, F^{n-1} \cdot \left(\sum_{q=1}^{4} \left(\frac{\mu_q \lambda_q \left(\prod_{k=1}^{4} \left(s + \mu_k\right)\right)}{s + \mu_q}\right)\right)} \tag{3.113}$$

$$P_{i-j}(s) = \frac{P_0(s)\,\lambda_j F^{(i-1)} \left(\prod_{v=1}^{i} (n - v + 1)\right)}{\left(\prod_{q=n-i}^{n-1} (s + qF)\right)} \tag{3.114}$$

$$P_{n-j}(s) = \frac{P_0(s)\,\lambda_j F^{(n-1)} \left(\prod_{v=1}^{n} (n - v + 1)\right)}{\left(s + \lambda_j\right) \cdot \left(\prod_{q=2}^{n} (s + (q-1)\,F)\right)} \tag{3.115}$$

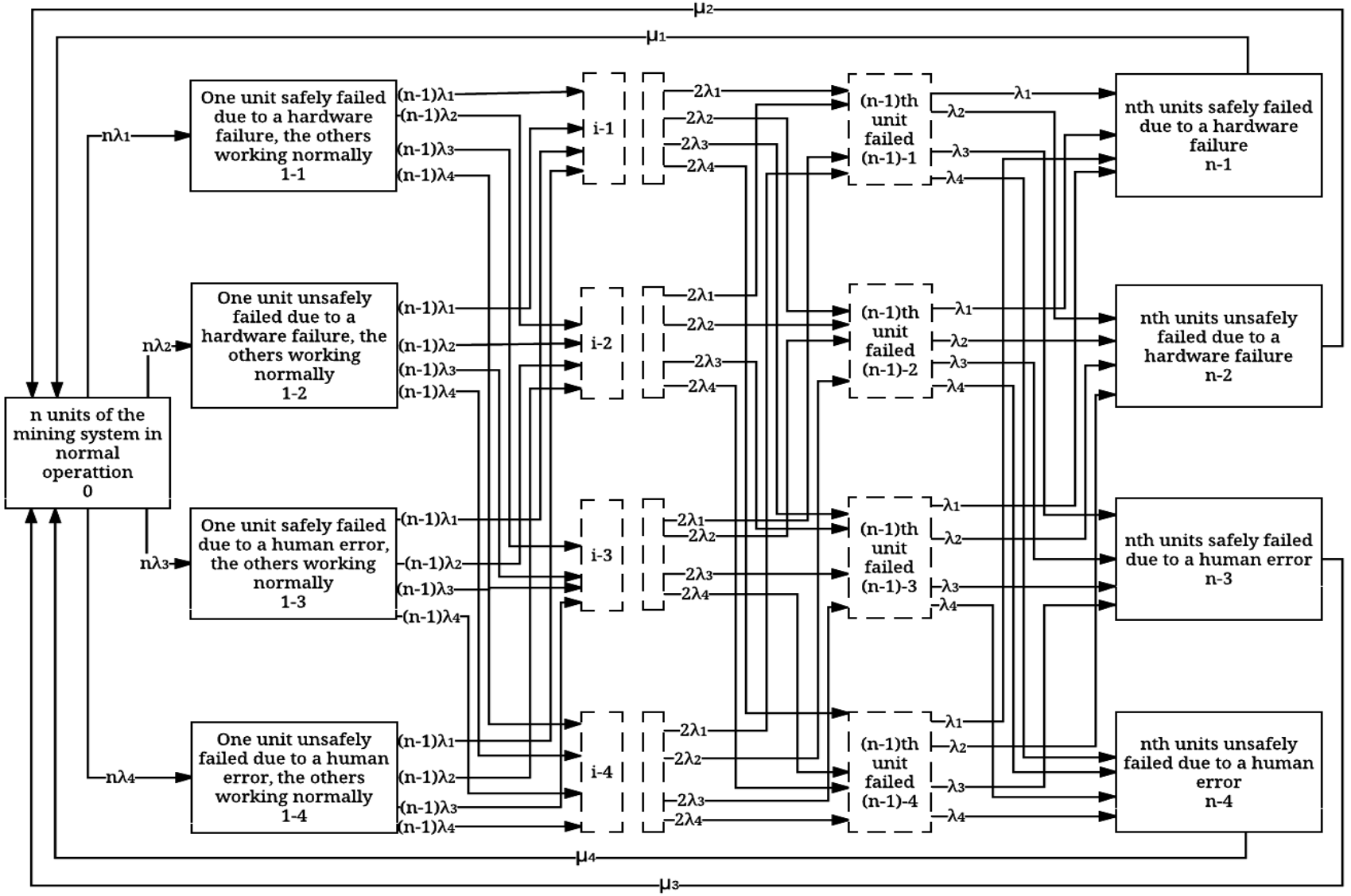

Figure 3-11 State space diagram of n-units with four failure modes and Type-I repair.

Where

$$F = \sum_{q=1}^{4} \lambda_q$$

The equations of time-dependent state probabilities can be obtained by taking the inverse Laplace transforms. However, the resulted equations were complicated and the common pattern was undistinguishable. Instead, the steady state probabilities were obtained and the general equations were developed as follows.

$$P_0 = \frac{\left(\prod_{i=2}^{n}((i-1))\right)\prod_{i=1}^{4}\mu_i}{\mathrm{n}\cdot\left(\sum_{i=1}^{n}\frac{(n-1)}{i}\right)\cdot\left(\prod_{i=1}^{4}\mu_i\right)+\mathrm{n}!\cdot\left(\sum_{q=1}^{4}\left(\frac{\lambda_q\left(\prod_{k=1}^{4}(\mu_k)\right)}{\mu_q}\right)\right)} \tag{3.116}$$

$$P_{i-j} = \frac{P_0\lambda_j\left(\prod_{v=1}^{i}(n-v+1)\right)}{\sum_{q=1}^{4}(\lambda_q)} \tag{3.117}$$

$$P_{n-j} = \frac{P_0\lambda_j\left(\prod_{v=1}^{i}(n-v+1)\right)}{\mu_j} \tag{3.118}$$

The steady state availability is obtained by finding the total probabilities of operating states.

$$AV_{SS} = \sum_{i=1}^{n-1}\left(\sum_{j=1}^{4}P_{j-i}\right) \tag{3.119}$$

MTTF has the following equation:

$$MTTF = \frac{1}{\sum_{q=1}^{4}\lambda_q}\cdot\sum_{i=0}^{n-1}\left(\frac{1}{n-i}\right) \tag{3.120}$$

3.3.2 **Special Case: One-Unit System with Type-I Repair**

The transition state diagram in Figure 3-12 shows a single unit model of mining system that has four failure modes. If this unit fails, the system fails and can be restored back to initial

state. By using the Markov method, the state space diagram described in Figure 3-12 are obtained as follows:

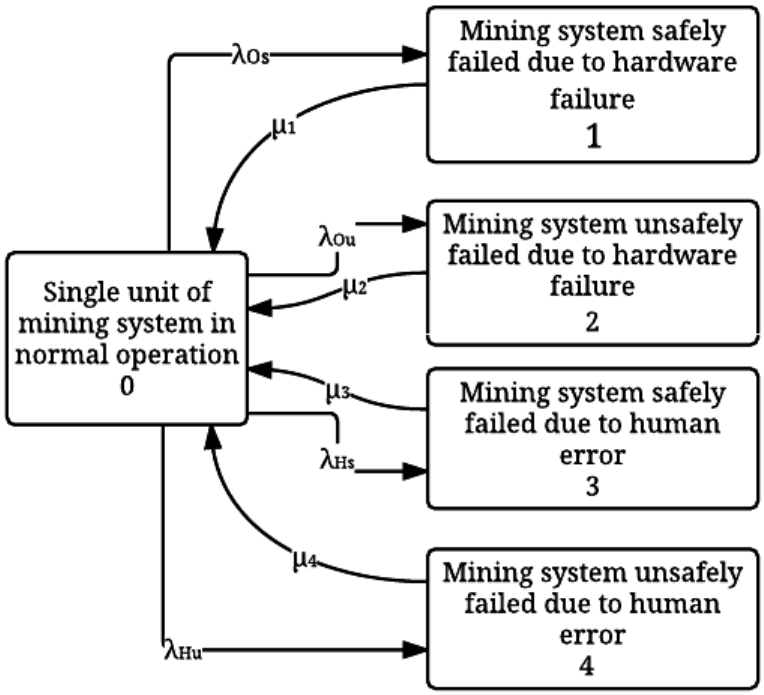

Figure 3-12 State space diagram of one-unit system with four failure modes and Type-I repair

$$\frac{dP_0(t)}{dt} + P_0(t)\left(\lambda_{Os} + \lambda_{Ou} + \lambda_{Hs} + \lambda_{Hu}\right) = P_1(t)\,\mu_1 + P_2(t)\,\mu_2 + P_3(t)\,\mu_3 + P_4(t)\,\mu_4 \quad (3.121)$$

$$\frac{dP_1(t)}{dt} + P_1(t)\,\mu_1 = P_0(t)\,\lambda_{Os} \quad (3.122)$$

$$\frac{dP_2(t)}{dt} + P_2(t)\,\mu_2 = P_0(t)\,\lambda_{Ou} \quad (3.123)$$

$$\frac{dP_3(t)}{dt} + P_3(t)\,\mu_3 = P_0(t)\,\lambda_{Hs} \quad (3.124)$$

$$\frac{dP_4(t)}{dt} + P_4(t)\,\mu_4 = P_0(t)\,\lambda_{Hu} \quad (3.125)$$

At time t= 0, $P_0(0)$= 1 and all other initial state probabilities are equal to zero. By taking the Laplace transforms of equations (3.121) – (3.125) the below set of equations are obtained:

$$P_0(s) = \frac{P_1(s)\,\mu_1 + P_2(s)\,\mu_2 + P_3(s)\,\mu_3 + P_4(s)\,\mu_4 + 1}{s + \lambda_{Os} + \lambda_{Ou} + \lambda_{Hs} + \lambda_{Hu}} \quad (3.126)$$

$$P_1(s) = \frac{P_0(s)\,\lambda_{Os}}{s+\mu_1} \tag{3.127}$$

$$P_2(s) = \frac{P_0(s)\,\lambda_{Ou}}{s+\mu_2} \tag{3.128}$$

$$P_3(s) = \frac{P_0(s)\,\lambda_{Hs}}{s+\mu_3} \tag{3.129}$$

$$P_4(s) = \frac{P_0(s)\,\lambda_{Hu}}{s+\mu_4} \tag{3.130}$$

By solving equations (3.126) – (3.130), we get the following equations:

$$P_0(s) = \frac{1}{(s+F-W)} \tag{3.131}$$

$$P_1(s) = \frac{\lambda_{Os}}{\left(s+\mu_1\right)(s+F-W)} \tag{3.132}$$

$$P_2(s) = \frac{\lambda_{Ou}}{\left(s+\mu_2\right)(s+F-W)} \tag{3.133}$$

$$P_3(s) = \frac{\lambda_{Hs}}{\left(s+\mu_3\right)(s+F-W)} \tag{3.134}$$

$$P_4(s) = \frac{\lambda_{Hu}}{\left(s+\mu_4\right)(s+F-W)} \tag{3.135}$$

Where

$$F = \lambda_{Os} + \lambda_{Ou} + \lambda_{Hs} + \lambda_{Hu}$$

$$W = \left(\frac{\lambda_{Os}\mu_1}{s+\mu_1} + \frac{\lambda_{Ou}\mu_2}{s+\mu_2} + \frac{\lambda_{Hs}\mu_3}{s+\mu_3} + \frac{\lambda_{Hu}\mu_4}{s+\mu_4} \right)$$

By taking the inverse Laplace transform of equations (3.131) – (3.135), we obtain the equations of time dependent state probabilities.

System Reliability and MTTF

To find the reliability and MTTF for this particular model, all μ_1, μ_2, μ_3, and μ_4 should be equal to zero which results into a similar model and equations as Special Case: One-Unit System

without Repair. The reliability equation (3.28) and MTTF equation (3.29) were used to develop plots in Figure 3-4 and Appendix C.1.

Availability and Steady state Probabilities

The availability is the total probabilities of system operating states.

$$AV(t) = P_0(t) \tag{3.136}$$

The system steady state probabilities can be obtained by applying final-value theorem on each state probability at s-domain. The following equations were obtained:

$$P_0 = \frac{\mu_1 \mu_2 \mu_3 \mu_4}{\lambda_1 \mu_2 \mu_3 \mu_4 + \lambda_2 \mu_1 \mu_3 \mu_4 + \lambda_3 \mu_1 \mu_2 \mu_4 + \lambda_4 \mu_1 \mu_2 \mu_3 + \mu_1 \mu_2 \mu_3 \mu_4} \tag{3.137}$$

$$P_1 = \frac{\lambda_1 \mu_2 \mu_3 \mu_4}{\lambda_1 \mu_2 \mu_3 \mu_4 + \lambda_2 \mu_1 \mu_3 \mu_4 + \lambda_3 \mu_1 \mu_2 \mu_4 + \lambda_4 \mu_1 \mu_2 \mu_3 + \mu_1 \mu_2 \mu_3 \mu_4} \tag{3.138}$$

$$P_2 = \frac{\lambda_2 \mu_1 \mu_3 \mu_4}{\lambda_1 \mu_2 \mu_3 \mu_4 + \lambda_2 \mu_1 \mu_3 \mu_4 + \lambda_3 \mu_1 \mu_2 \mu_4 + \lambda_4 \mu_1 \mu_2 \mu_3 + \mu_1 \mu_2 \mu_3 \mu_4} \tag{3.139}$$

$$P_3 = \frac{\lambda_3 \mu_1 \mu_2 \mu_4}{\lambda_1 \mu_2 \mu_3 \mu_4 + \lambda_2 \mu_1 \mu_3 \mu_4 + \lambda_3 \mu_1 \mu_2 \mu_4 + \lambda_4 \mu_1 \mu_2 \mu_3 + \mu_1 \mu_2 \mu_3 \mu_4} \tag{3.140}$$

$$P_4 = \frac{\lambda_4 \mu_1 \mu_2 \mu_3}{\lambda_1 \mu_2 \mu_3 \mu_4 + \lambda_2 \mu_1 \mu_3 \mu_4 + \lambda_3 \mu_1 \mu_2 \mu_4 + \lambda_4 \mu_1 \mu_2 \mu_3 + \mu_1 \mu_2 \mu_3 \mu_4} \tag{3.141}$$

To analyse the reliability parameters, they have to be plotted. To plots them, we assumed values of model parameters. If the values of model parameters were set as listed below, the inverse Laplace transforms of equations (3.131) – (3.135) were used to develop the plots of state probabilities in Figure 3-13 and availability equation (3.136) was used to develop the plots in Figure 3-14 and Figure 3-15. Detailed plots are presented in Appendix C.4.

$$\lambda_{Os} = 0.0008 \left(\frac{failure}{hour}\right) \quad \lambda_{Ou} = 0.00045 \left(\frac{failure}{hour}\right) \quad \mu_1 = 0.0025 \left(\frac{repair}{hour}\right) \quad \mu_2 = 0.0075 \left(\frac{repair}{hour}\right)$$

$$\lambda_{Hs} = 0.003 \left(\frac{failure}{hour}\right) \quad \lambda_{Hu} = 0.002 \left(\frac{failure}{hour}\right) \quad \mu_3 = 0.006 \left(\frac{repair}{hour}\right) \quad \mu_4 = 0.008 \left(\frac{repair}{hour}\right)$$

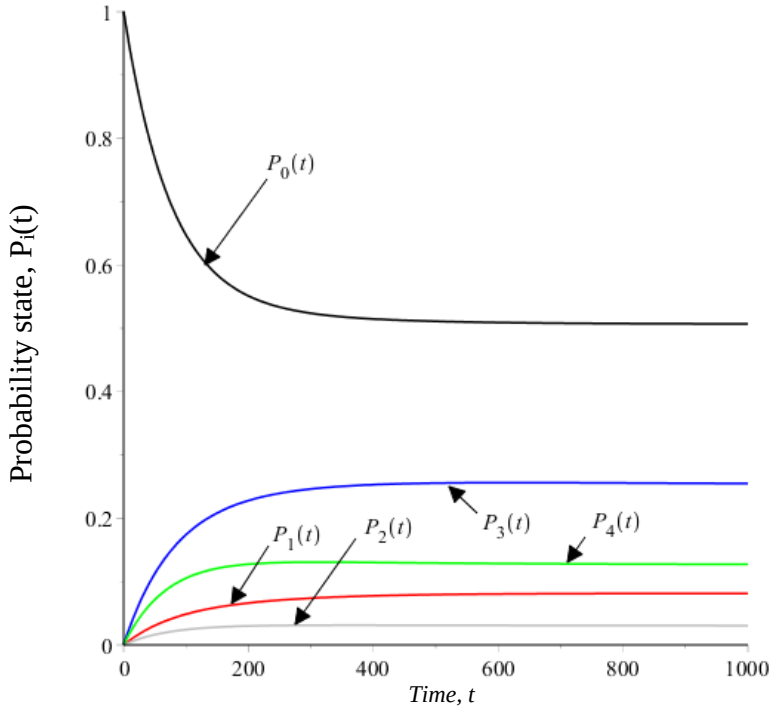

Figure 3-13 State probabilities of one-unit system with four failure modes and Type-I repair

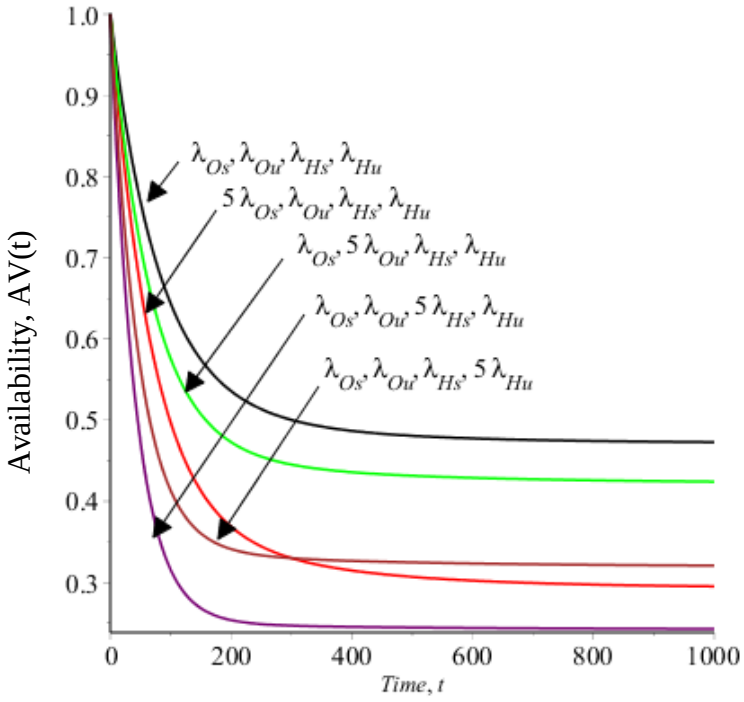

Figure 3-14 Availability plots of one-unit system with four failure modes and Type-I repair at different values of failure rates

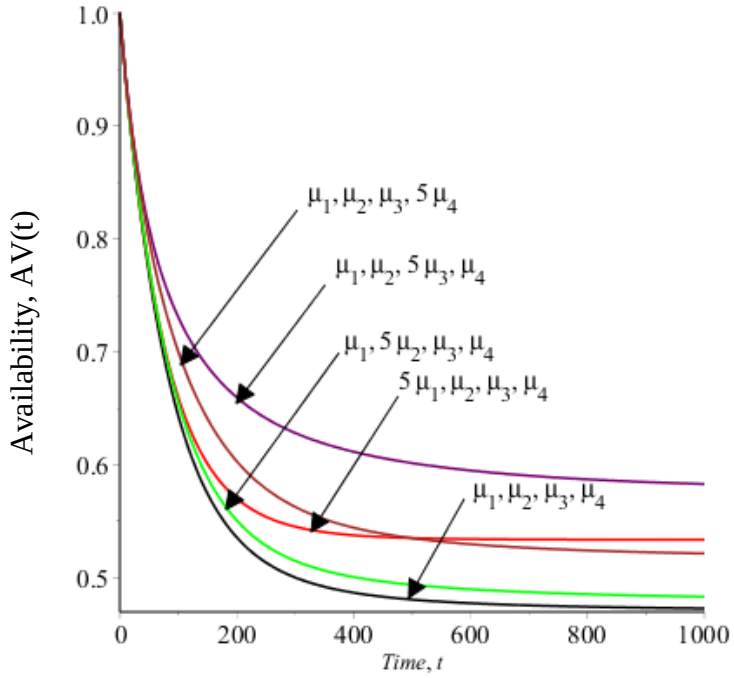

Figure 3-15 Availability plots of one-unit system with four failure modes and Type-I repair at different values of repair rates

3.3.3 **Special Case: Two-Units System with Type-I Repair**

The transition state diagram in Figure 3-16 shows a two units model of mining system that has four failure modes. If one unit fails, the other unit will sustain the operation. The system fails when both units fail. System repair is possible to restore the system to its initial state according to Type-I repair policy. By using the Markov method to perform analysis of the state space diagram in Figure 3-16, the following equations are obtained.

$$\frac{dP_0(t)}{dt} + 2P_0(t)\left(\lambda_{Os} + \lambda_{Ou} + \lambda_{Hs} + \lambda_{Hu}\right) = P_1(t)\,\mu_1 + P_2(t)\,\mu_2 + P_3(t)\,\mu_3 + P_4(t)\,\mu_4 \tag{3.142}$$

$$\frac{dP_1(t)}{dt} + P_1(t)\left(\lambda_{Os} + \lambda_{Ou} + \lambda_{Hs} + \lambda_{Hu}\right) = 2\lambda_{Os}P_0(t) \tag{3.143}$$

$$\frac{dP_2(t)}{dt} + P_2(t)\left(\lambda_{Os} + \lambda_{Ou} + \lambda_{Hs} + \lambda_{Hu}\right) = 2\lambda_{Ou}P_0(t) \tag{3.144}$$

$$\frac{dP_3(t)}{dt} + P_3(t)\left(\lambda_{Os} + \lambda_{Ou} + \lambda_{Hs} + \lambda_{Hu}\right) = 2\lambda_{Hs}P_0(t) \tag{3.145}$$

$$\frac{dP_4(t)}{dt} + P_4(t)\left(\lambda_{Os} + \lambda_{Ou} + \lambda_{Hs} + \lambda_{Hu}\right) = 2\lambda_{Hs}P_0(t) \tag{3.146}$$

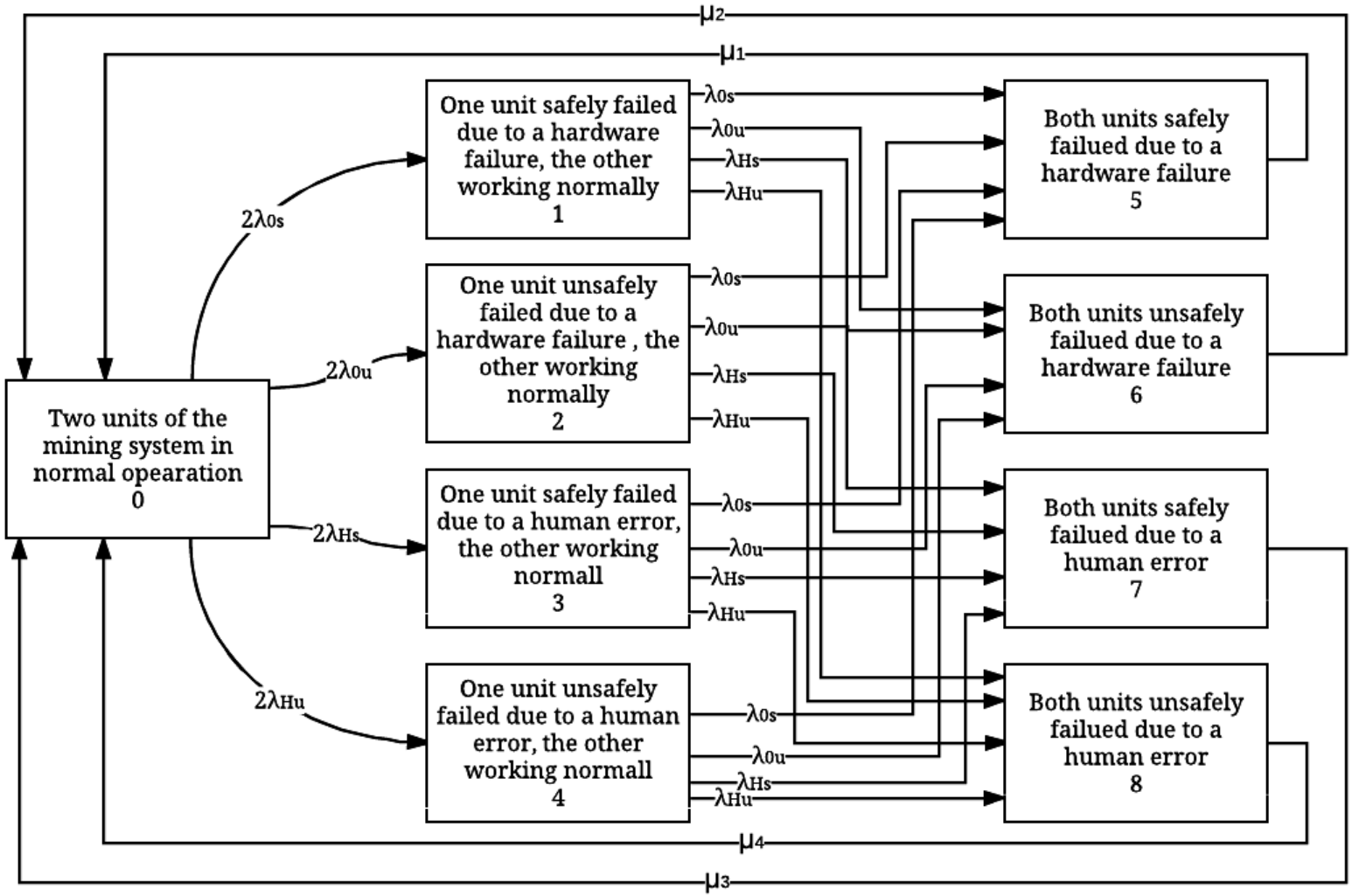

Figure 3-16 State space diagram of two-units system with four failure modes and Type-I repair

$$\frac{dP_5(t)}{dt} + P_5(t)\,\mu_1 = \lambda_{Os}\left(P_1(t) + P_2(t) + P_3(t) + P_4(t)\right) \tag{3.147}$$

$$\frac{dP_6(t)}{dt} + P_6(t)\,\mu_2 = \lambda_{Ou}\left(P_1(s) + P_2(s) + P_3(s) + P_4(s)\right) \tag{3.148}$$

$$\frac{dP_7(t)}{dt} + P_7(t)\,\mu_3 = \lambda_{Hs}\left(P_1(s) + P_2(s) + P_3(s) + P_4(s)\right) \tag{3.149}$$

$$\frac{dP_8(t)}{dt} + P_8(t)\,\mu_4 = \lambda_{Hu}\left(P_1(s) + P_2(s) + P_3(s) + P_4(s)\right) \tag{3.150}$$

At time t= 0, $P_0(0)$= 1 and all other initial state probabilities are equal to zero. By taking the Laplace transforms of equations (3.142) - (3.150), the following equations are obtained:

$$P_0(s) = \frac{P_5(s)\,\mu_1 + P_6(s)\,\mu_2 + P_7(s)\,\mu_3 + P_8(s)\,\mu_4 + 1}{s + 2\,\lambda_{Os} + 2\,\lambda_{Ou} + 2\,\lambda_{Hs} + 2\,\lambda_{Hu}} \tag{3.151}$$

$$P_1(s) = \frac{2\cdot\lambda_{Os}\cdot P_0(s)}{s + \lambda_{Os} + \lambda_{Ou} + \lambda_{Hs} + \lambda_{Hu}} \tag{3.152}$$

$$P_2(s) = \frac{2\cdot\lambda_{Ou}\cdot P_0(s)}{s + \lambda_{Os} + \lambda_{Ou} + \lambda_{Hs} + \lambda_{Hu}} \tag{3.153}$$

$$P_3(s) = \frac{2\cdot\lambda_{Hs}\cdot P_0(s)}{s + \lambda_{Os} + \lambda_{Ou} + \lambda_{Hs} + \lambda_{Hu}} \tag{3.154}$$

$$P_4(s) = \frac{2\cdot\lambda_{Hu}\cdot P_0(s)}{s + \lambda_{Os} + \lambda_{Ou} + \lambda_{Hs} + \lambda_{Hu}} \tag{3.155}$$

$$P_5(s) = \frac{\lambda_{Os}\cdot\left(P_1(s) + P_2(s) + P_3(s) + P_4(s)\right)}{s + \mu_1} \tag{3.156}$$

$$P_6(s) = \frac{\lambda_{Ou}\cdot\left(P_1(s) + P_2(s) + P_3(s) + P_4(s)\right)}{s + \mu_2} \tag{3.157}$$

$$P_7(s) = \frac{\lambda_{Hs}\cdot\left(P_1(s) + P_2(s) + P_3(s) + P_4(s)\right)}{s + \mu_3} \tag{3.158}$$

$$P_8(s) = \frac{\lambda_{Hu}\cdot\left(P_1(s) + P_2(s) + P_3(s) + P_4(s)\right)}{s + \mu_4} \tag{3.159}$$

By using equations (3.151) to (3.159), we get the following equations:

$$P_0(s) = \frac{1}{(s + 2F - 2\cdot\mathrm{F\,W})} \tag{3.160}$$

$$P_1(s) = \frac{2\cdot\lambda_{Os}}{(s+F)(s+2F-2\cdot \mathrm{F\,W})} \tag{3.161}$$

$$P_2(s) = \frac{2\cdot\lambda_{Ou}}{(s+F)(s+2F-2\cdot \mathrm{F\,W})} \tag{3.162}$$

$$P_3(s) = \frac{2\cdot\lambda_{Hs}}{(s+F)(s+2F-2\cdot \mathrm{F\,W})} \tag{3.163}$$

$$P_4(s) = \frac{2\cdot\lambda_{Hu}}{(s+F)(s+2F-2\cdot \mathrm{F\,W})} \tag{3.164}$$

$$P_5(s) = \frac{2\ \lambda_{Os}\cdot F}{\left(s+\mu_1\right)(s+F)(s+2F-2\cdot \mathrm{F\,W})} \tag{3.165}$$

$$P_6(s) = \frac{2\ \lambda_{Ou}\cdot F}{\left(s+\mu_2\right)(s+F)(s+2F-2\cdot \mathrm{F\,W})} \tag{3.166}$$

$$P_7(s) = \frac{2\ \lambda_{Hs}\cdot F}{\left(s+\mu_3\right)(s+F)(s+2F-2\cdot \mathrm{F\,W})} \tag{3.167}$$

$$P_8(s) = \frac{2\ \lambda_{Hu}\cdot F}{\left(s+\mu_4\right)(s+F)(s+2F-2\cdot \mathrm{F\,W})} \tag{3.168}$$

Where

$$F = \lambda_{Os} + \lambda_{Ou} + \lambda_{Hs} + \lambda_{Hu}$$

$$W = \left(\frac{\lambda_{Os}\,\mu_1}{\left(s+\mu_1\right)(s+F)} + \frac{\lambda_{Ou}\,\mu_2}{\left(s+\mu_2\right)(s+F)} + \frac{\lambda_{Hs}\,\mu_3}{\left(s+\mu_3\right)(s+F)} + \frac{\lambda_{Hu}\,\mu_4}{\left(s+\mu_4\right)(s+F)} \right)$$

By taking the inverse Laplace transform of equations (3.160) – (3.168), we get the equations of time dependent state probabilities.

System Reliability and MTTF

To find the reliability and MTTF, all μ_1, μ_2, μ_3, and μ_4 should be equal to zero. Then, system equations are solved. The resulted equations are similar to Special Case: Two-Units System without Repair. Therefore, the reliability equation (3.66) and MTTF equation (3.67) were used to develop the plots in Figure 3-7, and Appendix C.2.

Availability and Steady state Probabilities

The availability is the total probabilities of system operational states.

$$AV(t) = P_0(t) + P_1(t) + P_2(t) + P_3(t) + P_4(t) \tag{3.169}$$

The system steady state probabilities can be obtained by applying final-value theorem as follows:

$$P_0 = \frac{\mu_1 \mu_2 \mu_3 \mu_4}{2\lambda_{Hs}\mu_1\mu_2\mu_4 + 2\lambda_{Hu}\mu_1\mu_2\mu_3 + 2\lambda_{Os}\mu_2\mu_3\mu_4 + \lambda_{Ou}\mu_1\mu_3\mu_4 + 3\mu_1\mu_2\mu_3\mu_4} \tag{3.170}$$

$$P_1 = 2\lambda_{Os}\frac{\mu_1 \mu_2 \mu_3 \mu_4}{F\left(2\lambda_{Hs}\mu_1\mu_2\mu_4 + 2\lambda_{Hu}\mu_1\mu_2\mu_3 + 2\lambda_{Os}\mu_2\mu_3\mu_4 + 2\lambda_{Ou}\mu_1\mu_2\mu_3\mu_4 + 3\mu_1\mu_2\mu_3\mu_4\right)} \tag{3.171}$$

$$P_2 = \frac{2\lambda_{Ou}\mu_1 \mu_2 \mu_3 \mu_4}{F\left(2\lambda_{Hs}\mu_1\mu_2\mu_4 + 2\lambda_{Hu}\mu_1\mu_2\mu_3 + 2\lambda_{Os}\mu_2\mu_3\mu_4 + 2\lambda_{Ou}\mu_1\mu_2\mu_3\mu_4 + 3\mu_1\mu_2\mu_3\mu_4\right)} \tag{3.172}$$

$$P_3 = \frac{2\lambda_{Hs}\mu_1 \mu_2 \mu_3 \mu_4}{F\left(2\lambda_{Hs}\mu_1\mu_2\mu_4 + 2\lambda_{Hu}\mu_1\mu_2\mu_3 + 2\lambda_{Os}\mu_2\mu_3\mu_4 + 2\lambda_{Ou}\mu_1\mu_2\mu_3\mu_4 + 3\mu_1\mu_2\mu_3\mu_4\right)} \tag{3.173}$$

$$P_4 = \frac{2\lambda_{Hu}\mu_1 \mu_2 \mu_3 \mu_4}{F\left(2\lambda_{Hs}\mu_1\mu_2\mu_4 + 2\lambda_{Hu}\mu_1\mu_2\mu_3 + 2\lambda_{Os}\mu_2\mu_3\mu_4 + 2\lambda_{Ou}\mu_1\mu_2\mu_3\mu_4 + 3\mu_1\mu_2\mu_3\mu_4\right)} \tag{3.174}$$

$$P_5 = \frac{2\lambda_{Os}\mu_1 \mu_2 \mu_3 \mu_4}{F\left(2\lambda_{Hs}\mu_1\mu_2\mu_4 + 2\lambda_{Hu}\mu_1\mu_2\mu_3 + 2\lambda_{Os}\mu_2\mu_3\mu_4 + 2\lambda_{Ou}\mu_1\mu_2\mu_3\mu_4 + 3\mu_1\mu_2\mu_3\mu_4\right)} \tag{3.175}$$

$$P_6 = \frac{2\lambda_{Ou}\mu_1 \mu_2 \mu_3 \mu_4}{F\left(2\lambda_{Hs}\mu_1\mu_2\mu_4 + 2\lambda_{Hu}\mu_1\mu_2\mu_3 + 2\lambda_{Os}\mu_2\mu_3\mu_4 + 2\lambda_{Ou}\mu_1\mu_2\mu_3\mu_4 + 3\mu_1\mu_2\mu_3\mu_4\right)} \tag{3.176}$$

$$P_7 = \frac{2\lambda_{Hs}\mu_1 \mu_2 \mu_3 \mu_4}{F\left(2\lambda_{Hs}\mu_1\mu_2\mu_4 + 2\lambda_{Hu}\mu_1\mu_2\mu_3 + 2\lambda_{Os}\mu_2\mu_3\mu_4 + 2\lambda_{Ou}\mu_1\mu_2\mu_3\mu_4 + 3\mu_1\mu_2\mu_3\mu_4\right)} \tag{3.177}$$

$$P_8 = \frac{2\lambda_{Hu}\mu_1 \mu_2 \mu_3 \mu_4}{F\left(2\lambda_{Hs}\mu_1\mu_2\mu_4 + 2\lambda_{Hu}\mu_1\mu_2\mu_3 + 2\lambda_{Os}\mu_2\mu_3\mu_4 + 2\lambda_{Ou}\mu_1\mu_2\mu_3\mu_4 + 3\mu_1\mu_2\mu_3\mu_4\right)} \tag{3.178}$$

To analyse the model reliability parameters, specific values of failure and repair rates are assumed. Based on model parameter values, the inverse Laplace transforms of (3.160) – (3.168) were used to develop the plots of state probabilities in Figure 3-17, and availability equation (3.169) was used to develop the plots in Figure 3-18. Detailed plots are presented in Appendix C.5.

$$\lambda_{Os} = 0.0008\left(\frac{failure}{hour}\right) \quad \lambda_{Ou} = 0.00045\left(\frac{failure}{hour}\right) \quad \mu_1 = 0.0025\left(\frac{repair}{hour}\right) \quad \mu_2 = 0.0075\left(\frac{repair}{hour}\right)$$

$$\lambda_{Hs} = 0.003\left(\frac{failure}{hour}\right) \quad \lambda_{Hu} = 0.002\left(\frac{failure}{hour}\right) \quad \mu_3 = 0.006\left(\frac{repair}{hour}\right) \quad \mu_4 = 0.008\left(\frac{repair}{hour}\right)$$

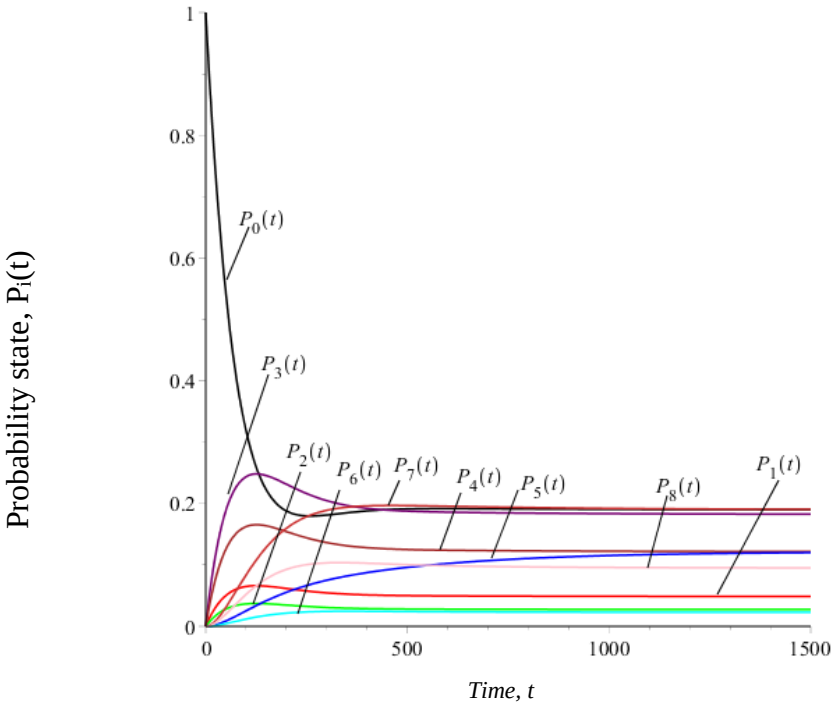

Figure 3-17 State probabilities of two-unit system with four failure modes and Type-I repair

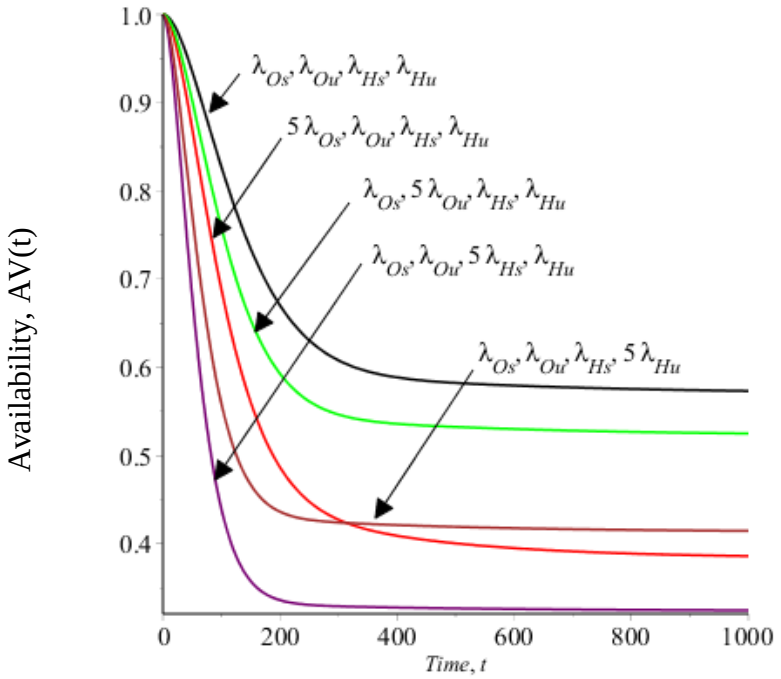

Figure 3-18 Availability plots of two-unit system with four failure modes and Type-I repair at different values of failure rates

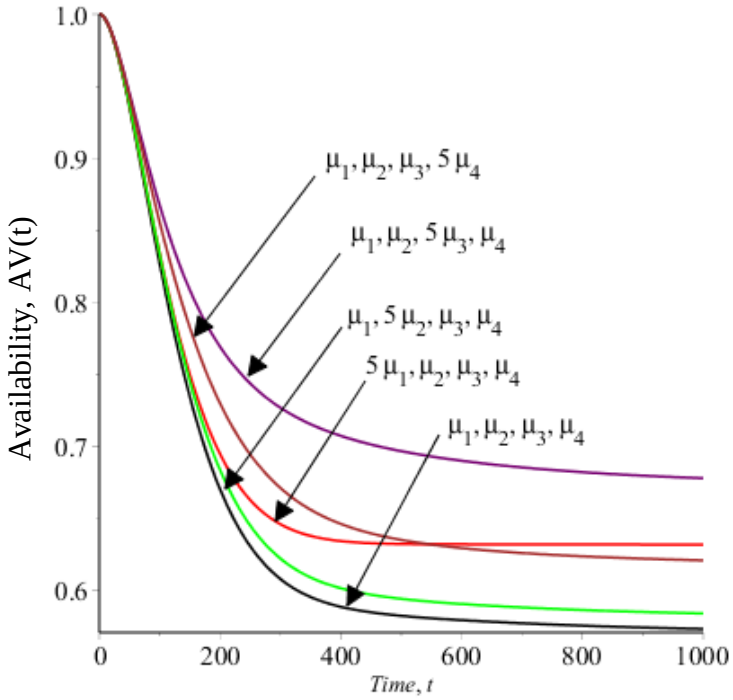

Figure 3-19 Availability plots of two-unit system with four failure modes and Type-I repair at different values of repair rates

3.3.1 Special Case: Three-Units System with Type-I Repair

The transition state diagram in Figure 3-20 shows three units model of mining system that has four failure modes. Each unit has the capability to operate the system at full capacity. Thus, the system fails when all units fail. When system completely fails, it can be restored to the initial state according to Type-I repair policy. By using the Markov method to perform analysis of the state space diagram in Figure 3-20, the follow equations are obtained.

$$\frac{dP_0(t)}{dt} + 3\,P_0(t)\left(\lambda_{Os} + \lambda_{Ou} + \lambda_{Hs} + \lambda_{Hu}\right) = \sum_{i=9}^{12} P_i(t)\,\mu_{(i-8)} \tag{3.179}$$

$$\frac{dP_1(t)}{dt} + 2\,P_1(t)\left(\lambda_{Os} + \lambda_{Ou} + \lambda_{Hs} + \lambda_{Hu}\right) = 3\,\lambda_{Os} P_0(t) \tag{3.180}$$

$$\frac{dP_2(t)}{dt} + 2\,P_2(t)\left(\lambda_{Os} + \lambda_{Ou} + \lambda_{Hs} + \lambda_{Hu}\right) = 3\,\lambda_{Ou} P_0(t) \tag{3.181}$$

$$\frac{dP_3(t)}{dt} + 2\,P_3(t)\left(\lambda_{Os} + \lambda_{Ou} + \lambda_{Hs} + \lambda_{Hu}\right) = 3\,\lambda_{Hs} P_0(t) \tag{3.182}$$

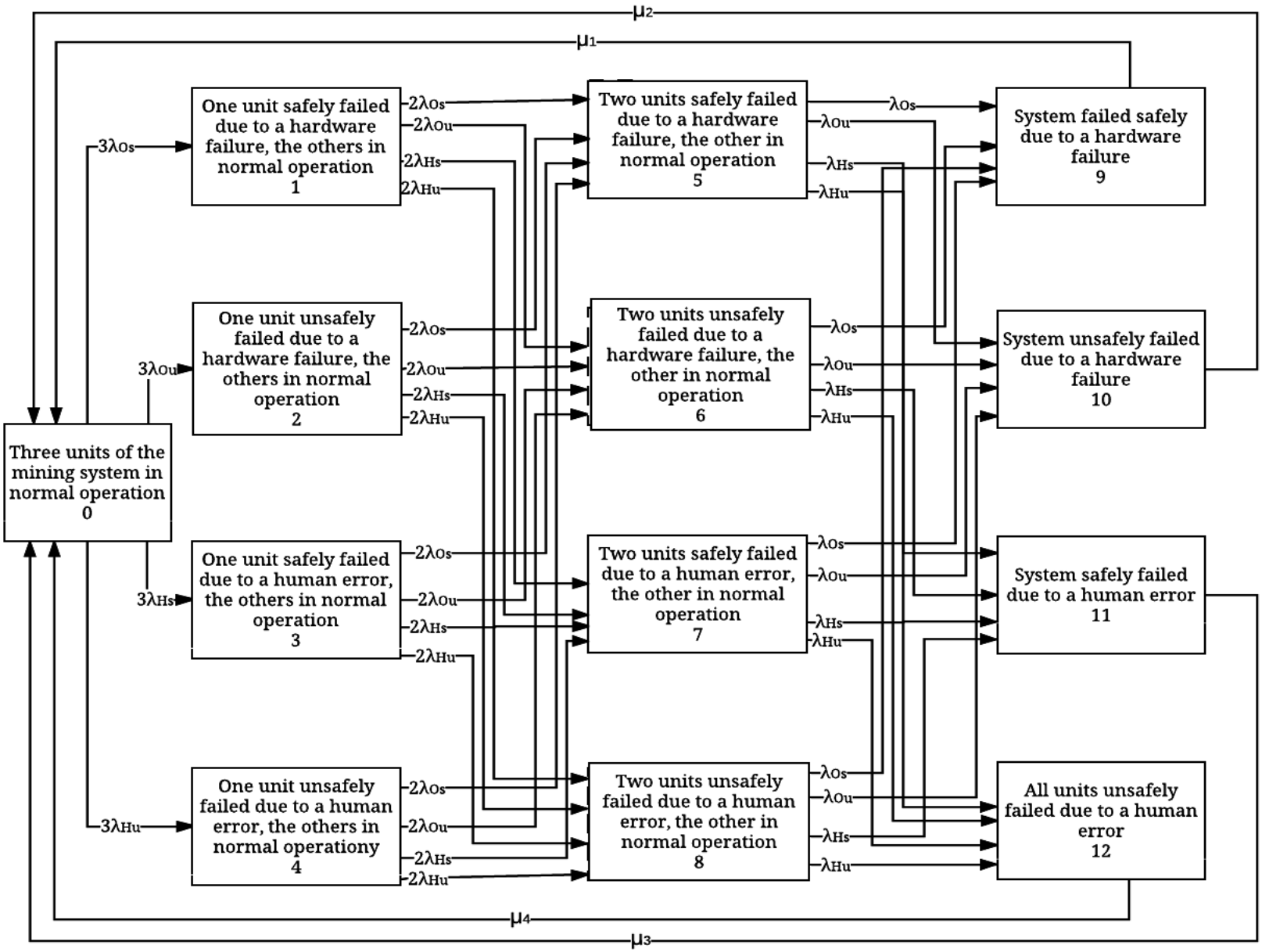

Figure 3-20 State space diagram of three-unit with four failure modes and Type-I repair

$$\frac{dP_4(t)}{dt} + 2P_4(t)\left(\lambda_{Os} + \lambda_{Ou} + \lambda_{Hs} + \lambda_{Hu}\right) = 3\lambda_{Hu} P_0(t) \tag{3.183}$$

$$\frac{dP_5(t)}{dt} + P_5(t)\left(\lambda_{Os} + \lambda_{Ou} + \lambda_{Hs} + \lambda_{Hu}\right) = 2\lambda_{Os} \cdot \sum_{i=1}^{4} P_i(t) \tag{3.184}$$

$$\frac{dP_6(t)}{dt} + P_6(t)\left(\lambda_{Os} + \lambda_{Ou} + \lambda_{Hs} + \lambda_{Hu}\right) = 2\lambda_{Ou} \cdot \sum_{i=1}^{4} P_i(t) \tag{3.185}$$

$$\frac{dP_7(t)}{dt} + P_7(t)\left(\lambda_{Os} + \lambda_{Ou} + \lambda_{Hs} + \lambda_{Hu}\right) = 2\lambda_{Hs} \cdot \sum_{i=1}^{4} P_i(t) \tag{3.186}$$

$$\frac{dP_8(t)}{dt} + P_8(t)\left(\lambda_{Os} + \lambda_{Ou} + \lambda_{Hs} + \lambda_{Hu}\right) = 2\lambda_{Hu} \cdot \sum_{i=1}^{4} P_i(t) \tag{3.187}$$

$$\frac{dP_9(t)}{dt} + P_9(t)\,\mu_1 = \lambda_{Os} \cdot \sum_{i=5}^{8} P_i(t) \tag{3.188}$$

$$\frac{dP_{10}(t)}{dt} + P_{10}(t)\,\mu_2 = \lambda_{Ou} \cdot \sum_{i=5}^{8} P_i(t) \tag{3.189}$$

$$\frac{dP_{11}(t)}{dt} + P_{11}(t)\,\mu_3 = \lambda_{Hs} \cdot \sum_{i=5}^{8} P_i(t) \tag{3.190}$$

$$\frac{dP_{12}(t)}{dt} + P_{12}(t)\,\mu_4 = \lambda_{Hu} \cdot \sum_{i=5}^{8} P_i(t) \tag{3.191}$$

At time t= 0, $P_0(0)$= 1 and all other initial state probabilities are equal to zero. By taking the Laplace transforms of equations 3.179 to 3.191, the following equations were obtained:

$$P_0(s) = \frac{\mu_1 \cdot P_9(s) + \mu_2 \cdot P_{10}(s) + \mu_3 \cdot P_{11}(s) + \mu_4 \cdot P_{12}(s) + 1}{s + 3 \cdot \left(\lambda_{Os} + \lambda_{Ou} + \lambda_{Hs} + \lambda_{Hu}\right)} \tag{3.192}$$

$$P_1(s) = \frac{3 \cdot \lambda_{Os} \cdot P_0(s)}{s + 2 \cdot \left(\lambda_{Os} + \lambda_{Ou} + \lambda_{Hs} + \lambda_{Hu}\right)} \tag{3.193}$$

$$P_2(s) = \frac{3 \cdot \lambda_{Ou} \cdot P_0(s)}{s + 2 \cdot \left(\lambda_{Os} + \lambda_{Ou} + \lambda_{Hs} + \lambda_{Hu}\right)} \tag{3.194}$$

$$P_3(s) = \frac{3 \cdot \lambda_{Hs} \cdot P_0(s)}{s + 2 \cdot \left(\lambda_{Os} + \lambda_{Ou} + \lambda_{Hs} + \lambda_{Hu}\right)} \tag{3.195}$$

$$P_4(s) = \frac{3 \cdot \lambda_{Hu} \cdot P_0(s)}{s + 2 \cdot \left(\lambda_{Os} + \lambda_{Ou} + \lambda_{Hs} + \lambda_{Hu}\right)} \tag{3.196}$$

$$P_5(s) = \frac{2 \cdot \lambda_{Os} \cdot \left(P_1(s) + P_2(s) + P_3(s) + P_4(s)\right)}{s + \left(\lambda_{Os} + \lambda_{Ou} + \lambda_{Hs} + \lambda_{Hu}\right)} \tag{3.197}$$

$$P_6(s) = \frac{2 \cdot \lambda_{Ou} \cdot \left(P_1(s) + P_2(s) + P_3(s) + P_4(s)\right)}{s + \left(\lambda_{Os} + \lambda_{Ou} + \lambda_{Hs} + \lambda_{Hu}\right)} \tag{3.198}$$

$$P_7(s) = \frac{2 \cdot \lambda_{Hs} \cdot \left(P_1(s) + P_2(s) + P_3(s) + P_4(s)\right)}{s + \left(\lambda_{Os} + \lambda_{Ou} + \lambda_{Hs} + \lambda_{Hu}\right)} \tag{3.199}$$

$$P_8(s) = \frac{2 \cdot \lambda_{Hu} \cdot \left(P_1(s) + P_2(s) + P_3(s) + P_4(s)\right)}{s + \left(\lambda_{Os} + \lambda_{Ou} + \lambda_{Hs} + \lambda_{Hu}\right)} \tag{3.200}$$

$$P_9(s) = \frac{\lambda_{Os} \cdot \left(P_5(s) + P_6(s) + P_7(s) + P_8(s)\right)}{s + \mu_1} \tag{3.201}$$

$$P_{10}(s) = \frac{\lambda_{Ou} \cdot \left(P_5(s) + P_6(s) + P_7(s) + P_8(s)\right)}{s + \mu_2} \tag{3.202}$$

$$P_{11}(s) = \frac{\lambda_{Hs} \cdot \left(P_5(s) + P_6(s) + P_7(s) + P_8(s)\right)}{s + \mu_3} \tag{3.203}$$

$$P_{12}(s) = \frac{\lambda_{Hu} \cdot \left(P_5(s) + P_6(s) + P_7(s) + P_8(s)\right)}{s + \mu_4} \tag{3.204}$$

By using equations (3.192) to (3.204), we get the following equations:

$$P_0(s) = \frac{(\mathrm{s} + \mathrm{F}) \cdot (\mathrm{s} + 2\,\mathrm{F})}{(\mathrm{s} + \mathrm{F}) \cdot (\mathrm{s} + 2\,\mathrm{F}) \cdot (\mathrm{s} + 3\,\mathrm{F}) - 6 \cdot F^2 \cdot W} \tag{3.205}$$

$$P_1(s) = \frac{3\,\lambda_{Os}(\mathrm{s} + \mathrm{F})}{(\mathrm{s} + \mathrm{F}) \cdot (\mathrm{s} + 2\,\mathrm{F}) \cdot (\mathrm{s} + 3\,\mathrm{F}) - 6 \cdot F^2 \cdot W} \tag{3.206}$$

$$P_2(s) = \frac{3\,\lambda_{Ou}(\mathrm{s} + \mathrm{F})}{(\mathrm{s} + \mathrm{F}) \cdot (\mathrm{s} + 2\,\mathrm{F}) \cdot (\mathrm{s} + 3\,\mathrm{F}) - 6 \cdot F^2 \cdot W} \tag{3.207}$$

$$P_3(s) = \frac{3\,\lambda_{Hs}(\mathrm{s} + \mathrm{F})}{(\mathrm{s} + \mathrm{F}) \cdot (\mathrm{s} + 2\,\mathrm{F}) \cdot (\mathrm{s} + 3\,\mathrm{F}) - 6 \cdot F^2 \cdot W} \tag{3.208}$$

$$P_4(s) = \frac{3\,\lambda_{Hu}(\mathrm{s} + \mathrm{F})}{(\mathrm{s} + \mathrm{F}) \cdot (\mathrm{s} + 2\,\mathrm{F}) \cdot (\mathrm{s} + 3\,\mathrm{F}) - 6 \cdot F^2 \cdot W} \tag{3.209}$$

$$P_5(s) = \frac{2\,\lambda_{Os} \cdot F}{(\mathrm{s} + \mathrm{F}) \cdot (\mathrm{s} + 2\,\mathrm{F}) \cdot (\mathrm{s} + 3\,\mathrm{F}) - 6 \cdot F^2 \cdot W} \tag{3.210}$$

$$P_6(s) = \frac{2\lambda_{Ou} \cdot F}{(s+F)\cdot(s+2F)\cdot(s+3F) - 6\cdot F^2 \cdot W} \tag{3.211}$$

$$P_7(s) = \frac{2\lambda_{Hs} \cdot F}{(s+F)\cdot(s+2F)\cdot(s+3F) - 6\cdot F^2 \cdot W} \tag{3.212}$$

$$P_8(s) = \frac{2\lambda_{Hu} \cdot F}{(s+F)\cdot(s+2F)\cdot(s+3F) - 6\cdot F^2 \cdot W} \tag{3.213}$$

$$P_9(s) = \frac{2\lambda_{Os} \cdot F^2}{(s+\mu_1)\cdot\left((s+F)\cdot(s+2F)\cdot(s+3F) - 6\cdot F^2 \cdot W\right)} \tag{3.214}$$

$$P_{10}(s) = \frac{2\lambda_{Ou} \cdot F^2}{(s+\mu_2)\cdot\left((s+F)\cdot(s+2F)\cdot(s+3F) - 6\cdot F^2 \cdot W\right)} \tag{3.215}$$

$$P_{11}(s) = \frac{2\lambda_{Hs} \cdot F^2}{(s+\mu_3)\cdot\left((s+F)\cdot(s+2F)\cdot(s+3F) - 6\cdot F^2 \cdot W\right)} \tag{3.216}$$

$$P_{12}(s) = \frac{2\lambda_{Hu} \cdot F^2}{(s+\mu_4)\cdot\left((s+F)\cdot(s+2F)\cdot(s+3F) - 6\cdot F^2 \cdot W\right)} \tag{3.217}$$

Where;

$$F = \lambda_{Os} + \lambda_{Ou} + \lambda_{Hs} + \lambda_{Hu}$$

$$W = \frac{\mu_1 \lambda_{Os}}{s+\mu_1} + \frac{\mu_2 \lambda_{Ou}}{s+\mu_2} + \frac{\mu_3 \lambda_{Hs}}{s+\mu_3} + \frac{\mu_4 \lambda_{Hu}}{s+\mu_4}$$

By taking the inverse Laplace transform of equations (3.205) – (3.217), the time dependent equations of state probabilities are obtained.

System Reliability and MTTF

To find the reliability and MTTF, μ_1, μ_2, μ_3, and μ_4 should be equal to zero. The resulted model and equations are similar to Special Case Three-Units without Repair. The reliability equation (3.107) and MTTF equation (3.108) were used to develop the plots in Figure 3-10 and in Appendix C.3.

Availability and Steady State Probabilities

This model has Type-I repair. Thus, the availability is the total probability of system operational states as follows.

$$AV(t) = \sum_{i=0}^{8} P_i(t) \tag{3.218}$$

The system steady state probabilities can be obtained by applying final-value theorem as follows:

$$P_0 = \frac{2\mu_1\mu_2\mu_3\mu_4}{6\lambda_{Hs}\mu_1\mu_2\mu_4 + 6\lambda_{Hu}\mu_1\mu_2\mu_3 + 6\lambda_{Os}\mu_2\mu_3\mu_4 + 6\lambda_{Ou}\mu_1\mu_3\mu_4 + 11\mu_1\mu_2\mu_3\mu_4} \tag{3.219}$$

$$P_1 = \frac{6\lambda_{Os}\mu_1\mu_2\mu_3\mu_4}{F\left(6\lambda_{Hs}\mu_1\mu_2\mu_4 + 6\lambda_{Hu}\mu_1\mu_2\mu_3 + 6\lambda_{Os}\mu_2\mu_3\mu_4 + 6\lambda_{Ou}\mu_1\mu_3\mu_4 + 11\mu_1\mu_2\mu_3\mu_4\right)} \tag{3.220}$$

$$P_2 = \frac{6\lambda_{Ou}\mu_1\mu_2\mu_3\mu_4}{F\left(6\lambda_{Hs}\mu_1\mu_2\mu_4 + 6\lambda_{Hu}\mu_1\mu_2\mu_3 + 6\lambda_{Os}\mu_2\mu_3\mu_4 + 6\lambda_{Ou}\mu_1\mu_3\mu_4 + 11\mu_1\mu_2\mu_3\mu_4\right)} \tag{3.221}$$

$$P_3 = \frac{6\lambda_{Hs}\mu_1\mu_2\mu_3\mu_4}{F\left(6\lambda_{Hs}\mu_1\mu_2\mu_4 + 6\lambda_{Hu}\mu_1\mu_2\mu_3 + 6\lambda_{Os}\mu_2\mu_3\mu_4 + 6\lambda_{Ou}\mu_1\mu_3\mu_4 + 11\mu_1\mu_2\mu_3\mu_4\right)} \tag{3.222}$$

$$P_4 = \frac{6\lambda_{Hu}\mu_1\mu_2\mu_3\mu_4}{F\left(6\lambda_{Hs}\mu_1\mu_2\mu_4 + 6\lambda_{Hu}\mu_1\mu_2\mu_3 + 6\lambda_{Os}\mu_2\mu_3\mu_4 + 6\lambda_{Ou}\mu_1\mu_3\mu_4 + 11\mu_1\mu_2\mu_3\mu_4\right)} \tag{3.223}$$

$$P_5 = \frac{6\lambda_{Os}\ \mu_1\mu_2\mu_3\mu_4}{F\left(6\lambda_{Hs}\mu_1\mu_2\mu_4 + 6\lambda_{Hu}\mu_1\mu_2\mu_3 + 6\lambda_{Os}\mu_2\mu_3\mu_4 + 6\lambda_{Ou}\mu_1\mu_3\mu_4 + 11\mu_1\mu_2\mu_3\mu_4\right)} \tag{3.224}$$

$$P_6 = \frac{6\lambda_{Ou}}{F\left(6\lambda_{Hs}\mu_1\mu_2\mu_4 + 6\lambda_{Hu}\mu_1\mu_2\mu_3 + 6\lambda_{Os}\mu_2\mu_3\mu_4 + 6\lambda_{Ou}\mu_1\mu_3\mu_4 + 11\mu_1\mu_2\mu_3\mu_4\right)} \tag{3.225}$$

$$P_7 = \frac{6\lambda_{Hs}\ \mu_1\mu_2\mu_3\mu_4}{F\left(6\lambda_{Hs}\mu_1\mu_2\mu_4 + 6\lambda_{Hu}\mu_1\mu_2\mu_3 + 6\lambda_{Os}\mu_2\mu_3\mu_4 + 6\lambda_{Ou}\mu_1\mu_3\mu_4 + 11\mu_1\mu_2\mu_3\mu_4\right)} \tag{3.226}$$

$$P_8 = \frac{6\lambda_{Hu}\ \mu_1\mu_2\mu_3\mu_4}{F\left(6\lambda_{Hs}\mu_1\mu_2\mu_4 + 6\lambda_{Hu}\mu_1\mu_2\mu_3 + 6\lambda_{Os}\mu_2\mu_3\mu_4 + 6\lambda_{Ou}\mu_1\mu_3\mu_4 + 11\mu_1\mu_2\mu_3\mu_4\right)} \tag{3.227}$$

To analyse the model reliability parameters, specific values of failure and repair rates are assumed. Based on assumed values, the inverse Laplace transforms of equation (3.205) – (3.217) were used to develop the plots in Figure 3-21 and availability equation (3.218) was used to develop the plots Figure 3-22. Detailed plots are presented in Appendix C.6.

$\lambda_{Os} = 0.0008 \left(\frac{failure}{hour} \right)$ $\lambda_{Ou} = 0.00045 \left(\frac{failure}{hour} \right)$ $\mu_1 = 0.0025 \left(\frac{repair}{hour} \right)$ $\mu_2 = 0.0075 \left(\frac{repair}{hour} \right)$

$\lambda_{Hs} = 0.003 \left(\frac{failure}{hour} \right)$ $\lambda_{Hu} = 0.002 \left(\frac{failure}{hour} \right)$ $\mu_3 = 0.006 \left(\frac{repair}{hour} \right)$ $\mu_4 = 0.008 \left(\frac{repair}{hour} \right)$

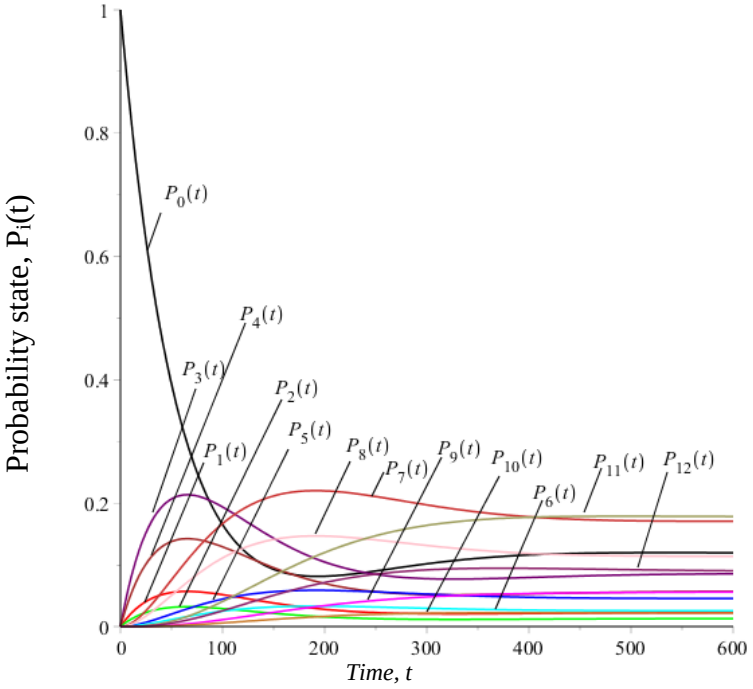

Figure 3-21 State probabilities of three –unit system with four failure modes and Type-I repair

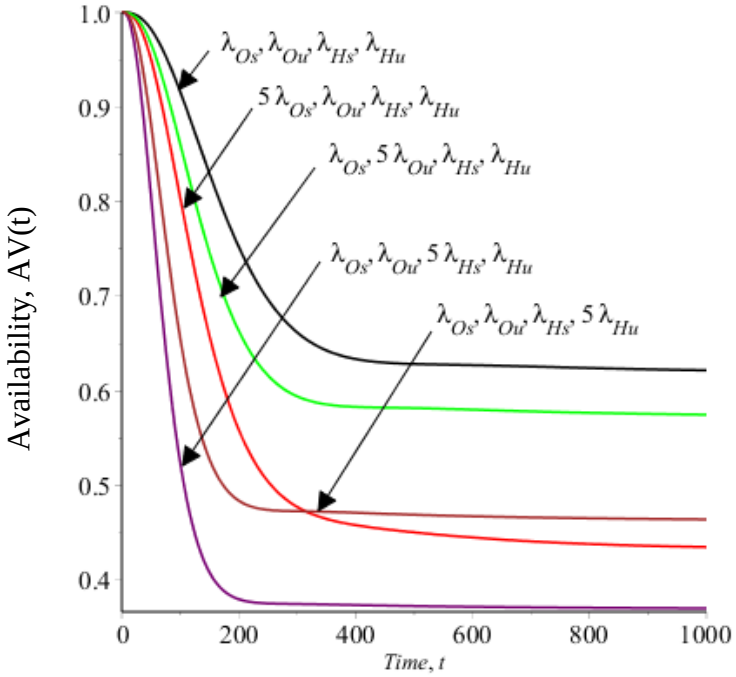

Figure 3-22 Availability plots of three -unit system with four failure modes and Type-I repair at different values of failure rates.

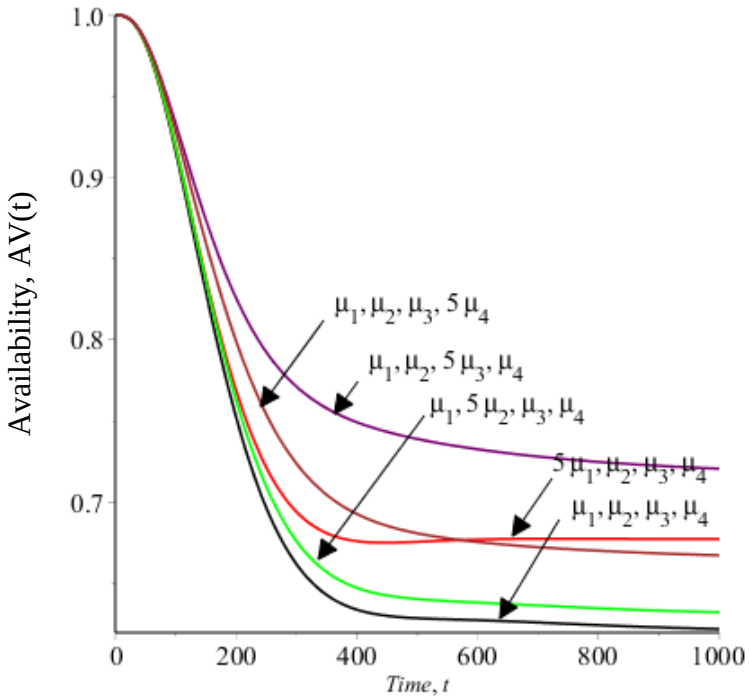

Figure 3-23 Availability plots of three –unit system with four failure modes and Type-I repair at different values of repair rates.

3.4 Discussion

This section compares the reliability of mining system models at different number of units in parallel configuration when safe and unsafe failure modes are considered. To demonstrate the influence of using different values of failure, repair rates and different number of units, the reliability plots of special cases one-unit, two-units and three-units are developed based on same assumed failure and repair rates.

The observation was similar to Chapter 2. However, Chapter 2 models considered two failure modes: hardware failure and human-error while Chapter 3 models considered four failure modes: safe hardware failure, unsafe hardware failure, safe human-error and unsafe human-error. The assumed value of failure rates in Chapter 2 are equal to the sum of safe and unsafe failure rates in Chapter 3. In other words, the total of safe and unsafe hardware failure rates ($\lambda_{os} + \lambda_{ou}$) equals the hardware failure rate (λ_o) and similarly is the human-error rates the total of safe and unsafe human-error rates ($\lambda_{Hs} + \lambda_{Hu}$) equals the hardware failure rate (λ_H). Therefore, the reliability plots for Chapter 2 and Chapter 3 models were identical when models have without repair or Type-I

repair. If the repair rate of safe failure is different than the repair rate of unsafe failure, as shown below, then the availability deviates as shown in Figure 3-32.

To investigate the influence of same failure rates on the different number of units in parallel configuration, Figure 3-24, Figure 3-26, Figure 3-28 and Figure 3-30 are developed. Figure 3-24, Figure 3-28, Figure 3-29 and Figure 3-30 clearly show that one-unit at current failure rate could have a higher reliability than two and three units model at a higher failure rate. Similarly, Figure 3-31 shows that one-unit model could have a higher reliability when failure rate was reduced than two and three units. Whereas reducing λ_{0s} and λ_{0u} do not have significant changes to the system reliability according to assumed failure rates.

Hence, it is not always advantageous to increase the number of units in parallel configuration if the failure rate will be increase. Also, it could be advantageous to control and reduce the failure rate or human-error rather than increase the number of parallel units.

To illustrate these points, model reliability equations 3.28, 3.66 and 3.107 for special cases were used to develop reliability plots based on assumed value as follows:

$$\lambda_{Os} = 0.0008 \left(\frac{failure}{hour} \right) \quad \lambda_{Ou} = 0.00045 \left(\frac{failure}{hour} \right) \quad \mu_1 = 0.0025 \left(\frac{repair}{hour} \right) \quad \mu_2 = 0.0075 \left(\frac{repair}{hour} \right)$$

$$\lambda_{Hs} = 0.003 \left(\frac{failure}{hour} \right) \quad \lambda_{Hu} = 0.002 \left(\frac{failure}{hour} \right) \quad \mu_3 = 0.006 \left(\frac{repair}{hour} \right) \quad \mu_4 = 0.008 \left(\frac{repair}{hour} \right)$$

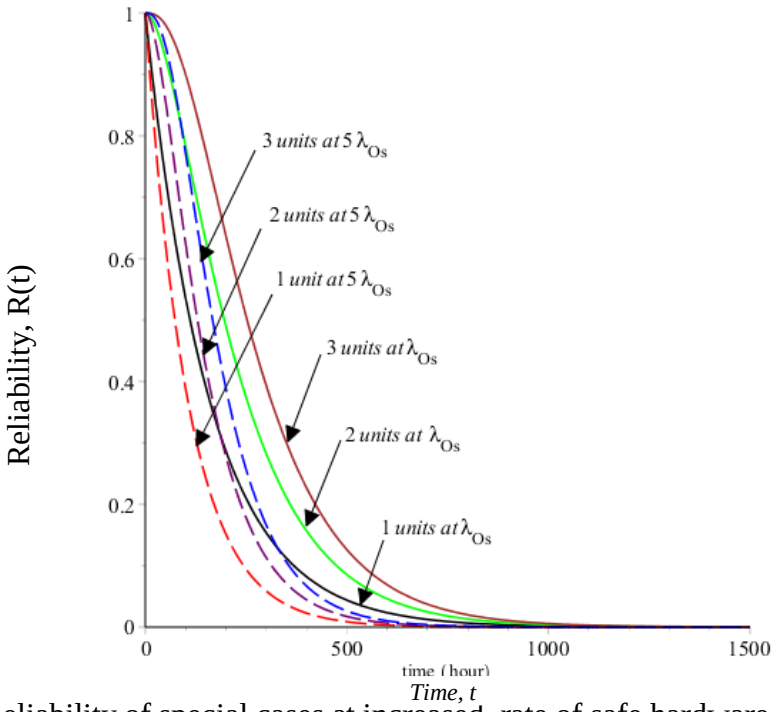

Figure 3-24 Reliability of special cases at increased rate of safe hardware failures

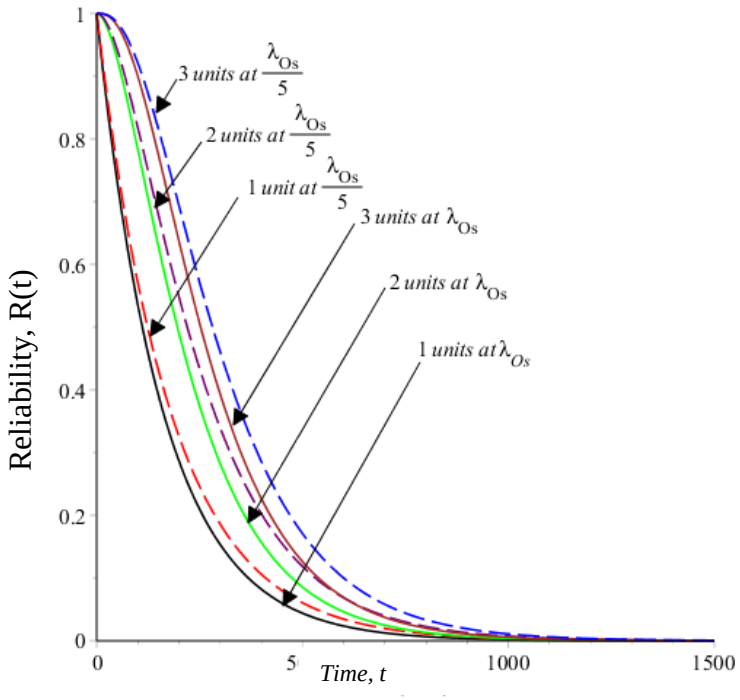

Figure 3-25 Reliability of special cases at decreased rate of safe hardware failures

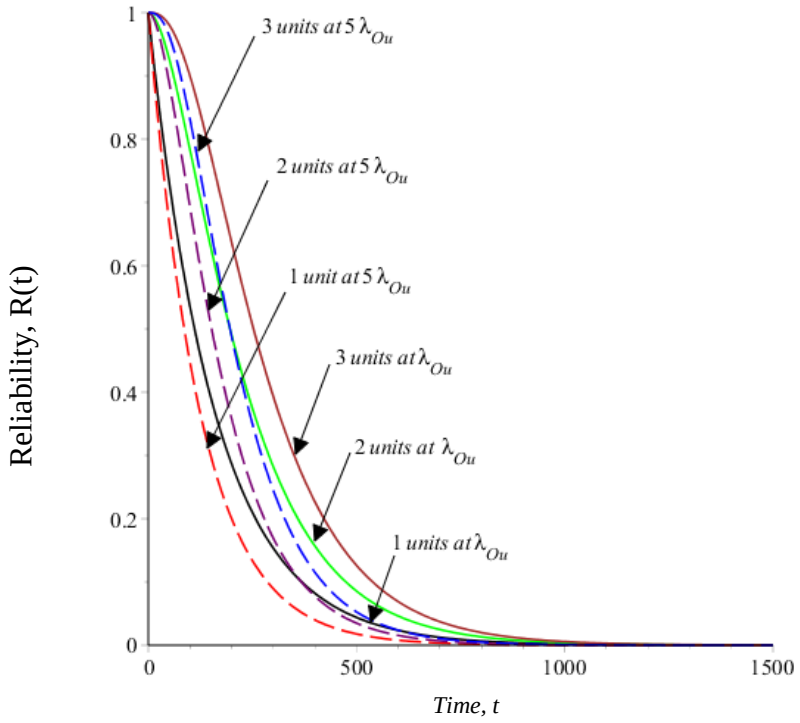

Figure 3-26 Reliability of special cases at increased rate of unsafe hardware failures

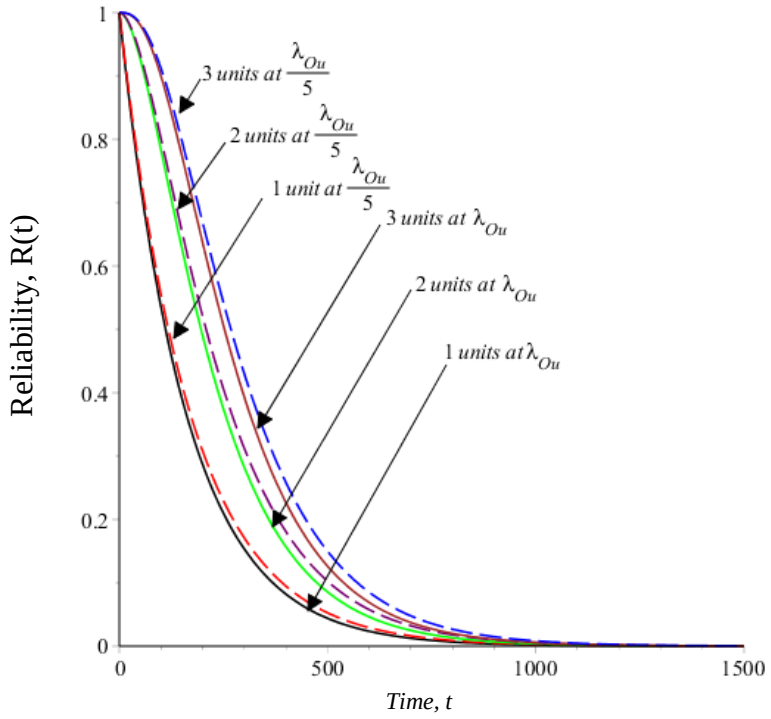

Figure 3-27 Reliability of special cases at decreased rate of unsafe hardware failures

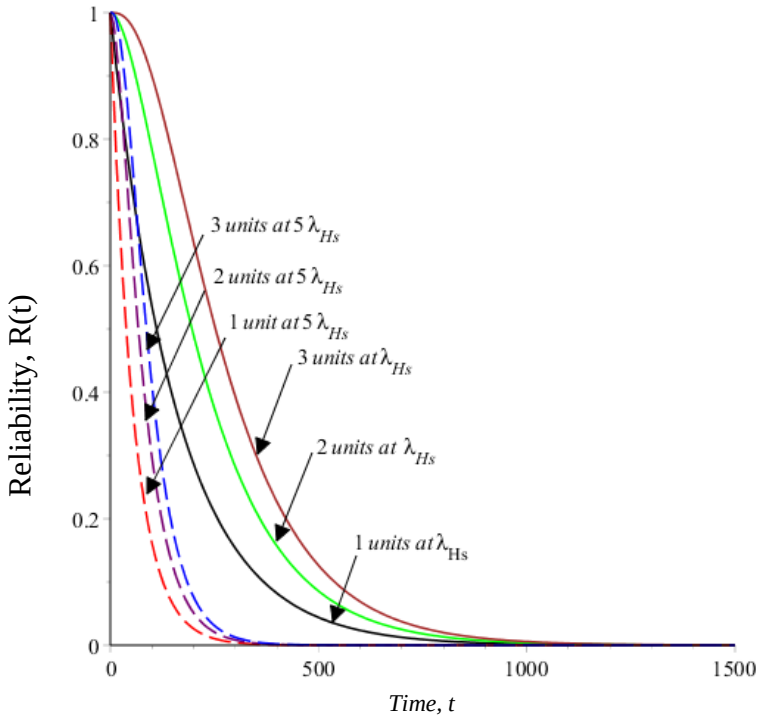

Figure 3-28 Reliability of special cases at increased rate of safe human-errors

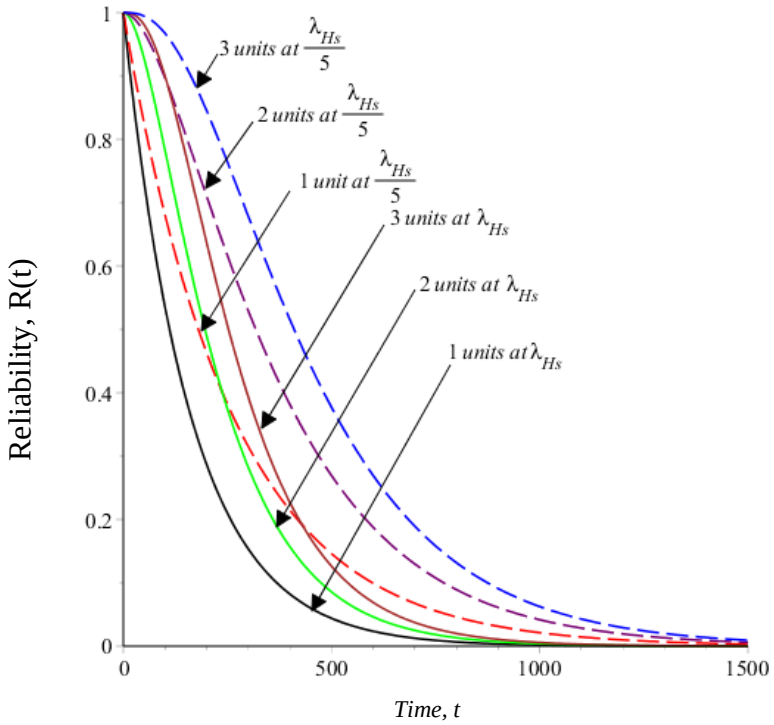

Figure 3-29 Reliability of special cases at decreased rate of safe human-errors

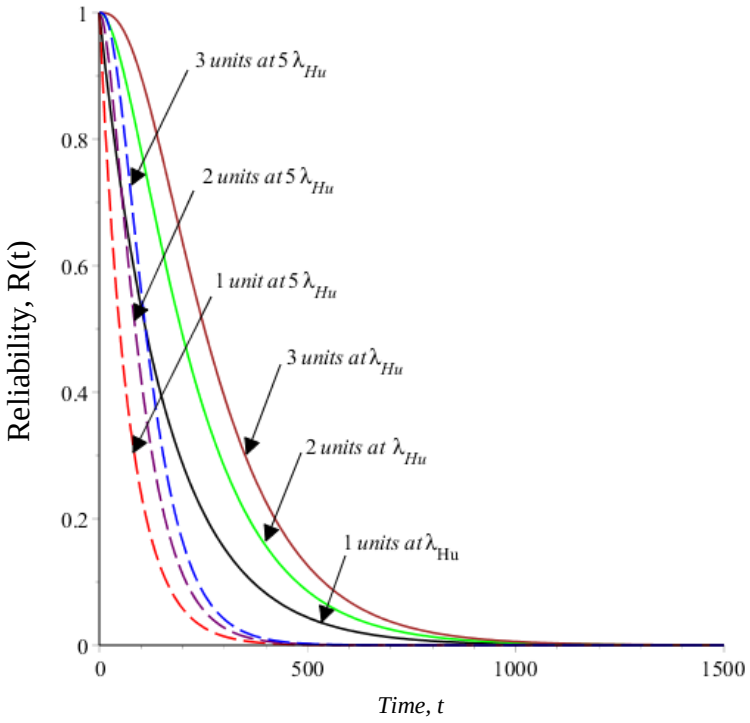

Figure 3-30 Reliability of special cases at increased rate of unsafe human-errors

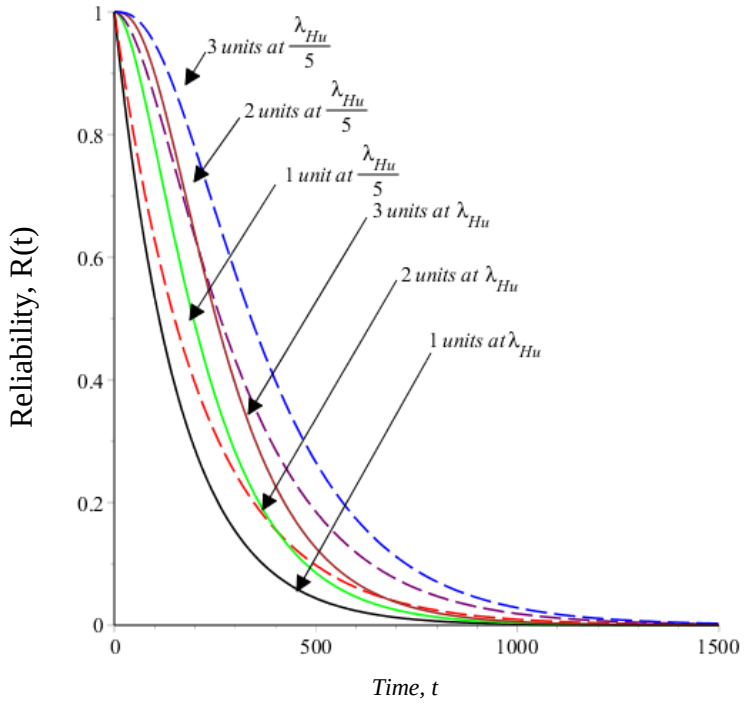

Figure 3-31 Reliability of special cases at decreased rate of unsafe human-errors

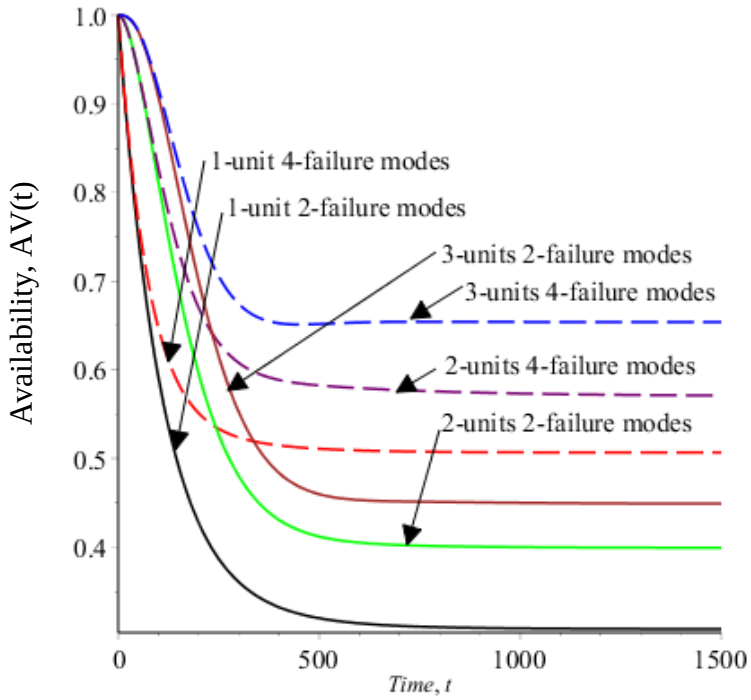

Figure 3-32 Availability of all special cases with two and four failure modes.

Chapter 4 : Reliability and Availability Analysis of Mining Systems with Partial and Complete Failures

4.1 Introduction

This chapter analyses a mining system with single unit in which system fails once this unit fails. The unit failure can be partially or completely. The former can be repaired on-site while the latter can only be repaired in repair workshop. The unit failure is instantly detected and required action is taken to restore the system to the initial state, while the unit on-site. Otherwise, the unit is sent to the repair shop, when on-side checks confirm a complete failure.

In this model, the system may fail due to hardware failure of human-error. Each failure mode has a partial and complete failure rate, and partial and complete repair rate. Whereas the workshop repair rate is the same for all failure modes.

Different values of failure and repair rates were assumed in reference to a certain value. Specifically, each parameter was multiplied by 5, 2, 1, 1/2 and 1/5. Then, the results were used to develop reliability parameters. This provided a reference plot and resulted plots that help in understanding the reliability measures behaviour. This approach was used because of limited data resources and database accesses.

Assumptions

The following assumptions are associated with this model:

i) All failure rate are constant.
ii) All repair rates are constant.
iii) The unit is in new condition at initial state.
iv) The repaired unit is as good as new.
v) There are two repair facilities.
vi) The unit can fail due to hardware failure or human-error.

Notation

n	Number of system states
t	Time in hours
s	Laplace transform variable
μ_1, μ_2	Constant repair rate of on-site facility.
μ_3	Constant repair rate of workshop facility.
λ_1, λ_2	Constant unit partial failure rate.
λ_3, λ_4	Constant unit total failure rate.
AV(t)	System availability at time (*t*)
$P_i(t)$	The probability that the system will be at state *i* at time (*t*), for *i*= 1, 2, 3, …,*n*
$P_i(s)$	The Laplace transform of state probability, for *i*= 1, 2, 3, …,*n*
P_i	Steady state probability for *i*= 1, 2, 3, …,*n*
R(t)	System reliability at time (*t*)
MTTF	System mean time to failure

4.2 System with Hardware Failure and Human-Error

State space diagram in Figure 4-1 presents a system with two failure modes: hardware failure and human-error. Each failure mode could be partial failure or complete failure. In this model, μ_1, λ_1 and μ_2, λ_2 refer to on-site repair and failure rate, λ_3 and λ_4 refer to complete failure rate, and μ_3 refers to workshop repair rate. By using the Markov method, the following equations are obtained:

$$\frac{dP_0(t)}{dt} + P_0(t)\left(\lambda_1 + \lambda_2\right) + P_1(t)\cdot\mu_1 = P_2(t)\cdot\mu_2 + P_3(t)\cdot\mu_3 \quad (4.1)$$

$$\frac{dP_1(t)}{dt} + P_1(t)\left(\lambda_3 + \mu_1\right) = P_0(t)\cdot\lambda_1 \quad (4.2)$$

$$\frac{dP_2(t)}{dt} + P_2(t)\left(\lambda_4 + \mu_2\right) = P_0(t)\cdot\lambda_2 \quad (4.3)$$

$$\frac{dP_3(t)}{dt} + P_3(t)\cdot\mu_3 + P_1(t)\cdot\lambda_3 = P_2(t)\cdot\lambda_4 \quad (4.4)$$

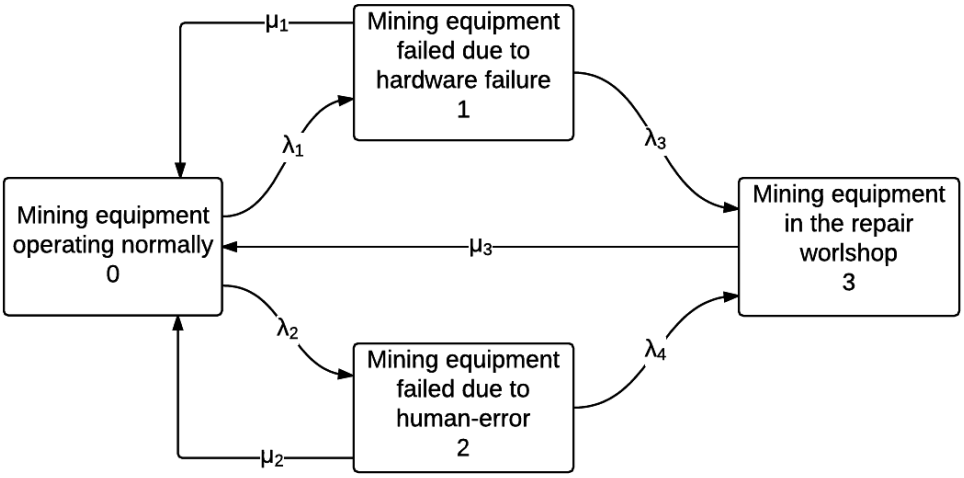

Figure 4-1 State space diagram of single unit with partial or complete failure

At time t=0, $P_0(0)=1$ and all other initial state probabilities are equal to zero. By taking the Laplace transforms of equations (4.1) – (4.4), the following equations are obtained:

$$P_0(s) = \frac{P_1(s)\cdot\mu_1 + P_2(s)\cdot\mu_2 + P_3(s)\cdot\mu_3 + 1}{s+\lambda_1+\lambda_2} \tag{4.5}$$

$$P_1(s) = \frac{P_0(s)\cdot\lambda_1}{s+\lambda_3+\mu_1} \tag{4.6}$$

$$P_2(s) = \frac{P_0(s)\cdot\lambda_2}{s+\lambda_4+\mu_2} \tag{4.7}$$

$$P_3(s) = \frac{P_1(s)\cdot\lambda_3 + P_2(s)\cdot\lambda_4}{s+\mu_3} \tag{4.8}$$

By using the equations (4.5) – (4.8), we get the following equations:

$$P_0(s) = \frac{1}{\left(s+\lambda_1+\lambda_2 - \left(\frac{\lambda_1\cdot\mu_1}{s+\lambda_3+\mu_1} + \frac{\lambda_2\cdot\mu_2}{s+\lambda_4+\mu_2} + \mathrm{K}\right)\right)} \tag{4.9}$$

$$P_1(s) = \frac{\lambda_1}{\left(s+\lambda_3+\mu_1\right)\left(s+\lambda_1+\lambda_2 - \left(\frac{\lambda_1\cdot\mu_1}{s+\lambda_3+\mu_1} + \frac{\lambda_2\cdot\mu_2}{s+\lambda_4+\mu_2} + \mathrm{K}\right)\right)} \tag{4.10}$$

$$P_2(s) = \frac{\lambda_2}{\left(s+\lambda_4+\mu_2\right)\left(s+\lambda_1+\lambda_2-\left(\frac{\lambda_1\cdot\mu_1}{s+\lambda_3+\mu_1}+\frac{\lambda_2\cdot\mu_2}{s+\lambda_4+\mu_2}+\mathrm{K}\right)\right)} \tag{4.11}$$

$$P_3(s) = \frac{\mathrm{K}}{\left(s+\lambda_1+\lambda_2-\left(\frac{\lambda_1\cdot\mu_1}{s+\lambda_3+\mu_1}+\frac{\lambda_2\cdot\mu_2}{s+\lambda_4+\mu_2}+\mathrm{K}\right)\right)} \tag{4.12}$$

Where

$$K = \frac{\left(\lambda_1\cdot\lambda_3\left(s+\lambda_4+\mu_2\right)+\lambda_2\cdot\lambda_4\cdot\left(s+\lambda_3+\mu_1\right)\right)\cdot\mu_3}{\left(s+\mu_3\right)\left(s+\lambda_3+\mu_1\right)\left(s+\lambda_4+\mu_2\right)}$$

The availability in this model equals the probability of initial state as follows:

$$AV(t) = P_0(t) \tag{4.13}$$

System Reliability, MTTF, Steady State Probability

The reliability in this model is the probability of the initial state when system failure is unrepairable. In other words, μ_1, μ_2 and μ_3 are equal zero. By taking the inverse Laplace transform, the time dependent equation of reliability is obtained.

$$R(t) = P_0(t) = \mathrm{e}^{-\left(\lambda_1+\lambda_2\right)t} \tag{4.14}$$

MTTF can be obtained as follows:

$$MTTF = \lim_{s\to o} R(s) = \frac{1}{\lambda_1+\lambda_2} \tag{4.15}$$

The system steady state probabilities can be obtained by applying the final-value theorem on each states probability at s-domain (4.9) – (4.12). The following equations were obtained:

$$P_0 = \frac{\mu_3\left(\lambda_4+\mu_2\right)\left(\lambda_3+\mu_1\right)}{\mathrm{F}+\mathrm{J}} \tag{4.16}$$

$$P_1 = \frac{\lambda_1\mu_3\left(\lambda_4+\mu_2\right)}{\mathrm{F}+\mathrm{J}} \tag{4.17}$$

$$P_2 = \frac{\lambda_2\mu_3\left(\lambda_3+\mu_1\right)}{\mathrm{F}+\mathrm{J}} \tag{4.18}$$

$$P_3 = \frac{\lambda_1\lambda_3\lambda_4 + \lambda_1\lambda_3\mu_2 + \lambda_2\lambda_3\lambda_4 + \lambda_2\lambda_4\mu_1}{\mathrm{F} + \mathrm{J}} \tag{4.19}$$

Where

$$F = \lambda_1\lambda_3\lambda_4 + \lambda_1\lambda_3\mu_2 + \lambda_1\lambda_4\mu_3 + \lambda_1\mu_2\mu_3 + \lambda_2\lambda_3\lambda_4 + \lambda_2\lambda_3\mu_3$$

$$J = \lambda_2\lambda_4\mu_1 + \lambda_2\mu_1\mu_3 + \lambda_3\lambda_4\mu_3 + \lambda_3\mu_2\mu_3 + \lambda_4\mu_1\mu_3 + \mu_1\mu_2\mu_3$$

To analyse the model reliability perimeters, specific values of failure and repair rates are assumed. According to the assumed values, the inverse Laplace transform of state probability equations (4.9) – (4.13) the state probability plot was developed in Figure 4-2, the reliability equation (4.14) was used to develop the plots in Figure 4-3, and availability equations (4.12) was used to develop the plots in Figure 4-4. Detailed plots are presented in Appendix D.1.

$$\lambda_1 = 0.003\ \left(\frac{failure}{hour}\right) \quad \lambda_2 = 0.00027\left(\frac{failure}{hour}\right) \quad \mu_1 = 0.0075\left(\frac{repair}{hour}\right) \quad \mu_2 = 0.004\left(\frac{repair}{hour}\right)$$

$$\lambda_3 = 0.004\ \left(\frac{failure}{hour}\right) \quad \lambda_4 = 0.0052\left(\frac{failure}{hour}\right) \quad \mu_3 = 0.002\ \left(\frac{repair}{hour}\right)$$

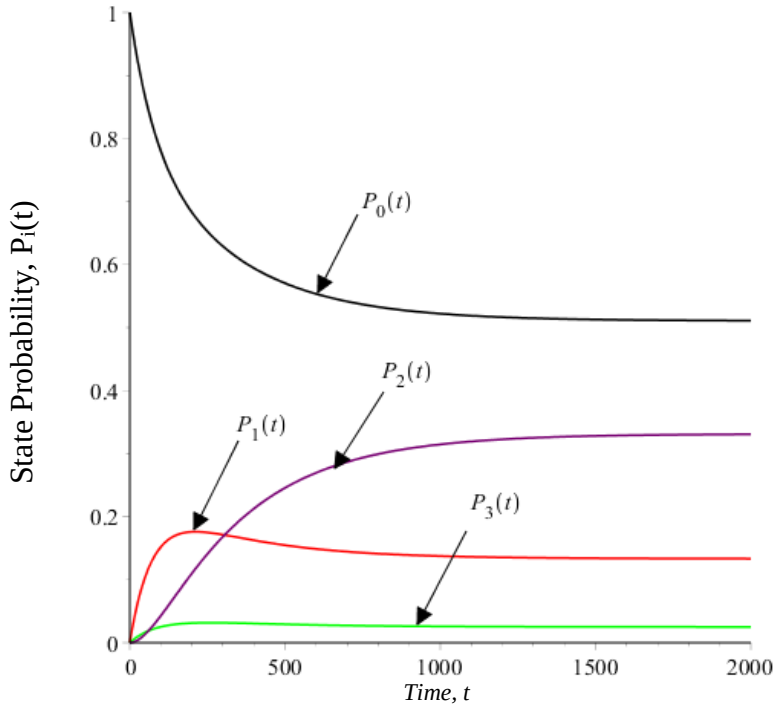

Figure 4-2 State probabilities of single unit with partial or complete failure

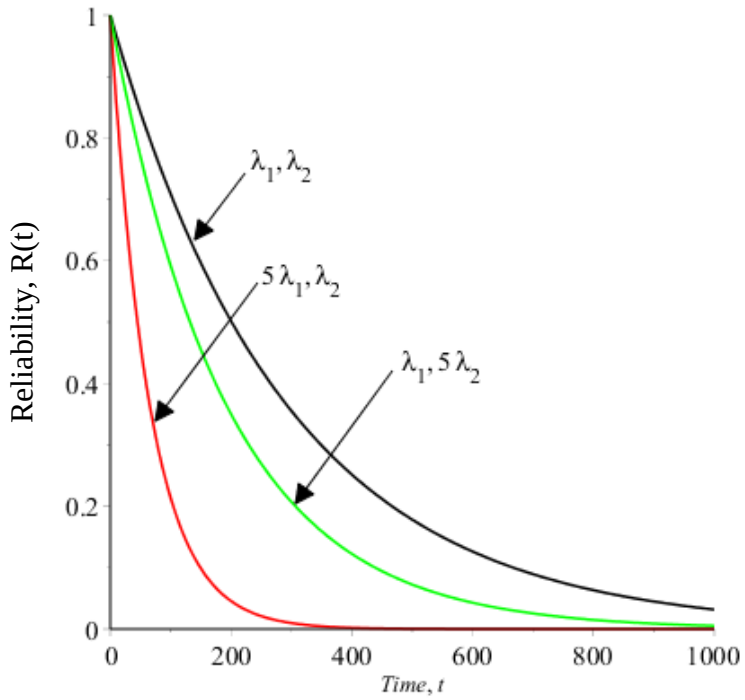

Figure 4-3 Reliability plots of single unit with partial or complete failure at different values of failure rates

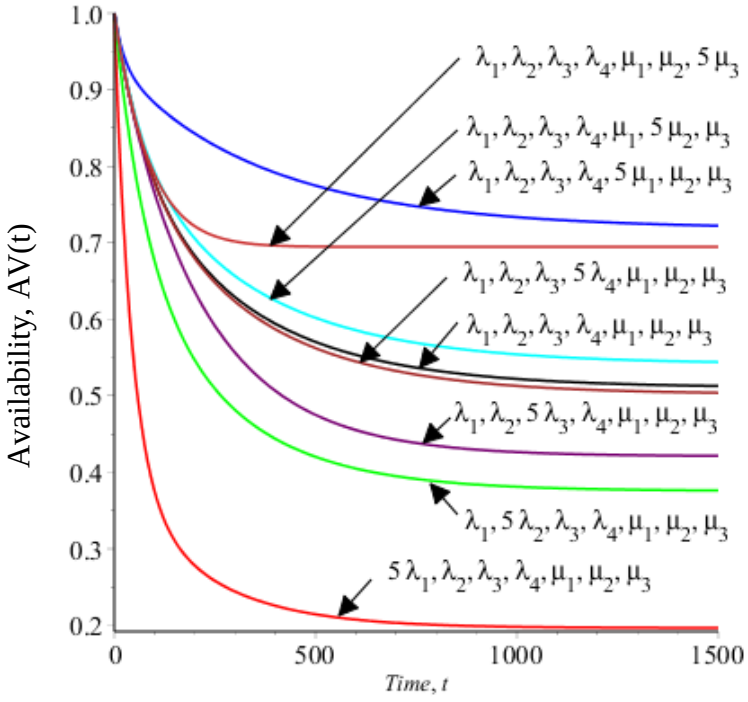

Figure 4-4 Availability of single unit with partial or complete failure at different values of model parameters

4.3 System Safe and Unsafe Failures of Hardware and Human-Error

State space diagram in Figure 4-5 presents a system with on operating state and four failure modes: safe hardware failure, unsafe hardware failure, safe human-error and unsafe human-error. In this model, λ_1, μ_1, λ_2, μ_2, λ_3, μ_3, λ_4, and μ_4, refer to on-site failure and repair rates. Also, λ_5, λ_6, λ_7 and λ_8 refer to complete failure rate, and μ_5 refers to workshop repair rate. By using the Markov method, the following equations were obtained:

$$\frac{dP_0(t)}{dt} + P_0(t)\cdot\sum_{i=1}^{4}\lambda_i = \sum_{i=1}^{5}P_i(t)\cdot\mu_i \tag{4.20}$$

$$\frac{dP_1(t)}{dt} + P_1(t)\left(\mu_1+\lambda_5\right) = P_0(t)\cdot\lambda_1 \tag{4.21}$$

$$\frac{dP_2(t)}{dt} + P_2(t)\left(\mu_2+\lambda_6\right) = P_0(t)\cdot\lambda_2 \tag{4.22}$$

$$\frac{dP_3(t)}{dt} + P_3(t)\left(\mu_3+\lambda_7\right) = P_0(t)\cdot\lambda_3 \tag{4.23}$$

$$\frac{dP_4(t)}{dt} + P_4(t)\left(\mu_4+\lambda_8\right) = P_0(t)\cdot\lambda_4 \tag{4.24}$$

$$\frac{dP_5(t)}{dt} + P_5(t)\cdot\mu_5 = \sum_{i=1}^{4}P_i(t)\cdot\lambda_{i+4} \tag{4.25}$$

At time t=0, $P_0(0)=1$ and all other initial state probabilities are equal to zero. By taking the Laplace transforms of equations (4.20) – (4.25) the following equations are obtained:

$$P_0(s) = \frac{\sum_{i=1}^{5}P_i(s)\cdot\mu_i + 1}{s+\sum_{i=1}^{4}\lambda_i} \tag{4.26}$$

$$P_1(s) = \frac{P_0(s)\,\lambda_1}{s+\mu_1+\lambda_5} \tag{4.27}$$

$$P_2(s) = \frac{P_0(s)\,\lambda_2}{s+\mu_2+\lambda_6} \tag{4.28}$$

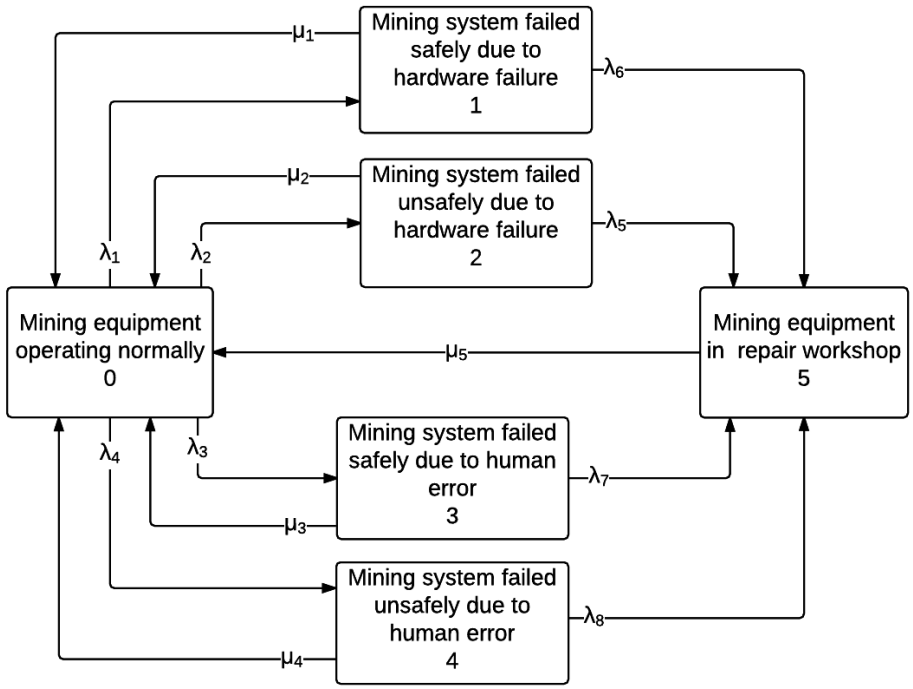

Figure 4-5 State space diagram of single unit with safe and unsafe partial failure modes of hardware failure and human-error

$$P_3(s) = \frac{P_0(s)\,\lambda_3}{s + \mu_3 + \lambda_7} \tag{4.29}$$

$$P_4(s) = \frac{P_0(s)\,\lambda_4}{s + \mu_4 + \lambda_8} \tag{4.30}$$

$$P_5(s) = \frac{P_1(s)\,\lambda_5 + P_2(s)\,\lambda_6 + P_3(s)\,\lambda_7 + P_4(s)\,\lambda_8}{s + \mu_5} \tag{4.31}$$

By using equations (4.26) – (4.31), we get the following equations:

$$P_0(s) = \frac{1}{\left(s + \lambda_1 + \lambda_2 + \lambda_3 + \lambda_4 - \left(J + K\cdot\mu_5\right)\right)} \tag{4.32}$$

$$P_1(s) = \frac{\lambda_1}{\left(s + \mu_1 + \lambda_5\right)\left(s + \lambda_1 + \lambda_2 + \lambda_3 + \lambda_4 - \left(J + K\cdot\mu_5\right)\right)} \tag{4.33}$$

$$P_2(s) = \frac{\lambda_2}{\left(s + \mu_2 + \lambda_6\right)\left(s + \lambda_1 + \lambda_2 + \lambda_3 + \lambda_4 - \left(J + K\cdot\mu_5\right)\right)} \tag{4.34}$$

$$P_3(s) = \frac{\lambda_3}{\left(s + \mu_3 + \lambda_7\right)\left(s + \lambda_1 + \lambda_2 + \lambda_3 + \lambda_4 - \left(J + K\cdot\mu_5\right)\right)} \tag{4.35}$$

$$P_4(s) = \frac{\lambda_4}{\left(s+\mu_4+\lambda_8\right)\left(s+\lambda_1+\lambda_2+\lambda_3+\lambda_4-\left(J+K\cdot\mu_5\right)\right)} \tag{4.36}$$

$$P_5(s) = \frac{\left(\frac{\lambda_1\cdot\lambda_5}{s+\mu_1+\lambda_5}+\frac{\lambda_2\cdot\lambda_6}{s+\mu_2+\lambda_6}+\frac{\lambda_3\cdot\lambda_7}{s+\mu_3+\lambda_7}+\frac{\lambda_4\cdot\lambda_8}{s+\mu_4+\lambda_8}\right)}{\left(s+\mu_5\right)\left(s+\lambda_1+\lambda_2+\lambda_3+\lambda_4-\left(J+K\cdot\mu_5\right)\right)} \tag{4.37}$$

Where

$$J = \frac{\lambda_1\cdot\mu_1}{s+\mu_1+\lambda_5}+\frac{\lambda_2\cdot\mu_2}{s+\mu_2+\lambda_6}+\frac{\lambda_3\cdot\mu_3}{s+\mu_3+\lambda_7}+\frac{\lambda_4\cdot\mu_4}{s+\mu_4+\lambda_8}$$

$$K = \frac{\left(\frac{\lambda_1\cdot\lambda_5}{s+\mu_1+\lambda_5}+\frac{\lambda_2\cdot\lambda_6}{s+\mu_2+\lambda_6}+\frac{\lambda_3\cdot\lambda_7}{s+\mu_3+\lambda_7}+\frac{\lambda_4\cdot\lambda_8}{s+\mu_4+\lambda_8}\right)}{s+\mu_5}$$

The availability in this model equals the probability of initial state as follows:

$$AV(t) = P_0(t) \tag{4.38}$$

System Reliability, MTTF and Steady State Probabilities

In general, the reliability of a system is total probabilities of all operating states when system failure is unrepairable. Thus, this model reliability probability of $P_o(t)$ when $\mu_1 = \mu_2 = \mu_3 = \mu_4 = 0$. Then, reliability can be obtained as follows:

$$R(t) = P_0(t) = e^{-\left(\lambda_1+\lambda_2+\lambda_3+\lambda_4\right)t} \tag{4.39}$$

MTTF can be drived from the relibility equation as follows:

$$MTTF = \lim_{s\to 0} R(s) = \frac{1}{\lambda_1+\lambda_2+\lambda_3+\lambda_4} \tag{4.40}$$

By using the final-value theorem, the equation of steady state probabilities are obtained as follows:

$$P_0 = \frac{\left(\mu_1+\lambda_5\right)\left(\mu_2+\lambda_6\right)\left(\mu_3+\lambda_7\right)\left(\mu_4+\lambda_8\right)\mu_5}{W_5} \tag{4.41}$$

$$P_1 = \frac{\lambda_1 \left(\mu_2 + \lambda_6\right)\left(\mu_3 + \lambda_7\right)\left(\mu_4 + \lambda_8\right)\mu_5}{W_5} \tag{4.42}$$

$$P_2 = \frac{\lambda_2 \left(\mu_1 + \lambda_5\right)\left(\mu_3 + \lambda_7\right)\left(\mu_4 + \lambda_8\right)\mu_5}{W_5} \tag{4.43}$$

$$P_3 = \frac{\lambda_3 \left(\mu_1 + \lambda_5\right)\left(\mu_2 + \lambda_6\right)\left(\mu_4 + \lambda_8\right)\mu_5}{W_5} \tag{4.44}$$

$$P_4 = \frac{\lambda_4 \left(\mu_1 + \lambda_5\right)\left(\mu_2 + \lambda_6\right)\left(\mu_3 + \lambda_7\right)\mu_5}{W_5} \tag{4.45}$$

$$P_5 = \frac{\prod_{i=1}^{4}\left(\mu_i + \lambda_{i+4}\right)}{\mu_5 W_5}\left(\frac{\lambda_1 \cdot \mu_5 \cdot \lambda_5}{\left(\mu_1 + \lambda_5\right)} + \frac{\lambda_2 \cdot \mu_5 \cdot \lambda_6}{\left(\mu_2 + \lambda_6\right)} + \frac{\lambda_3 \cdot \mu_5 \cdot \lambda_7}{\left(\mu_3 + \lambda_7\right)} + \frac{\lambda_4 \cdot \mu_5 \cdot \lambda_8}{\left(\mu_4 + \lambda_8\right)}\right) \tag{4.46}$$

Where

$$\begin{aligned}
W_5 = {} & \lambda_1\lambda_5\lambda_6\lambda_7\lambda_8 + \lambda_1\lambda_5\lambda_6\lambda_7\mu_4 + \lambda_1\lambda_5\lambda_6\lambda_8\mu_3 + \lambda_1\lambda_5\lambda_6\mu_3\mu_4 + \lambda_1\lambda_5\lambda_7\lambda_8\mu_2 \\
& + \lambda_1\lambda_5\lambda_7\mu_2\mu_4 + \lambda_1\lambda_5\lambda_8\mu_2\mu_3 + \lambda_1\lambda_5\mu_2\mu_3\mu_4 + \lambda_1\lambda_6\lambda_7\lambda_8\mu_5 + \lambda_1\lambda_6\lambda_7\mu_4\mu_5 \\
& + \lambda_1\lambda_6\lambda_8\mu_3\mu_5 + \lambda_1\lambda_6\mu_3\mu_4\mu_5 + \lambda_1\lambda_7\lambda_8\mu_2\mu_5 + \lambda_1\lambda_7\mu_2\mu_4\mu_5 + \lambda_1\lambda_8\mu_2\mu_3\mu_5 \\
& + \lambda_1\mu_2\mu_3\mu_4\mu_5 + \lambda_2\lambda_5\lambda_6\lambda_7\lambda_8 + \lambda_2\lambda_5\lambda_6\lambda_7\mu_4 + \lambda_2\lambda_5\lambda_6\lambda_8\mu_3 + \lambda_2\lambda_5\lambda_6\mu_3\mu_4 \\
& + \lambda_2\lambda_5\lambda_7\lambda_8\mu_5 + \lambda_2\lambda_5\lambda_7\mu_4\mu_5 + \lambda_2\lambda_5\lambda_8\mu_3\mu_5 + \lambda_2\lambda_5\mu_3\mu_4\mu_5 + \lambda_2\lambda_6\lambda_7\lambda_8\mu_1 \\
& + \lambda_2\lambda_6\lambda_7\mu_1\mu_4 + \lambda_2\lambda_6\lambda_8\mu_1\mu_3 + \lambda_2\lambda_6\mu_1\mu_3\mu_4 + \lambda_2\lambda_7\lambda_8\mu_1\mu_5 + \lambda_2\lambda_7\mu_1\mu_4\mu_5 \\
& + \lambda_2\lambda_8\mu_1\mu_3\mu_5 + \lambda_2\mu_1\mu_3\mu_4\mu_5 + \lambda_3\lambda_5\lambda_6\lambda_7\lambda_8 + \lambda_3\lambda_5\lambda_6\lambda_7\mu_4 + \lambda_3\lambda_5\lambda_6\lambda_8\mu_5 \\
& + \lambda_3\lambda_5\lambda_6\mu_4\mu_5 + \lambda_3\lambda_5\lambda_7\lambda_8\mu_2 + \lambda_3\lambda_5\lambda_7\mu_2\mu_4 + \lambda_3\lambda_5\lambda_8\mu_2\mu_5 + \lambda_3\lambda_5\mu_2\mu_4\mu_5 \\
& + \lambda_3\lambda_6\lambda_7\lambda_8\mu_1 + \lambda_3\lambda_6\lambda_7\mu_1\mu_4 + \lambda_3\lambda_6\lambda_8\mu_1\mu_5 + \lambda_3\lambda_6\mu_1\mu_4\mu_5 + \lambda_3\lambda_7\lambda_8\mu_1\mu_2 \\
& + \lambda_3\lambda_7\mu_1\mu_2\mu_4 + \lambda_3\lambda_8\mu_1\mu_2\mu_5 + \lambda_3\mu_1\mu_2\mu_4\mu_5 + \lambda_4\lambda_5\lambda_6\lambda_7\lambda_8 + \lambda_4\lambda_5\lambda_6\lambda_7\mu_5 \\
& + \lambda_4\lambda_5\lambda_6\lambda_8\mu_3 + \lambda_4\lambda_5\lambda_6\mu_3\mu_5 + \lambda_4\lambda_5\lambda_7\lambda_8\mu_2 + \lambda_4\lambda_5\lambda_7\mu_2\mu_5 + \lambda_4\lambda_5\lambda_8\mu_2\mu_3 \\
& + \lambda_4\lambda_5\mu_2\mu_3\mu_5 + \lambda_4\lambda_6\lambda_7\lambda_8\mu_1 + \lambda_4\lambda_6\lambda_7\mu_1\mu_5 + \lambda_4\lambda_6\lambda_8\mu_1\mu_3 + \lambda_4\lambda_6\mu_1\mu_3\mu_5 \\
& + \lambda_4\lambda_7\lambda_8\mu_1\mu_2 + \lambda_4\lambda_7\mu_1\mu_2\mu_5 + \lambda_4\lambda_8\mu_1\mu_2\mu_3 + \lambda_4\mu_1\mu_2\mu_3\mu_5 + \lambda_5\lambda_6\lambda_7\lambda_8\mu_5 \\
& + \lambda_5\lambda_6\lambda_7\mu_4\mu_5 + \lambda_5\lambda_6\lambda_8\mu_3\mu_5 + \lambda_5\lambda_6\mu_3\mu_4\mu_5 + \lambda_5\lambda_7\lambda_8\mu_2\mu_5 + \lambda_5\lambda_7\mu_2\mu_4\mu_5 \\
& + \lambda_5\lambda_8\mu_2\mu_3\mu_5 + \lambda_5\mu_2\mu_3\mu_4\mu_5 + \lambda_6\lambda_7\lambda_8\mu_1\mu_5 + \lambda_6\lambda_7\mu_1\mu_4\mu_5 + \lambda_6\lambda_8\mu_1\mu_3\mu_5 \\
& + \lambda_6\mu_1\mu_3\mu_4\mu_5 + \lambda_7\lambda_8\mu_1\mu_2\mu_5 + \lambda_7\mu_1\mu_2\mu_4\mu_5 + \lambda_8\mu_1\mu_2\mu_3\mu_5 + \mu_1\mu_2\mu_3\mu_4\mu_5
\end{aligned}$$

To analyse the model reliability, specific values of failure and repair rates are assumed. Accordingly, the inverse Laplace transforms of equations (4.32) – (4.37) were used to develop plots in Figure 4-6, the reliability equation (4.39) was used to develop the plots in Figure 4-7, the availability equation(4.38) was used to develop the plots in Figure 4-8 and Figure 4-9. Detailed plots are presented in Appendix D.2.

$\lambda_1 = 0.0025 \left(\frac{failure}{hour}\right)$ $\mu_1 = 0.005 \left(\frac{repair}{hour}\right)$ $\lambda_5 = 0.002 \left(\frac{failure}{hour}\right)$ $\lambda_6 = 0.0002 \left(\frac{failure}{hour}\right)$

$\lambda_2 = 0.00025 \left(\frac{failure}{hour}\right)$ $\mu_2 = 0.0025 \left(\frac{repair}{hour}\right)$ $\lambda_7 = 0.002 \left(\frac{failure}{hour}\right)$ $\lambda_8 = 0.005 \left(\frac{failure}{hour}\right)$

$\lambda_3 = 0.0005 \left(\frac{failure}{hour}\right)$ $\mu_3 = 0.0025 \left(\frac{repair}{hour}\right)$ $\mu_5 = 0.002 \left(\frac{repair}{hour}\right)$

$\lambda_4 = 0.0002 \left(\frac{failure}{hour}\right)$ $\mu_4 = 0.0015 \left(\frac{repair}{hour}\right)$

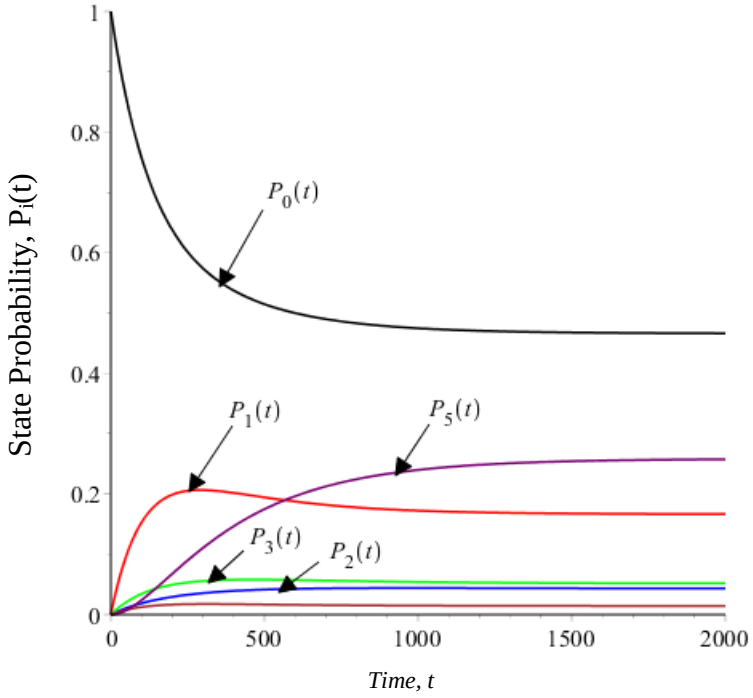

Figure 4-6 State probabilities of single unit with safe and unsafe partial failures of hardware and human-error

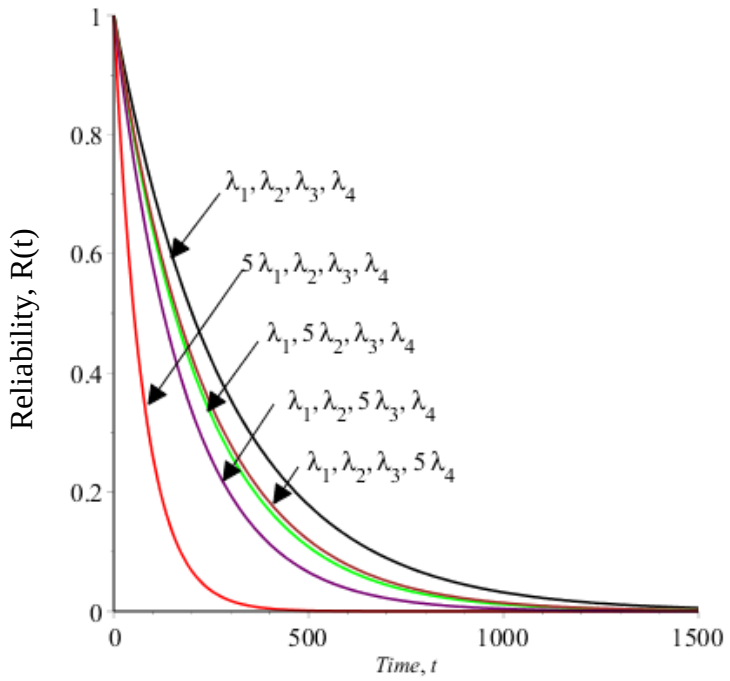

Figure 4-7 Reliability of single unit with safe and unsafe partial failures of hardware and human-error at different values of failure rates

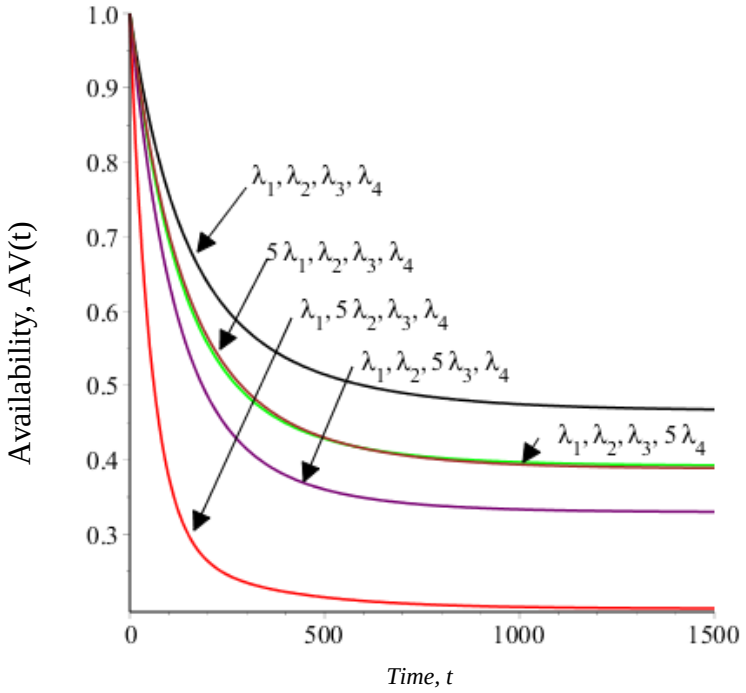

Figure 4-8 Availability of single unit with safe and unsafe partial failures of hardware and human-error at different values of failure rates

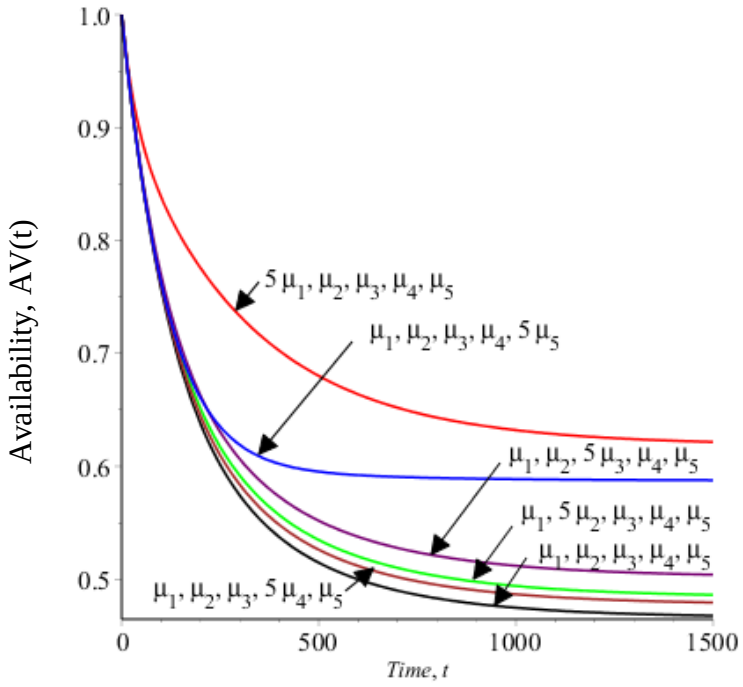

Figure 4-9 Availability of single unit with safe and unsafe partial failures of hardware and human-error at different values of repair rates

4.4 Discussion

The models of this chapter shows the reliability and availability of system when two repair facilities were used: on-site and workshop. It was noticed that, state probabilities plots give a general overview of model behaviour to identify critical states and model parameters. According to assumed model parameters, the reliability measures are significantly influenced by the on-site repair rates.

Chapter 5 Miscellaneous Models

5.1 Mining System Maintenance with Human-Error

This section discusses the human performance in mining task that may be performed normally or with human-error. If the human-error was classified into non-critical and critical, the following models were analysed:

1- Critical and non-critical human-error.

2- Critical and non-critical human-error considering the environment and stress level.

Different values of transfer rates were assumed in reference to a certain value. Specifically, each parameter was multiplied by 5, 2, 1, 1/2 and 1/5. Then, the results were used to develop reliability parameter. This provides a reference plot and resulted plots that help in understanding the reliability measures behaviour. This approach was used because of limited data resources and database accesses.

Assumptions

The following assumptions are associated with this model:

vii) Worker critical and non-critical error rates are constant
viii) All errors occur independently.
ix) The worker performs a time continuous task.

Notation

n	Number of states
t	Time in hours
s	Laplace transform variable

α_1	Constant transition rate associated with changing the work environment from normal to abnormal.
α_2	Constant transition rate associated with changing the work environment from abnormal to normal.
λ_i	Constant error rate for i= 1, 2, 3…n
$P_i(t)$	The probability that the worker will be at state *i* at time (*t*), for *i*= 1, 2, 3, …,*n*
$P_i(s)$	The Laplace transform of state probability, for *i*= 1, 2, 3, …,*n*
R(t)	worker reliability at time (*t*)
MTTF	worker mean time to error

5.1.1 **Worker Performance with Critical and Non-Critical Human-Error**

The state space diagram in Figure 5-1shows a model of worker task performance that can be performed normally, non-critical human-error or critical human-error.

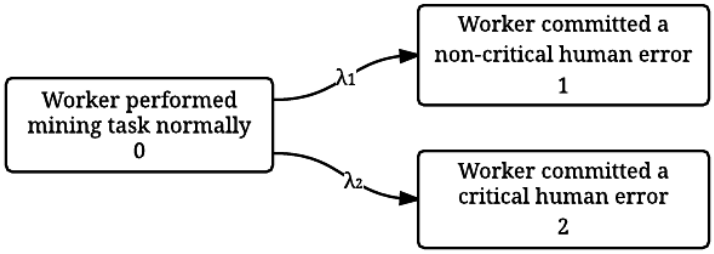

Figure 5-1 State space diagram of maintenance work

By using the Markov method to analyse this model, the associated differential equations are obtained as follows:

$$\frac{dP_0(t)}{dt} + P_0(t)\left(\lambda_1 + \lambda_2\right) = 0 \tag{5.1}$$

$$\frac{dP_1(t)}{dt} = P_0(t)\cdot\lambda_1 \tag{5.2}$$

$$\frac{dP_2(t)}{dt} = P_0(t)\cdot\lambda_2 \tag{5.3}$$

At time t=0, $P_0(0)=1$ and all other initial state probabilities are equal to zero. By taking the Laplace transforms of equations (5.1) – (5.3), the following equations are obtained:

$$P_0(s) = \frac{1}{s + \lambda_1 + \lambda_2} \tag{5.4}$$

$$P_1(s) = \frac{P_0(s) \cdot \lambda_1}{s} \tag{5.5}$$

$$P_2(s) = \frac{P_0(s) \cdot \lambda_2}{s} \tag{5.6}$$

By taking the inverse Laplace Transform of equations (5.4) – (5.6), time dependent probabilities are obtained.

$$P_0(t) = e^{-(\lambda_1 + \lambda_2)t} \tag{5.7}$$

$$P_1(t) = \frac{\lambda_1 \left(1 - e^{-(\lambda_1 + \lambda_2)t}\right)}{\lambda_1 + \lambda_2} \tag{5.8}$$

$$P_2(t) = \frac{\lambda_2 \left(1 - e^{-(\lambda_1 + \lambda_2)t}\right)}{\lambda_1 + \lambda_2} \tag{5.9}$$

Human Reliability, MTTF and Steady State Probabilities

In this simple model, human reliability is when worker perform maintenance work normally.

$$R(t) = P_0(t) \tag{5.10}$$

MTTF can be drived from the relibility equation as follows:

$$MTTF = \lim_{s \to 0} R(s) = \frac{1}{\lambda_1 + \lambda_2} \tag{5.11}$$

To develop reliability plots, specific values of error rates are assumed. Accordingly, the state probability equations (5.7) – (5.9) were used to develop the plots in Figure 5-2, and reliability equation (5.10) was used to develop the plots in Figure 5-3. Detailed plots are presented in Appendix E.1.

$$\lambda_1 = 0.001 \left(\frac{error}{hour}\right) \quad \lambda_2 = 0.0005 \left(\frac{error}{hour}\right)$$

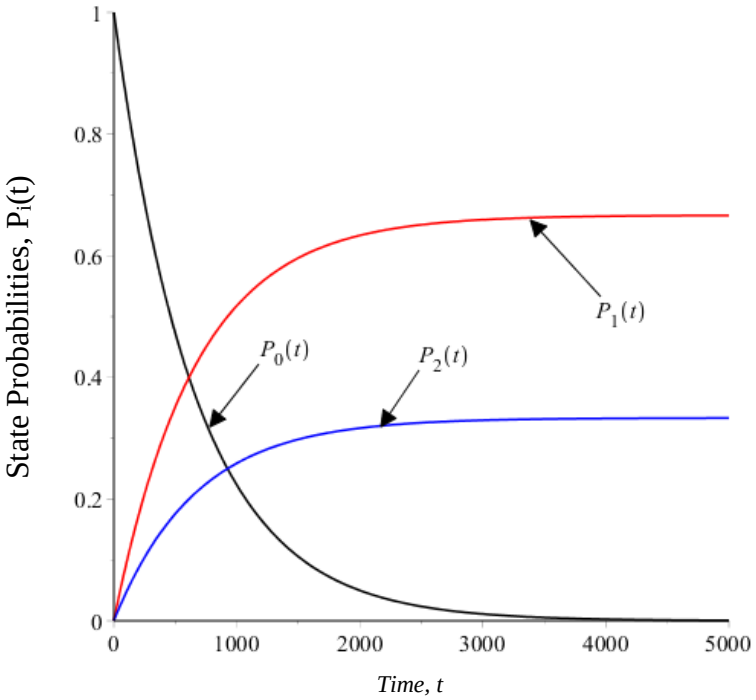

Figure 5-2 State probabilities of task performance

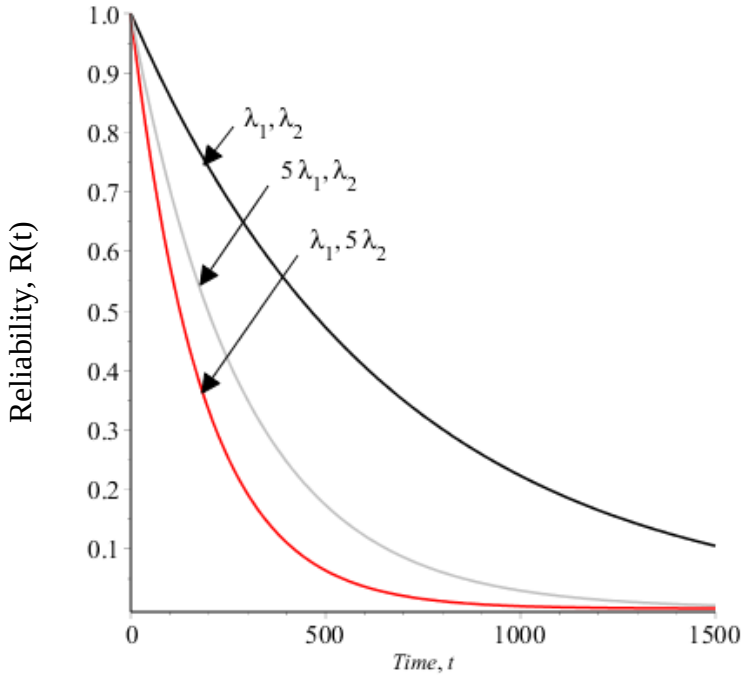

Figure 5-3 Reliability of task performance at different values of failure rates

5.1.1 **Worker Performance under Different levels of Stress.**

This model, Figure 5-4, is similar to last one, however, the task performance may be committed non-critical or critical human-error under different level of work environment and stress level. By using the Markov method to perform reliability analysis of the state space diagram in Figure 5-4, the following differential equations are obtained.

$$\frac{dP_0(t)}{dt} + P_0(t)\left(\lambda_1 + \lambda_2 + \alpha_1\right) = P_5(t)\cdot\alpha_2 \tag{5.12}$$

$$\frac{dP_1(t)}{dt} = P_0(t)\cdot\lambda_1 \tag{5.13}$$

$$\frac{dP_2(t)}{dt} = P_0(t)\cdot\lambda_2 \tag{5.14}$$

$$\frac{dP_3(t)}{dt} = P_5(t)\cdot\lambda_3 \tag{5.15}$$

$$\frac{dP_4(t)}{dt} = P_5(t)\cdot\lambda_4 \tag{5.16}$$

$$\frac{dP_5(t)}{dt} + P_5(t)\left(\lambda_3 + \lambda_4 + \alpha_2\right) = P_0\cdot\alpha_1 \tag{5.17}$$

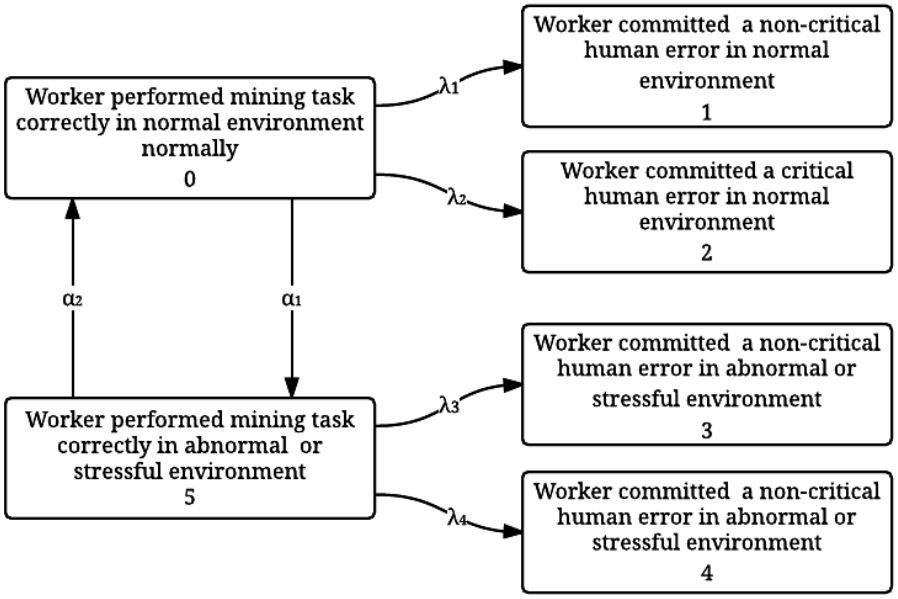

Figure 5-4 State space diagram of task performance considering the work environment

The task starts under normal environment that at time t=0, $P_0(0)=1$ and all other initial state probabilities are equal to zero. By taking the Laplace transforms of equations (5.12) – (5.17), the following equations are obtained:

$$P_0(s) = \frac{\left(P_5(s)\cdot\alpha_2 + 1\right)}{s + \lambda_1 + \lambda_2 + \alpha_1} \tag{5.18}$$

$$P_1(s) = \frac{P_0(s)\cdot\lambda_1}{s} \tag{5.19}$$

$$P_2(s) = \frac{P_0(s)\cdot\lambda_2}{s} \tag{5.20}$$

$$P_3(s) = \frac{P_5(s)\cdot\lambda_3}{s} \tag{5.21}$$

$$P_4(s) = \frac{P_5(s)\cdot\lambda_4}{s} \tag{5.22}$$

$$P_5(s) = \frac{P_0(s)\cdot\alpha_1}{s + \lambda_3 + \lambda_4 + \alpha_2} \tag{5.23}$$

By using the equations (5.18) – (5.23), we get the following equations:

$$P_0(s) = \frac{\left(s + \lambda_3 + \lambda_4 + \alpha_2\right)}{\left(\left(s + \lambda_1 + \lambda_2 + \alpha_1\right)\left(s + \lambda_3 + \lambda_4 + \alpha_2\right) - \alpha_1\cdot\alpha_2\right)} \tag{5.24}$$

$$P_1(s) = \frac{\lambda_1\cdot\left(s + \lambda_3 + \lambda_4 + \alpha_2\right)}{s\cdot\left(\left(s + \lambda_1 + \lambda_2 + \alpha_1\right)\left(s + \lambda_3 + \lambda_4 + \alpha_2\right) - \alpha_1\cdot\alpha_2\right)} \tag{5.25}$$

$$P_2(s) = \frac{\lambda_2\cdot\left(s + \lambda_3 + \lambda_4 + \alpha_2\right)}{s\cdot\left(\left(s + \lambda_1 + \lambda_2 + \alpha_1\right)\left(s + \lambda_3 + \lambda_4 + \alpha_2\right) - \alpha_1\cdot\alpha_2\right)} \tag{5.26}$$

$$P_3(s) = \frac{\lambda_3\cdot\alpha_1}{s\left(\left(s + \lambda_1 + \lambda_2 + \alpha_1\right)\left(s + \lambda_3 + \lambda_4 + \alpha_2\right) - \alpha_1\cdot\alpha_2\right)} \tag{5.27}$$

$$P_4(s) = \frac{\lambda_4\cdot\alpha_1}{s\left(\left(s + \lambda_1 + \lambda_2 + \alpha_1\right)\left(s + \lambda_3 + \lambda_4 + \alpha_2\right) - \alpha_1\cdot\alpha_2\right)} \tag{5.28}$$

$$P_5(s) = \frac{\alpha_1}{\left(\left(s + \lambda_1 + \lambda_2 + \alpha_1\right)\left(s + \lambda_3 + \lambda_4 + \alpha_2\right) - \alpha_1\cdot\alpha_2\right)} \tag{5.29}$$

System Reliability, MTTF, Steady State Probability

The reliability of the model is the states where worker performed the task normally, whether under normal or abnormal environment.

$$R(t) = P_0(t) + P_5(t) \tag{5.30}$$

MTTF can be drived from the reliability equation by using $\lim_{s \to 0} R(s)$ as follows.

$$MTTF = \frac{\lambda_3 + \lambda_4 + \alpha_2 + \alpha_1}{\alpha_1 \lambda_3 + \alpha_1 \lambda_4 + \alpha_2 \lambda_1 + \alpha_2 \lambda_2 + \lambda_1 \lambda_3 + \lambda_1 \lambda_4 + \lambda_2 \lambda_3 + \lambda_2 \lambda_4} \tag{5.31}$$

To develop reliability plots, specific values of error and environment transition rates are assumed. Accordingly, the inverse Laplace transforms of equations (5.24) – (5.29) were used to develop the plots in Figure 5-5, and the reliability equation (5.30) was used to develop the plots in Figure 5-6. Detailed plots are presented in Appendix E.2.

$$\alpha_1 = 0.002\left(\frac{transition}{hour}\right) \quad \alpha_2 = 0.002\left(\frac{transition}{hour}\right) \quad \lambda_1 = 0.0015\left(\frac{error}{hour}\right)$$
$$\lambda_2 = 0.0005\left(\frac{error}{hour}\right) \quad \lambda_3 = 0.0005\left(\frac{error}{hour}\right) \quad \lambda_4 = 0.001\left(\frac{error}{hour}\right)$$

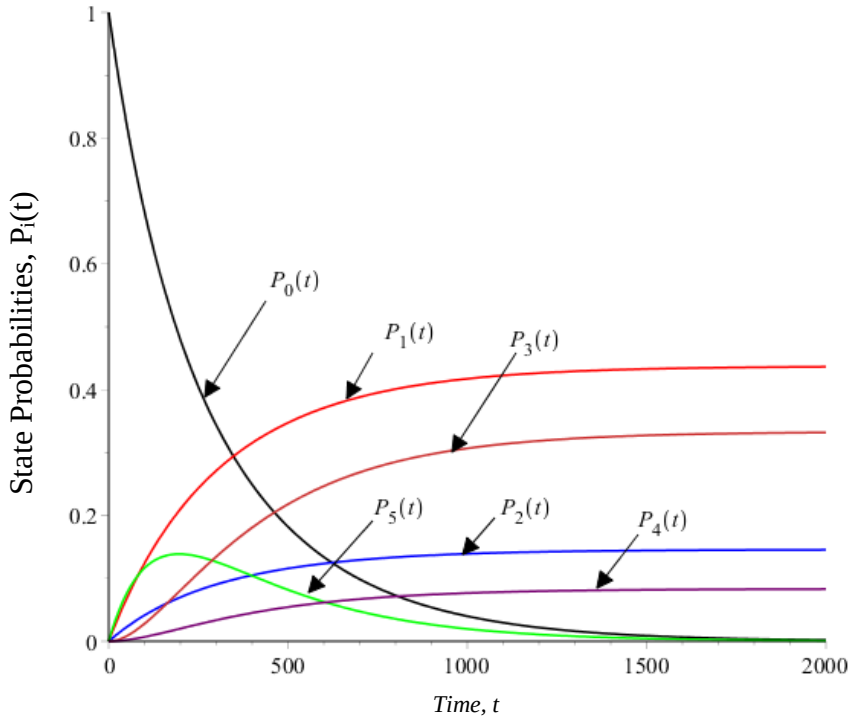

Figure 5-5 State probabilities of task performance considering the work environment

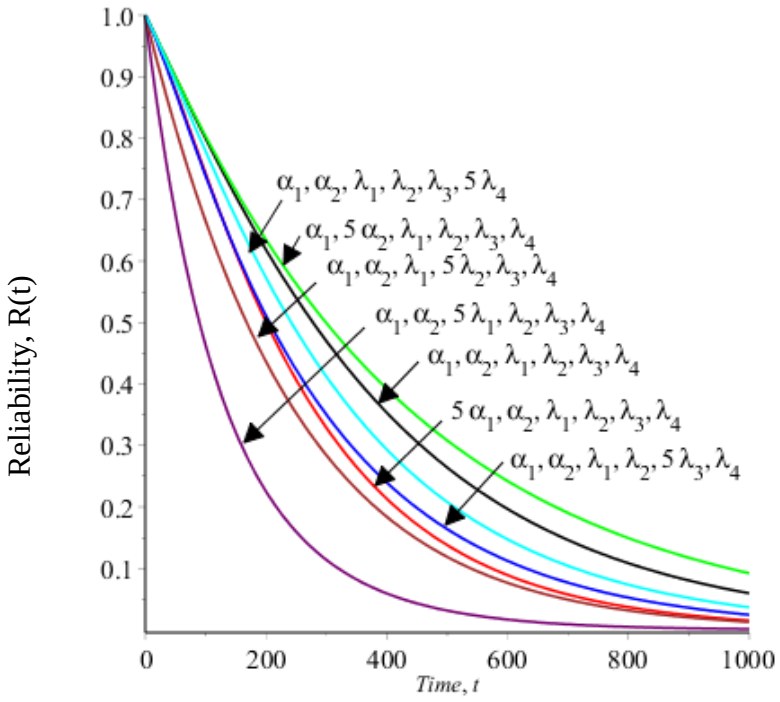

Figure 5-6 Reliability plots of task performance considering the work environment at different values of model parameters

5.2 One- Unit System with Three Operational States and One Failure Mode

This section studies the behaviour of a system with different working conditions. The space state diagram in Figure 5-7 shows a single unit mining system that could be working normally or unsafely due to either a non-human-error or a human-error. The system unsafe working conditions might be identified and appropriate step is taken to restore the system to the normal working state. The system failure is possible at any working state. When the system fails, failure is instantly identified and appropriate step is taken to restore the system to one of the working conditions, namely, normal, unsafe due to non-human-error or unsafe due to human-error.

Assumptions:

The following assumptions are associated with this model:

i) All failures are statistically independent.

ii) All failure and repair rates are constant.

iii) The repaired system is as good as new.

iv) There are two repair facilities.

v) The system may fail due to hardware failure or human-error.

Notation

n	Number of system states units
t	Time in hours
s	Laplace transform variable
λ_u	Constant transition rate of unsafe working state due to non-human-error
λ_h	Constant transition rate of unsafe working state due to human-error
$\lambda_1, \lambda_2, \lambda_f$	Constant failure rate
μ_u, μ_h	Constant repair rate of unsafe working states
μ_1, μ_2, μ_f	Constant repair rate of system failure
AV(t)	System availability at time (*t*)
$P_i(t)$	The probability that the system will be at state *i* at time (*t*), for *i*= 1, 2, 3, …,*n*
$P_i(s)$	The Laplace transform of state probability, for *i*= 1, 2, 3, …,*n*
R(t)	System reliability at time (*t*)
MTTF	System mean time to failure

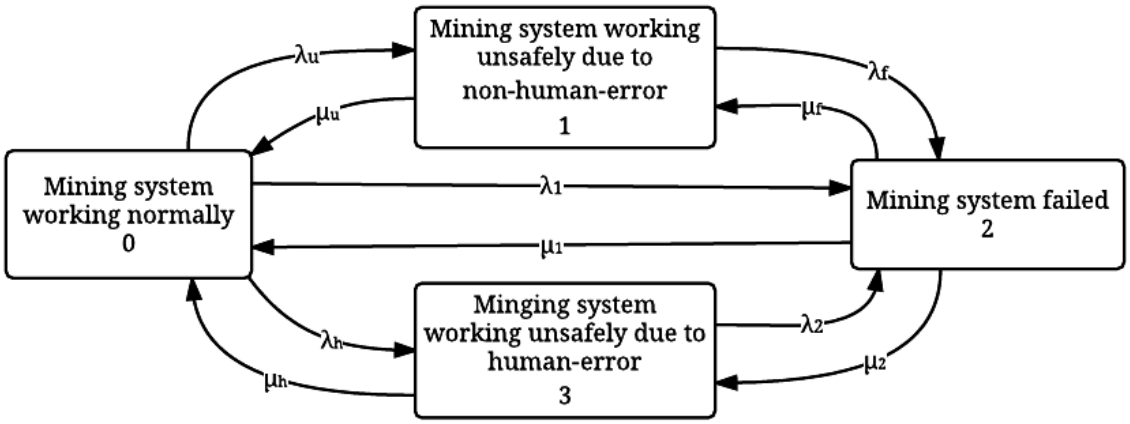

Figure 5-7 State space diagram for a system with three operating states and one failure mode with repair.

By using the Markov method to analyse this model, associated differential equations are obtained as follows:

$$\frac{dP_0(t)}{dt} + P_0(t)\left(\lambda_1 + \lambda_h + \lambda_u\right) = P_1(t)\cdot\mu_u + P_3(t)\cdot\mu_h + P_2(t)\cdot\mu_1 \tag{5.32}$$

$$\frac{dP_1(t)}{dt} + P_1(t)\left(\mu_u + \lambda_f\right) = P_0(t)\cdot\lambda_u + P_2(t)\cdot\mu_f \tag{5.33}$$

$$\frac{dP_2(t)}{dt} + P_2(t)\left(\mu_1 + \mu_f + \mu_2\right) = P_0(t)\cdot\lambda_1 + P_1(t)\cdot\lambda_f + P_3(t)\cdot\lambda_2 \tag{5.34}$$

$$\frac{dP_3(t)}{dt} + P_3(t)\left(\mu_h + \lambda_2\right) = P_0(t)\cdot\lambda_h + P_2(t)\cdot\mu_2 \tag{5.35}$$

The model is in normal working operation at the initial state, which means that at time t = 0, $P_0(0) = 1$ and all other initial state probabilities are equal to zero. By taking the Laplace transforms of equations (5.32) – (5.35), the following equations are obtained:

$$P_0(s) = \frac{P_1(t)\,\mu_u + P_3(t)\,\mu_h + P_2(t)\,\mu_1 + 1}{s + \lambda_1 + \lambda_h + \lambda_u} \tag{5.36}$$

$$P_1(s) = \frac{P_0(s)\,\lambda_u + P_2(s)\,\mu_f}{s + \mu_u + \lambda_f} \tag{5.37}$$

$$P_2(s) = \frac{P_0(s)\,\lambda_1 + P_1(s)\,\lambda_f + P_3(s)\,\lambda_2}{s + \mu_1 + \mu_f + \mu_2} \tag{5.38}$$

$$P_3(s) = \frac{P_0(s)\,\lambda_h + P_2(s)\,\mu_2}{s + \mu_h + \lambda_2} \tag{5.39}$$

By using the equations (5.36) to (5.39), we get the following equations:

$$P_0(s) = \frac{1}{\left(s + \lambda_1 + \lambda_h + \lambda_u - K - J\cdot\left(\frac{\mu_f\cdot\mu_u}{s + \mu_u + \lambda_f} + \frac{\mu_2\cdot\mu_h}{s + \mu_h + \lambda_2} + \mu_1\right)\right)} \tag{5.40}$$

$$P_1(s) = \frac{\left(\lambda_u + J\cdot\mu_f\right)}{\left(s + \mu_u + \lambda_f\right)\left(s + \lambda_1 + \lambda_h + \lambda_u - K - J\cdot\left(\frac{\mu_f\cdot\mu_u}{s + \mu_u + \lambda_f} + \frac{\mu_2\cdot\mu_h}{s + \mu_h + \lambda_2} + \mu_1\right)\right)} \tag{5.41}$$

$$P_2(s) = \frac{J}{\left(s + \lambda_1 + \lambda_h + \lambda_u - K - J\cdot\left(\frac{\mu_f\cdot\mu_u}{s + \mu_u + \lambda_f} + \frac{\mu_2\cdot\mu_h}{s + \mu_h + \lambda_2} + \mu_1\right)\right)} \tag{5.42}$$

$$P_3(s) = \frac{\left(\lambda_h + J\cdot\mu_2\right)}{\left(s+\mu_h+\lambda_2\right)\left(s+\lambda_1+\lambda_h+\lambda_u - K - J\cdot\left(\frac{\mu_f\cdot\mu_u}{s+\mu_u+\lambda_f}+\frac{\mu_2\cdot\mu_h}{s+\mu_h+\lambda_2}+\mu_1\right)\right)} \tag{5.43}$$

Where

$$K = \frac{\lambda_u\cdot\mu_u}{s+\mu_u+\lambda_f} + \frac{\lambda_h\cdot\mu_h}{s+\mu_h+\lambda_2}$$

$$J = \frac{\left(\lambda_1 + \frac{\lambda_u\lambda_f}{\left(s+\mu_u+\lambda_f\right)} + \frac{\lambda_h\lambda_2}{\left(s+\mu_h+\lambda_2\right)}\right)}{\left(s+\mu_1+\mu_2+\mu_f\right) - \frac{\mu_f\lambda_f}{\left(s+\mu_u+\lambda_f\right)} - \frac{\mu_2\lambda_2}{\left(s+\mu_h+\lambda_2\right)}}$$

By taking the inverse Laplace transform, the equations of time dependent state probabilities are obtained.

System Reliability and MTTF

The reliability is equal to the probability of $P_o(t)$, $P_1(t)$ and $P_3(t)$ when system unrepairable i.e $\mu_1 = \mu_f = \mu_2 = 0$. The model reliability is obtained as follows:

$$R(t) = P_0(t) + P_1(t) + P_3(t) \tag{5.44}$$

MTTF can be drived from the relibility equation as follows:

$$MTTF = \lim_{s\to 0} R(s) = \frac{\lambda_2\lambda_f + \lambda_2\lambda_u + \lambda_2\mu_u + \lambda_f\lambda_h + \lambda_f\mu_h + \lambda_h\mu_u + \lambda_u\mu_h + \mu_h\mu_u}{\lambda_1\lambda_2\lambda_f + \lambda_1\lambda_2\mu_u + \lambda_1\lambda_f\mu_h + \lambda_1\mu_h\mu_u + \lambda_2\lambda_f\lambda_h + \lambda_2\lambda_f\lambda_u + \lambda_2\lambda_h\mu_u + \lambda_f\lambda_u\mu_h} \tag{5.45}$$

Availability and Steady state Probabilities

Availability is the total probability of system operational states.

$$AV(t) = P_0(t) + P_1(t) + P_2(t) \tag{5.46}$$

By using the final-value theorem, we can find the model steady state probabilities.

$$P_0 = \frac{\lambda_2 \lambda_f \mu_1 + \lambda_2 \mu_1 \mu_u + \lambda_2 \mu_f \mu_u + \lambda_f \mu_1 \mu_h + \lambda_f \mu_2 \mu_h + \mu_1 \mu_h \mu_u + \mu_2 \mu_h \mu_u + \mu_f \mu_h \mu_u}{Y} \quad (5.47)$$

$$P_1 = \frac{\lambda_1 \lambda_2 \mu_f + \lambda_1 \mu_f \mu_h + \lambda_2 \lambda_h \mu_f + \lambda_2 \lambda_u \mu_1 + \lambda_2 \lambda_u \mu_f + \lambda_u \mu_1 \mu_h + \lambda_u \mu_2 \mu_h + \lambda_u \mu_f \mu_h}{Y} \quad (5.48)$$

$$P_2 = \frac{\lambda_1 \lambda_2 \lambda_f + \lambda_1 \lambda_2 \mu_u + \lambda_1 \lambda_f \mu_h + \lambda_1 \mu_h \mu_u + \lambda_2 \lambda_f \lambda_h + \lambda_2 \lambda_f \lambda_u + \lambda_2 \lambda_h \mu_u + \lambda_f \lambda_u \mu_h}{Y} \quad (5.49)$$

$$P_3 = \frac{\lambda_1 \lambda_f \mu_2 + \lambda_1 \mu_2 \mu_u + \lambda_f \lambda_h \mu_1 + \lambda_f \lambda_h \mu_2 + \lambda_f \lambda_u \mu_2 + \lambda_h \mu_1 \mu_u + \lambda_h \mu_2 \mu_u + \lambda_h \mu_f \mu_u}{Y} \quad (5.50)$$

Where

$$\begin{aligned} Y = {} & \lambda_1 \lambda_2 \lambda_f + \lambda_1 \lambda_2 \mu_f + \lambda_1 \lambda_2 \mu_u + \lambda_1 \lambda_f \mu_2 + \lambda_1 \lambda_f \mu_h + \lambda_1 \mu_2 \mu_u + \lambda_1 \mu_f \mu_h + \lambda_1 \mu_h \mu_u \\ & + \lambda_2 \lambda_f \lambda_h + \lambda_2 \lambda_f \lambda_u + \lambda_2 \lambda_f \mu_1 + \lambda_2 \lambda_h \mu_f + \lambda_2 \lambda_h \mu_u + \lambda_2 \lambda_u \mu_1 + \lambda_2 \lambda_u \mu_f + \lambda_2 \mu_1 \mu_u \\ & + \lambda_2 \mu_f \mu_u + \lambda_f \lambda_h \mu_1 + \lambda_f \lambda_h \mu_2 + \lambda_f \lambda_u \mu_2 + \lambda_f \lambda_u \mu_h + \lambda_f \mu_1 \mu_h + \lambda_f \mu_2 \mu_h + \lambda_h \mu_1 \mu_u \\ & + \lambda_h \mu_2 \mu_u + \lambda_h \mu_f \mu_u + \lambda_u \mu_1 \mu_h + \lambda_u \mu_2 \mu_h + \lambda_u \mu_f \mu_h + \mu_1 \mu_h \mu_u + \mu_2 \mu_h \mu_u + \mu_f \mu_h \mu_u \end{aligned}$$

To analyse the model reliability, specific values of failure and repair rates are assumed. Accordingly, the inverse Laplace transforms of equations (5.40) – (5.43) were used to develop the plots in Figure 5-8, the reliability equation (5.44) was used to develop the plots in Figure 5-9 and Figure 5-10, the availability equation (5.46) was used to develop the plots in Figure 5-11 and Figure 5-12. Detailed plots are presented in Appendix E.3.

$\lambda_1 = 0.0005 \left(\frac{failure}{hour} \right)$ $\lambda_2 = 0.006 \left(\frac{failure}{hour} \right)$
$\lambda_u = 0.002 \left(\frac{failure}{hour} \right)$ $\lambda_f = 0.0025 \left(\frac{failure}{hour} \right)$
$\lambda_h = 0.0035 \left(\frac{failure}{hour} \right)$ $\mu_1 = 0.007 \left(\frac{repair}{hour} \right)$
$\mu_2 = 0.005 \left(\frac{repair}{hour} \right)$ $\mu_u = 0.0035 \left(\frac{repair}{hour} \right)$
$\mu_f = 0.0035 \left(\frac{repair}{hour} \right)$ $\mu_h = 0.005 \left(\frac{repair}{hour} \right)$

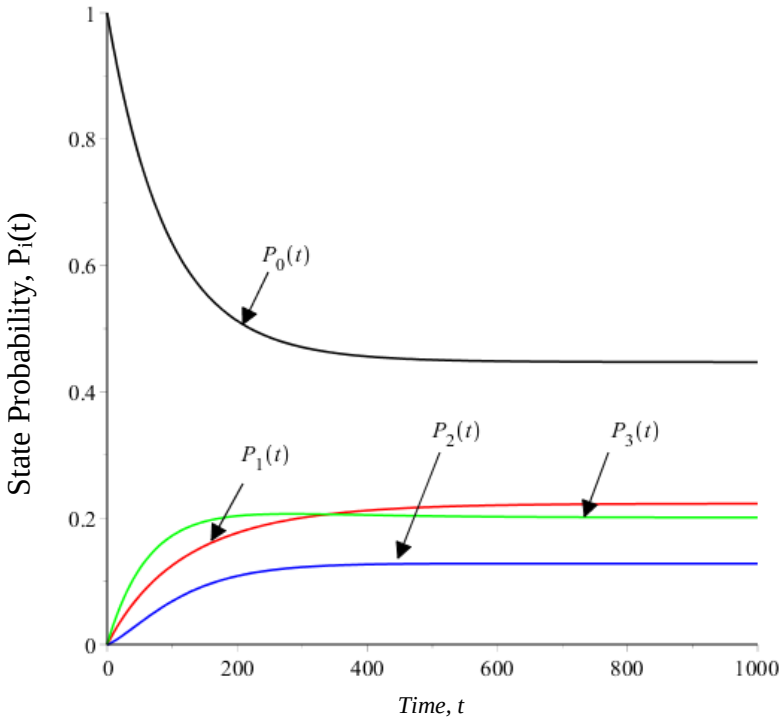

Figure 5-8 State probabilities of a system with three operation states and one failure mode

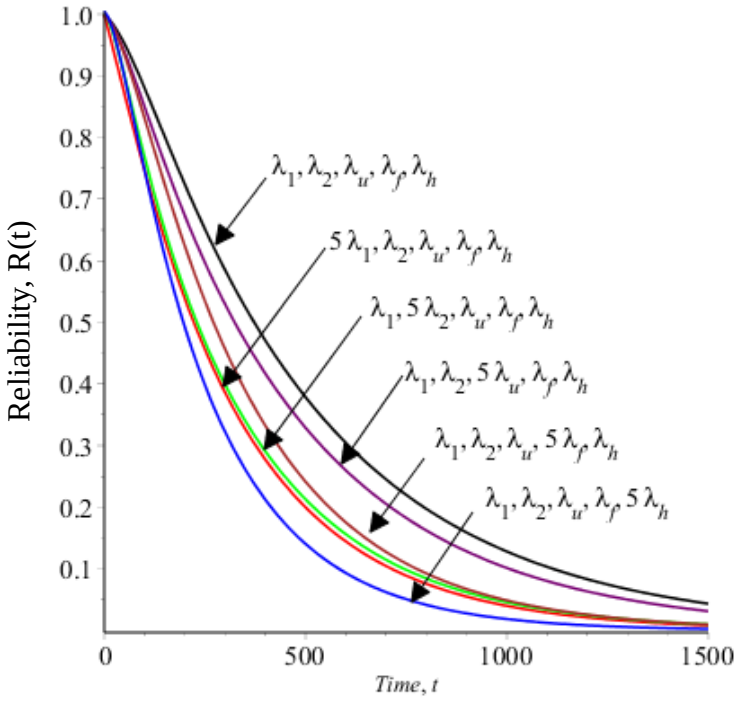

Figure 5-9 Reliability plots of a system with three operation states at different values of failure rates

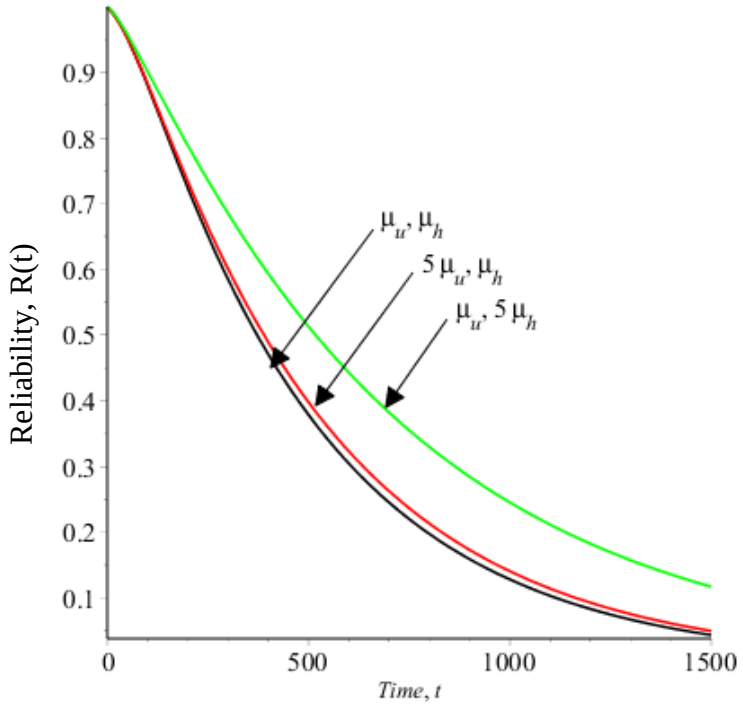

Figure 5-10 Reliability plots of a system with three operation states at different values of repair rates

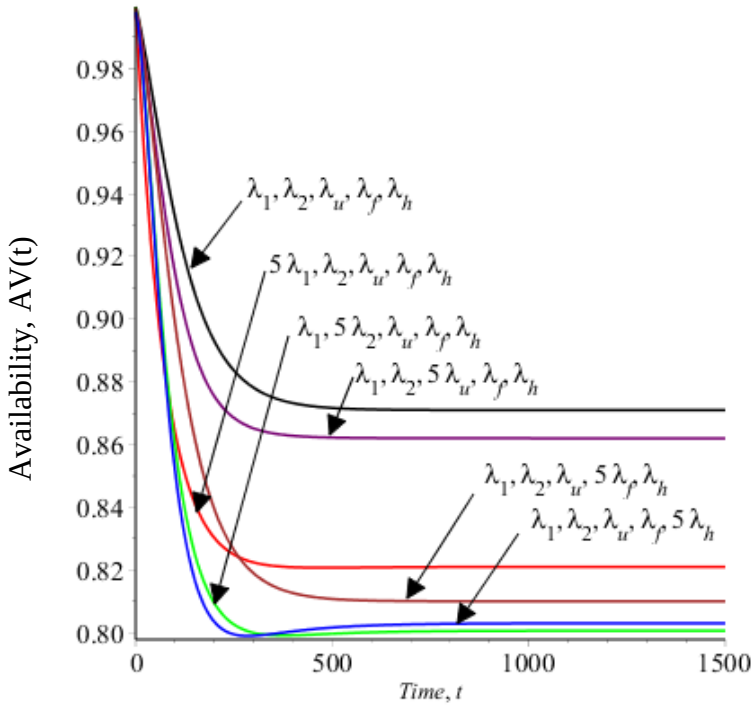

Figure 5-11 Availability plots of the system with three operation states at different values of failure rates

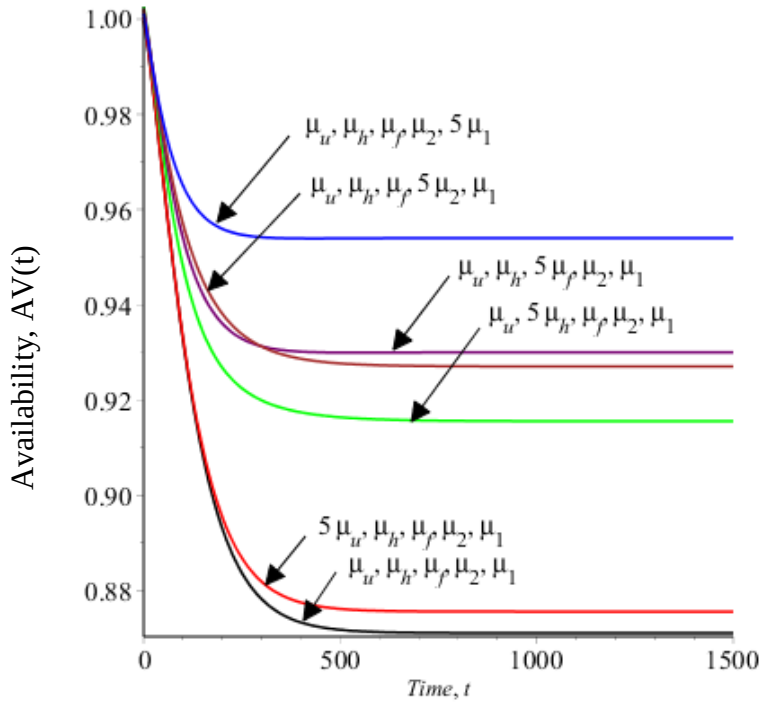

Figure 5-12 Availability plots of the system with three operation states at different values of repair rate

5.3 Discussion

Worker performance in mining is subjected to different levels of work environment and stress. Therefore, the realistic reliability analysis should consider them in predicting the worker performance. In general, the detailed models provide a better understanding of system reliability behaviour.

The second model has three operating conditions in which the normal operation usually should have lower failure rated than the other unsafe operation conditions. However, if the failure rate for normal operation condition increases significantly, the system reliability and availability may increase by increasing the probability to operate at unsafe conditions. Figure 5-11 shows that the availability plot when model parameters equals ($5\lambda_1$, λ_2, λ_u, λ_f, λ_h) has lower availability than plot with model parameters equals (λ_1, λ_2, $5\lambda_u$, λ_f, λ_h).

Chapter 6 : Conclusion and Recommendations

6.1 Conclusion

This study analysed number of models representing mining systems to understand reliability and availability behaviour when different values of model failure rates, repair rates, number of identical units in parallel configuration, repair policies and when considering the safety of unit failures. General equations were developed to express time dependent reliability and steady state availability of n-number of identical units in parallel configurations. The outcome of study can be summarized in six main points as follows:

1. The mining system reliability increases as the number of units in parallel configuration increase. However, it was noticed that the probability to be at initial state decreases as the number of unit increases, which in turn required more maintenance work to keep the system at "as-built" condition.

2. The detailed models of mining systems provide a better understanding about system availability. However, as the number of states increases, the associated Markov method equations become more complicated.

3. The reliability and availability plots follow the same pattern at different values of model parameters. Therefore, generating reliability and availability plots with assumed model parameters may help in understanding their behaviours.

4. The process of improving the reliability and availability of any mining system is a multiple factors process that need optimization.

5. The mining system reliability, availability and MTTF increase as number of units increase when units have the same failure and repair rates. Also, they increase as the failure rate decrease and repair rate increase.

6. The instant unit repair policy has a slight improvement effect in the system overall reliability and availability. Whereas after total system failure repair has a significant improvement effect in the overall availability.

6.2 Recommendations

1. The models representing mining systems in this study have constant repair and failure rates. The study can be extended to include time dependent failure and repair rates.

2. All units in parallel configurations are assumed to be identical. Non-identical unit can be considered for future studies to understand mining systems reliability and availability behaviours.

3. This study investigated the effect of different repair policies at parallel configuration system with two-units. Future study may extend the investigation to more than two-units.

References

1- Dhillon, B. S., “Mining equipment reliability, maintainability, and safety”, Springer, London, U.K. 2008.

2- Sudano, J. J., “Minimizing human-machine interface failures in high risk systems”, *Proceeding of IEEE Conference of Aerospace and Electronics (NAECON),* 1994, pp. 749-752.

3- Reason, J., "Human Error: Models and Management", *BMJ: British Medical Journal,* Vol. 320, No.7237, 2000, pp. 768-770.

4- Dragan, I.M., Alexandru I.M. "The Reliability of the Human Factor", *Procedia Economics and Finance Journal, Vol. 15,* 2014, pp. 1486-1494.

5- Williams, H. L., “Reliability Evaluation of the Human Component in Man-Machine Systems”, Electrical Manufacturing, 1958, pp. 78 -82.

6- Hitchcock, L., Sanders, M., “Survey of Human Factors in Underground Bituminous Coal Mining Naval Ammunition Depot”, Crane, Indiana, 1971.

7- Gross, B., Schurick, J., “Hazard Analysis and Safety Economics in Mineral Processing Plants”, *Canyon Research Group,* Westlake Village, California, 1982.

8- Conway E.J., Sanders M.S., “Recommendations for Human Factors Research and Development Projects in Surface Mining”. Report No. OFR-211-83. Bureau of Mines, United States Department of the Interior. Washington, D.C., 1982.

9- Shooman, M.L., “Probabilistic Reliability: An Engineering Approach”, McGraw-Hill, New York, 1968.

10- Garrett, J. W., & Teizer, J., “Human Factors Analysis Classification System Relating to Human Error Awareness Taxonomy in Construction Safety”, *Journal of Construction Engineering and Management,* Vol. 135, No. 8, 2009, pp.754-763.

11- Clark, D., “Tribology – its applications to equipment reliability and maintainability design in the underground coal mining industry’, *Proceedings of the Institution of Engineers Australia Tribology Conference,* 1990, pp. 38–44.

12- Salvendy, G., “Handbook of human factors and ergonomics*”,*. John Wiley & Sons, New York, 2012.

13- Sanders, M. S., Ernest J. M., “Human Factors in Engineering and Design”, McGraw- Hill Book Company, New York, 1987.
14- Sheridan, T. B., “Humans and Automation: System Design and Research Issues”. John Wiley & Sons, New York, 2002.
15- Parasuraman, R., Sheridan, T. B., Wickens, C. D., “A model for types and levels of human interaction with automation”, *IEEE Transactions on systems, man, and cybernetics-Part A: Systems and Humans*, Vol. 30, No.3, 2000, pp. 286-297.
16- Degani, A., Shafto, M., Kirlik, A., “Modes in human machine systems: Review, classification, and application”. *International Journal of Aviation Psychology*, Vol. 9, No. 2, 1999, pp. 125–138.
17- Dhillon, B. S., “Human reliability, error, and human factors in engineering maintenance: with reference to aviation and power generation*”,* CRC Press, Boca Raton, Florida, 2009.
18- Haight, J. M., "Automated Control Systems Do They Reduce Human Error and Incidents?", Journal of Professional Safety, Vol. 52, No.05, 2007, pp. 20 – 27.
19- Dhillon, B.S., “Design Reliability: Fundamentals and Application”, CRC Press, Boca Raton, Florida, 1999.
20- Dhillon, B.S., Singh, C., “Engineering Reliability: New Techniques and Applications*”,* John Wiley & Sons, New York, 1981.
21- Chaturvedi, S. K., “Network Reliability: Measures and Evaluation”, John Wiley & Sons, Hoboken, New Jersey, 2016.
22- Arezes, P. M., de Carvalho, P. V., “Ergonomics and Human Factors in Safety Management”, CRC Press, New York, 2016.
23- Dhillon, B. S., "Bibliography of Literature on Mining Equipment Reliability", *Microelectronics and Reliability*, Vol. 26, 1986, pp. 1131-1138.
24- Lewis, M. W., & Steinberg, L., "Maintenance of Mobile Mine Equipment in the Information Age." *Journal of Quality in Maintenance Engineering,* Vol. 7, No. 4, 2001, pp. 264-274.
25- Endsley, M. R., "Level of Automation Effects on Performance, Situation Awareness and Workload in a Dynamic Control Task." *Ergonomics,* Vol. 42, No.3, 1999, pp. 462-92.

26- Mistriotis, G. D., “Some properties of Markov chains and Markov chain aggregates”, Thesis of Master of Applied Science, Electrical Department, University of Ottawa, Ottawa, Canada, 1974.
27- Basharin, G. P., Amy N. L., and Valeriy A. N. "The life and work of AA Markov", *Linear Algebra and its Applications,* Vol. 386, 2004, pp. 3-26.
28- Buzacott, J. A., "Markov Approach to Finding Failure Times of Repairable Systems", *IEEE Transactions on Reliability,* Vol. R-19 No. 4, 1970, pp. 128-34.
29- Rothrock, L., Wysk, R., Kim, N., Shin, D., Son, Y. J., Joo, J., "A Modelling Formalism for Human-Machine Cooperative Systems." *International Journal of Production Research,* Vol. 49, No. 14, 2011, pp. 4263-4273.
30- Givi, Z. S., Jaber, M. Y., Neumann, W. P., “Modelling worker reliability with learning and fatigue”, *Applied Mathematical Modelling*, Vol. 39, No. 17, 2015, pp. 5186-5199.
31- McLeod, R. W., “Designing for human reliability: human factors engineering in the oil, gas, and process industries”, Gulf Professional Publishing, Waltham, Massachusetts, 2015.
32- Dhillon, B. S., Yang N., "Comparisons of Block Diagram and Markov Method System Reliability and Mean Time to Failure Results for Constant and Non-Constant Unit Failure Rates." *Microelectronics and Reliability*, Vol. 37, No. 3, 1997, pp. 505-509.
33- Stapelberg, R. F., “Handbook of reliability, availability, maintainability and safety in engineering design”, Springer, Queensland, Australia, 2009.
34- Lynas, D., & Horberry, T., “Human factor issues with automated mining equipment”. *Ergonomics Open Journal*, Vol. 4, 2011, pp. 74-80.
35- Sarter N.B., Woods D.D., Billings C.E., “Automation surprises”, *Handbook of Human Factors and Ergonomics*. John Wiley & Sons, New York, 1997, pp. 1926-1943
36- Endsley, M. R. “Towards a new paradigm for automation: Designing for situation awareness”, *Proceeding of the 6th IFAC/IFIP/IFORS/IEA Symposium on Analysis, Design and Evaluation of Man-Machine Systems,* Vol. 1, 1995, pp. 365-370.
37- Simon, F., Javad, B., Abbas, B., “Availability analysis of the main conveyor in the Svea Coal Mine in Norway”, *International Journal of Mining Science and Technology*, Vol. 24, No. 5, 2014, pp. 587-591.

38- Butorin, Y. M., Gavrilenko, V. A., “Some aspects of the reliability of drilling equipment”, *Journal of Mining Science*, Vol. 12, No. 1, 1976, pp. 62-65.

39- Dhillon, B. S., “Maintainability, maintenance, and reliability for engineers”, CRC Press, New York, 2006.

40- Barlow, R. E. Proschan, F., “Statistical Theory of Reliability and Life Testing”, John Wiley & Sons, New York, 1965.

41- Hauskrecht, M., Meuleau, N., Kaelbling, L. P., Dean, T., Boutilier, C., “Hierarchical solution of Markov decision processes using macro-actions”, *Proceedings of the Fourteenth conference on Uncertainty in artificial intelligence*, 1998, pp. 220-229.

42- Bello, G. C., Avogadri, S., “Offshore pipeline system—how to decide the optimal redundancies using reliability engineering”, *Reliability Engineering*, Vol. 3, No. 2, 1982, pp. 89-99.

43- Ushakov, I. A., “Handbook of reliability engineering*”*. John Wiley & Sons, New York, 1994.

44- Lisnianski, A., Levitin, G., Ben-Haim, H., Elmakis, D., “Power system structure optimization subject to reliability constraints”, *Electric Power Systems Research*, Vol. 39, No. 2, 1996, pp. 145-152.

45- Kuo, W., Prasad, V. R., “An annotated overview of system-reliability optimization”. *IEEE Transactions on reliability*, Vol. 49, No. 2, 2000, pp. 176-187.

46- Li, D., Sun, X., McKinnon, K., “An exact solution method for reliability optimization in complex systems”, *Annals of Operations Research*, Vol.133 No. 4, 2005, pp. 129-148.

47- Dhillon, B. S., Rayapati, S. N., “Reliability analysis of non-maintained parallel systems subject to hardware failure and human error”, *Microelectronics Reliability*, Vol. 25, No. 1, 1985, pp. 111-122.

48- Levitin, G., “The universal generating function in reliability analysis and optimization”, Springer, London, U.K., 2005.

49- Lee, S. B., Katz, A., Hillman, C., “Getting the quality and reliability terminology straight”. *IEEE Transactions on Components, Packaging, and Manufacturing Technology: Part A*, Vol. 21, No. 3, 1998, pp. 521-523.

50- Krarti, M., “An overview of artificial intelligence-based methods for building energy systems”, *Journal of solar energy engineering*, Vol. *125, No.* 3, 2003, pp. 331-342.

51- Reason, J., Cognitive Engineering in Aviation Domain, Lawrence Erlbaum Associates, Mahwah, New Jersey, 2000.

52- Dhillon, B. S., Liu. Y., "Human Error in Maintenance: A Review." *Journal of Quality in Maintenance Engineering*, Vol. 12, No. 1, 2006, pp. 21-36.

53- Norman, D. A., "Stages and levels in human-machine interaction", *International journal of man-machine studies*, Vol. 21, No. 4, 1984, pp. 365-375.

54- Rouse, W. B., Rouse, S. H., "Analysis and classification of human error", *IEEE Transactions on Systems, Man, and Cybernetics*, Vol. 13, No. 4, 1983, pp. 539-549.

55- Buchnan, D.J., *"*What is the Role of Mining Health and Safety Research in the 21st Century?" *Proceeding of Mine safe International Conference*, 2000, pp. 309 – 317.

56- MISHC, "Causes of Fatalities and Significant Injury in the Australian Mining Industry", *Queensland Resources Council*, University of Queensland Minerals Industry Safety and Health Centre, 2005.

57- Heinrich, H.W., *"Industrial Accident Prevention: A Scientific Approach*", McGraw-Hill, New York, 1931.

58- Rasmussen, J., "Reasons, causes, and human error". *Journal of Organizational Behavior: New technology and human error*, Vol. 9, No. 2, 1987, pp. 293 – 301.

59- Reason, J., "A framework for classifying errors", *Journal of Organizational Behavior: New technology and human error*, Vol. 9, No. 2, 1987, pp. 5-14.

60- Dhillon, B. S., "Mine safety: a modern approach", Springer, London, U.K. 2010.

61- Cox, S. Tait, R., "Safety, Reliability and Risk Management: An Integrated Approach" Oxford, Butterworth-Heinemann, U.K., 2011.

62- Horberry, T., Burgess -Limerick, R., Cooke, T., Steiner, L., "Improving Mining Equipment Safety Through Human-Centered Design". *Ergonomics in Design: The Quarterly of Human Factors Applications*, 2016.

63- Reason, J.T., "The Contribution of Latent Failure to the Breakdown of Complex Systems". *The Royal Society*, Riso National Laboratory, Denmark, 1989.

64- Reason, J.T., "Management Risk and Risk Management", *Proceeding of Human Reliability in Nuclear Power Conference*, Confederation of British Industry, London, Conference.

65- HSE, "Human Factors in Industrial Safety", HMSO, London, U.K, 1989.

66- Xiong, X., Yu-Liang W., Wen-Ben J., "Reliability Model for MEMS Accelerometers." *Novel Algorithms and Techniques in Telecommunications, Automation and Industrial Electronics*, Springer Netherlands, 2008, pp. 261-266.

67- Reliability Design Handbook, RDG-376, Reliability Analysis Center, Rom Air Development Center, Griffis Air Force Base, Rome, New York, 1976.

68- Klutke, G., Kiessler P. C., Wortman, M. A., "A critical look at the bathtub curve." *IEEE Transactions on Reliability*, Vol. 52, No.1, 2003, pp. 125-129.

69- Geraci, A., Katki, F., McMonegal, L., Meyer, B., Lane, J., Wilson, P., Springsteel, F. "IEEE standard computer dictionary: Compilation of IEEE standard computer glossaries". IEEE Press, 1991.

70- ISO, EN. "6385. 2004." *Ergonomic principles in the design of work systems*, (2004).

71- Kirwan, B., "Human error identification in human reliability assessment. Part 1: Overview of approaches". *Applied ergonomics*, Vol. 23, No. 5, 1992, pp. 299-318.

72- Kirwan, B., "Human error identification in human reliability assessment. Part 2: Detailed comparison of techniques", *Applied ergonomics*, Vol. 23, No. 6, 1992, pp. 371-381.

73- Young, M. S., Neville A. S., "Attention and Automation: New Perspectives on Mental Underload and Performance", Theoretical Issues in Ergonomics Science, Vol.3, No. 2, 2002, pp. 178-94.

74- Naresky, J.J., "Reliability definitions", *IEEE Transportation Reliability*, 19, 1970, 198-200.

75- Zhao, Hai-xiang, and Frédéric Magoulès. "A Review on the Prediction of Building Energy Consumption." *Renewable and Sustainable Energy Reviews*, Vol. 16, No.6, 2012, pp. 3586-92.

76- Barlow, R.E., Proschan F., "Availability theory for multicomponent system, multivariate analysis III", *Academic Press Inc*., New York, 1973, pp 319–335.

77- Verma, A. K., Srividya, A., Karanki, D. R., "Reliability and safety engineering", Springer, London, U.K., 2010.

78- Cavallaro, J. R., Walker, I. D., "A survey of NASA and military standards on fault tolerance and reliability applied to robotics", *In proceeding with Conference on Intelligent Robotics in Field, Factory, Service, and Space*, Vol. 1, 1994, pp. 282-286.

79- Everett, W. W., Honiden, S., “Reliability and safety of real-time systems”, *IEEE Software*, Vol. 12, No. 3, 1995, pp. 13-16.

80- Shewhart, W. A., “Economic control of quality of manufactured product”, ASQ Quality Press, New York, 1931.

81- Sun, Y., Li, X. S., Guo, H., “Enhance Mining System Reliability through System Integration Approach”, *CSIRO Earth Science and Resource Engineering,* Australia, 2013.

82- Yuriy, G., Vayenas, N., “Discrete-event simulation of mine equipment systems combined with a reliability assessment model based on generic algorithms”. *International Journal of Mining, Reclamation and Environment*, Vol 22, No. 1, 2008, pp. 70-83.

83- Peng, S., Vayenas, N., “Maintainability Analysis of Underground Mining Equipment Using Generic Algorithms: Case Studies with an LHD Vehicle”. *Journal of Mining,* Vol.20, No. 1, 2014, pp. 32-50.

84- Basu, A. J., Baafi, E. Y., “Discrete event simulation of mining systems: current practice in Australia”. *International Journal of Surface Mining, Reclamation and Environment*, Vol. 13, No. 2, 1999, pp. 79-84.

85- Hall, R. A., Daneshmend, L. K., “Reliability and maintainability models for mobile underground haulage equipment”. *CIM bulletin*, Vol. 96, No. 1072, 2003, 159-165.

86- Song, Z., Schunnesson, H., Rinne, M., Sturgul, J., “Intelligent scheduling for underground mobile mining equipment”. *PloS one*, Vol 10, No. 6, 2015, e0131003.

87- Panagiotou, G. N., “Discrete mine system simulation in Europe”. *International Journal of Surface Mining, Reclamation and Environment*, Vol. 13, No. 2, 1999, pp. 43-46.

88- Jianhua, L., Xiaoyan, S., “Countermeasures of Mine Safety Management based on Behavior Safety Mode”. *Procedia Engineering*, 84, 2014, pp.144-150.

89- Lynas, D., Horberry, T., “Human factor issues with automated mining equipment”. *Ergonomics Open Journal*, Vol *4*, 2011, pp. 74-80.

90- Dhillon, B. S., & Yang, N., Availability of a man-machine system with critical and non-critical human error. *Microelectronics Reliability*, Vol. 33, No. 10, 1993, pp. 1511-1521.

91- Mirmohammadi, M., Gholamnejad, J., Fattahpour, V., Seyedsadri, P., Ghorbani, Y., “Designing of an environmental assessment algorithm for surface mining projects”. *Journal of environmental management*, Vol. 90, No. 8, 2009, pp. 2422-2435.

92- McPhee, B., “Ergonomics in mining”. *Occupational Medicine*, Vol. 54, No. 5, 2004, pp. 297-303.

93- Elías A., “Ergonomics in Mining: The Chilean Experience”. *The Journal of Human Factors and Ergonomics Society*, Vol. 56, No. 6, 2012, pp.901-907

94- Piedrahita, L., “Some Experiences on the Ergonomics Application in Mining”. *Revista Ciencias de la Salud*, Vol. 12, No. 1, 2014, pp. 69-76.

95- Horberry, T., Burgess-Limerick, R., Fuller, R., “The contributions of human factors and ergonomics to a sustainable minerals industry”. *Ergonomics*, Vol. 56, No. 3, 2013, pp. 556-564.

96- Horberry, T., Burgess-Limerick, R., Steiner, L. J., *Human factors for the design, operation, and maintenance of mining equipment*. CRC Press, New York, 2016.

97- Fioroni, M. M., Franzese, L. A. G., Bianchi, T. J., Ezawa, L., Pinto, L. R., de Miranda, G. “Concurrent simulation and optimization models for mining planning”. *In proceeding of IEEE 2008 Winter Simulation Conference*, 2008, pp. 759-767

98- Barabady, J., Kumar, U. “Reliability and maintainability analysis of crushing plants in Jajarm Bauxite Mine of Iran”. *In Proceedings of the Annual Reliability and Maintainability Symposium*, 2005, pp. 109-115

99- Dhillon, B. S., Rayapati, S. N. “Human performance reliability modelling”. *Microelectronics Reliability*, Vol. 28, No. 4, 1988, pp.573-580.

100- Gaver, D. P. “Time to failure and availability of paralleled systems with repair”. *IEEE Transactions on Reliability*, Vol. 12, No. 2, 1963, 30-38.

101- Chao, M. T., Fu, J. C. “The reliability of a large series system under Markov structure”. *Advances in Applied Probability*, Vol. 23, No. 4, 1991, pp. 894-908.

102- Lam, Y., Zhang, Y. L. “Analysis of a two-component series system with a geometric process model”. *Naval Research Logistics (NRL)*, Vol. 43, No. 4, 1996, pp. 491-502.

103- Freiheit, T., Hu, S. J., “Impact of machining parameters on machine reliability and system productivity”. *Journal of manufacturing science and engineering*, Vol. 124, No. 2, 2002, 296-304.

104- Haldane J. S., “The human factor in coil mining”, Nature, 1924, Vol.114, No. 2869, 1924, pp.598.

105- Hitchcock, L., Sanders, M. “Survey of Human Factors in Underground Bituminous Coal Mining Naval Ammunition Depot”, Crane, Indiana, 1971.

106- Sanders M. S., Peay J. M., “Human Factor in Mining”. *Bureau of Mines Information Circular*, IC-9182, United States Department of the Interior, 1988.

107- *National Institute for Occupational Safety and Health, Mining Program*. Retrieved November 15, 2015, from http://www.cdc.gov/niosh/mining/statistics/allmining.html

108- Hamilton, D. D., Hopper, J. E. andJones, J. H., “Inherently Safe Mining Systems, Report No. USBM OFR 124 –77*”. United States Bureau of Mines (USBM)*, Washington, DC, 1977.

109- *Historical Data on Mine Disasters in the United States*, Washington, DC: U.S. Department of Labor. Available at www.msha.gov/MSHAINFO/FactSheets/MSHAFACTS8.htm

110- Dhillon, B. S., “Mining equipment safety: a review, analysis methods and improvement strategies”. *International Journal of Mining, Reclamation and Environment*, Vol. 23, No. 3, 2009, pp. 168-179.

111- Rushworth, A. M., Talbot, C. F., Von Glehn, F. H., Lomas, R. M., “Investigate the causes of transport and tramming accidents on coal mines”. *Safety in Mines Research Advisory Committee*, COL 506, 1999, pp. 1-121

112- Willamson, A., Feyer, A. M., “Behavioural epidemiology as a tool for accident research”. *Journal of Occupational Accidents*, Vol. 12, No. 1, 1990, pp. 207-222. Dhillon, B. S., “Stochastic models for predicting human reliability”. *Microelectronics Reliability*, Vol. 22, No. 3, 1982, pp. 491-496.

113- Dhillon, B. S., Rayapati, S. N., “Reliability evaluation of human operators under stress”. *Microelectronics Reliability*, Vol. 25, No. 4, 1985, pp. 729-752.

114- Dhillon, B. S., “Stochastic models for evaluating probability of system failure due to human error”. *Microelectronics Reliability*, Vol. 24, No. 5, 1984, pp. 921-924.

115- Kumar, A., Garg, S. C. “Reliability analysis of a system with a human operator and subject to two failure modes. *Microelectronics Reliability”*, Vol. 31, No. 2, 1991, pp. 277-283.

116- Kumar, A., Agarwal, M., Garg, S. C., "Reliability analysis of a two-unit redundant system with critical human error". *Microelectronics Reliability*, Vol. 26, No. 5, 1986, pp. 867-871.

117- Chung, W. K., "Reliability analysis of a human operator under several levels of stress". *Microelectronics Reliability*, Vol. 31 No. 2-3, 1991, pp. 367-370.

118- Chung, W. K. "Reliability evaluation of a human operator under various levels of stress". *Microelectronics Reliability*, Vol. 31, No. 6, 1991, pp. 1251-1255.

119- Goel, L. R., Sharma, G. C., Gupta, R. "Cost analysis of a two unit cold standby system under different weather conditions". *Microelectronics Reliability*, Vol. 25, No. 4, 1985, pp. 655-659.

120- Guo, T., Cao, J., "Reliability analysis of a multistate one-unit repairable system operating under a changing environment". *Microelectronics Reliability*, Vol. 32, No. 3, 1992, pp. 439-443.

121- Deng, Y., Song, S., "Reliability analysis of a multicomponent system in a multistate Markovian environment". *Microelectronics Reliability*, Vol. 33, No. 9, 1993, pp. 1237-1239.

122- Savita, D., "Stochastic analysis of repairable systems of non-identical units operating under different weather conditions", *Maharshi Dayanand University Thesis Research*, 2015, available at http://hdl.handle.net/10603/39149.

123- Chaudhuri, M., Agarwal, M. "Availability Analysis of a Non-Markovian System with Parallel Repairs Operating Under Fluctuating Environments". *Recent Developments in Operational Research*, 2002, pp. 73-87.

124- Song, S., Deng, Y., "Reliability analysis of a three-unit system in a changing environment". *Microelectronics Reliability*, Vol. 33, No. 5, 1993, pp. 637-639.

125- Li, W., Alfa, A. S., Zhao, Y. Q. "Stochastic analysis of a repairable system with three units and two repair facilities". *Microelectronics Reliability*, Vol. 38, No. 4, 1998, pp. 585-595.

126- Cao, J. "Stochastic behaviour of a man-machine system operating under changing environment subject to a Markov process with two states". *Microelectronics Reliability*, Vol. 29, No. 4, 1989, pp. 529-531.

127- Agarwal, M. A., Templeton, J. G.”Stochastic analysis of a repairable system under fluctuating weather”. *International journal of systems science*, Vol.21 No. 10, 1990, pp. 2019-2028.

128- Goel, L. R., Shrivastava, P., “A single unit man-machine system with varying physical conditions of the repairman”. *Microelectronics Reliability*, Vol. 32 No. 3, 1992, pp. 313-317.

129- Mokaddis, G. S., Tawfek, M. L., Elhssia, S. A., “Some characteristics of a man-machine system operating subject to different weather conditions”. *Microelectronics Reliability*, Vol. 37, No. 3, 1997, pp. 493-496.

130- Singh, S. K., Singh, R. B., “Cost analysis of a man-machine system operating under changing operator conditions”. *Microelectronics Reliability*, Vol. 33, No 9, 1993, pp. 1267-1274.

131- Mokaddis, G. S., Ayed, Y. M., Al-Hajeri, H. S., “Propabilistic Analysis of a Man-Machine System Operating Subject To Different Physical Conditions”. *International Journal of Modern Engineering Research (IJMER)*, Vol. 1, No 4, 2014, pp. 12-22.

132- Li, X., McKee, D. J., Horberry, T., Powell, M. S. “The control room operator: The forgotten element in mineral process control”. *Minerals Engineering*, Vol. 24, No. 8, 2011, pp. 894-902.

133- Levitin, G., Lisnianski, A. “A new approach to solving problems of multi-state system reliability optimization”. *Quality and reliability engineering international*, Vol. 17 No. 2, 2001, pp. 93-104.

134- Horberry, T., “Better integration of human factors considerations within safety in design”. *Theoretical Issues in Ergonomics Science*, Vol. 15, No. 3, 2014, pp. 293-304.

135- Horberry, T., Burgess-Limerick, R., “Applying a human-centred process to re-design equipment and work environments”. *Safety*, Vol.1, No. 1, 2015, pp. 7-15.

136- Pazell, S., Burgess-Limerick, R., Horberry, T., McGuire, R. “Human-centred design for road construction: Optimising productivity by reducing safety and health risks”. *In proceeding of Ergoship 2016,* 6-7 April 2016.

137- Horberry, T., Cooke, T., “Safe and inclusive design of equipment used in the minerals industry”. In proceeding of the 6th Cambridge Workshop on Universal Access and Assistive Technology, 2012, pp. 23-32.

138- Horberry, T., Lynas, D. ,"Human interaction with automated mining equipment: The development of an emerging technologies database. *Ergonomic Australia*, Vol. 8, No. 1, 2012, pp. 1-6.

139- Boudreau-Trudel, B., Zaras, K., Nadeau, S., Deschamps, I., "Introduction of Innovative Equipment in Mining: Impact on Productivity". *American Journal of Industrial and Business Management*, Vol.4, No.1, 2014.

140- Boudreau-Trudel, B., Nadeau, S., Zaras, K., Deschamps, I., "Introduction of Innovative Equipment in Mining: Impact on Occupational Health and Safety." *Open Journal of Safety Science and Technology*, Vol. 4, No. 1, 2014.

141- Boudreau-Trudel, B., Nadeau, S., Zaras, K., "Innovative Mining Equipment: Key Factors for Successful Implementation". *American Journal of Industrial and Business Management*, Vol.5, No. 4, 2015, pp.161-171.

142- Oliveira, A., Araujo, R., Jardine, A., "Human-Centered Interfaces for Situation Awareness in Maintenance". *In proceeding of International Conference on Human Interface and the Management of Information*, Vol. 8522, 2014, pp. 193-204.

143- Ruckart, P. Z., Burgess, P. A., "Human error and time of occurrence in hazardous material events in mining and manufacturing". *Journal of hazardous materials*, Vol. 142, No. 3, 2007, pp. 747-753.

144- Patterson, J. "Human error in mining: A multivariable analysis of mining accidents/incidents in Queensland, Australia and the United States of America using the human factors analysis and classification system framework". Clemson University Thesis Research, 2009, available at http://tigerprints.clemson.edu/all_dissertations/464/

145- Ruff, T., Coleman, P., Martini, L., "Machine-related injuries in the US mining industry and priorities for safety research". *International journal of injury control and safety promotion*, Vol. 18, No. 1, 2011, pp. 11-20.

146- Hobbs, A., Williamson, A. "Associations between errors and contributing factors in aircraft maintenance. *Human Factors: The Journal of the Human Factors and Ergonomics Society*, Vol. 45, No. 2, 2003, pp. 186-201.

147- Kumar, P., Gupta, S., Agarwal, M., Singh, U. "Categorization and standardization of accidental risk-criticality levels of human error to develop risk and safety management policy. *Safety Science*, Vol. 85, pp. 88-98.

148- Chung, W. K., “Reliability analysis of a repairable parallel system with standby involving human error and common-cause failures. *Microelectronics Reliability*, Vol. 27, No. 2, 1987, pp. 269-271.

149- Chung, W. K., “Reliability analysis of a series repairable system with multiple failures”. *Microelectronics Reliability*, Vol. 31, No. 2, 1991, pp. 371-373.

150- Chung, W. K., “Reliability and availability analysis of cold standby system with repair and multiple non-critical and critical errors”. *Microelectronics Reliability*, Vol. 34, No. 12, 1994, pp. 1891-1896.

151- Chung, W. K., “Reliability analysis of a human operator under different levels of stress”. *Microelectronics Reliability*, Vol. 32, No. 1-2, 1992, pp. 127-131.

152- Mahmoud, M. A. W., Esmail, M. A., “Probabilistic analysis of a two-unit warm standby system subject to hardware and human error failures”. *Microelectronics Reliability*, Vol. 36, No. 10, 1996, 1565-1568.

153- Gupta, P. P., & Kumar, A., “Reliability and MTTF analysis of a non-repairable parallel redundant complex system under hardware and human failures”. *Microelectronics Reliability*, Vol. 26, No. 2, 1986, pp. 229-234.

154- Manna, D. K. , “A note on a paper by Gupta and Kumar” .*Microelectronics Reliability*, Vol. 32, No. 5, 1992, pp. 733-735.

Appendix A: Steps to Solve Inverse Laplace Transforms

Appendix A is about steps to solve Markov equations and obtain time dependent state probabilities by solving inverse Laplace transform.

A.1 Two identical units with two failure modes and Type-I repair

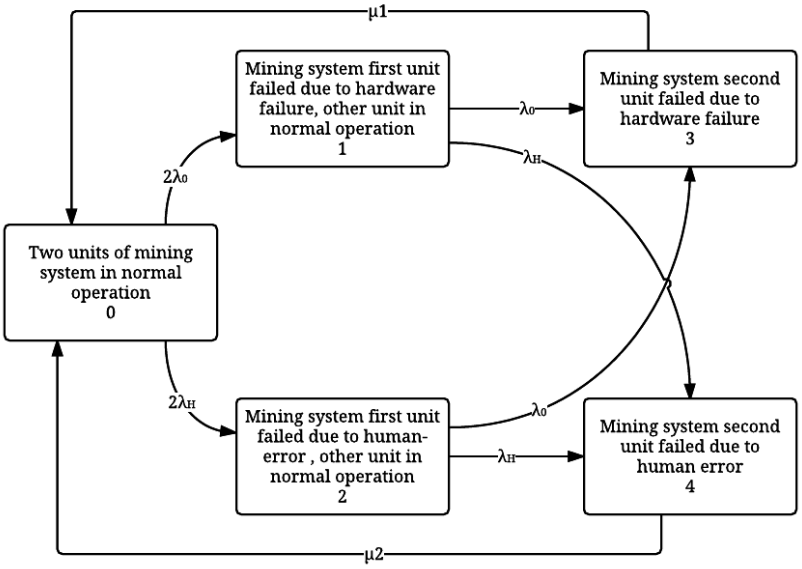

Figure A-1 State space diagram of two identical units with two failure modes and Type-I repair

First the differential equations were obtained by using the Markov method as follows:

$$\frac{dP_0(t)}{dt} + P_0(t)\left(2\cdot\lambda_0 + 2\,\lambda_H\right) = P_3(t)\cdot\mu_1 + P_4(t)\cdot\mu_2$$

$$\frac{dP_1(t)}{dt} + P_1(t)\left(\lambda_0 + \lambda_H\right) = P_0(t)\cdot 2\,\lambda_0$$

$$\frac{dP_2(t)}{dt} + P_2(t)\left(\lambda_0 + \lambda_H\right) = P_0(t)\cdot 2\,\lambda_H$$

$$\frac{dP_3(t)}{dt} + P_3(t)\cdot\mu_1 = \lambda_0\left(P_1(t) + P_2(t)\right)$$

$$\frac{dP_4(t)}{dt} + P_4(t)\cdot\mu_2 = \lambda_H\left(P_1(t) + P_2(t)\right)$$

Then, the s-domain equations were obtained by taking the Laplace transforms when time t=0, $P_0(0)=1$, and all other initial state probabilities are equal to zero.

$$P_0(s) = \frac{P_3(s)\cdot\mu_1 + P_4(s)\cdot\mu_2 + 1}{s + 2\lambda_0 + 2\lambda_H}$$

$$P_1(s) = \frac{P_0(s)\cdot 2\cdot\lambda_0}{s + \lambda + \lambda_H}$$

$$P_2(s) = \frac{P_0(s)\cdot 2\cdot\lambda_H}{s + \lambda_0 + \lambda_H}$$

$$P_3(s) = \frac{\lambda_0\cdot\left(P_1(s) + P_2(s)\right)}{s + \mu_1}$$

$$P_4(s) = \frac{\lambda_H\cdot\left(P_1(s) + P_2(s)\right)}{s + \mu_2}$$

Next, the equations are rearranged as follows:

$$P_0(s) = \frac{\left(s+\mu_1\right)\left(s+\mu_2\right)\cdot\left(s+\lambda_0+\lambda_H\right)}{s\cdot\left(s^3 + s^2\beta + s\gamma + \delta\right)}$$

$$P_1(s) = \frac{2\lambda_0\left(s+\mu_1\right)\left(s+\mu_2\right)}{s\cdot\left(s^3 + s^2\beta + s\gamma + \delta\right)}$$

$$P_2(s) = \frac{2\lambda_H\left(s+\mu_1\right)\left(s+\mu_2\right)}{s\cdot\left(s^3 + s^2\beta + s\gamma + \delta\right)}$$

$$P_3(s) = \frac{2\lambda_0\left(s+\mu_2\right)\left(\lambda+\sigma\right)}{s\cdot\left(s^3 + s^2\beta + s\gamma + \delta\right)}$$

$$P_4(s) = \frac{2\lambda_H\left(s+\mu_2\right)\left(\lambda+\sigma\right)}{s\cdot\left(s^3 + s^2\beta + s\gamma + \delta\right)}$$

Where;

$$\beta = 3\lambda_H + \mu_1 + \mu_2 + 3\lambda_0$$

$$\gamma = 2\lambda_0^2 + 4\lambda_0\lambda_H + 3\lambda_0\mu_1 + 3\lambda_0\mu_2 + 2\lambda_H^2 + 3\lambda_H\mu_1 + 3\lambda_H\mu_2 + \mu_1\mu_2$$

$$\delta = 2\lambda_0^2 + 4\lambda_0\lambda_H + 3\lambda_0\mu_1 + 3\lambda_0\mu_2 + 2\lambda_H^2 + 3\lambda_H\mu_1 + 3\lambda_H\mu_2 + \mu_1\mu_2$$

After that, Cardano's Method was used to find the roots of cubic equations as follows:

$$q = \frac{\left(3\gamma - \beta^2\right)}{9}$$

$$r = 9\gamma\beta - 27\delta - 2\beta^3$$

$$\zeta = \sqrt{r + \sqrt{q^3 + r^2}}$$

$$\tau = \sqrt{r - \sqrt{q^3 + r^2}}$$

$$n_1 = \zeta + \tau - \frac{1}{3}\beta$$

$$n_2 = -\frac{1}{2}(\zeta + \tau) - \frac{1}{3}\beta + \frac{1}{2}i\sqrt{3}\,(\zeta - \tau)$$

$$n_2 = -\frac{1}{2}(\zeta + \tau) - \frac{1}{3}\beta - \frac{1}{2}i\sqrt{3}\,(\zeta - \tau)$$

The above *i* is associated with complex number

$$-\beta = n_1 + n_2 + n_3$$

$$\gamma = n_1 n_2 + n_2 n_3 + n_3 n_1$$

$$-\delta = n_1 n_2 n_3$$

Then, the partial fraction was obtained as follows:

$$P_0(s) = \frac{\left(s + \mu_1\right)\left(s + \mu_2\right)\cdot\left(s + \lambda + \sigma\right)}{s\cdot\left(s - n_1\right)\left(s - n_2\right)\left(s_3 - n_3\right)} = \frac{A_0}{s} + \frac{B_0}{\left(s - n_1\right)} + \frac{C_0}{\left(s - n_2\right)} + \frac{D_0}{\left(s - n_3\right)}$$

The value of A_0, B_0 and C_0 are as follows:

$$A_0 = -\frac{\mu_1\mu_2\left(\lambda + \sigma\right)}{n_1 n_2 n_3}$$

$$B_0 = \frac{\left(n_1 + \mu_1\right)\left(n_1 + \mu_2\right)\cdot\left(n_1 + \lambda + \sigma\right)}{n_1\cdot\left(n_1 - n_2\right)\left(n_1 - n_3\right)}$$

$$C_0 = \frac{\left(n_2 + \mu_1\right)\left(n_2 + \mu_2\right)\cdot\left(n_2 + \lambda + \sigma\right)}{n_1\cdot\left(n_2 - n_1\right)\left(n_2 - n_3\right)}$$

$$\mathrm{D}_0 = \frac{\left(n_3 + \mu_1\right)\left(n_3 + \mu_2\right)\cdot\left(n_3 + \lambda + \sigma\right)}{n_1\cdot\left(n_3 - n_1\right)\left(n_3 - n_2\right)}$$

Then, time dependent probability can be obtained by taking the inverse Laplace transform.

$$P_0(t) = A_0 + B_0\ \mathrm{e}^{-t n_1} + C_0\ \mathrm{e}^{-t n_2} + \mathrm{D}_0\ \mathrm{e}^{-t n_3}$$

By following the same steps, we can find next state time dependent probability.

$$P_1(s) = \frac{2\lambda_0\left(s + \mu_1\right)\left(s + \mu_2\right)}{s\left(s - n_1\right)\left(s - n_2\right)\left(s_3 - n_3\right)} = \frac{A_1}{s} + \frac{B_1}{\left(s - n_1\right)} + \frac{C_1}{\left(s - n_2\right)} + \frac{\mathrm{D}_1}{\left(s - n_3\right)}$$

$$A_1 = -\frac{2\lambda_0\mu_1\mu_2}{n_1 n_2 n_3}$$

$$B_1 = \frac{2\lambda_0\ \left(n_1 + \mu_1\right)\left(n_1 + \mu_2\right)}{n_1\cdot\left(n_1 - n_2\right)\left(n_1 - n_3\right)}$$

$$C_1 = \frac{2\lambda_0\ \left(n_2 + \mu_1\right)\left(n_2 + \mu_2\right)}{n_1\cdot\left(n_2 - n_1\right)\left(n_2 - n_3\right)}$$

$$\mathrm{D}_1 = \frac{2\lambda_0\ \left(n_3 + \mu_1\right)\left(n_3 + \mu_2\right)}{n_1\cdot\left(n_3 - n_1\right)\left(n_3 - n_2\right)}$$

By following the same steps, we can find next state time dependent probability.

$$P_2(s) = \frac{2\lambda_H\left(s + \mu_1\right)\left(s + \mu_2\right)}{s\cdot\left(s^3 + s^2\beta + \mathrm{s}\gamma + \delta\right)} = \frac{A_2}{s} + \frac{B_2}{\left(s - n_1\right)} + \frac{C_2}{\left(s - n_2\right)} + \frac{\mathrm{D}_2}{\left(s - n_3\right)}$$

$$A_2 = -\frac{2\lambda_H\mu_1\mu_2}{n_1 n_2 n_3}$$

$$B_2 = \frac{2\lambda_H\left(n_1 + \mu_1\right)\left(n_1 + \mu_2\right)}{n_1\cdot\left(n_1 - n_2\right)\left(n_1 - n_3\right)}$$

$$C_2 = \frac{2\lambda_H\left(n_2 + \mu_1\right)\left(n_2 + \mu_2\right)}{n_1\cdot\left(n_2 - n_1\right)\left(n_2 - n_3\right)}$$

$$D_2 = \frac{2\lambda_H \left(n_3 + \mu_1\right)\left(n_3 + \mu_2\right)}{n_1 \cdot \left(n_3 - n_1\right)\left(n_3 - n_2\right)}$$

$$P_2(t) = A_2 + B_2\, e^{-t n_1} + C_2\, e^{-t n_2} + D_2\, e^{-t n_3}$$

By following the same steps, we can find next state time dependent probability.

$$P_3(s) = \frac{2\lambda_0 \left(s + \mu_2\right)(\lambda + \sigma)}{s \cdot \left(s^3 + s^2 \beta + s\gamma + \delta\right)} = \frac{A_3}{s} + \frac{B_3}{\left(s - n_1\right)} + \frac{C_3}{\left(s - n_2\right)} + \frac{D_3}{\left(s - n_3\right)}$$

$$A_3 = -\frac{2\lambda_0\, \mu_2(\lambda + \sigma)}{n_1 n_2 n_3}$$

$$B_3 = \frac{2\lambda_0 (\lambda + \sigma)\left(n_1 + \mu_2\right)}{n_1 \cdot \left(n_1 - n_2\right)\left(n_1 - n_3\right)}$$

$$C_3 = \frac{2\lambda_0\ (\lambda + \sigma)\left(n_2 + \mu_2\right)}{n_1 \cdot \left(n_2 - n_1\right)\left(n_2 - n_3\right)}$$

$$D_3 = \frac{2\lambda_0\ (\lambda + \sigma)\left(n_3 + \mu_2\right)}{n_1 \cdot \left(n_3 - n_1\right)\left(n_3 - n_2\right)}$$

$$P_3(t) = A_3 + B_3\, e^{-t n_1} + C_3\, e^{-t n_2} + D_3\, e^{-t n_3}$$

By following the same steps, we can find next state time dependent probability.

$$P_4(s) = \frac{2\lambda_H \left(s + \mu_1\right)(\lambda + \sigma)}{s \cdot \left(s^3 + s^2 \beta + s\gamma + \delta\right)} = \frac{A_4}{s} + \frac{B_4}{\left(s - n_1\right)} + \frac{C_4}{\left(s - n_2\right)} + \frac{D_4}{\left(s - n_3\right)}$$

$$A_4 = -\frac{2\lambda_H\, \mu_2(\lambda + \sigma)}{n_1 n_2 n_3}$$

$$B_4 = \frac{2\lambda_H (\lambda + \sigma)\left(n_1 + \mu_2\right)}{n_1 \cdot \left(n_1 - n_2\right)\left(n_1 - n_3\right)}$$

$$C_4 = \frac{2\lambda_H (\lambda + \sigma)\left(n_2 + \mu_2\right)}{n_1 \cdot \left(n_2 - n_1\right)\left(n_2 - n_3\right)}$$

$$D_4 = \frac{2\lambda_H (\lambda + \sigma)\left(n_3 + \mu_2\right)}{n_1 \cdot \left(n_3 - n_1\right)\left(n_3 - n_2\right)}$$

$$P_4(t) = A_4 + B_4\, e^{-t n_1} + C_4\, e^{-t n_2} + D_4\, e^{-t n_3}$$

A.2 Two identical units with two failure modes and Type-II repair

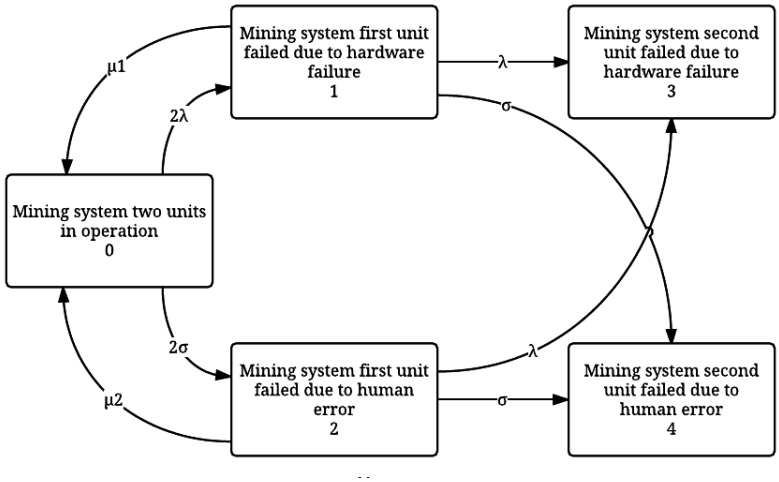

Figure A-2 State space diagram of two identical units with two failure modes and Type-II repair

First the differential equations were obtained by the Markov method as follows:

$$\frac{dP_0(t)}{dt} + P_0(t)\left(2\cdot\lambda_0 + 2\lambda_H\right) = P_1(t)\cdot\mu_1 + P_2(t)\cdot\mu_2$$

$$\frac{dP_1(t)}{dt} + P_1(t)\left(\lambda_0 + \lambda_H + \mu_1\right) = P_0(t)\cdot 2\lambda_0$$

$$\frac{dP_2(t)}{dt} + P_2(t)\left(\lambda_0 + \lambda_H + \mu_2\right) = P_0(t)\cdot 2\lambda_H$$

$$\frac{dP_3(t)}{dt} = \lambda_0\left(P_1(t) + P_2(t)\right)$$

$$\frac{dP_4(t)}{dt} = \lambda_H\left(P_1(t) + P_2(t)\right)$$

Then, the s-domain equations were obtained by taking the Laplace transforms when time t=0, $P_0(0)=1$, and all other initial state probabilities are equal to zero.

$$P_0(s) = \frac{P_1(s)\cdot\mu_1 + P_2(s)\cdot\mu_2 + 1}{s + 2\lambda_0 + 2\lambda_H}$$

$$P_1(s) = \frac{P_0(s) \cdot 2 \cdot \lambda_0}{s + \lambda_0 + \lambda_H + \mu_1}$$

$$P_2(s) = \frac{P_0(s) \cdot 2 \cdot \lambda_H}{s + \lambda_0 + \lambda_H + \mu_2}$$

$$P_3(s) = \frac{\lambda_0 \cdot \left(P_1(s) + P_2(s)\right)}{s}$$

$$P_4(s) = \frac{\lambda_H \cdot \left(P_1(s) + P_2(s)\right)}{s}$$

Next, the equation were rearranged as follows:

$$P_0(s) = \frac{\left(s + \lambda_0 + \lambda_H + \mu_1\right)\left(s + \lambda_0 + \lambda_H + \mu_2\right)}{\left(s^3 + s^2\beta + s\gamma + \delta\right)}$$

$$P_1(s) = \frac{2\lambda_0\left(s + \lambda_0 + \lambda_H + \mu_2\right)}{\left(s^3 + s^2\beta + s\gamma + \delta\right)}$$

$$P_2(s) = \frac{2\lambda_H\left(s + \lambda_0 + \lambda_H + \mu_1\right)}{\left(s^3 + s^2\beta + s\gamma + \delta\right)}$$

$$P_3(s) = \frac{2\lambda_0\left(\lambda_0\left(s + \lambda_0 + \lambda_H + \mu_1\right) + \lambda_H\left(s + \lambda_0 + \lambda_H + \mu_2\right)\right)}{s \cdot \left(s^3 + s^2\beta + s\gamma + \delta\right)}$$

$$P_4(s) = \frac{2\lambda_H\left(\lambda_0\left(s + \lambda_0 + \lambda_H + \mu_1\right) + \lambda_H\left(s + \lambda_0 + \lambda_H + \mu_2\right)\right)}{s \cdot \left(s^3 + s^2\beta + s\gamma + \delta\right)}$$

Where;

$$\beta = 4\lambda_H + \mu_1 + \mu_2 + 4\lambda_0$$

$$\gamma = 5\lambda_0^2 + 10\lambda_0\lambda_H + \lambda_0\mu_1 + 3\lambda_0\mu_2 + 5\lambda_H^2 + 3\lambda_H\mu_1 + \lambda_H\mu_2 + \mu_1\mu_2$$

$$\delta = 2\lambda_0^3 + 6\lambda_0^2\lambda_H + 2\lambda_0^2\mu_2 + 6\lambda_0\lambda_H^2 + 2\lambda_0\lambda_H\mu_1 + 2\lambda_0\lambda_H\mu_2 + 2\lambda_H^3 + 2\lambda_H^2\mu_1$$

After that, Cardano's Method was used to find the roots of cubic equations as follows:

$$q = \frac{\left(3\gamma - \beta^2\right)}{9}$$

$$r = 9\gamma\beta - 27\delta - 2\beta^3$$

$$\zeta = \sqrt{r + \sqrt{q^3 + r^2}}$$

$$\tau = \sqrt{r - \sqrt{q^3 + r^2}}$$

$$n_1 = \zeta + \tau - \frac{1}{3}\beta$$

$$n_2 = -\frac{1}{2}(\zeta + \tau) - \frac{1}{3}\beta + \frac{1}{2} i\sqrt{3}\,(\zeta - \tau)$$

$$n_2 = -\frac{1}{2}(\zeta + \tau) - \frac{1}{3}\beta - \frac{1}{2} i\sqrt{3}\,(\zeta - \tau)$$

The above *i* is associated with complex number

$$-\beta = n_1 + n_2 + n_3$$

$$\gamma = n_1 n_2 + n_2 n_3 + n_3 n_1$$

$$-\delta = n_1 n_2 n_3$$

Then, the equation partial fraction was obtained as follows:

$$P_0(s) = \frac{\left(s + \lambda_0 + \lambda_H + \mu_1\right)\left(s + \lambda_0 + \lambda_H + \mu_2\right)}{\left(s - n_1\right)\left(s - n_2\right)\left(s - n_3\right)} = \frac{A_0}{\left(s - n_1\right)} + \frac{B_0}{\left(s - n_2\right)} + \frac{C_0}{\left(s - n_3\right)}$$

The value of A_0, B_0 and C_0 can be found to be as below.

$$A_0 = \frac{\left(n_1 + \lambda_0 + \lambda_H + \mu_1\right)\left(n_1 + \lambda_0 + \lambda_H + \mu_2\right)}{\left(n_1 - n_2\right)\left(n_1 - n_3\right)}$$

$$B_0 = \frac{\left(n_2 + \lambda_0 + \lambda_H + \mu_1\right)\left(n_2 + \lambda_0 + \lambda_H + \mu_2\right)}{\left(n_2 - n_1\right)\left(n_2 - n_3\right)}$$

$$C_0 = \frac{\left(n_3 + \lambda_0 + \lambda_H + \mu_1\right)\left(n_3 + \lambda_0 + \lambda_H + \mu_2\right)}{\left(n_3 - n_1\right)\left(n_3 - n_2\right)}$$

Then, we can find the inverse Laplace transform.

$$P_0(t) = A_0 e^{-t n_1} + B_0\, e^{-t n_2} + C_0\, e^{-t n_3}$$

By following the same steps, we can find next state time dependent probability.

$$P_1(s) = \frac{A_1}{(s - n_1)} + \frac{B_1}{(s - n_2)} + \frac{C_1}{(s - n_3)}$$

$$A_1 = \frac{2\lambda_0 \left(n_1 + \lambda_0 + \lambda_H + \mu_2\right)}{(n_1 - n_2)(n_1 - n_3)}$$
$$B_1 = \frac{2\lambda_0 \left(n_2 + \lambda_0 + \lambda_H + \mu_2\right)}{(n_2 - n_1)(n_2 - n_3)}$$
$$C_1 = \frac{2\lambda_0 \left(n_3 + \lambda_0 + \lambda_H + \mu_2\right)}{(n_3 - n_1)(n_3 - n_2)}$$

Then, we can find the inverse Laplace transform.

$$P_1(t) = + A_1 e^{-tn_1} + B_1 e^{-tn_2} + C_1 e^{-tn_3}$$

By following the same steps, we can find next state time dependent probability.

$$P_2(s) = \frac{A_2}{(s - n_1)} + \frac{B_2}{(s - n_2)} + \frac{C_2}{(s - n_3)}$$

$$A_2 = \frac{2\lambda_H \left(n_1 + \lambda_0 + \lambda_H + \mu_1\right)}{(n_1 - n_2)(n_1 - n_3)}$$
$$B_2 = \frac{2\lambda_H \left(n_2 + \lambda_0 + \lambda_H + \mu_1\right)}{(n_2 - n_1)(n_2 - n_3)}$$
$$C_2 = \frac{2\lambda_H \left(n_3 + \lambda_0 + \lambda_H + \mu_1\right)}{(n_3 - n_1)(n_3 - n_2)}$$

Then, we can find the inverse Laplace transform.

$$P_2(t) = A_2 e^{-tn_1} + B_2 e^{-tn_2} + C_2 e^{-tn_3}$$

By following the same steps, we can find next state time dependent probability.

$$P_3(s) = \frac{A_3}{s} + \frac{B_3}{(s - n_1)} + \frac{C_3}{(s - n_2)} + \frac{\mathrm{D}_3}{(s - n_3)}$$

$$A_3 = - \frac{2\lambda_0 \left(\lambda_0 \left(\lambda_0 + \lambda_H + \mu_1\right) + \lambda_H \left(\lambda_0 + \lambda_H + \mu_2\right)\right)}{n_1 n_2 n_3}$$

$$B_3 = \frac{2\lambda_0 \left(\lambda_0 \left(n_1 + \lambda_0 + \lambda_H + \mu_1\right) + \sigma \left(n_1 + \lambda_0 + \lambda_H + \mu_2\right)\right)}{n_1 \cdot (n_1 - n_2)(n_1 - n_3)}$$

$$C_3 = \frac{2\lambda_0 \left(\lambda_0 \left(n_2 + \lambda_0 + \lambda_H + \mu_1\right) + \lambda_H \left(n_2 + \lambda_0 + \lambda_H + \mu_2\right)\right)}{n_2 \cdot (n_2 - n_1)(n_2 - n_3)}$$

$$\mathrm{D}_3 = \frac{2\lambda_0 \left(\lambda_0 \left(n_3 + \lambda_0 + \lambda_H + \mu_1\right) + \lambda_H \left(n_3 + \lambda_0 + \lambda_H + \mu_2\right)\right)}{n_3 \cdot (n_3 - n_1)(n_3 - n_2)}$$

Then, we can find the inverse Laplace transform.

$$P_3(t) = A_3 + B_3\, \mathrm{e}^{-t n_1} + C_3\, \mathrm{e}^{-t n_2} + \mathrm{D}_3\, \mathrm{e}^{-t n_3}$$

By following the same steps, we can find next state time dependent probability.

$$P_4(s) = \frac{A_4}{s} + \frac{B_4}{(s - n_1)} + \frac{C_4}{(s - n_2)} + \frac{\mathrm{D}_4}{(s - n_3)}$$

$$A_4 = - \frac{2\lambda_H \left(\lambda_0 \left(\lambda_0 + \lambda_H + \mu_1\right) + \lambda_H \left(\lambda_0 + \lambda_H + \mu_2\right)\right)}{n_1 n_2 n_3}$$

$$B_4 = \frac{2\lambda_H \left(\lambda_0 \left(n_1 + \lambda_0 + \lambda_H + \mu_1\right) + \lambda_H \left(n_1 + \lambda_0 + \lambda_H + \mu_2\right)\right)}{n_1 \cdot (n_1 - n_2)(n_1 - n_3)}$$

$$C_4 = \frac{2\lambda_H \left(\lambda_0 \left(n_2 + \lambda_0 + \lambda_H + \mu_1\right) + \lambda_H \left(n_2 + \lambda_0 + \lambda_H + \mu_2\right)\right)}{n_2 \cdot (n_2 - n_1)(n_2 - n_3)}$$

$$\mathrm{D}_4 = \frac{2\lambda_H \left(\lambda_0 \left(n_3 + \lambda_0 + \lambda_H + \mu_1\right) + \lambda_H \left(n_3 + \lambda_0 + \lambda_H + \mu_2\right)\right)}{n_3 \cdot (n_3 - n_1)(n_3 - n_2)}$$

Then, we can find the inverse Laplace transform.

$$P_4(t) = A_4 + B_4\, \mathrm{e}^{-t n_1} + C_4\, \mathrm{e}^{-t n_2} + \mathrm{D}_4\, \mathrm{e}^{-t n_3}$$

A.3 Two identical units with two failure modes and Type-III repair

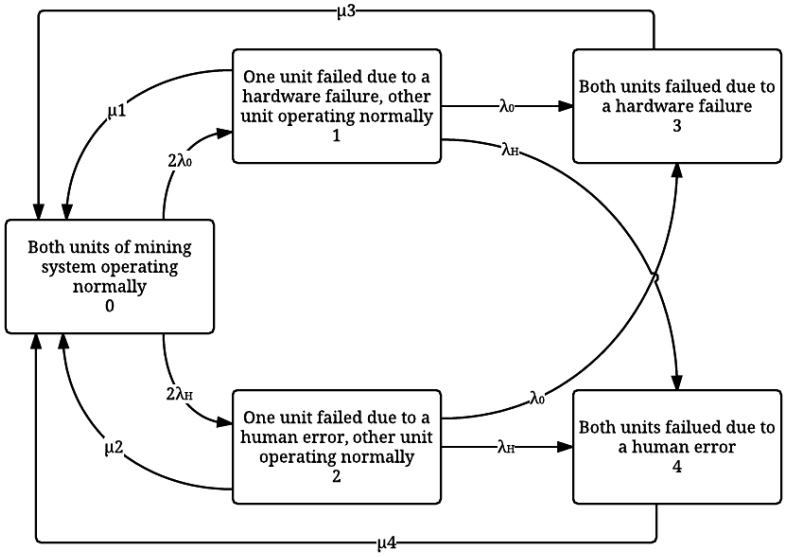

Figure A-3 State space diagram of two identical units with two failure modes and Type-III repair

First the differential equations were obtained by using the Markov method as follows:

$$\frac{dP_0(t)}{dt} + P_0(t)\left(2\lambda_0 + 2\lambda_H\right) = P_1(t)\,\mu_1 + P_2(t)\,\mu_2 + P_3(t)\,\mu_3 + P_4(t)\,\mu_4$$

$$\frac{dP_1(t)}{dt} + P_1(t)\left(\lambda_0 + \lambda_H + \mu_1\right) = P_0(t)\cdot 2\lambda_0$$

$$\frac{dP_2(t)}{dt} + P_2(t)\left(\lambda_0 + \lambda_H + \mu_2\right) = + P_0(t)\cdot 2\lambda_H$$

$$\frac{dP_3(t)}{dt} + P_3(t)\cdot\mu_3 = P_1(t)\cdot\lambda_0 + P_2(t)\cdot\lambda_0$$

$$\frac{dP_4(t)}{dt} + P_4(t)\cdot\mu_4 = P_1(t)\cdot\lambda_H + P_2(t)\cdot\lambda_H$$

Then, the s-domain equations were obtained by taking the Laplace transforms when time t=0, $P_0(0)=1$, and all other initial state probabilities are equal to zero.

$$P_0(s) = \frac{P_1(s)\cdot\mu_1 + P_2(s)\cdot\mu_2 + P_3(s)\cdot\mu_3 + P_4(s)\cdot\mu_4 + 1}{s + 2\cdot\lambda_0 + 2\cdot\lambda_H}$$

$$P_1(s) = \frac{2 \cdot \lambda_0 \cdot P_0(s)}{s + \lambda_0 + \lambda_H + \mu_1}$$

$$P_2(s) = \frac{2 \cdot \lambda_H \cdot P_0(s)}{s + \lambda_0 + \lambda_H + \mu_2}$$

$$P_3(s) = \frac{\lambda_0 \cdot \left(P_1(s) + P_2(s)\right)}{s + \mu_3}$$

$$P_4(s) = \frac{\lambda_H \cdot \left(P_1(s) + P_2(s)\right)}{s + \mu_4}$$

Next, the equations were rearranged as follows:

$$P_0(s) = \frac{\left(s + \mu_3\right)\left(s + \mu_4\right)\left(s + \lambda_0 + \lambda_H + \mu_1\right)\left(s + \lambda_0 + \lambda_H + \mu_2\right)}{s\left(s^4 + s^3\beta + s^2\gamma + s\delta + \epsilon\right)}$$

$$P_1(s) = \frac{2\lambda\left(s + \mu_3\right)\left(s + \mu_4\right)\left(s + \lambda + \sigma + \mu_2\right)}{s\left(\beta s^3 + s^4 + \gamma s^2 + \delta s + \epsilon\right)}$$

$$P_2(s) = \frac{2\sigma\left(s + \mu_3\right)\left(s + \mu_4\right)\left(s + \lambda + \sigma + \mu_1\right)}{s\left(\beta s^3 + s^4 + \gamma s^2 + \delta s + \epsilon\right)}$$

$$P_3(s) = \frac{2\lambda\left(\left(s + \lambda + \sigma + \mu_2\right)\lambda + \left(s + \lambda + \sigma + \mu_1\right)\sigma\right)\left(s + \mu_3\right)}{s\left(s^4 + s^3\beta + s^2\gamma + s\delta + \epsilon\right)}$$

$$P_4(s) = \frac{2\sigma\left(\left(s + \lambda + \sigma + \mu_2\right)\lambda + \left(s + \lambda + \sigma + \mu_1\right)\sigma\right)\left(s + \mu_3\right)}{s\left(s^4 + s^3\beta + s^2\gamma + s\delta + \epsilon\right)}$$

Where;

$$\beta = 4\lambda + 4\lambda_H + \mu_1 + \mu_2 + \mu_3 + \mu_4$$

$$\gamma = 5\lambda_0^2 + 10\lambda_0\lambda_H + \lambda_0\mu_1 + 3\lambda_0\mu_2 + 4\lambda_0\mu_3 + 4\lambda_0\mu_4 + 5\lambda_H^2 + 3\lambda_H\mu_1 + \lambda_H\mu_2 + 4\lambda_H\mu_3 + 4\lambda_H\mu_4 + \mu_1\mu_2 + \mu_1\mu_3 + \mu_1\mu_4 + \mu_2\mu_3 + \mu_2\mu_4 + \mu_3\mu_4$$

$$\begin{aligned}\delta = {} & 2\lambda_0^3 + 6\lambda_0^2\lambda_H + 2\lambda_0^2\mu_2 + 3\lambda_0^2\mu_3 + 5\lambda_0^2\mu_4 + 6\lambda_0\lambda_H^2 + 2\lambda_0\lambda_H\mu_1 + 2\lambda_0\lambda_H\mu_2 \\ & + 8\lambda_0\lambda_H\mu_3 + 8\lambda_0\lambda_H\mu_4 + \lambda_0\mu_1\mu_3 + \lambda_0\mu_1\mu_4 + 3\lambda_0\mu_2\mu_3 + 3\lambda_0\mu_2\mu_4 + 4\lambda_0\mu_3\mu_4 \\ & + 2\lambda_H^3 + 2\lambda_H^2\mu_1 + 5\lambda_H^2\mu_3 + 3\lambda_H^2\mu_4 + 3\lambda_H\mu_1\mu_3 + 3\lambda_H\mu_1\mu_4 + \lambda_H\mu_2\mu_3 + \lambda_H\mu_2\mu_4 \\ & + 4\lambda_H\mu_3\mu_4 + \mu_1\mu_2\mu_3 + \mu_1\mu_2\mu_4 + \mu_1\mu_3\mu_4 + \mu_2\mu_3\mu_4\end{aligned}$$

$$\epsilon = 2\lambda_0^3\mu_4 + 2\lambda_0^2\lambda_H\mu_3 + 4\lambda_0^2\lambda_H\mu_4 + 2\lambda_0^2\mu_2\mu_4 + 3\lambda_0^2\mu_3\mu_4 + 4\lambda_0\lambda_H^2\mu_3 + 2\lambda_0\lambda_H^2\mu_4 + 2\lambda_0\lambda_H\mu_1\mu_4 + 2\lambda_0\lambda_H\mu_2\mu_3 + 6\lambda_0\lambda_H\mu_3\mu_4 + \lambda_0\mu_1\mu_3\mu_4 + 3\lambda_0\mu_2\mu_3\mu_4 + 2\lambda_H^3\mu_3 + 2\lambda_H^2\mu_1\mu_3 + 3\lambda_H^2\mu_3\mu_4 + 3\lambda_H\mu_1\mu_3\mu_4 + \lambda_H\mu_2\mu_3\mu_4 + \mu_1\mu_2\mu_3\mu_4$$

After that, Cardano's Method was used to find the roots of cubic equations as follows:

$$q = 27\beta^2\epsilon - 9\beta\delta\gamma + 2\gamma^3 + 27\delta^2 - 72\epsilon\gamma$$

$$r = q + \sqrt{q^2 - 4\left(-3\beta\delta + 12\epsilon + \gamma\right)^3}$$

$$v = \frac{1}{3}\frac{\left(-3\beta\delta + \gamma^2 + 12\epsilon\right)2^{1/3}}{r^{1/3}} + \frac{1}{6}2^{2/3}r^{1/3}$$

$$\zeta = \frac{1}{6}\sqrt{9\beta - 24\gamma + 36v}$$

$$\tau = \frac{1}{2}\beta^2 - \frac{4}{3}\gamma - v$$

$$\omega = \frac{1}{4}\frac{-\beta^3 + 4\beta\gamma - 8\delta}{\zeta}$$

$$n_1 = \frac{1}{4}\beta + \frac{1}{2}\zeta - \frac{1}{2}i\sqrt{\tau - \omega}$$

$$n_2 = -\frac{1}{4}\beta - \frac{1}{2}\zeta + \frac{1}{2}i\sqrt{\tau - \omega}$$

$$n_3 = -\frac{1}{4}\beta + \frac{1}{2}\zeta - \frac{1}{2}i\sqrt{\tau - \omega}$$

$$n_4 = -\frac{1}{4}\beta + \frac{1}{2}\zeta + \frac{1}{2}i\sqrt{\tau - \omega}$$

Then, the equation partial fraction was obtained as follows:

$$P_0(s) = \frac{\left(s + \mu_3\right)\left(s + \mu_4\right)\left(s + \lambda_0 + \lambda_H + \mu_1\right)\left(s + \lambda_0 + \lambda_H + \mu_2\right)}{s\left(s - n_1\right)\left(s - n_2\right)\left(s - n_3\right)\left(s - n_4\right)} = \frac{A_0}{s} + \frac{B_0}{s - n_1} + \frac{C_0}{s - n_2} + \frac{\mathrm{D}_0}{s - n_3} + \frac{E_0}{s - n_4}$$

The value of A_0, B_0 and C_0 can be found to be as below.

$$A_0 = \frac{\mu_1\mu_2\left(\lambda_0 + \lambda_H + \mu_1\right)\left(\lambda_0 + \lambda_H + \mu_2\right)}{n_1 n_2 n_3 n_4}$$

$$B_0 = \frac{(n_1+\mu_3)(n_1+\mu_4)(n_1+\lambda_0+\lambda_H+\mu_1)(n_1+\lambda_0+\lambda_H+\mu_2)}{n_1(n_1-n_2)(n_1-n_3)(n_1-n_4)}$$

$$C_0 = \frac{(n_2+\mu_3)(n_2+\mu_4)(n_2+\lambda_0+\lambda_H+\mu_1)(n_2+\lambda_0+\lambda_H+\mu_2)}{n_2(n_2-n_1)(n_2-n_3)(n_2-n_4)}$$

$$D_0 = \frac{(n_3+\mu_3)(n_3+\mu_4)(n_3+\lambda_0+\lambda_H+\mu_1)(n_3+\lambda_0+\lambda_H+\mu_2)}{n_3(n_3-n_1)(n_3-n_2)(n_3-n_4)}$$

$$E_0 = \frac{(n_4+\mu_3)(n_4+\mu_4)(n_4+\lambda_0+\lambda_H+\mu_1)(n_4+\lambda_0+\lambda_H+\mu_2)}{n_4(n_4-n_1)(n_4-n_2)(n_4-n_3)}$$

Then, we can find the inverse Laplace transform.

$$P_0(t) = A_0 + B_0 e^{-n_1 t} + C_0 e^{-n_2 t} + D_0 e^{-n_3 t} + E_0 e^{-n_4 t}$$

By following the same steps, we can find next state time dependent probability.

$$P_1(s) = \frac{2\lambda_0(s+\mu_3)(s+\mu_4)(s+\lambda_0+\lambda_H+\mu_2)}{s(s-n_1)(s-n_2)(s-n_3)(s-n_4)}$$
$$= \frac{A_1}{s} + \frac{B_1}{s-n_1} + \frac{C_1}{s-n_2} + \frac{D_1}{s-n_3} + \frac{E_1}{s-n_4}$$

$$A_1 = \frac{2\lambda_0\mu_3\mu_4(\lambda_0+\lambda_H+\mu_2)}{n_1 n_2 n_3 n_4}$$

$$B_1 = \frac{2\lambda_0(n_1+\mu_3)(n_1+\mu_4)(n_1+\lambda_0+\lambda_H+\mu_2)}{n_1(n_1-n_2)(n_1-n_3)(n_1-n_4)}$$

$$C_1 = \frac{2\lambda_0(n_2+\mu_3)(n_2+\mu_4)(n_2+\lambda_0+\lambda_H+\mu_2)}{n_2(n_2-n_1)(n_2-n_3)(n_2-n_4)}$$

$$D_1 = \frac{2\lambda_0(n_3+\mu_3)(n_3+\mu_4)(n_3+\lambda_0+\lambda_H+\mu_2)}{n_3(n_3-n_1)(n_3-n_2)(n_3-n_4)}$$

$$E_1 = \frac{2\lambda_0(n_4+\mu_3)(n_4+\mu_4)(n_4+\lambda_0+\lambda_H+\mu_2)}{n_4(n_4-n_1)(n_4-n_2)(n_4-n_3)}$$

Then, we can find the inverse Laplace transform.

$$P_1(t) = A_1 + B_1 e^{-n_1 t} + C_1 e^{-n_2 t} + D_1 e^{-n_3 t} + E_1 e^{-n_4 t}$$

By following the same steps, we can find next state time dependent probability.

$$P_2(s) = \frac{2\lambda_H (s+\mu_3)(s+\mu_4)(s+\lambda_0+\lambda_H+\mu_1)}{s(s-n_1)(s-n_2)(s-n_3)(s-n_4)} = \frac{A_2}{s} + \frac{B_2}{s-n_1} + \frac{C_2}{s-n_2} + \frac{D_2}{s-n_3} + \frac{E_2}{s-n_4}$$

$$A_2 = \frac{2\lambda_H \mu_3 \mu_4 (\lambda_0+\lambda_H+\mu_2)}{n_1 n_2 n_3 n_4}$$

$$B_2 = \frac{2\lambda_H (n_1+\mu_3)(n_1+\mu_4)(n_1+\lambda+\sigma+\mu_2)}{n_1 (n_1-n_2)(n_1-n_3)(n_1-n_4)}$$

$$C_2 = \frac{2\lambda_H (n_2+\mu_3)(n_2+\mu_4)(n_2+\lambda_0+\lambda_H+\mu_2)}{n_2 (n_2-n_1)(n_2-n_3)(n_2-n_4)}$$

$$D_2 = \frac{2\lambda_H (n_3+\mu_3)(n_3+\mu_4)(n_3+\lambda_0+\lambda_H+\mu_2)}{n_3 (n_3-n_1)(n_3-n_2)(n_3-n_4)}$$

$$E_2 = \frac{2\lambda_H (n_4+\mu_3)(n_4+\mu_4)(n_4+\lambda_0+\lambda_H+\mu_2)}{n_4 (n_4-n_1)(n_4-n_2)(n_4-n_3)}$$

Then, we can find the inverse Laplace transform.

$$P_2(t) = A_2 + B_2 e^{-n_1 t} + C_2 e^{-n_2 t} + D_2 e^{-n_3 t} + E_2 e^{-n_4 t}$$

By following the same steps, we can find next state time dependent probability.

$$P_3(s) = \frac{2\lambda_0 \left(\left(s+\lambda_0+\lambda_H+\mu_2\right)\lambda_0 + \left(s+\lambda_0+\lambda_H+\mu_1\right)\lambda_H \right)(s+\mu_3)}{s(s-n_1)(s-n_2)(s-n_3)(s-n_4)} = \frac{A_3}{s} + \frac{B_3}{s-n_1} + \frac{C_3}{s-n_2} + \frac{D_3}{s-n_3} + \frac{E_3}{s-n_4}$$

$$A_3 = \frac{2\lambda_0 \mu_3 \left(\left(\lambda_0+\lambda_H+\mu_2\right)\lambda_0 + \left(\lambda_0+\lambda_H+\mu_1\right)\lambda_H \right)}{n_1 n_2 n_3 n_4}$$

$$B_3 = \frac{2\lambda_0 \left(\left(n_1+\lambda_0+\lambda_H+\mu_2\right)\lambda_0 + \left(n_1+\lambda_0+\lambda_H+\mu_1\right)\lambda_H \right)(n_1+\mu_3)}{n_1 (n_1-n_2)(n_1-n_3)(n_1-n_4)}$$

$$C_3 = \frac{2\lambda_0 \left(\left(n_2+\lambda_0+\lambda_H+\mu_2\right)\lambda_0 + \left(n_2+\lambda_0+\lambda_H+\mu_1\right)\lambda_H \right)(n_2+\mu_3)}{n_2 (n_2-n_1)(n_2-n_3)(n_2-n_4)}$$

$$D_3 = \frac{2\lambda_0\left(\left(n_3+\lambda_0+\lambda_H+\mu_2\right)\lambda_0+\left(n_3+\lambda_0+\lambda_H+\mu_1\right)\lambda_H\right)\left(n_3+\mu_3\right)}{n_3\left(n_3-n_1\right)\left(n_3-n_2\right)\left(n_3-n_4\right)}$$

$$E_3 = \frac{2\lambda_0\left(\left(n_4+\lambda_0+\lambda_H+\mu_2\right)\lambda_0+\left(n_3+\lambda_0+\lambda_H+\mu_1\right)\lambda_H\right)\left(n_4+\mu_3\right)}{n_4\left(n_4-n_1\right)\left(n_4-n_2\right)\left(n_4-n_3\right)}$$

Then, we can find the inverse Laplace transform.

$$P_3(t) = A_3 + B_3\,\mathrm{e}^{-n_1 t} + C_3\,\mathrm{e}^{-n_2 t} + D_3\,\mathrm{e}^{-n_3 t} + E_3\,\mathrm{e}^{-n_4 t}$$

By following the same steps, we can find next state time dependent probability.

$$P_4(s) = \frac{2\sigma\left(\left(s+\lambda_0+\lambda_H+\mu_2\right)\lambda_H+\left(s+\lambda_0+\lambda_H+\mu_1\right)\lambda_H\right)\left(s+\mu_3\right)}{s\left(s-n_1\right)\left(s-n_2\right)\left(s-n_3\right)\left(s-n_4\right)}$$
$$= \frac{A_4}{s} + \frac{B_4}{s-n_1} + \frac{C_4}{s-n_2} + \frac{\mathrm{D}_4}{s-n_3} + \frac{E_4}{s-n_4}$$

$$A_4 = \frac{2\lambda_H\mu_3\left(\left(\lambda_0+\lambda_H+\mu_2\right)\lambda_H+\left(\lambda_0+\lambda_H+\mu_1\right)\lambda_H\right)}{n_1 n_2 n_3 n_4}$$

$$B_4 = \frac{2\lambda_H\left(\left(n_1+\lambda_0+\lambda_H+\mu_2\right)\lambda_H+\left(n_1+\lambda_0+\lambda_H+\mu_1\right)\lambda_H\right)\left(n_1+\mu_3\right)}{n_1\left(n_1-n_2\right)\left(n_1-n_3\right)\left(n_1-n_4\right)}$$

$$C_4 = \frac{2\lambda_H\left(\left(n_2+\lambda_0+\lambda_H+\mu_2\right)\lambda_H+\left(n_2+\lambda_0+\lambda_H+\mu_1\right)\lambda_H\right)\left(n_2+\mu_3\right)}{n_2\left(n_2-n_1\right)\left(n_2-n_3\right)\left(n_2-n_4\right)}$$

$$\mathrm{D}_4 = \frac{2\lambda_H\left(\left(n_3+\lambda_0+\lambda_H+\mu_2\right)\lambda_H+\left(n_3+\lambda_0+\lambda_H+\mu_1\right)\lambda_H\right)\left(n_3+\mu_3\right)}{n_3\left(n_3-n_1\right)\left(n_3-n_2\right)\left(n_3-n_4\right)}$$

$$E_4 = \frac{2\lambda_H\left(\left(n_4+\lambda_0+\lambda_H+\mu_2\right)\lambda_H+\left(n_3+\lambda_0+\lambda_H+\mu_1\right)\lambda_H\right)\left(n_4+\mu_3\right)}{n_4\left(n_4-n_1\right)\left(n_4-n_2\right)\left(n_4-n_3\right)}$$

Then, we can find the inverse Laplace transform.

$$P_4(t) = A_4 + B_4\,\mathrm{e}^{-n_1 t} + C_4\,\mathrm{e}^{-n_2 t} + D_4\,\mathrm{e}^{-n_3 t} + E_4\,\mathrm{e}^{-n_4 t}$$

Appendix B: Reliability Parameter Plots of Chapter 2

B.1 Special Case: One-Unit without repair

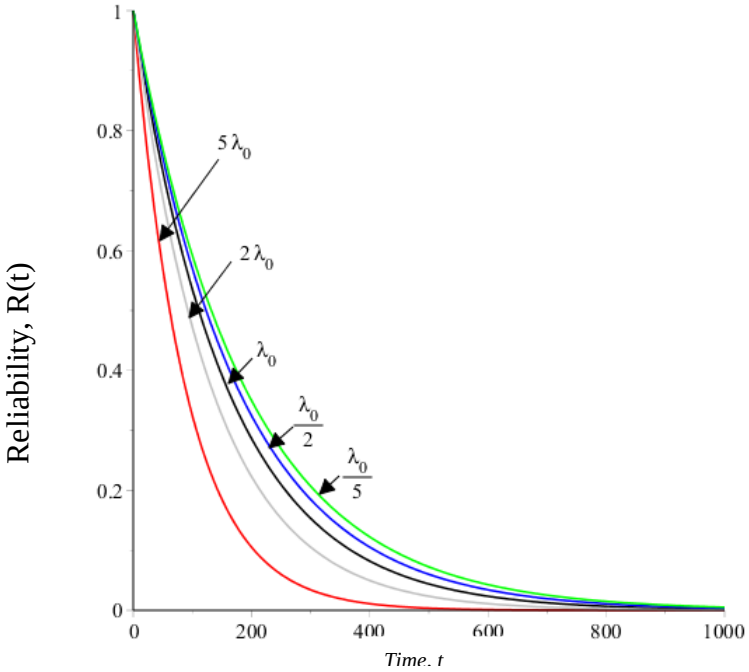

Figure B-1 Reliability plots of one-unit system with two failure modes without repair at different values of hardware failure rate ($\lambda_{0)}$.

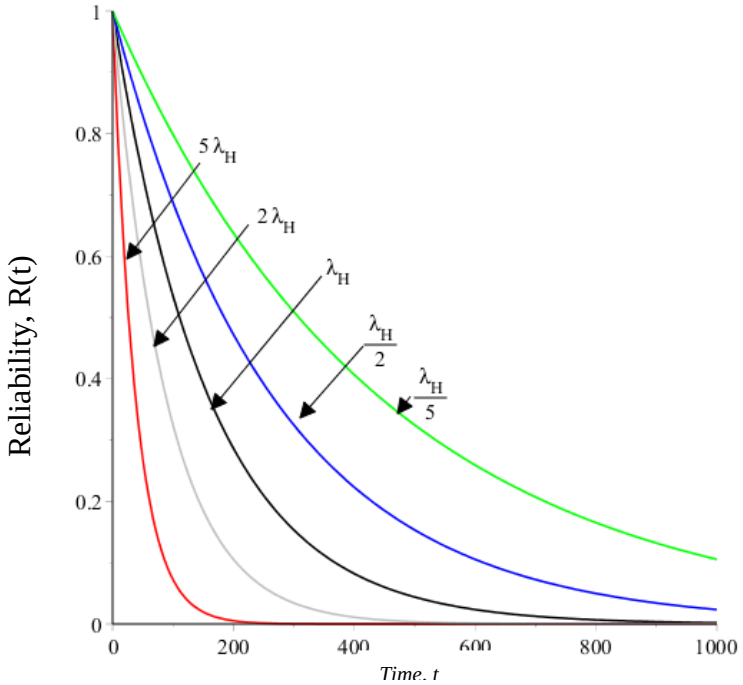

Figure B-2 Reliability plots of one-unit system with two failure modes without repair at different values of human-error rate (λ_H).

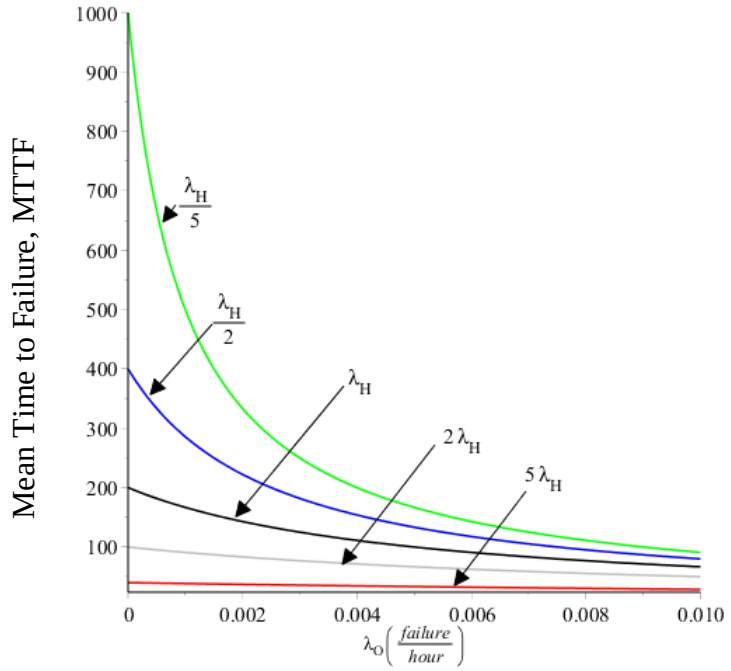

Figure B-3 MTTF plots of one-unit system with two failure modes without repair at different values of human-error rate (λ_H).

B.2 Special Case: Two-Unit without repair

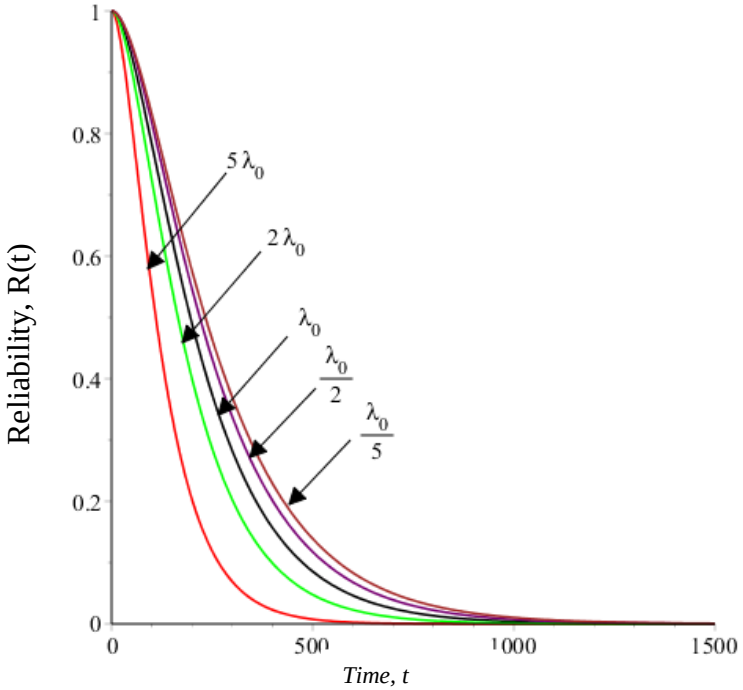

Figure B-4 Reliability plots of two-units system with two failure modes without repair at different values of hardware failure rate (λ_0).

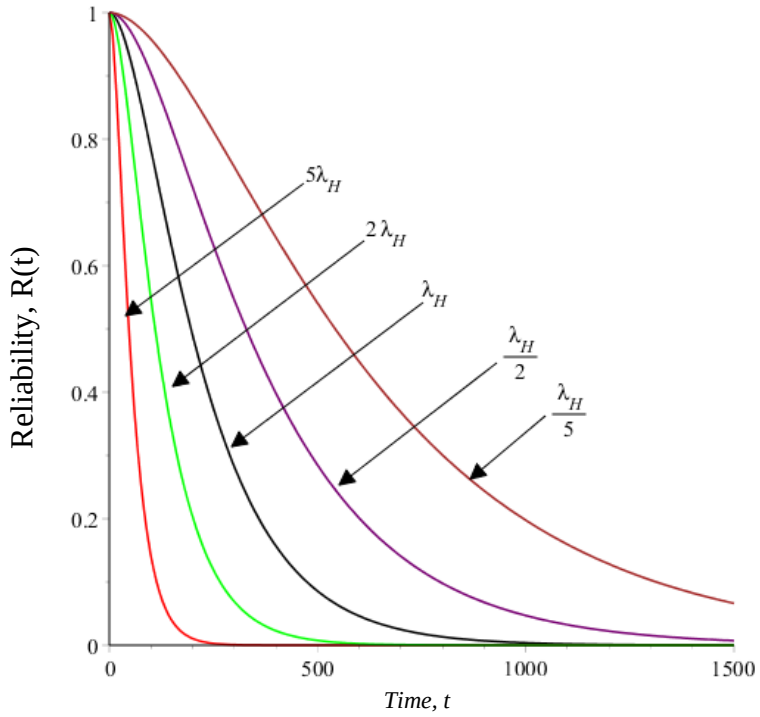

Figure B-5 Reliability plots of two-units system with two failure modes without repair at different values of human-error rate (λ_H).

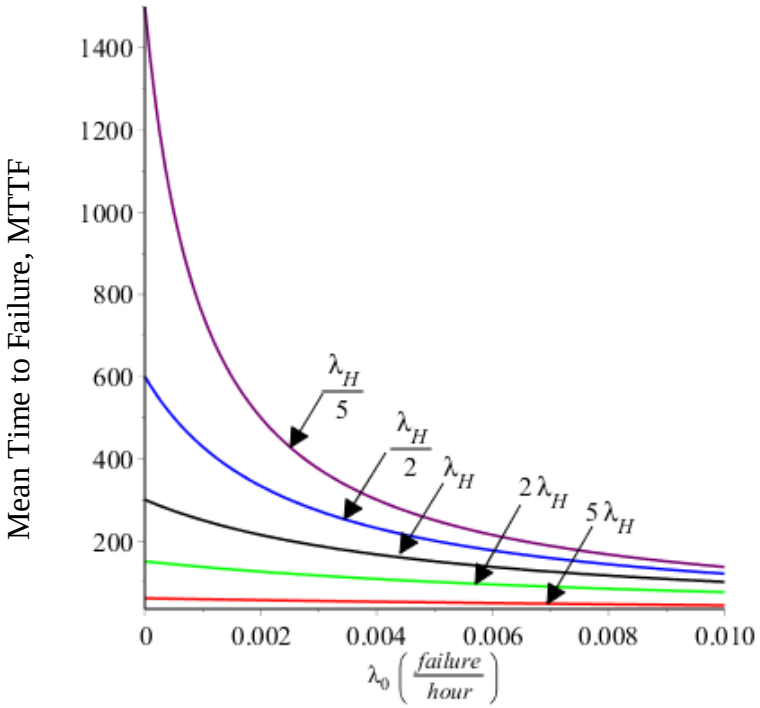

Figure 0B-6 MTTF Plots of two-units system with two failure modes and without repair at different values of human-error rate (λ_H).

B.3 Special Case: Three-Unit without repair

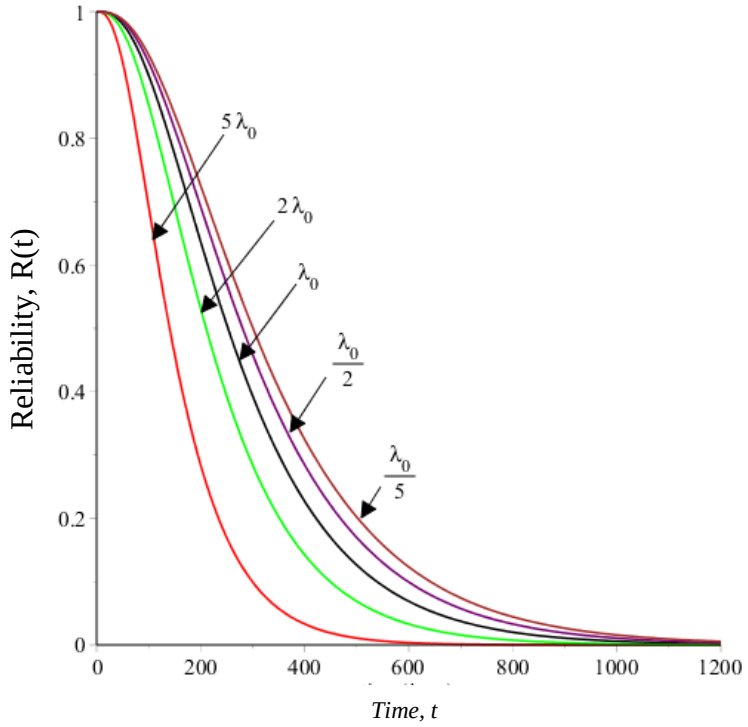

Figure B-7 Reliability plots of three-units system with two failure modes without repair at different values of hardware failure rate (λ_0).

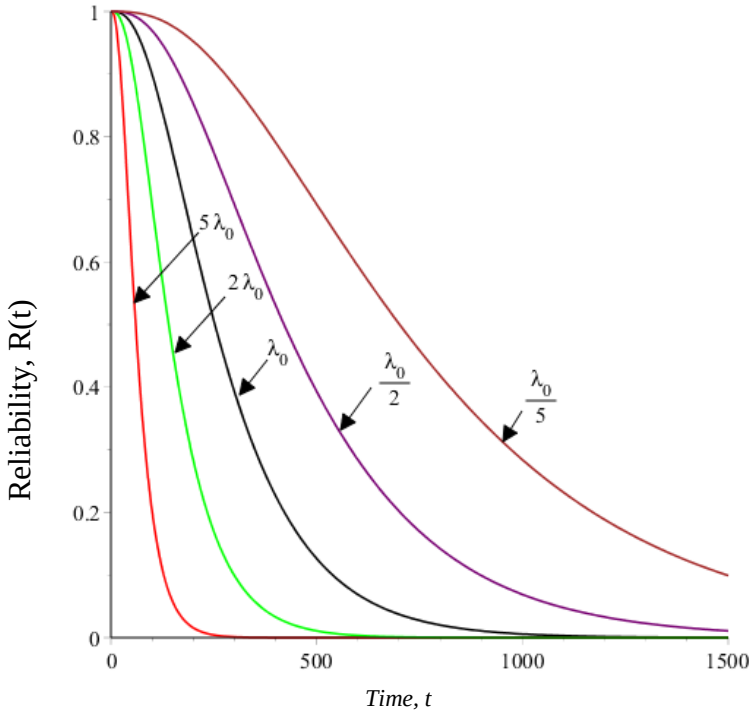

Figure B-8 Reliability plots of three-units system with two failure modes without repair at different values of human-error rate (λ_H).

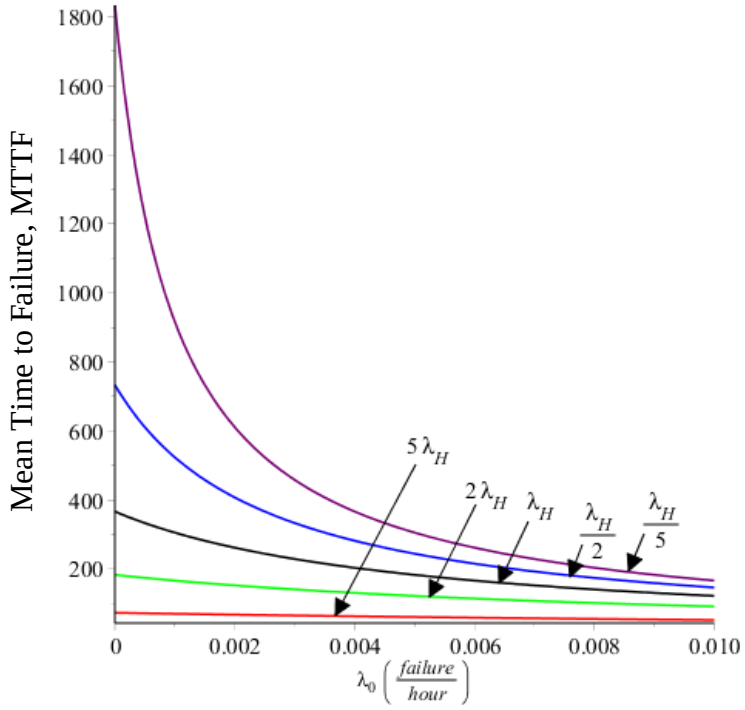

Figure B-9 MTTF plots of three-units system with two failure modes and without repair at different values of human-error rate (λ_H).

B.4 Special Case: One-Unit with Type-I repair

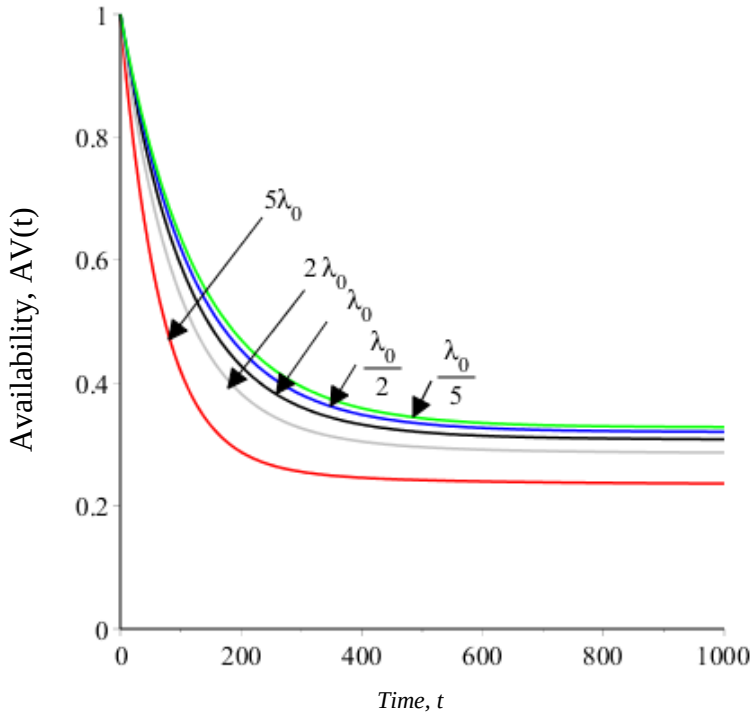

Figure B-10 Availability plots of one-unit system with two failure modes and Type-I repair at different values of hardware failure rate (λ_0).

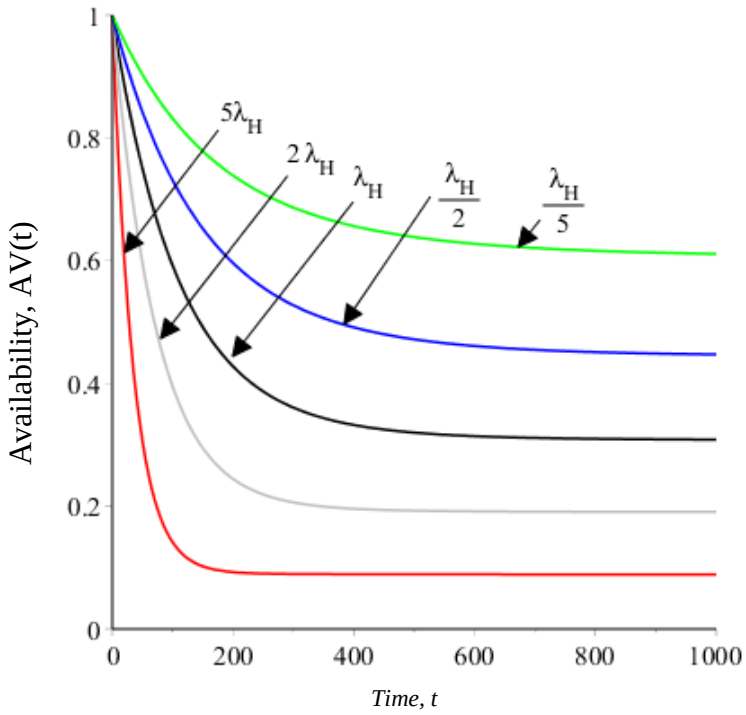

Figure B-11 Availability plots of one-unit system with two failure modes and Type-I repair at different values of human-error rate (λ_H).

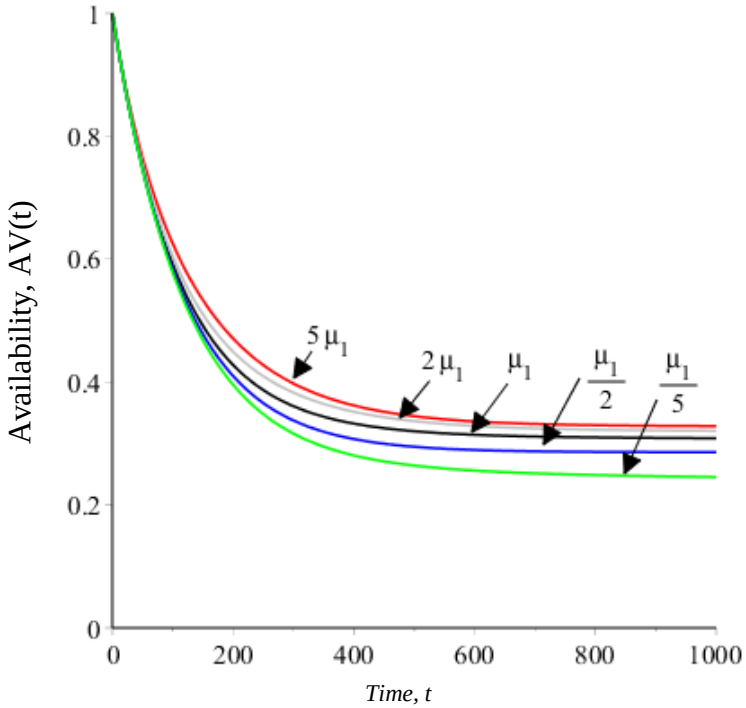

Figure B-12 Availability plots of one-unit system with two failure modes and Type-I repair at different values of repair rate (μ_1).

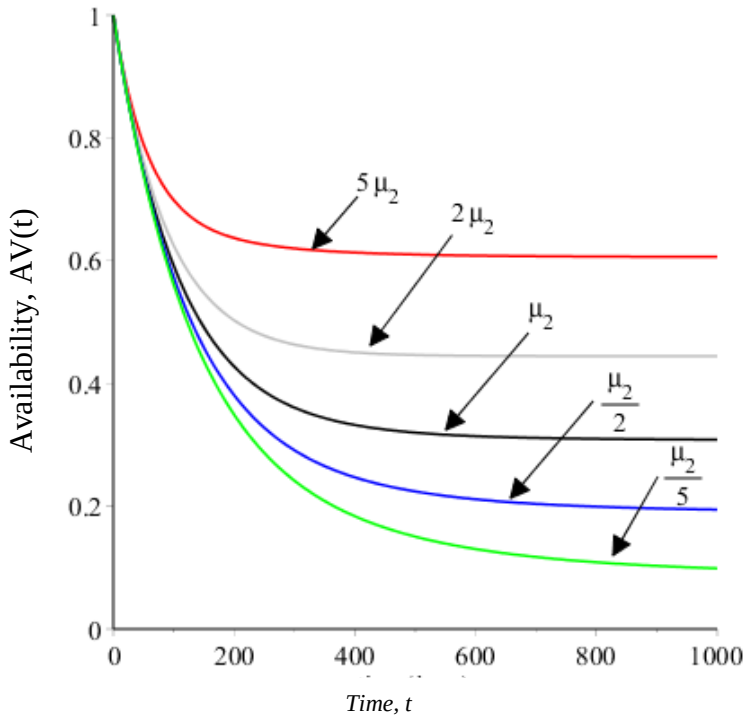

Figure B-13 Availability plots of one-unit system with two failure modes and Type-I repair at different values of repair rate (μ_2).

B.5 Special Case: Two-Unit with Type-I repair

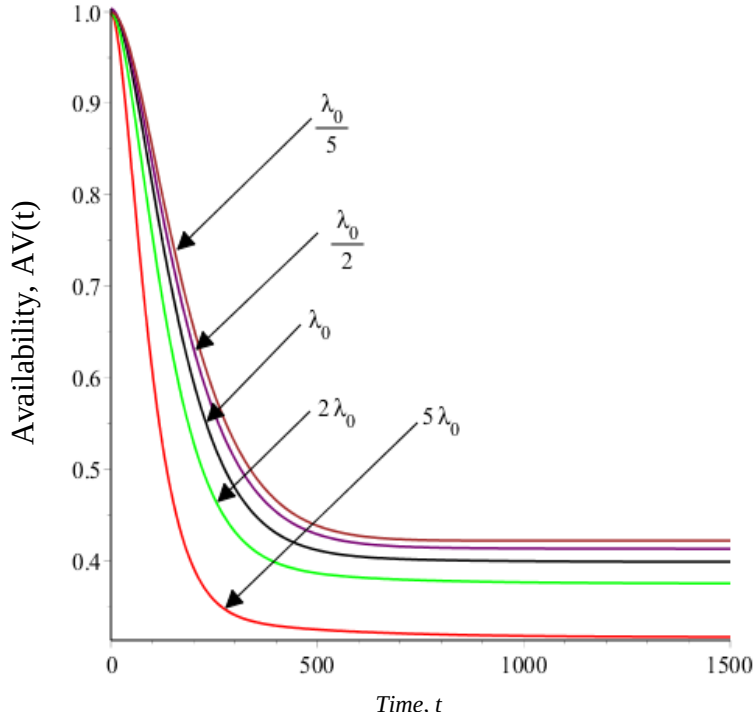

Figure B-14 Availability plots of two-units system mining with two failure modes and Type-I repair at different values of λ_0.

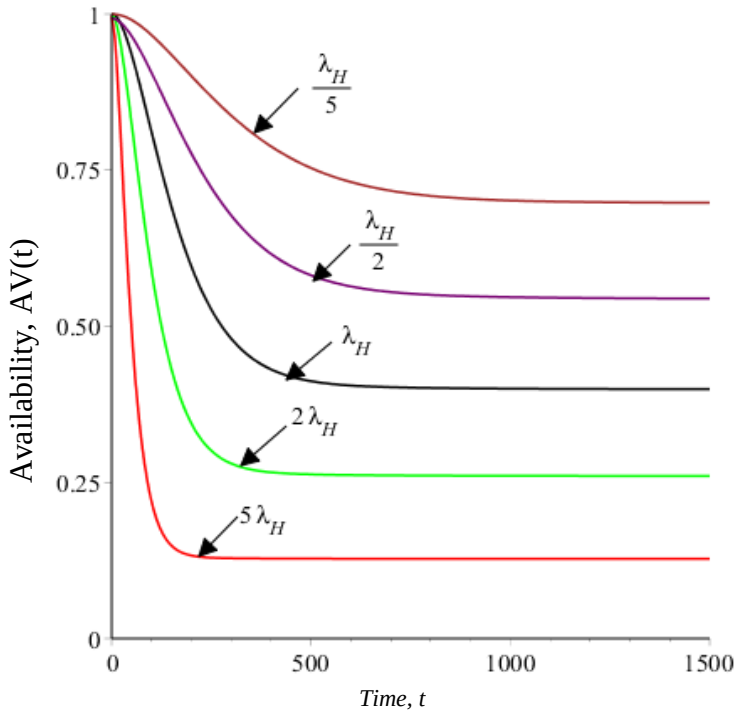

Figure B-15 Availability plots of two-units system with two failure modes and Type-I repair at different values of hardware failure (λ_H).

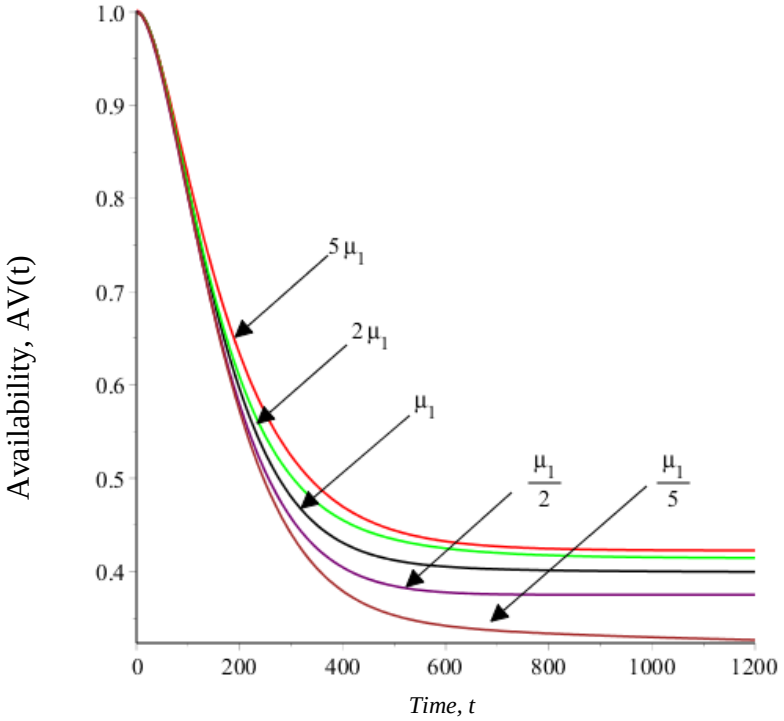

Figure B-16 Availability plots of two-units system mining system with two failure modes and Type-I repair at different values of repair rate (μ_1).

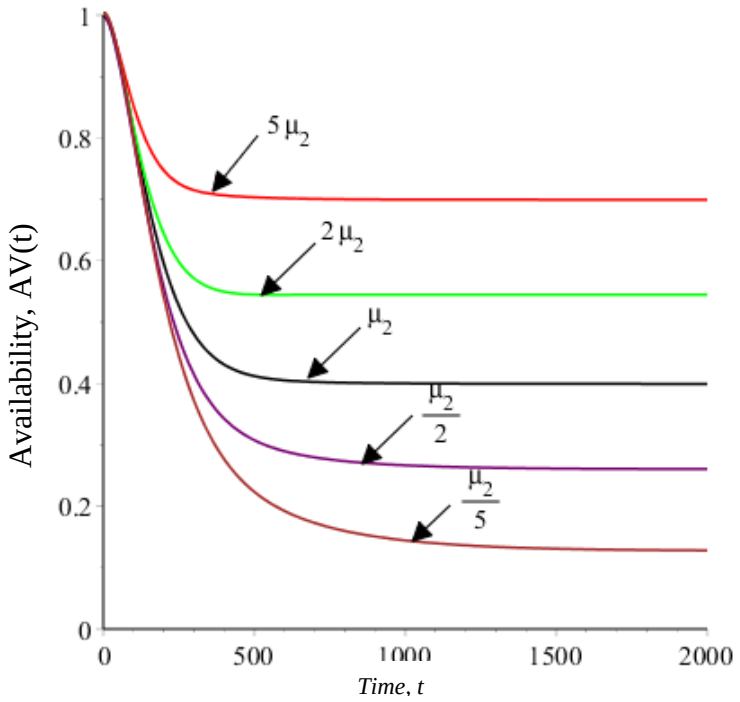

Figure B-17 Availability plots of two-units system with two failure modes and Type-I repair at different values of repair rate (μ_2).

B.6 Special Case: Three-Unit with Type-I repair

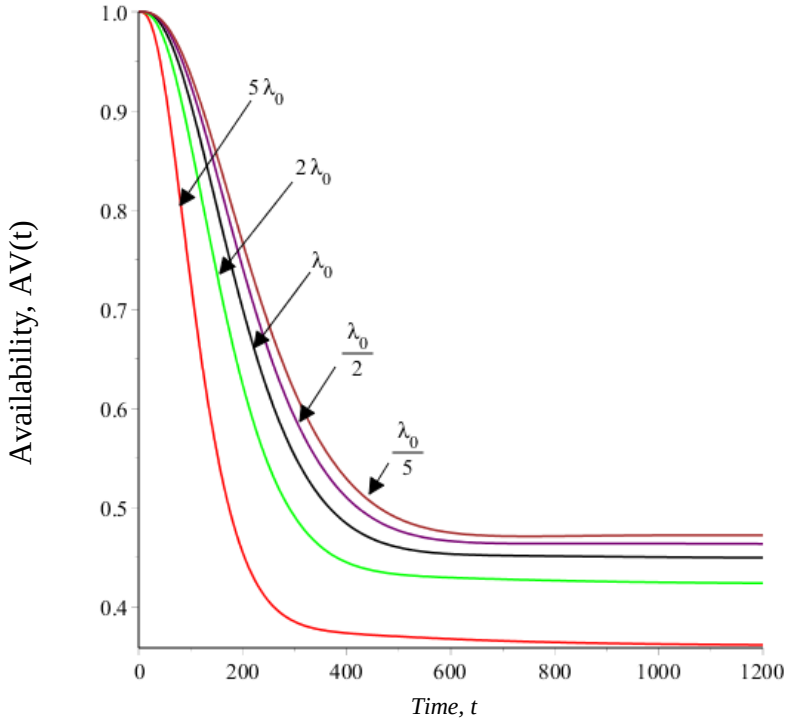

Figure B-18 Availability plots of three-units system with two failure modes and Type-I policy at different values of λ_0.

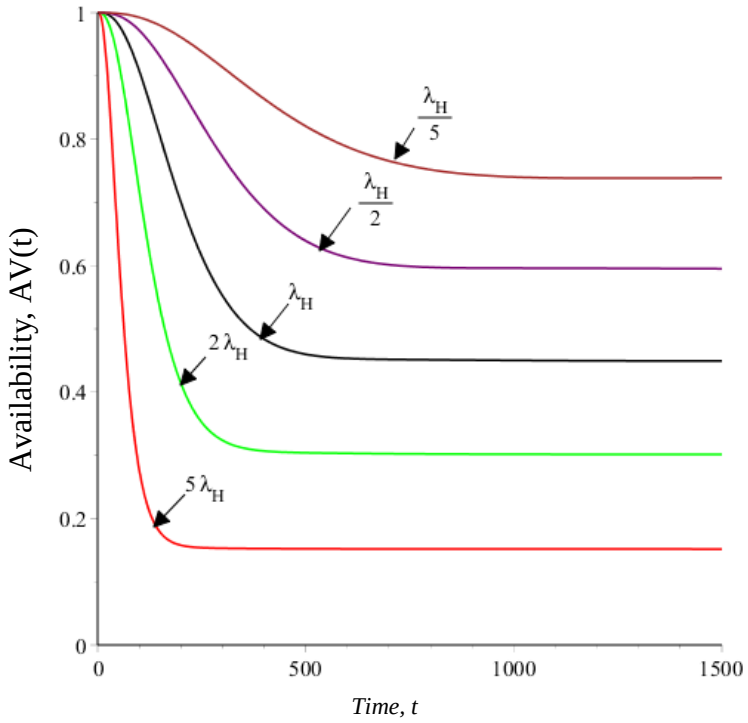

Figure B-19 Availability plots of three-units system with two failure modes and Type-I repair at different values of λ_H.

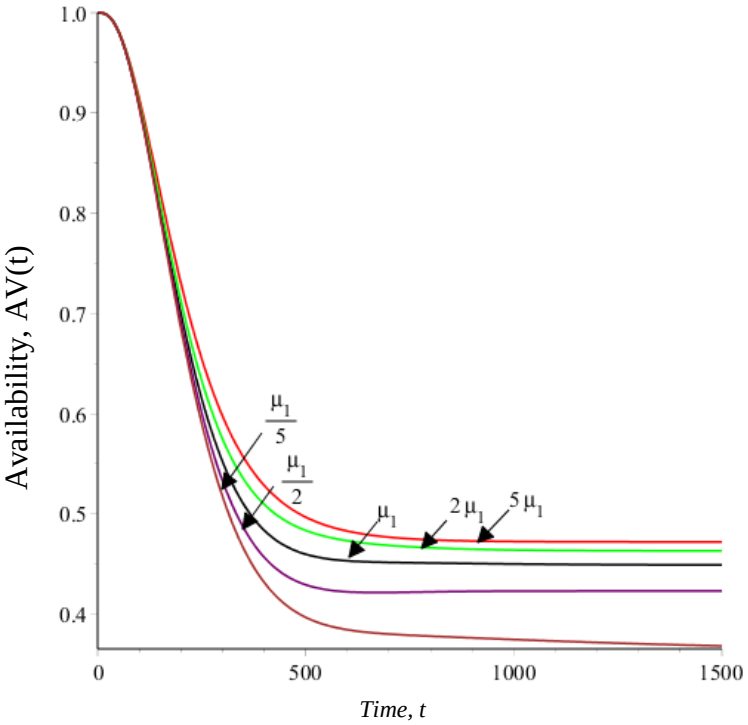

Figure B-20 Availability plots of three-units system with two failure modes and Type-I repair at different values of μ_1.

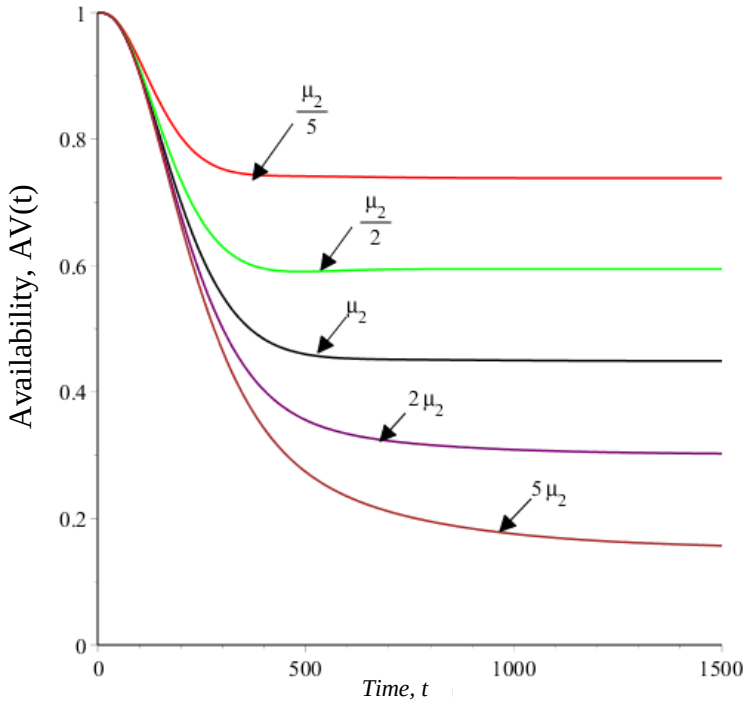

Figure B-21 Availability plots of three-units system with two failure modes and Type-I repair at different values of μ_2.

B.7 Special Case: Two-Unit with Type-II repair

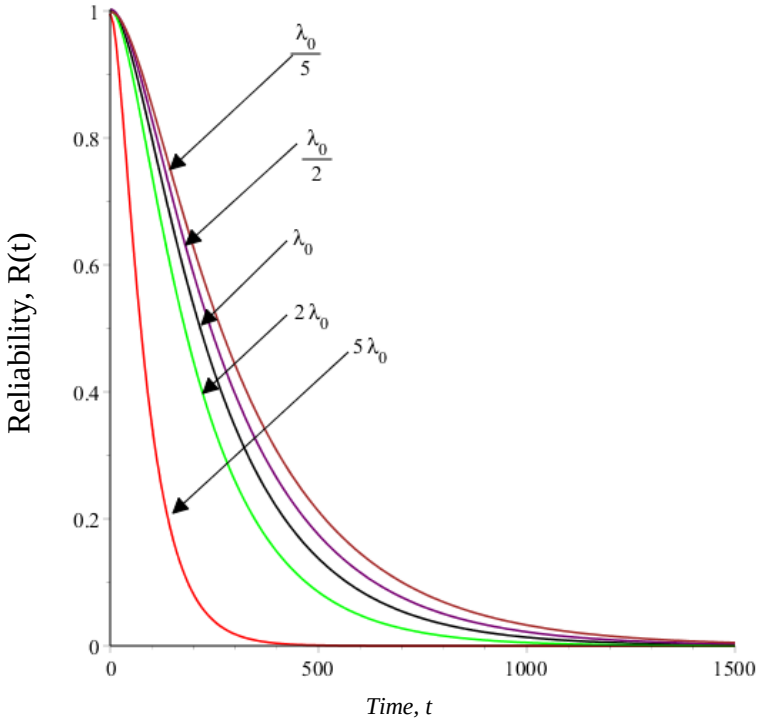

Figure B-22 Reliability plots of two-units system with two failure modes and Type-II repair at different values of λ_0.

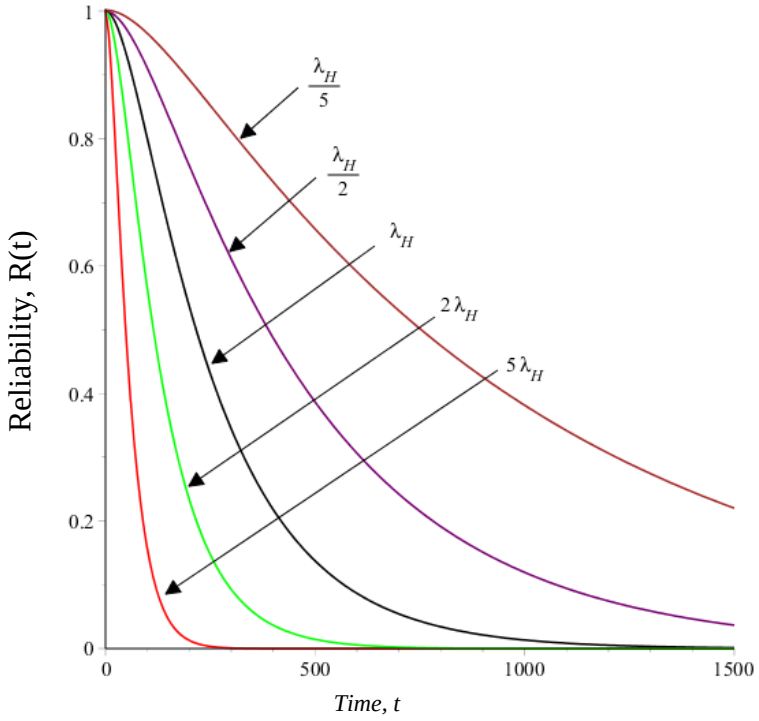

Figure B-23 Reliability plots of two-units system with two failure modes and Type-II repair at different values of λ_0.

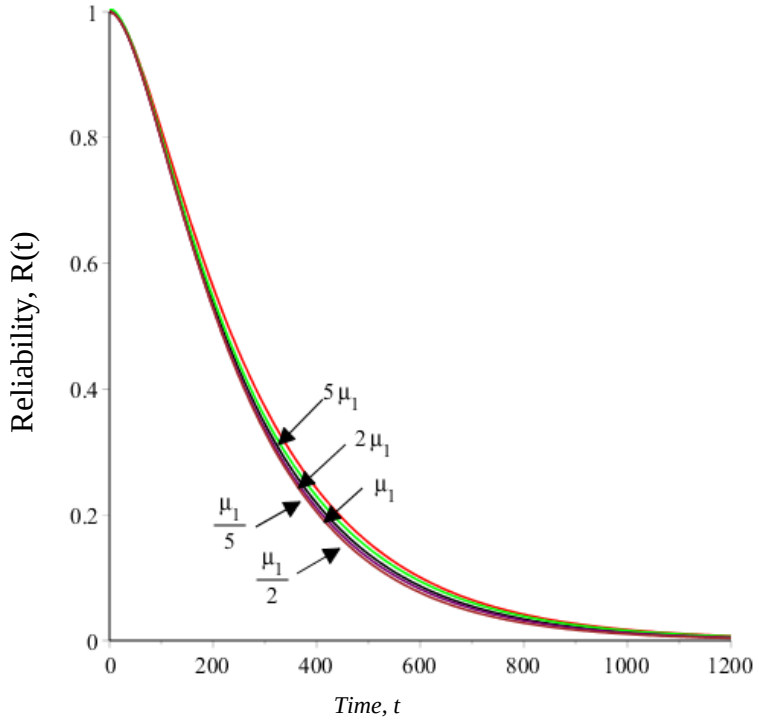

Figure B-24 Reliability plots of two-units system with two failure modes and Type-II repair at different values of μ_1.

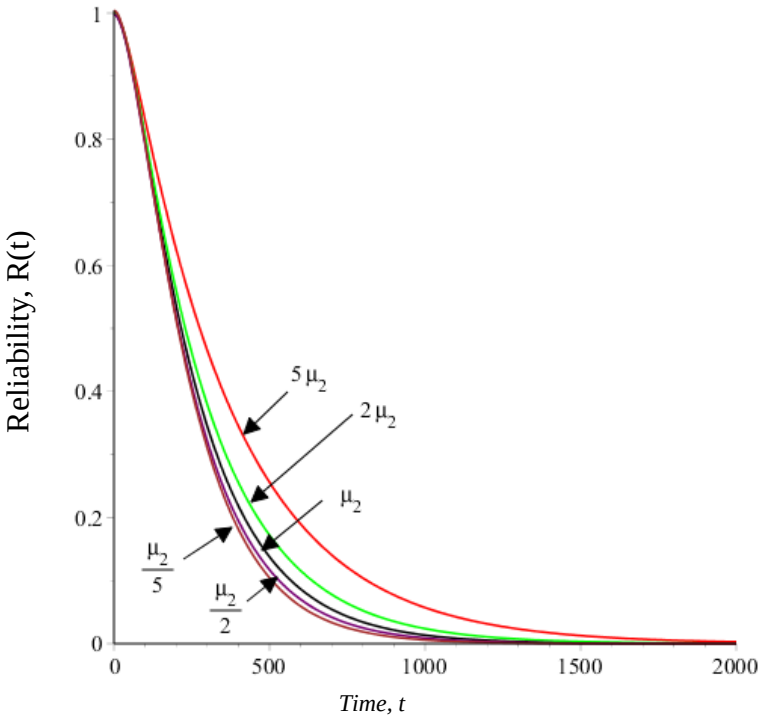

Figure B-25 Reliability plots of two-units system with two failure modes and Type-II repair at different values of μ_1.

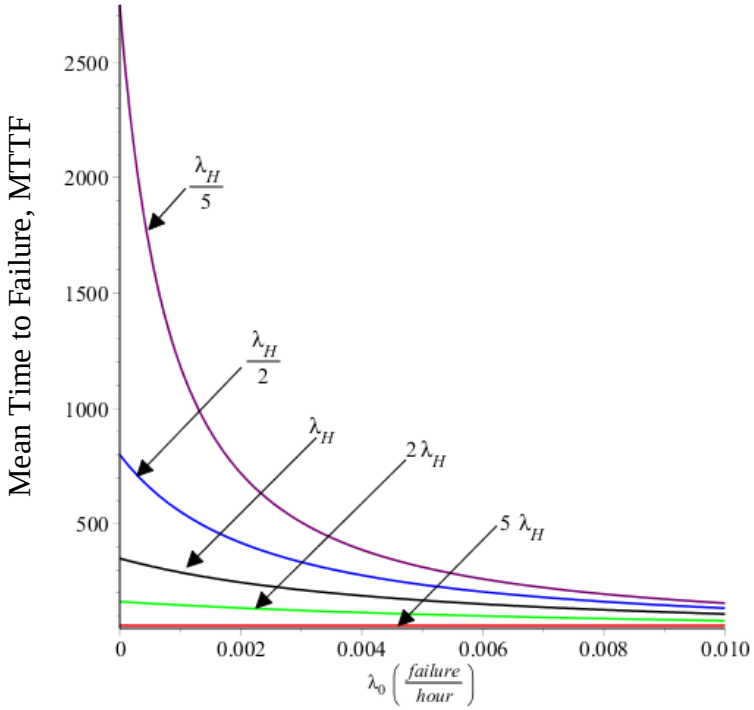

Figure B-26 MTTF plots of two-units system with two failure modes and Type-II repair at different values of λ_H.

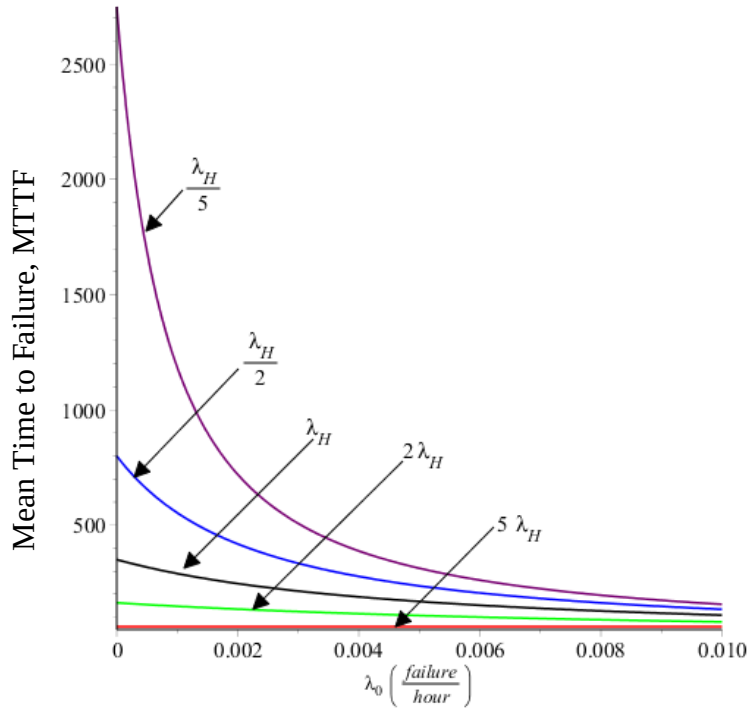

Figure B-27 MTTF plots of two-units system with two failure modes and without repair at different values of λ_H.

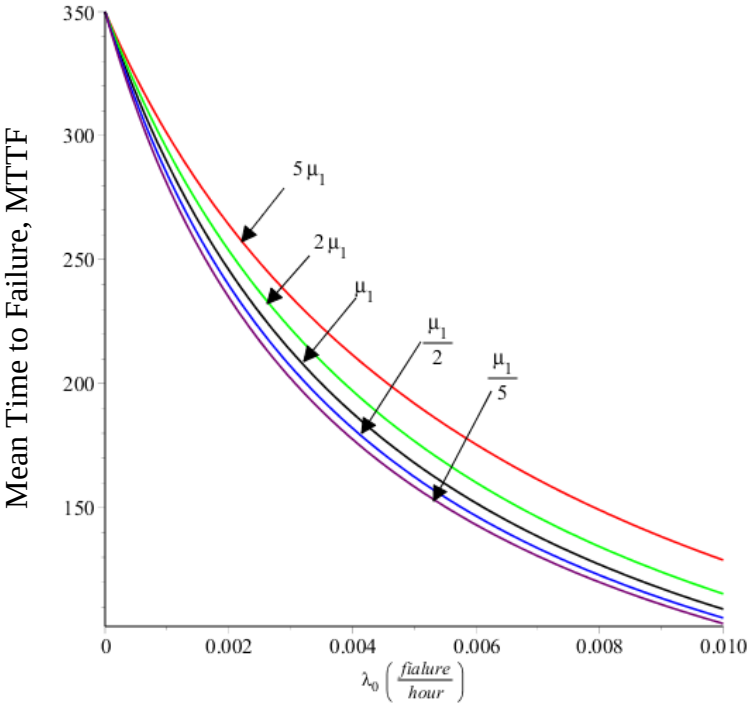

Figure B-28 MTTF plots of two-units system with two failure modes and without repair at different values of μ_1.

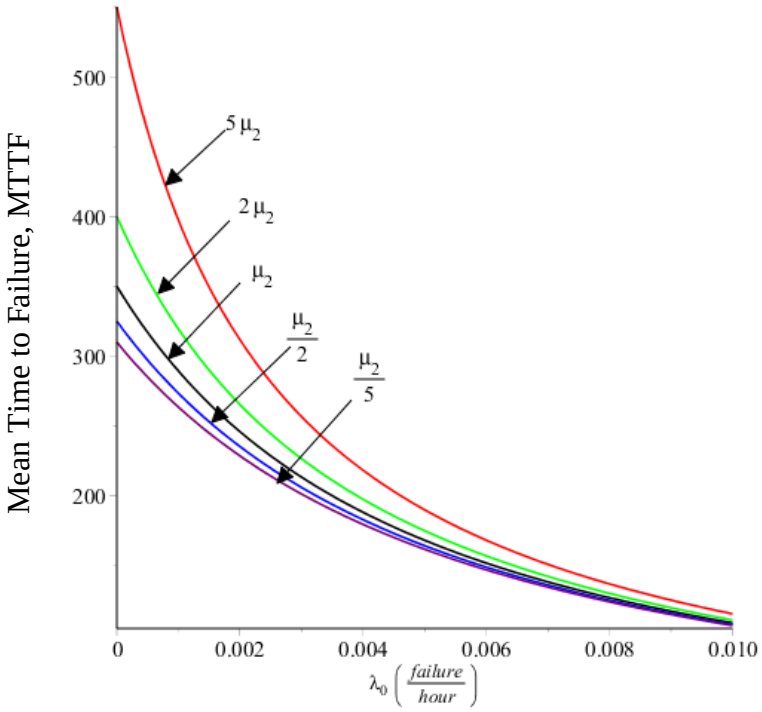

Figure B-29 MTTF plots of two-units system with two failure modes and without repair at different values of μ_2.

B.8 Special Case: Two-Unit with Type-III repair

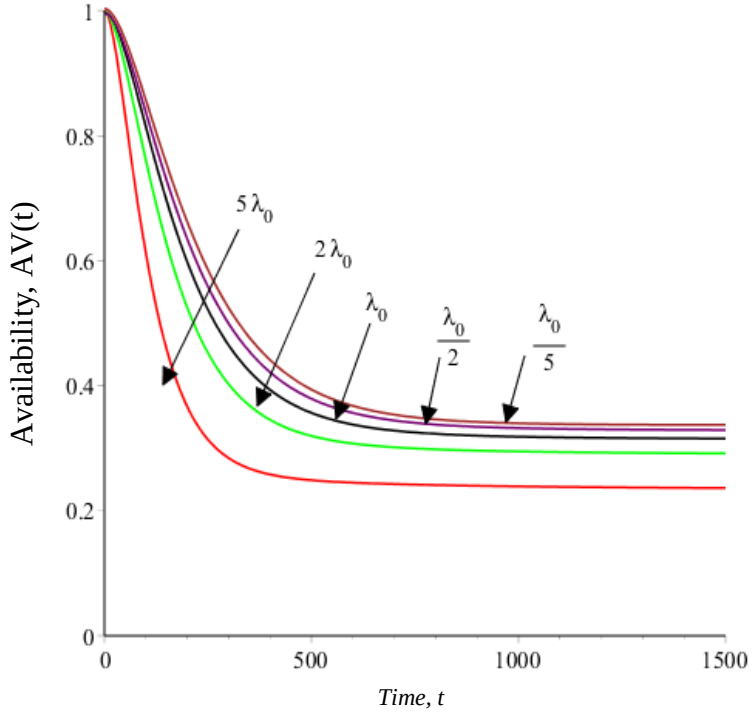

Figure B-30 Availability plots of two-units system with two failure modes and Type-III repair at different values of λ_0.

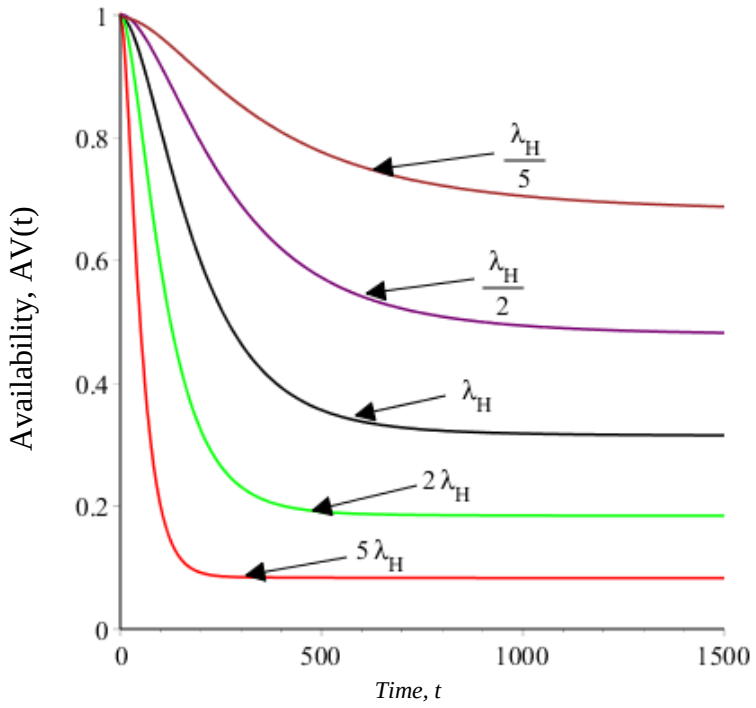

Figure B-31 Availability plots of two-units system with two failure modes and Type-III repair at different values of λ_H.

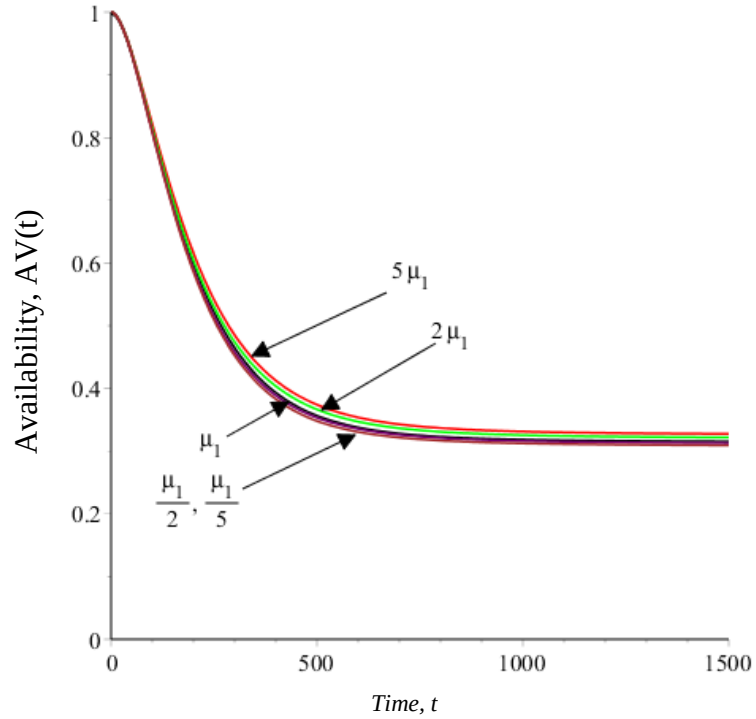

Figure B-32 Availability plots of two-units system with two failure modes and Type-III repair at different values of μ_1.

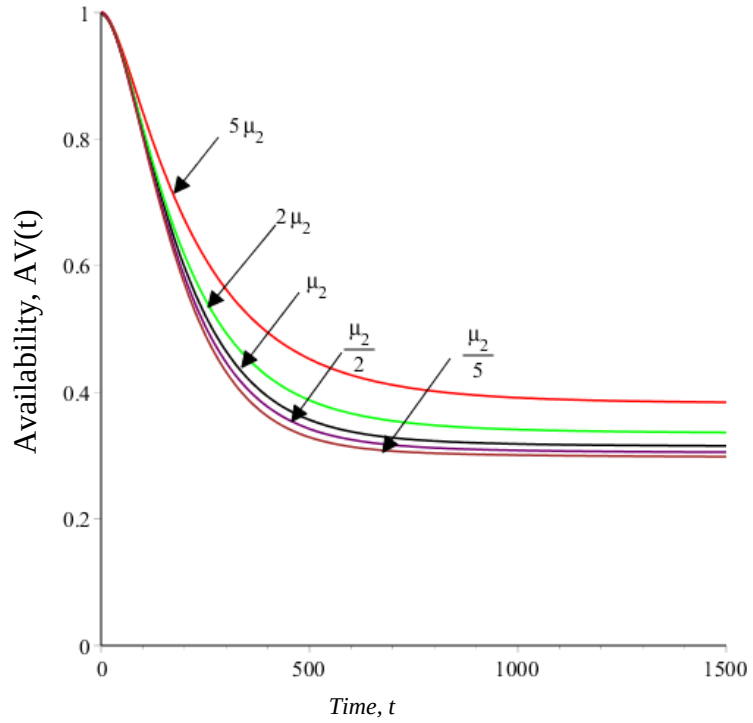

Figure B-33 Availability plots of two-units system with two failure modes and Type-III repair at different values of μ_2.

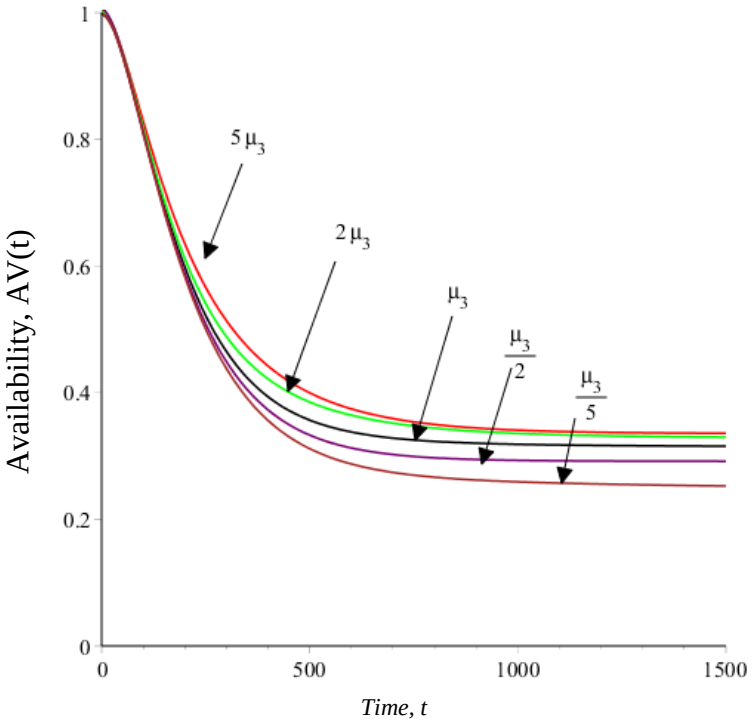

Figure B-34 Availability plots of two-units system with two failure modes and Type-III repair at different values of μ_3.

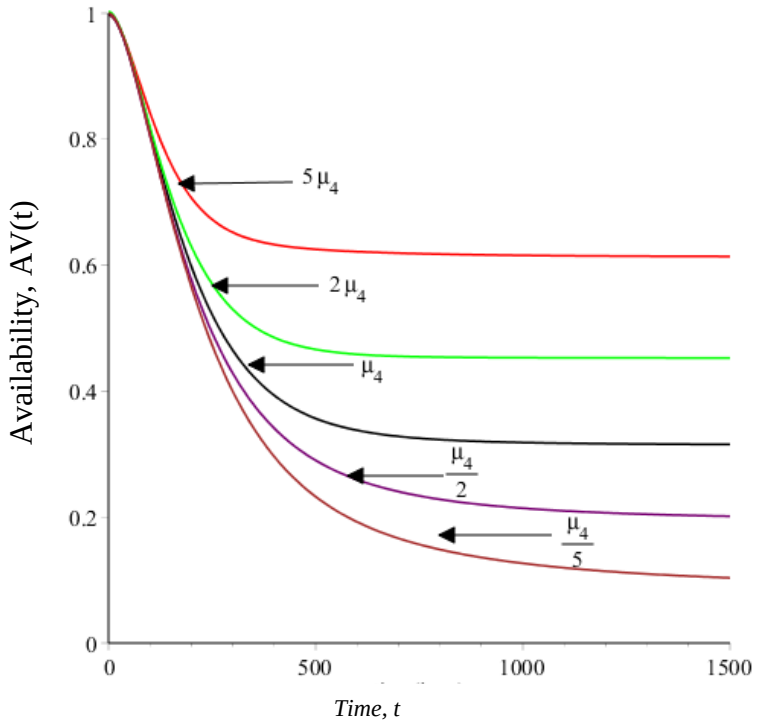

Figure B-35 Availability plots of two-units system with two failure modes and Type-III repair at different values of μ_4.

Appendix C: Reliability Parameter Plots of Chapter 3

C.1 Special Case: One-Unit without repair

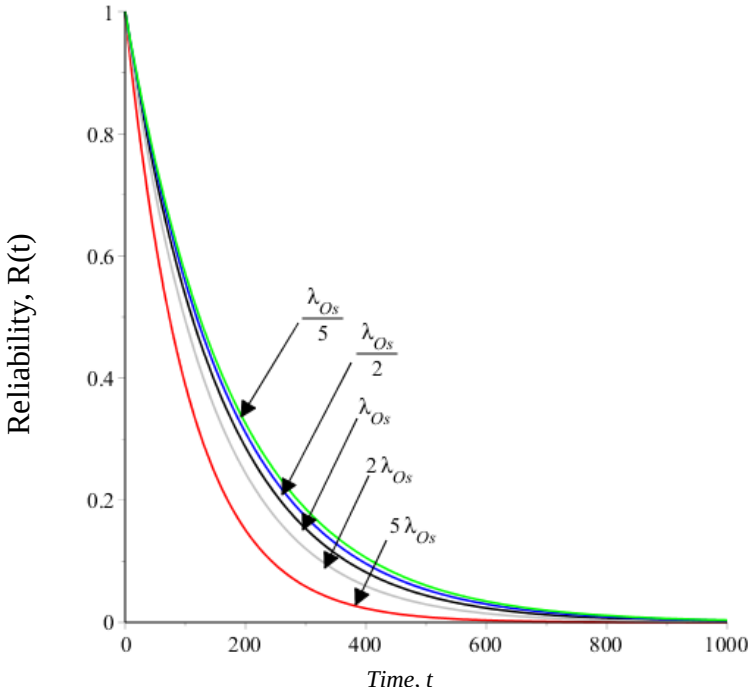

Figure C-1 Reliability plots of one-unit system with four failure modes without repair at different values of λ_{Os}.

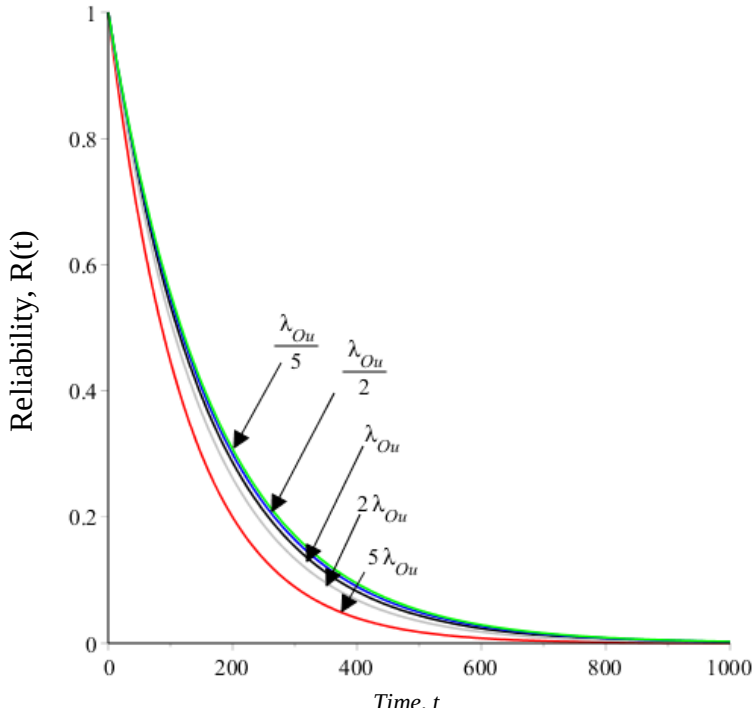

Figure C-2 Reliability plots of one-unit system with four failure modes without repair at different values of λ_{Ou}.

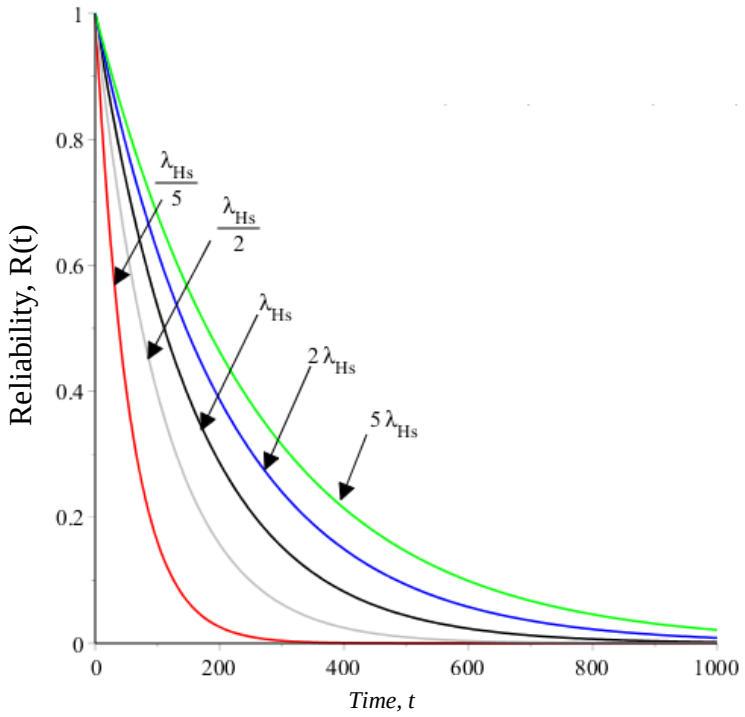

Figure C-3 Reliability plots of one-unit system with four failure modes without repair at different values of λ_{Hs}.

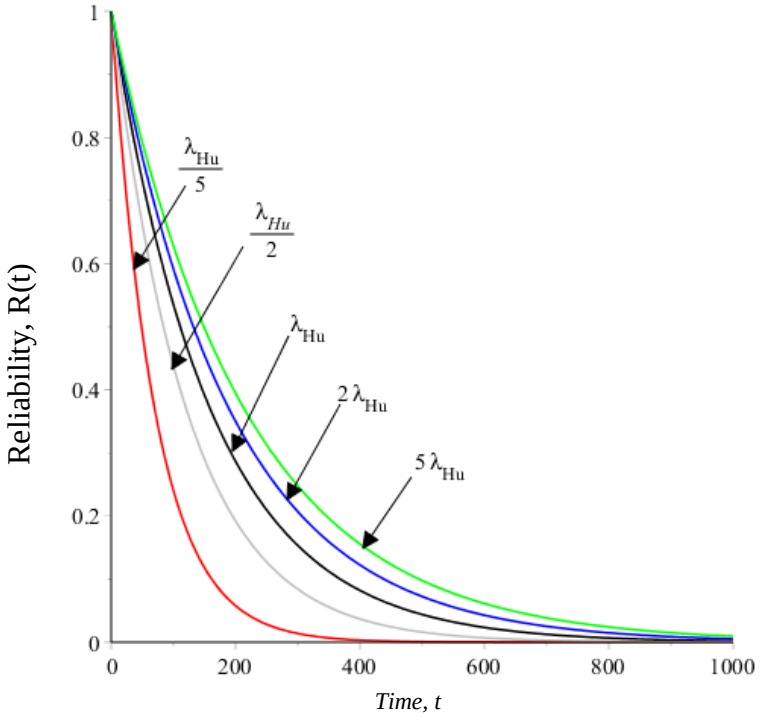

Figure C-4 Reliability plots of one-unit system with four failure modes without repair at different values of λ_{Hu}.

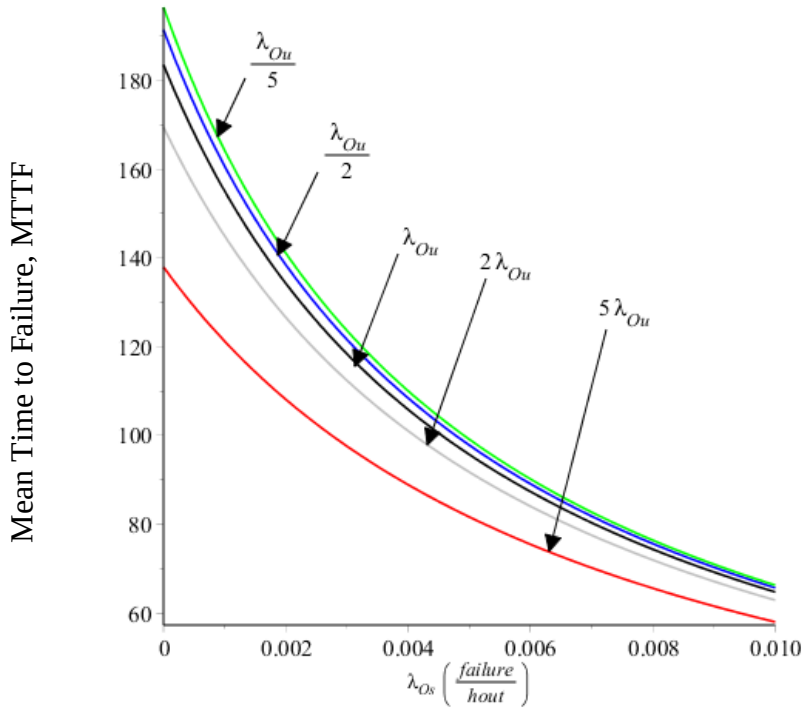

Figure C-5 MTTF plots of one-unit system with four failure modes without repair at different values of λ_{Ou}.

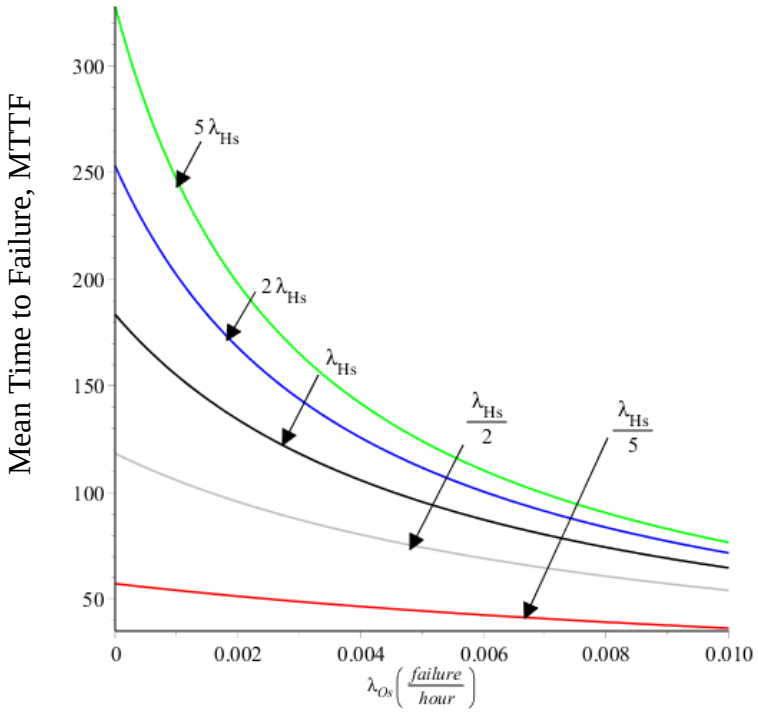

Figure C-6 MTTF plots of one-unit system with four failure modes without repair at different values of λ_{Hs}.

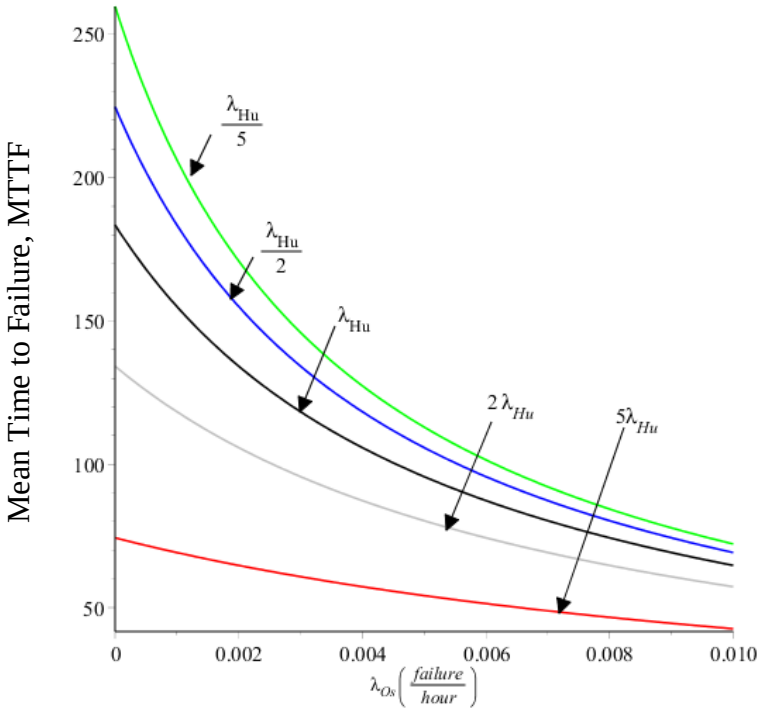

Figure C-7 MTTF plots of one-unit system with four failure modes without repair at different values of λ_{Hu}.

C.2 Special Case: Two-Unit without repair

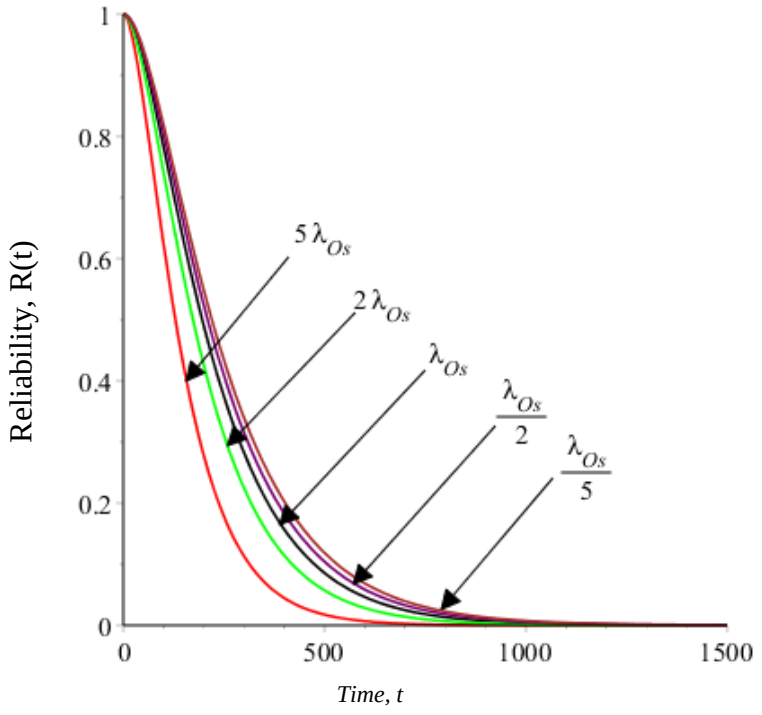

Figure C-8 Reliability plots of two-units system with four failure modes without repair at different values of λ_{0s}.

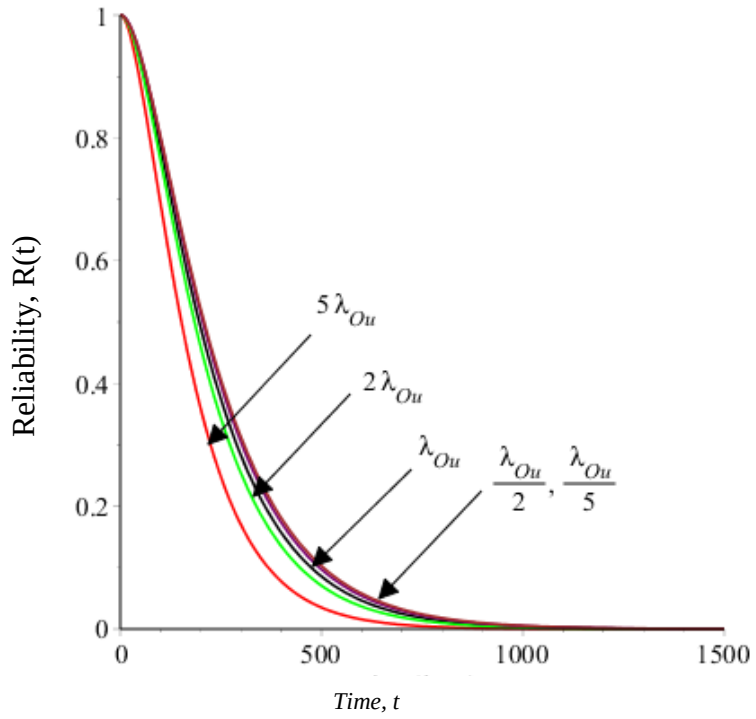

Figure C-9 Reliability plots of two-units system with four failure modes without repair at different values of λ_{0u}.

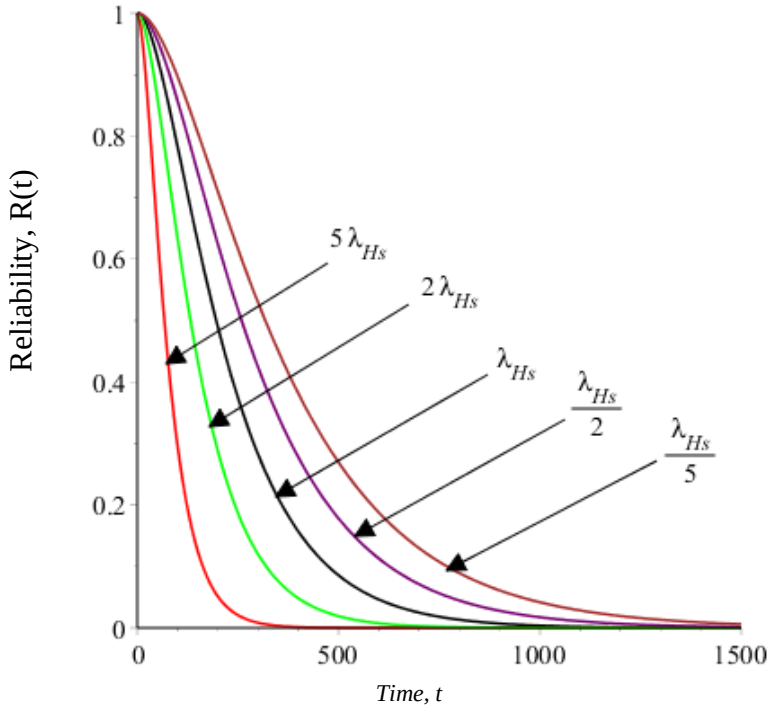

Figure C-10 Reliability plots of two-units system with four failure modes without repair at different values of λ_{Hs}.

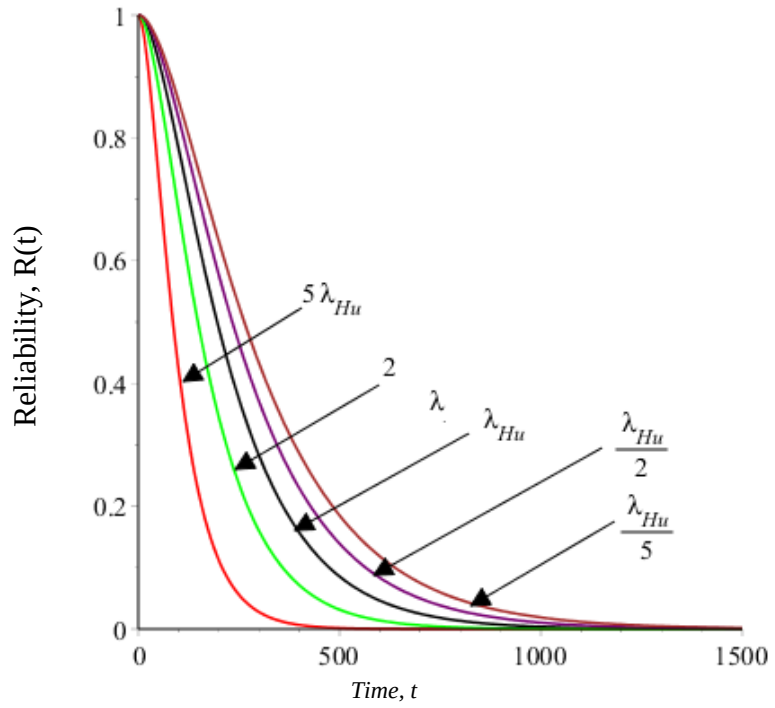

Figure C-11 Reliability plots of two-units system with four failure modes without repair at different values of λ_{Hu}.

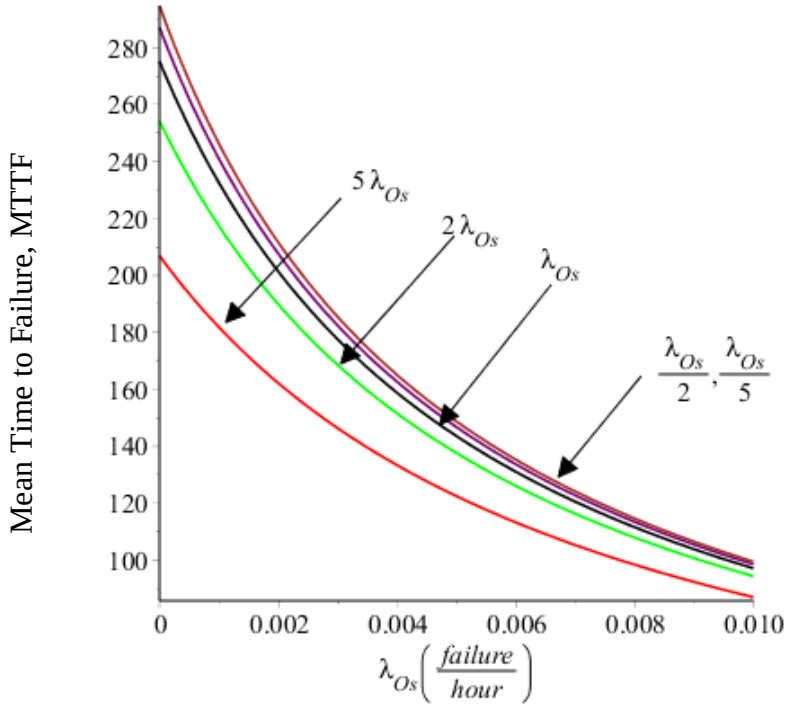

Figure C-12 MTTF plots of two-units system with three failure modes without repair at different values of λ_{0u}.

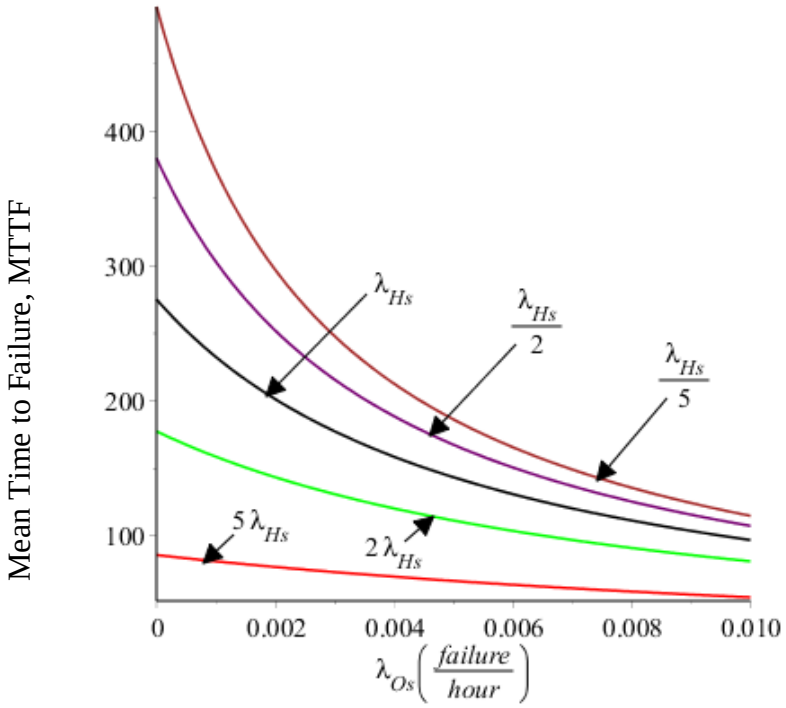

Figure C-13 MTTF plots of two-units system with three failure modes without repair at different values of λ_{Hs}.

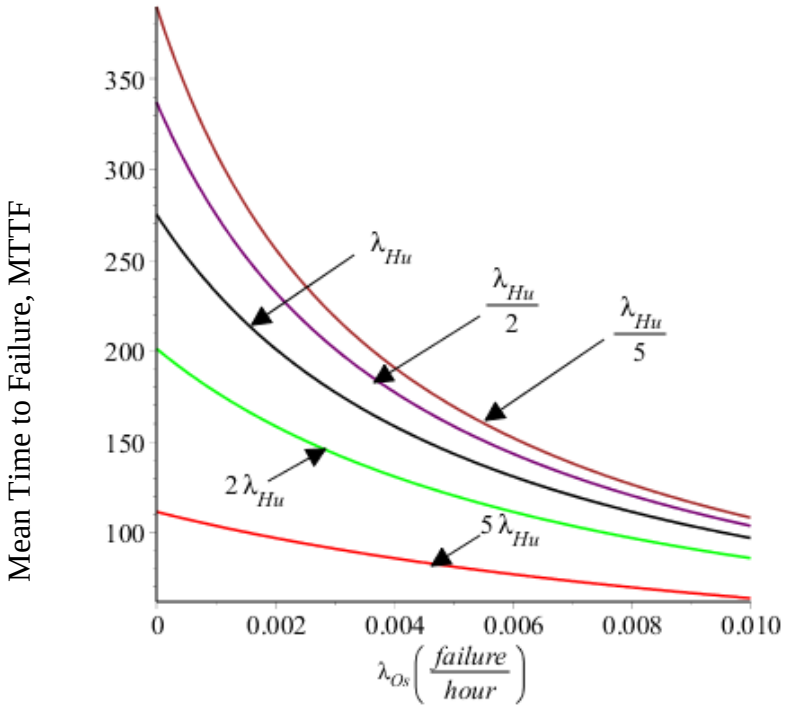

Figure C-14 MTTF plots of two-units system with three failure modes without repair at different values of λ_{Hu}.

C.3 Special Case: Thee-Unit without repair

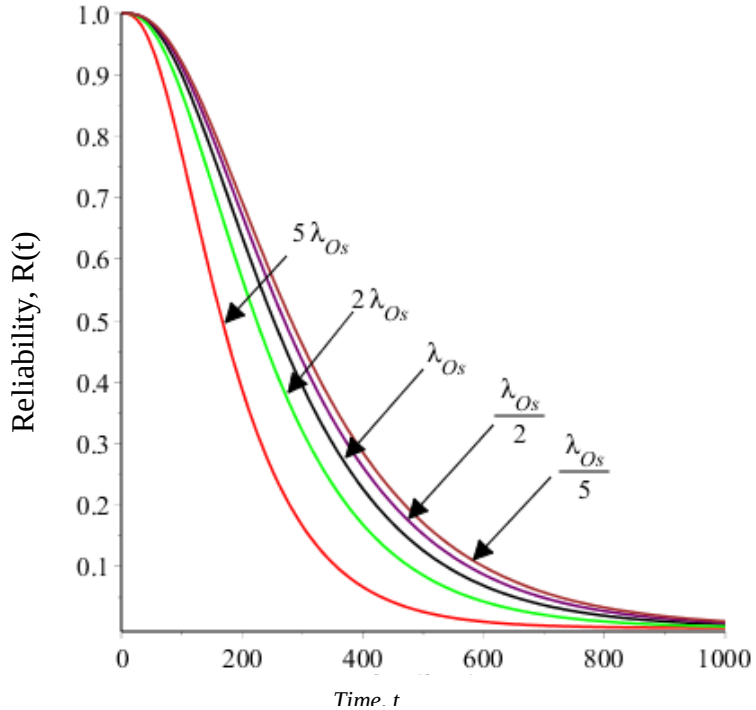

Figure C-15 Reliability plots of three-units system with four failure modes without repair at different values of λ_{0s}.

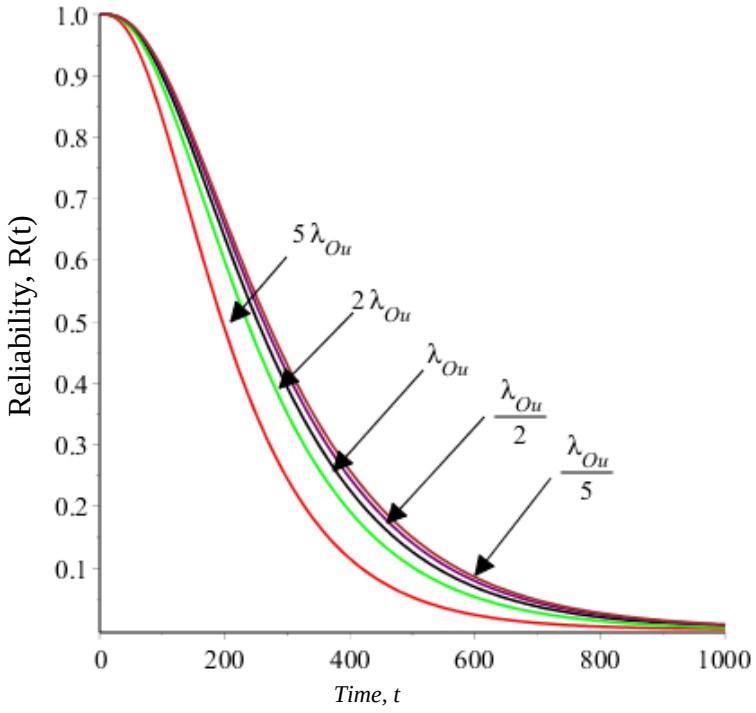

Figure C-16 Reliability plots of three-units system with four failure modes without repair at different values of λ_{0u}.

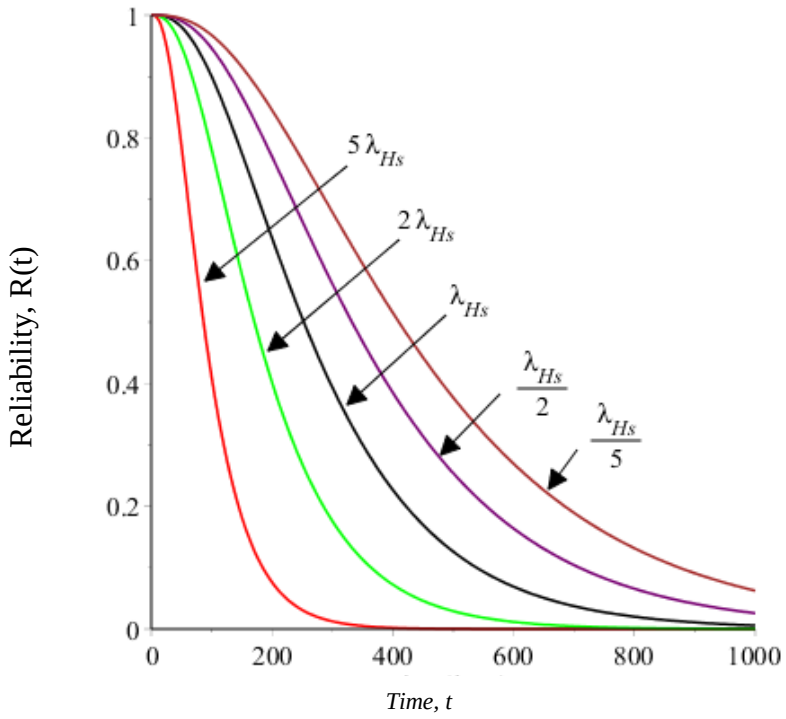

Figure C-17 Reliability plots of three-units system with four failure modes without repair at different values of λ_{Hs}.

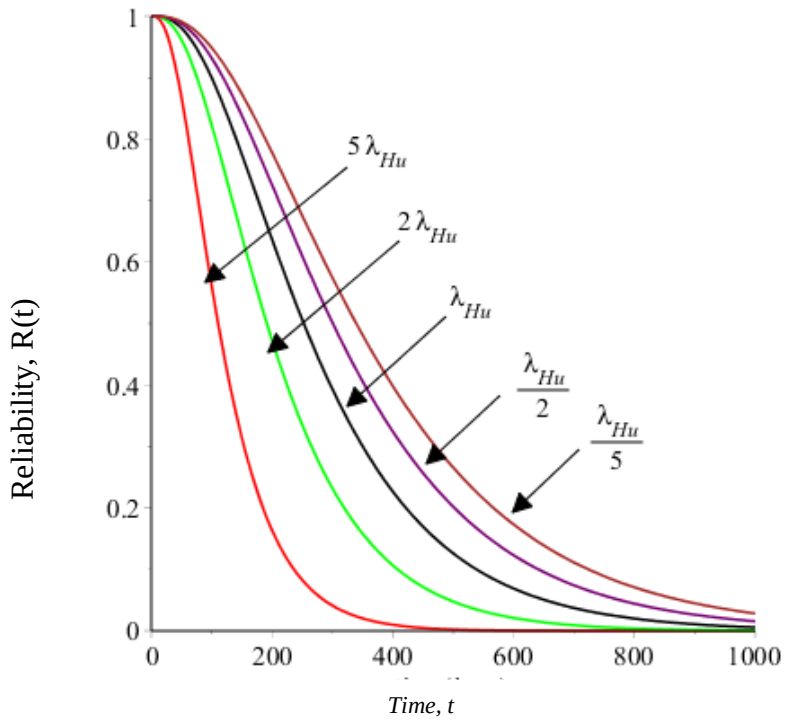

Figure C-18 Reliability plots of three-units system with four failure modes without repair at different values of λ_{Hu}.

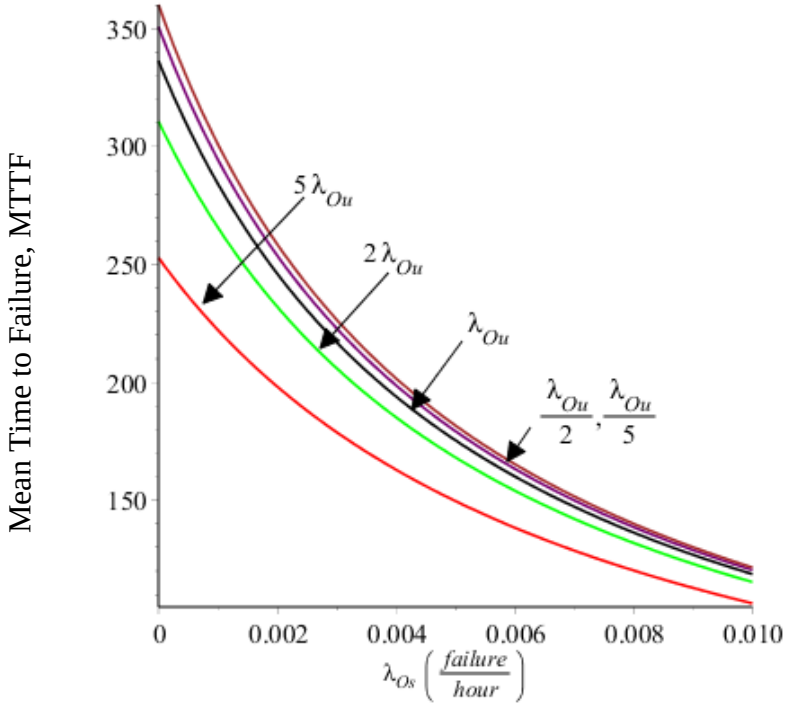

Figure C-19 MTTF plots of three-units system with four failure modes and without repair at different values of λ_{0u}.

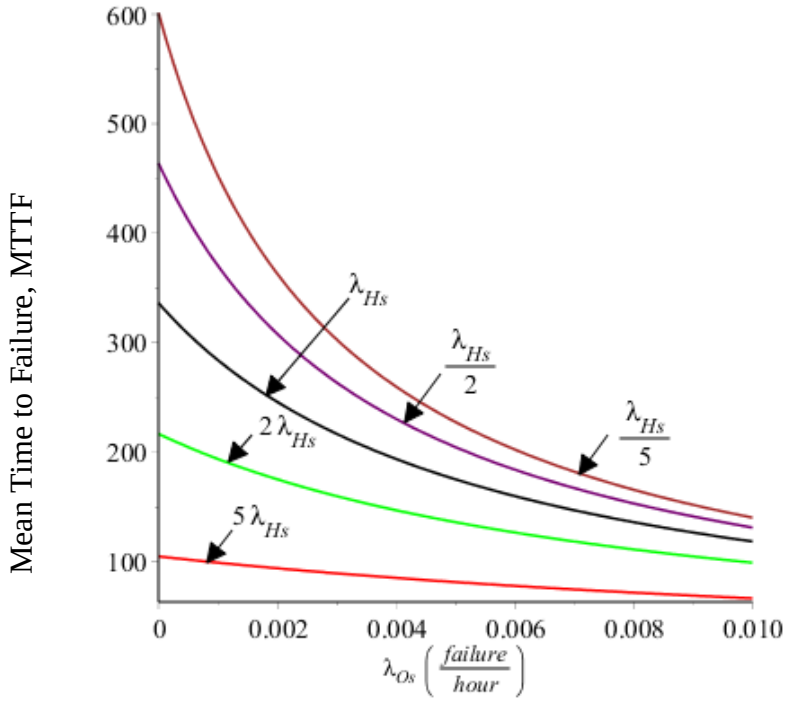

Figure C-20 MTTF plots of three-units system with four failure modes and without repair at different values of λ_{Hs}.

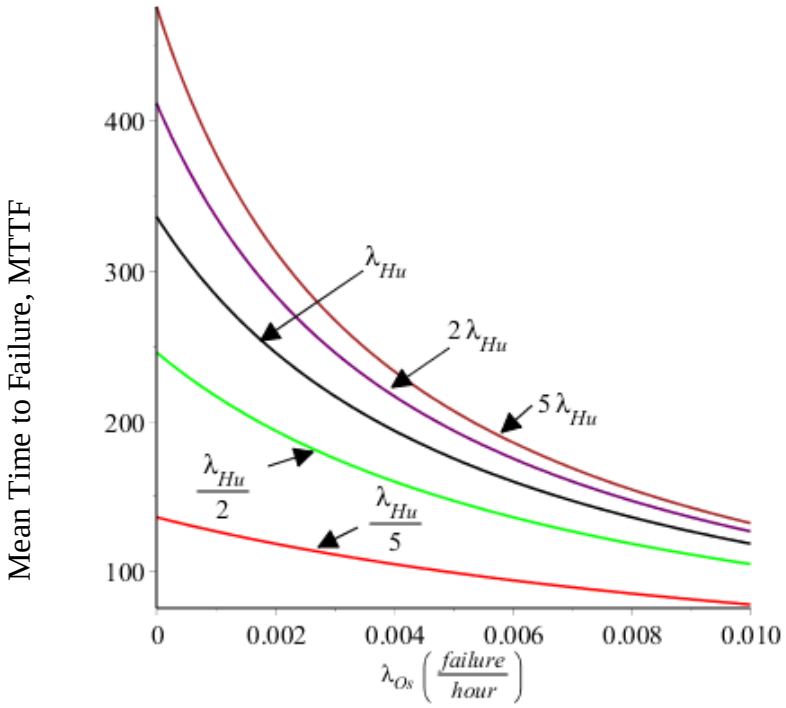

Figure C-21 MTTF plots of three-units system with four failure modes and without repair at different values of λ_{Hu}.

C.4 Special Case One-Unit with Type-I repair

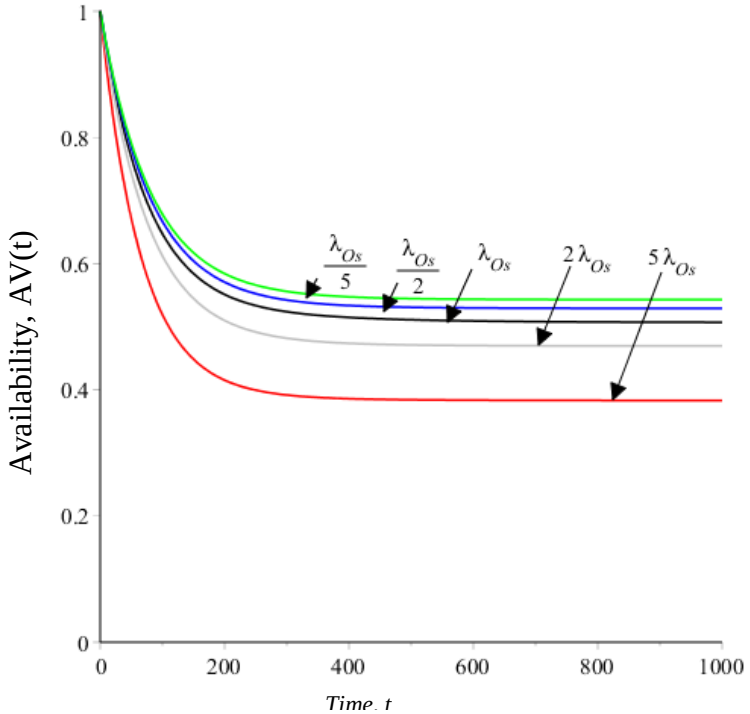

Figure C-22 Availability plots of one-unit system with four failure modes with Type-I repair at different values of λ_{Os}.

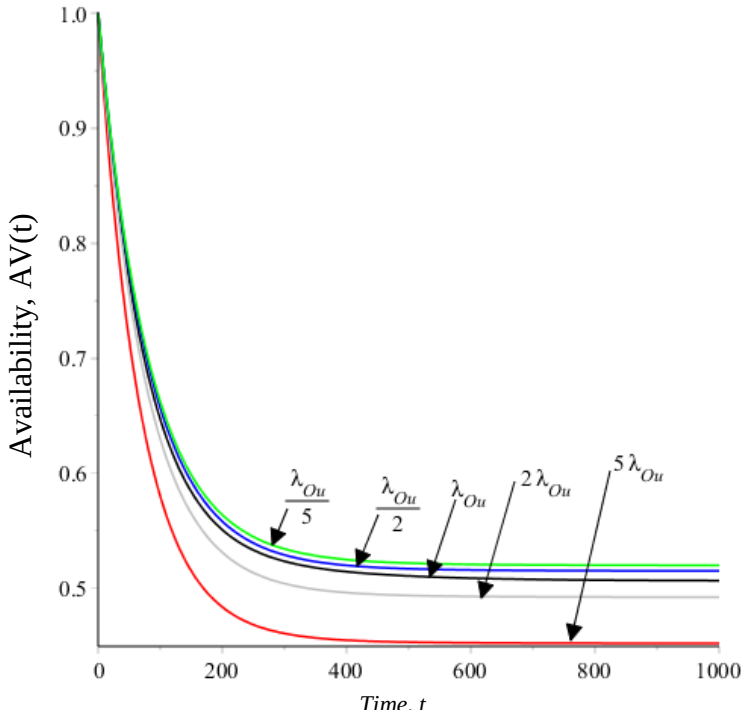

Figure C-23 Availability plots of one-unit system with four failure modes with Type-I repair at different values of λ_{Ou}.

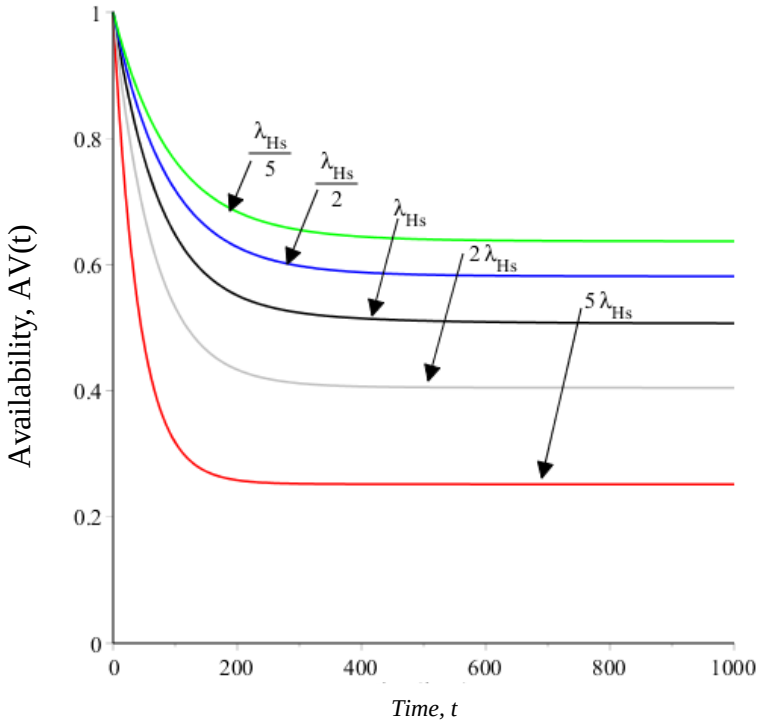

Figure C-24 Availability plots of one-unit system with four failure modes with Type-I repair at different values of λ_{Hs}.

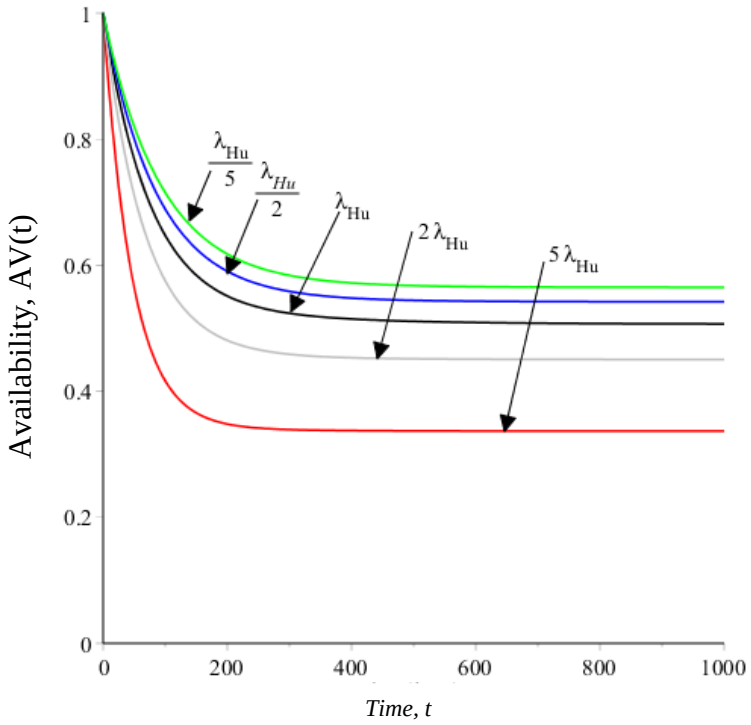

Figure C-25 Availability plots of one-unit system with four failure modes with Type-I repair at different values of λ_{Hs}.

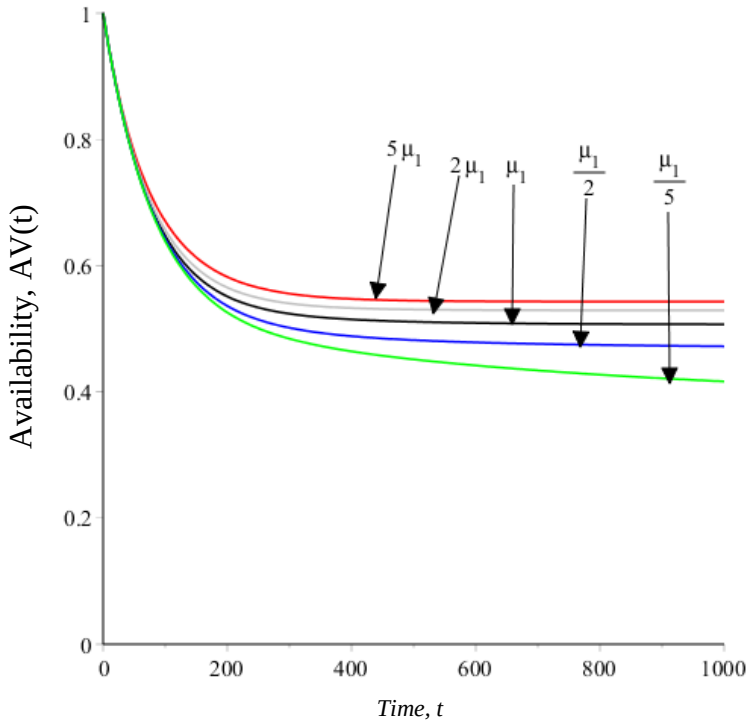

Figure C-26 Availability plots of one-unit system with four failure modes with Type-I repair at different values of μ_1.

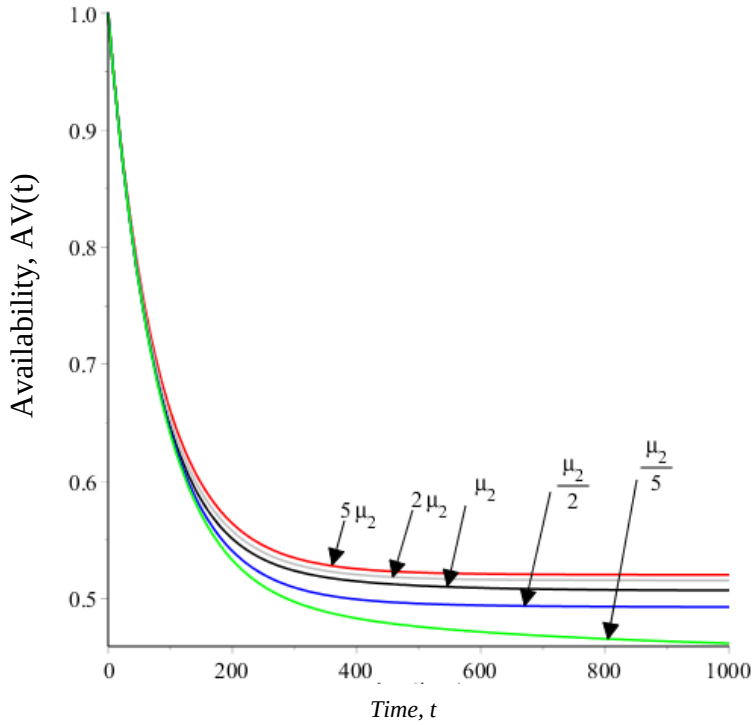

Figure C-27 Availability plots of one-unit system with four failure modes with Type-I repair at different values of μ_2.

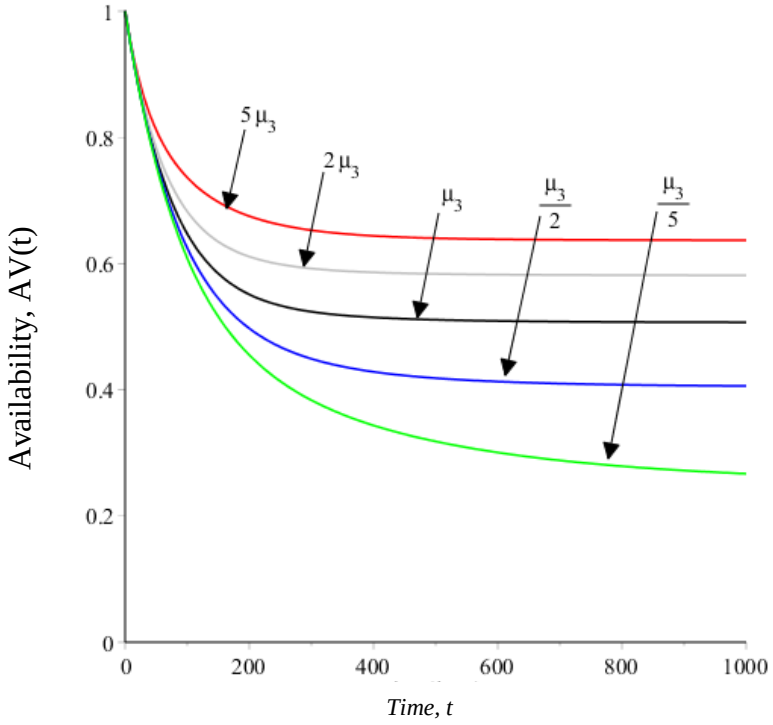

Figure C-28 Availability plots of one-unit system with four failure modes with Type-I repair at different values of μ_3.

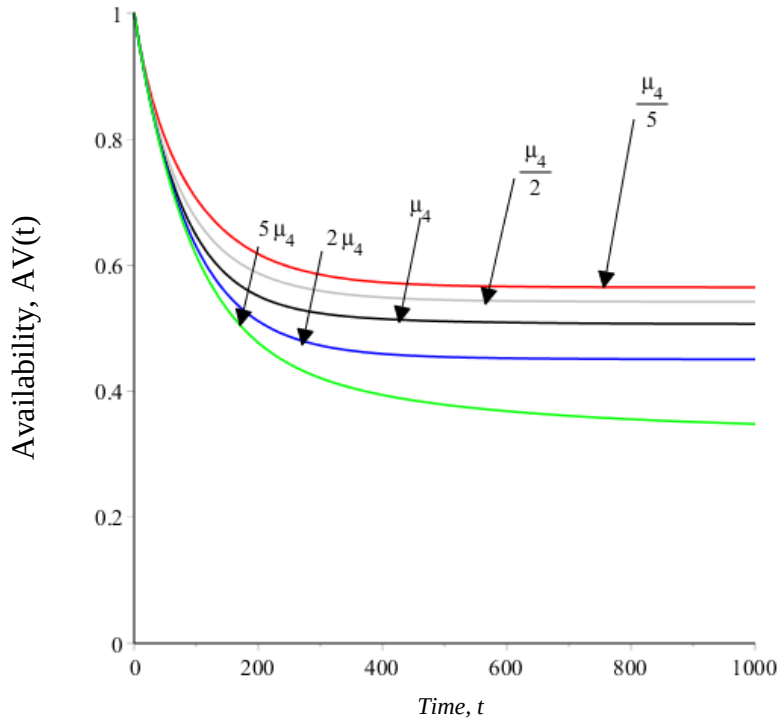

Figure C-29 Availability plots of one-unit system with four failure modes with Type-I repair at different values of μ_4.

C.2 Special Case: Two-Unit with Type-I repair

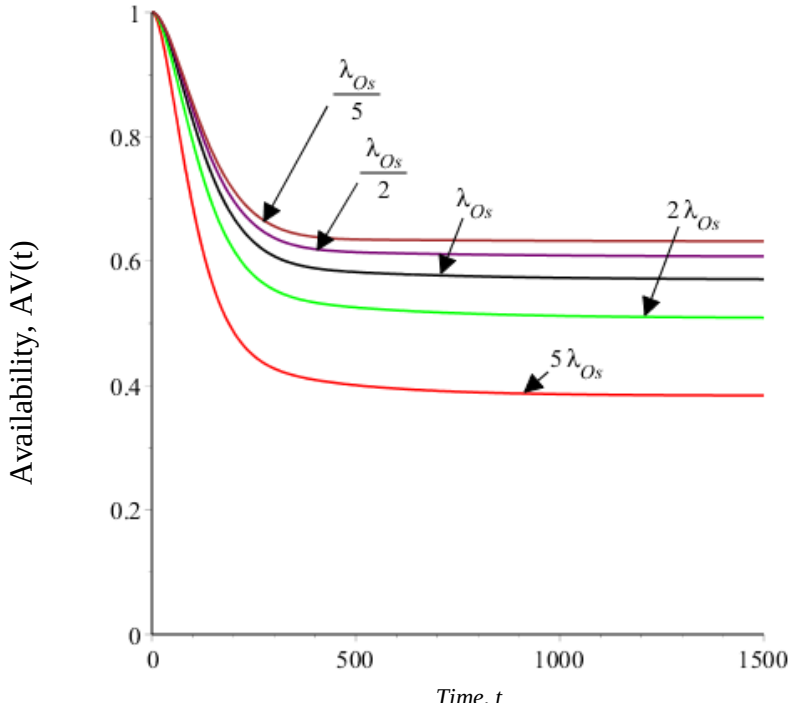

Figure C-30 Availability plots of two-unit system with four failure modes with Type-I repair at different values of λ_{Os}.

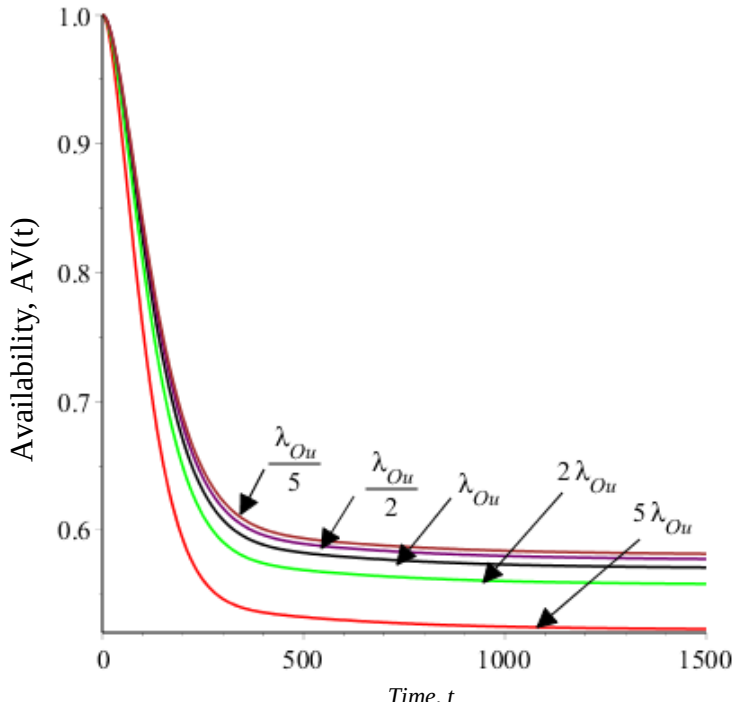

Figure C-31 Availability plots of two-unit system with four failure modes with Type-I repair at different values of λ_{Ou}.

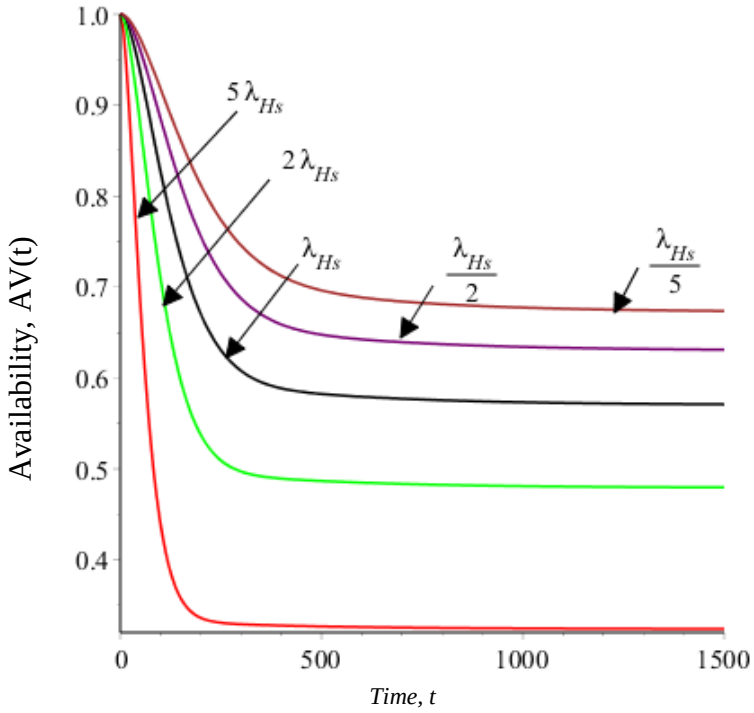

Figure C-32 Availability plots of two-unit system with four failure modes with Type-I repair at different values of λ_{Hs}.

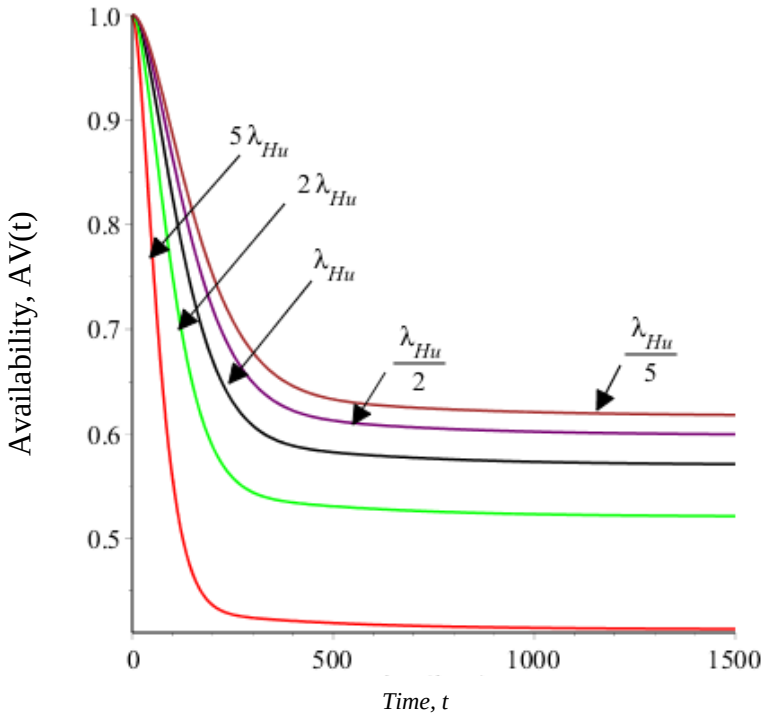

Figure C-33 Availability plots of two-unit system with four failure modes with Type-I repair at different values of λ_{Hu}.

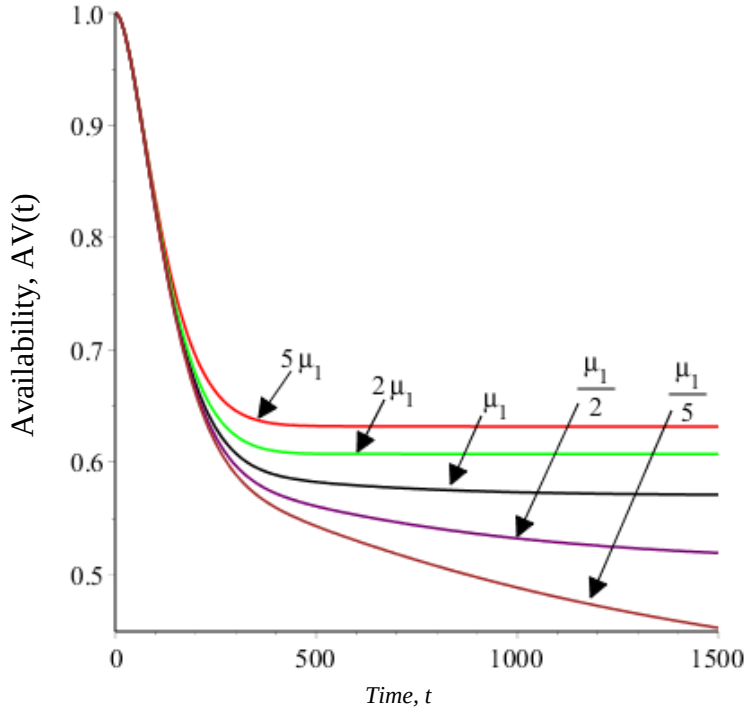

Figure C-34 Availability plots of two-unit system with four failure modes with Type-I repair at different values of μ_1.

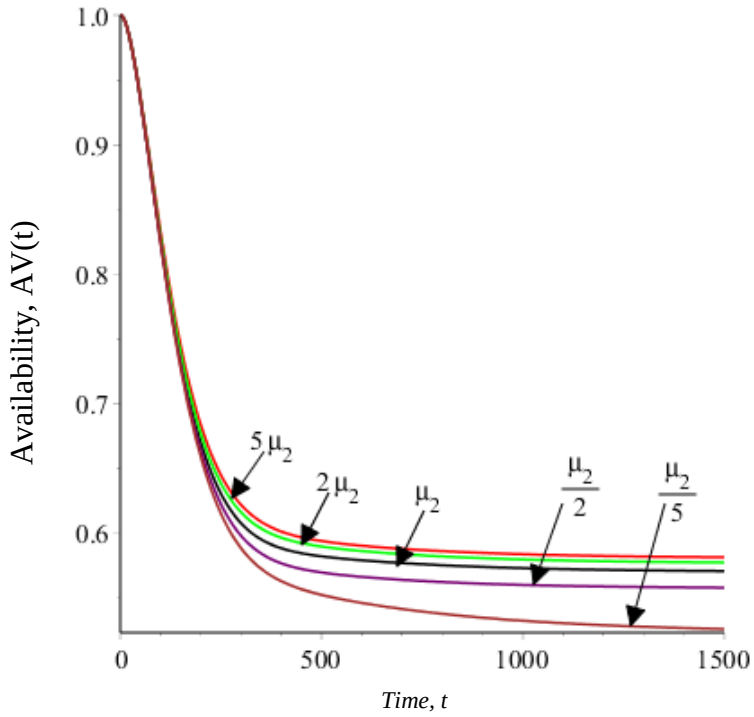

Figure C-35 Availability plots of two-unit system with four failure modes with Type-I repair at different values of μ_2.

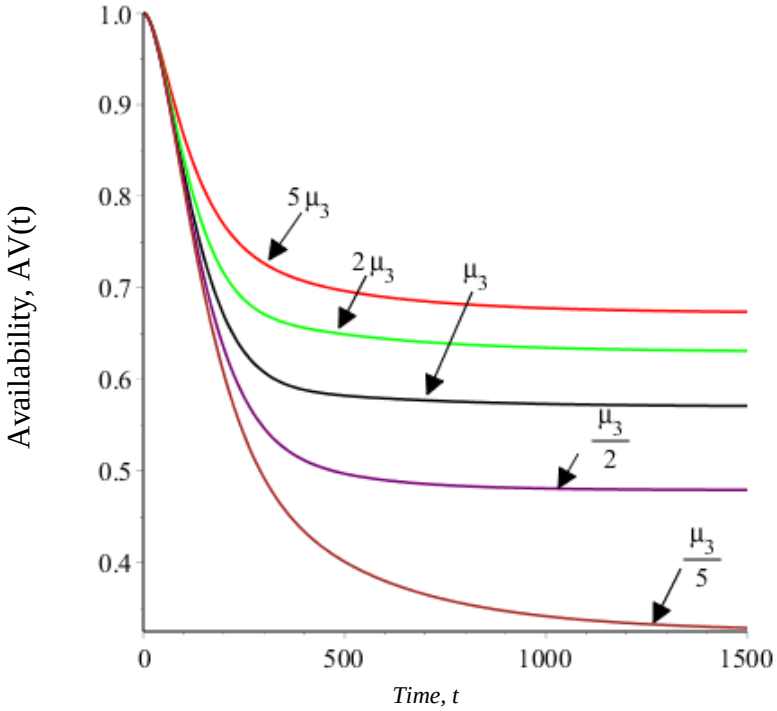

Figure C-36 Availability plots of two-unit system with four failure modes with Type-I repair at different values of μ_3.

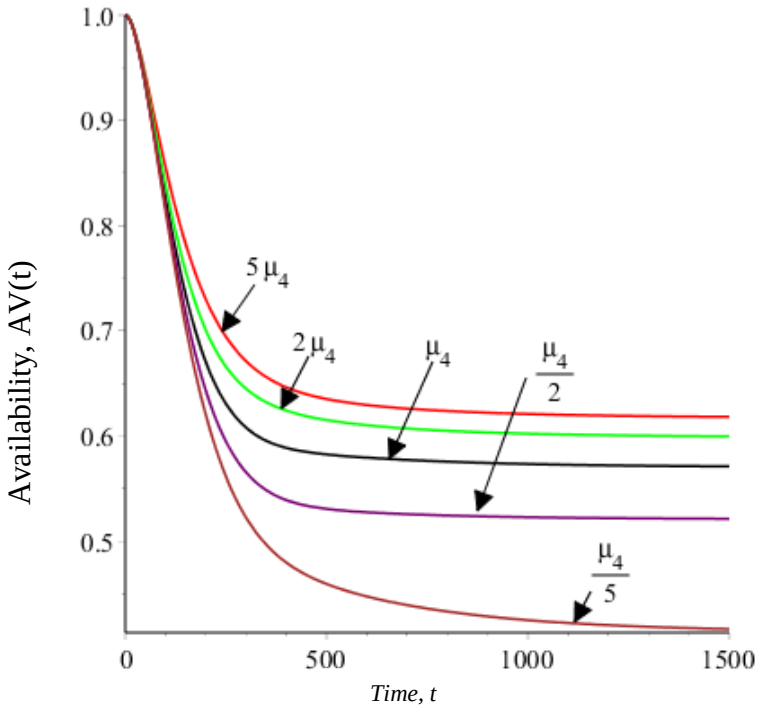

Figure C-37 Availability plots of two-unit system with four failure modes with Type-I repair at different values of μ_4.

C.2 Special Case Three-Unit with Type-I repair

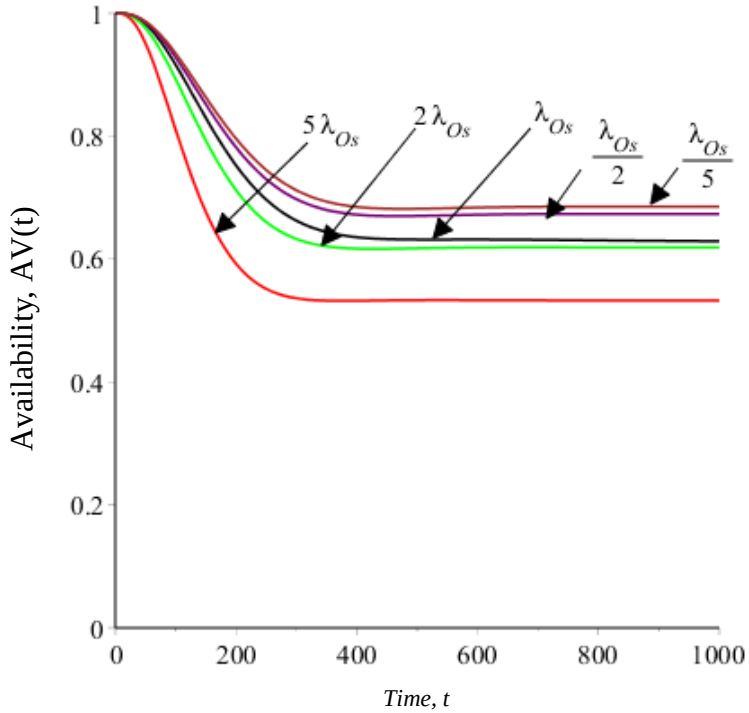

Figure C-38 Availability plots of three -unit system with four failure modes with Type-I repair at different values of λ_{Os}.

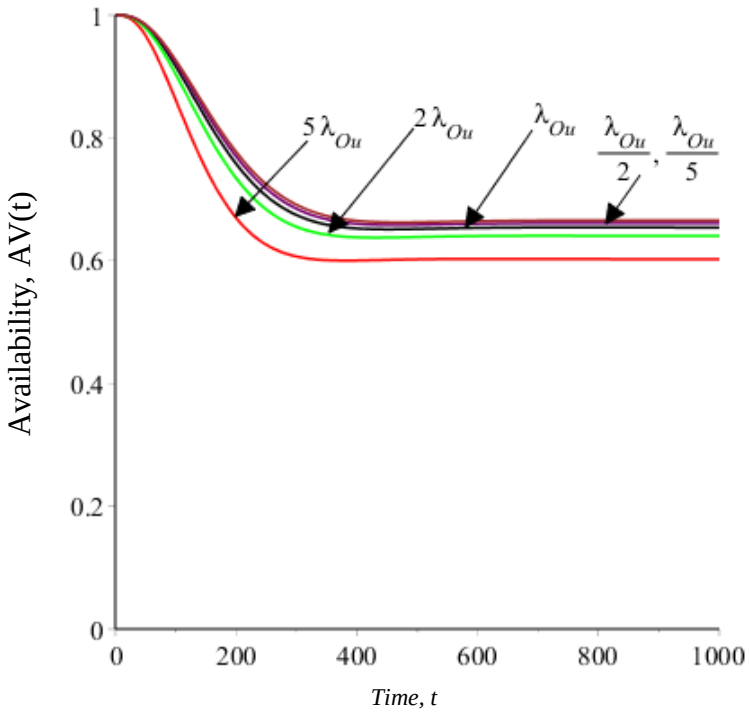

Figure C-39 Availability plots of three -unit system with four failure modes with Type-I repair at different values of λ_{Ou}.

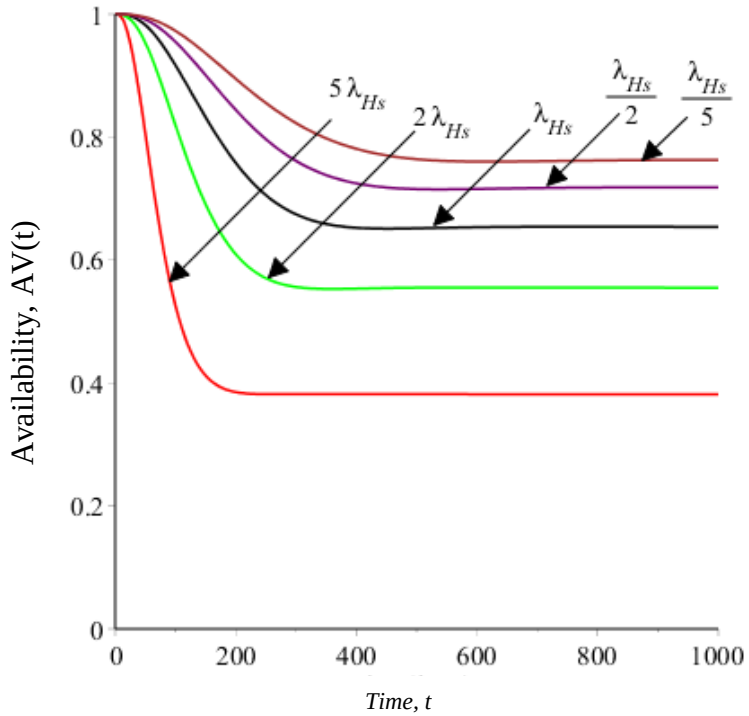

Figure C-40 Availability plots of three -unit system with four failure modes with Type-I repair at different values of λ_{Hs}.

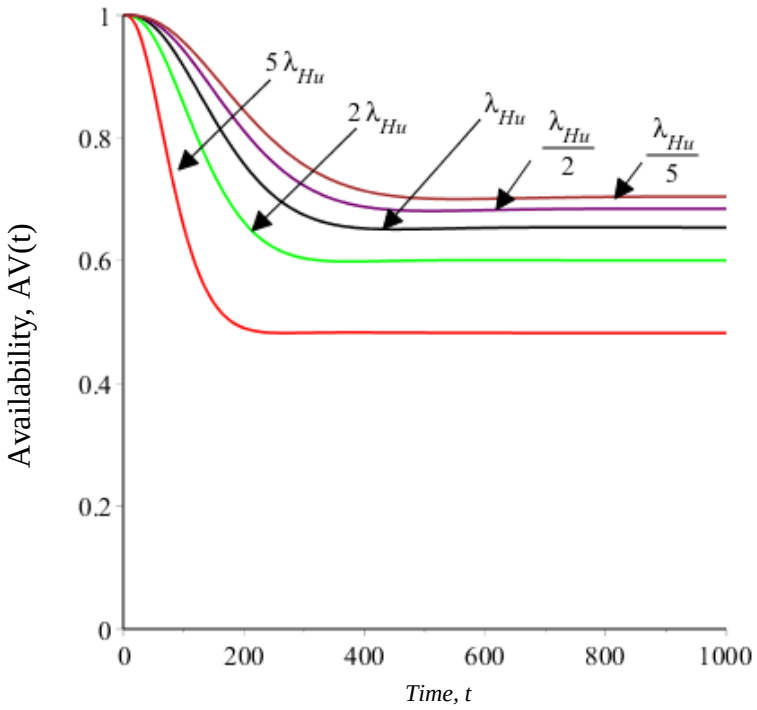

Figure C-41 Availability plots of three -unit system with four failure modes with Type-I repair at different values of λ_{Hu}.

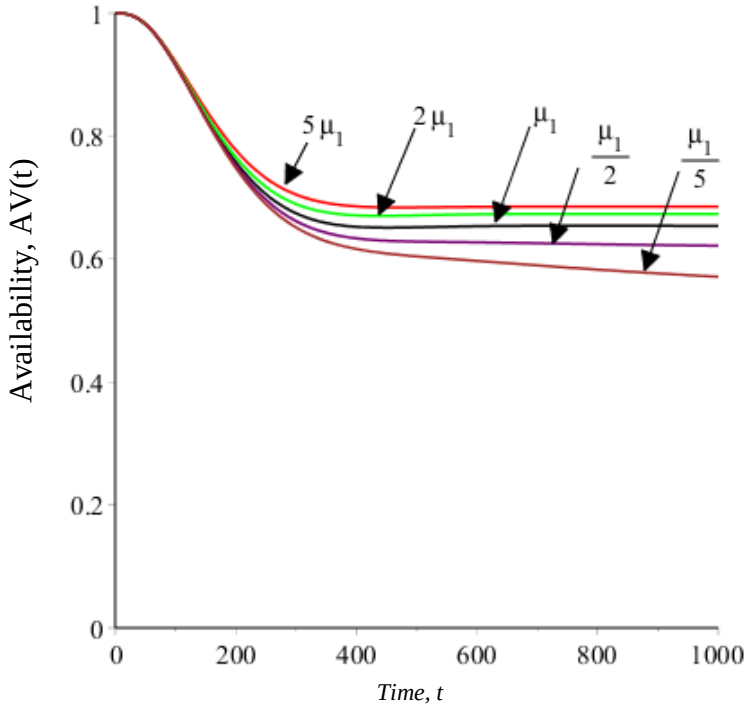

Figure C-42 Availability plots of three -unit system with four failure modes with Type-I repair at different values of μ_1.

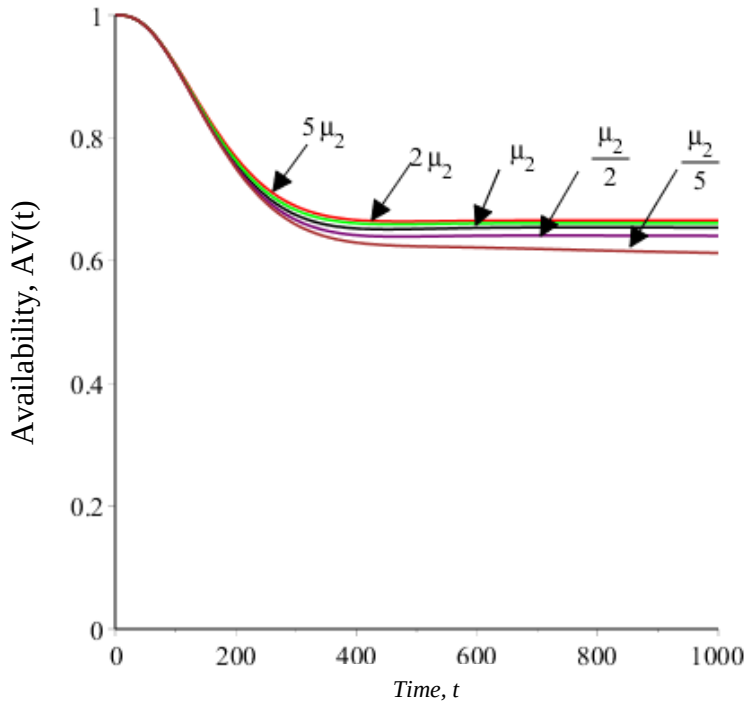

Figure C-43 Availability plots of three -unit system with four failure modes with Type-I repair at different values of μ_2.

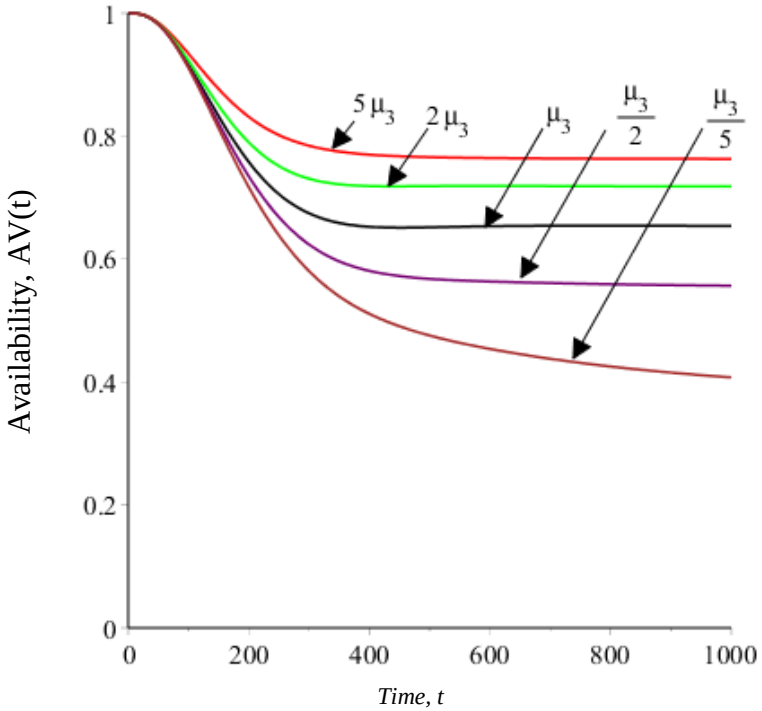

Figure C-44 Availability plots of three -unit system with four failure modes with Type-I repair at different values of μ_3.

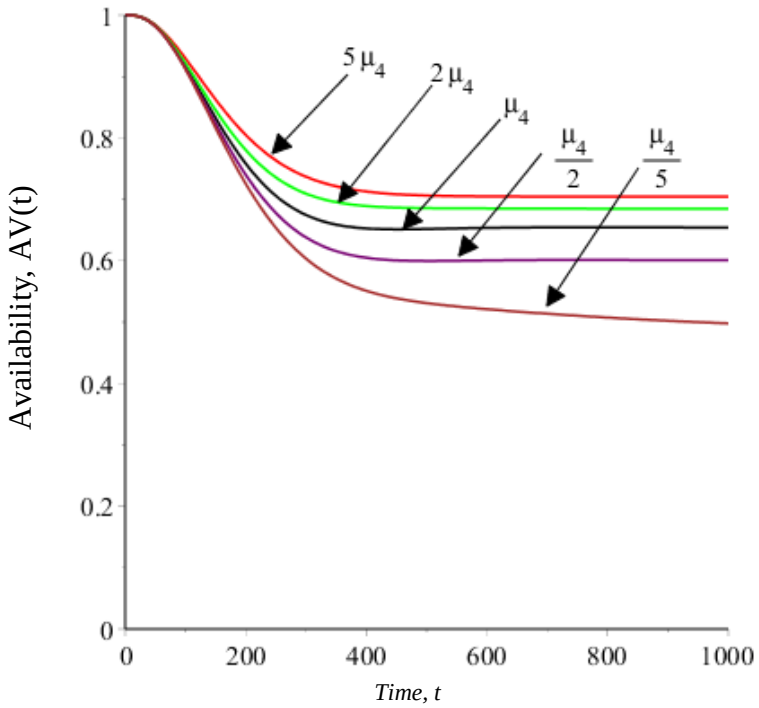

Figure C-45 Availability plots of three-unit system with four failure modes with Type-I repair at different values of μ_4.

Appendix D: Reliability Parameter Plots of Chapter 4

D.1 Single Unit with Hardware and Human-Error

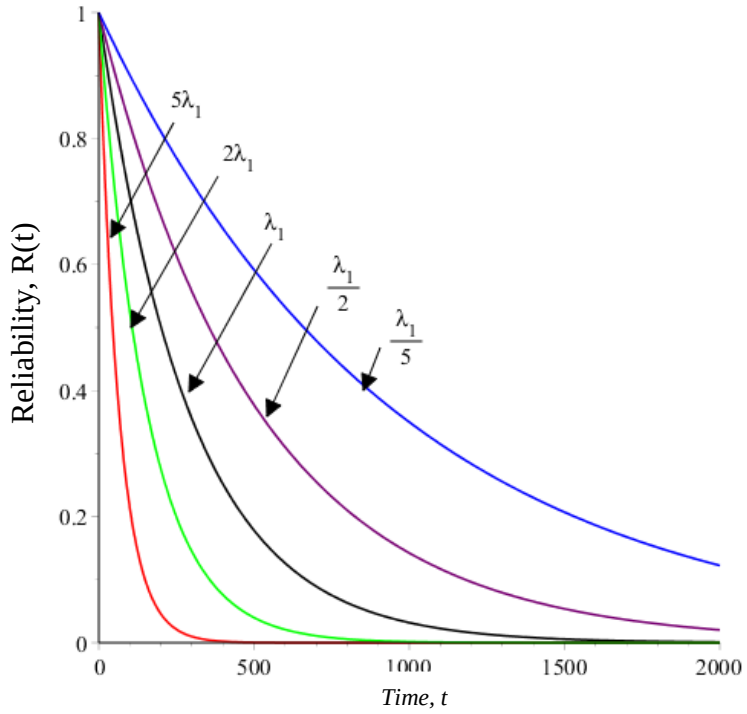

Figure D-1 Reliability plots of single unit system with partially or completely failures at different values of λ_1

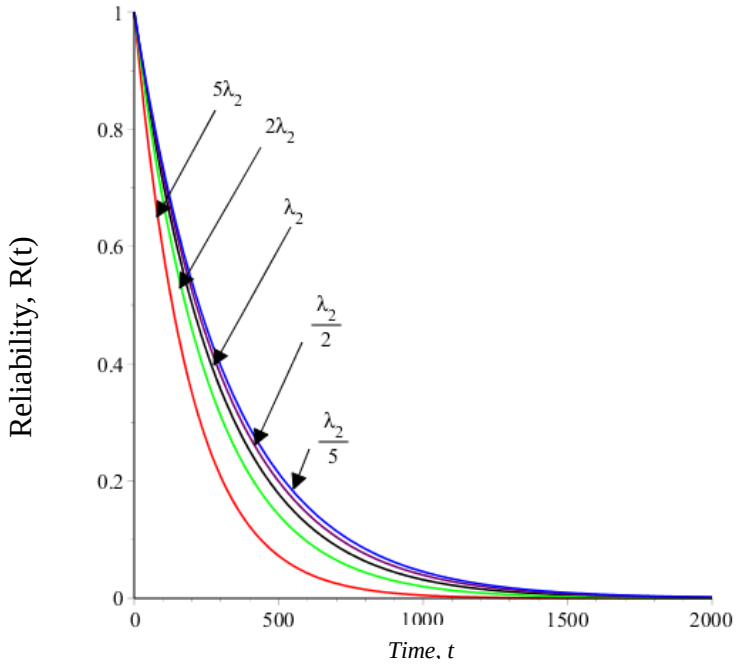

Figure D-2 MTTF of single unit system with partially or completely failures at different values of λ_2

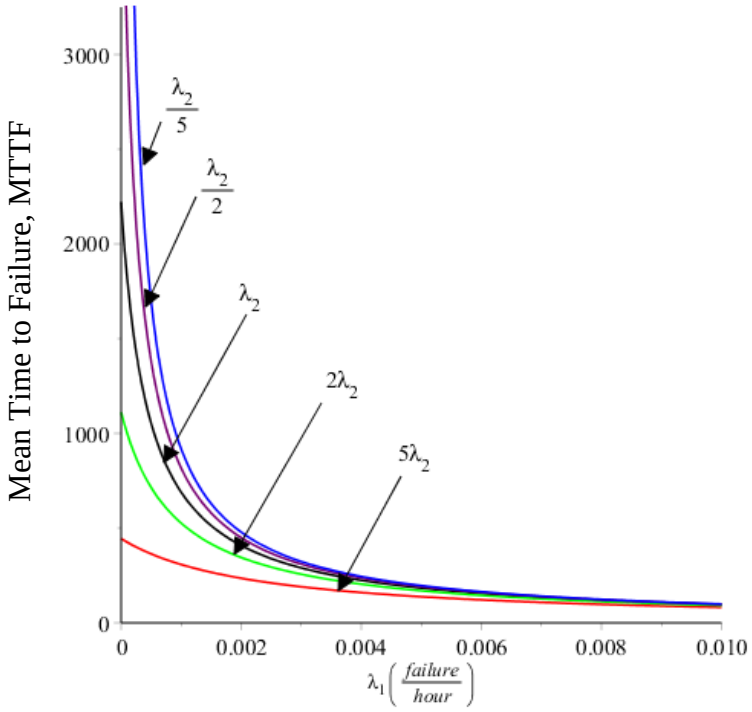

Figure D-3 Reliability of single unit system with partially or completely failures at different values of λ_2

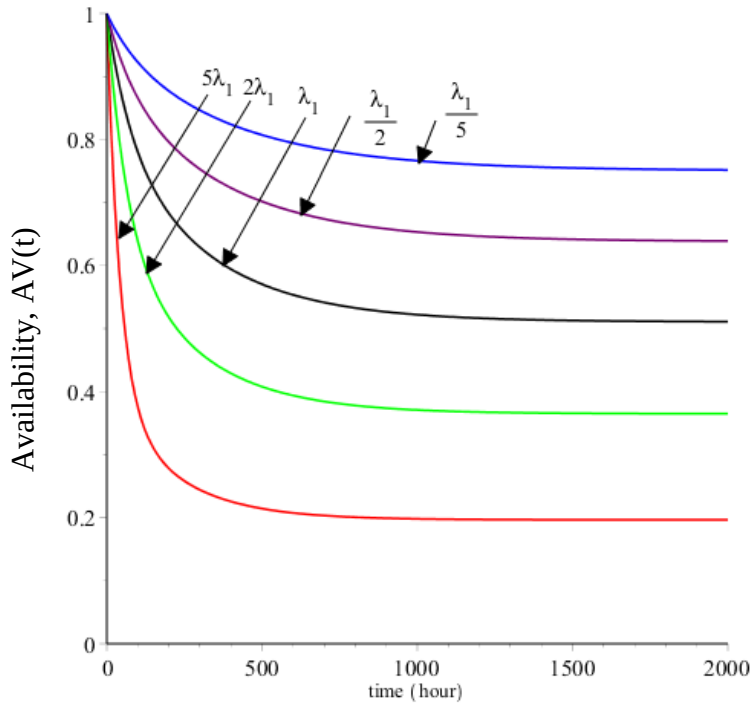

Figure D-4 Availability of single unit system with partially or completely failures at different values of λ_1

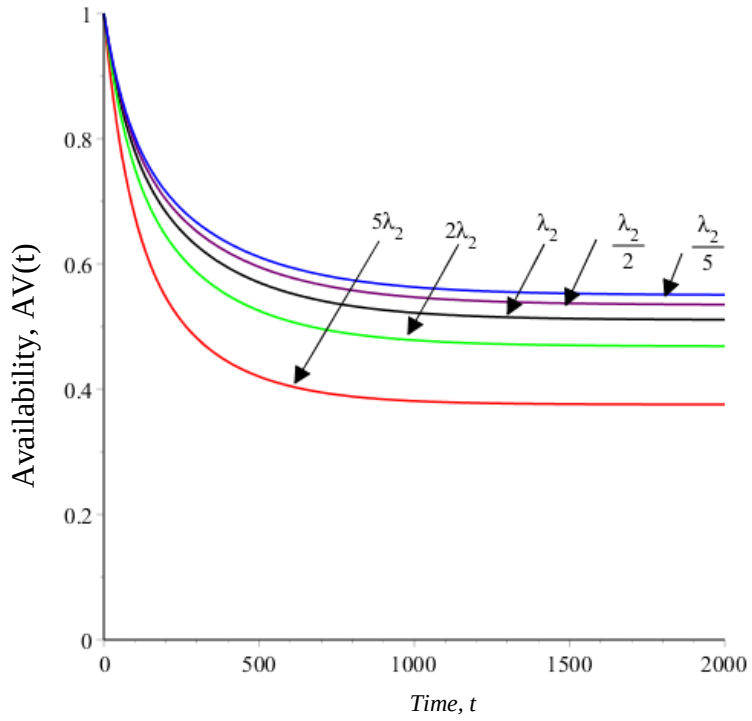

Figure D-5 Availability of single unit system with partially or completely failures at different values of λ_2

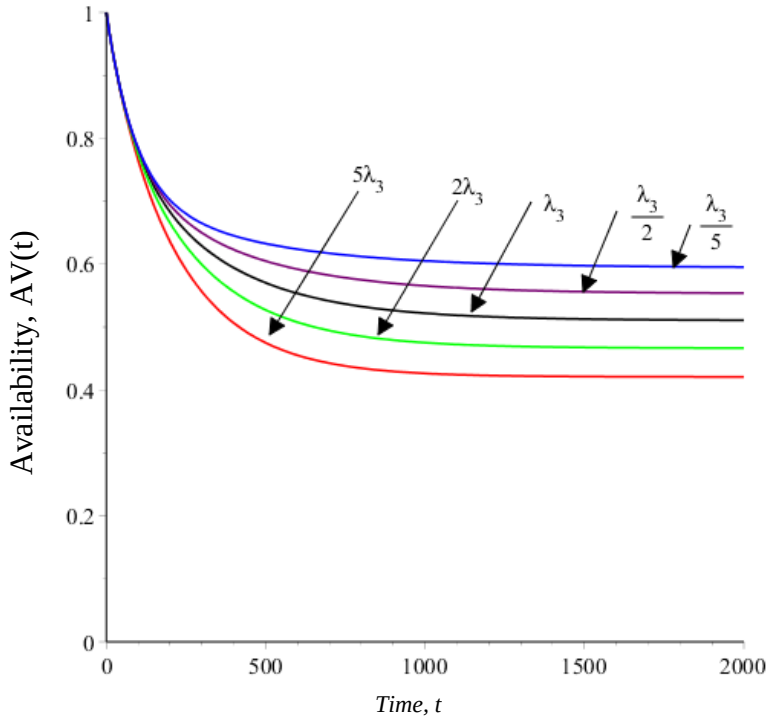

Figure D-6 Availability of single unit system with partially or completely failures at different values of λ_3

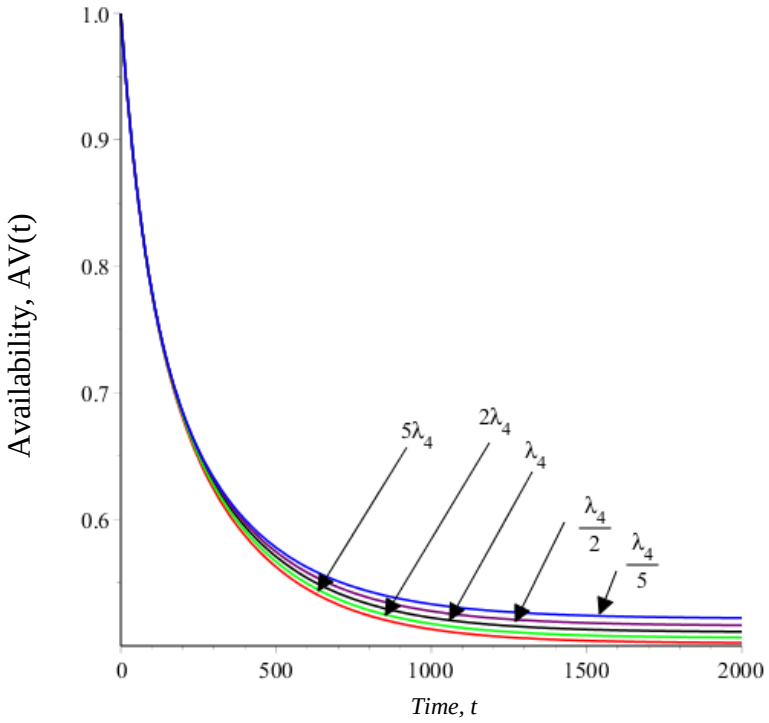

Figure D-7 Availability of single unit system with partially or completely failures at different values of λ_4

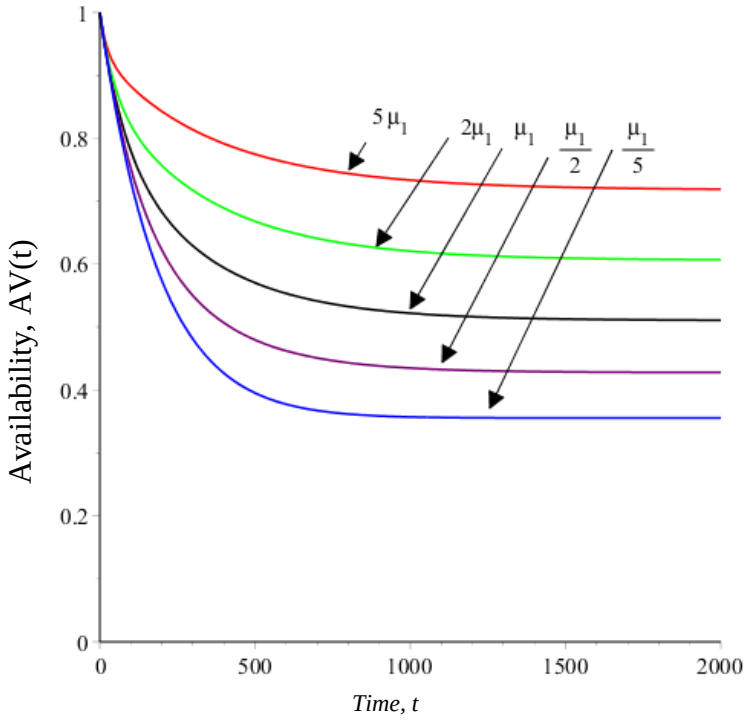

Figure D-8 Availability of single unit system with partially or completely failures at different values of μ_1

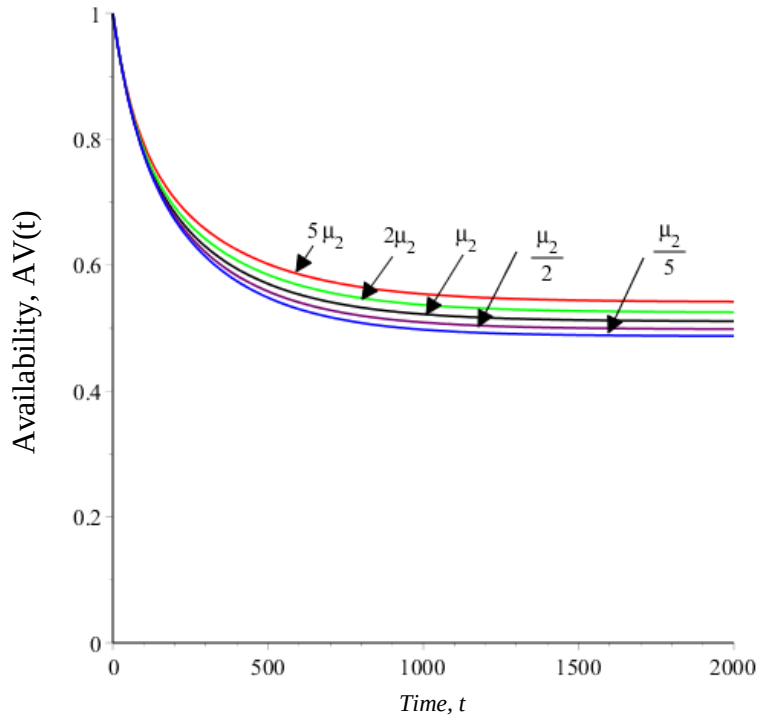

Figure D-9 Availability of single unit system with partially or completely failures at different values of μ_2

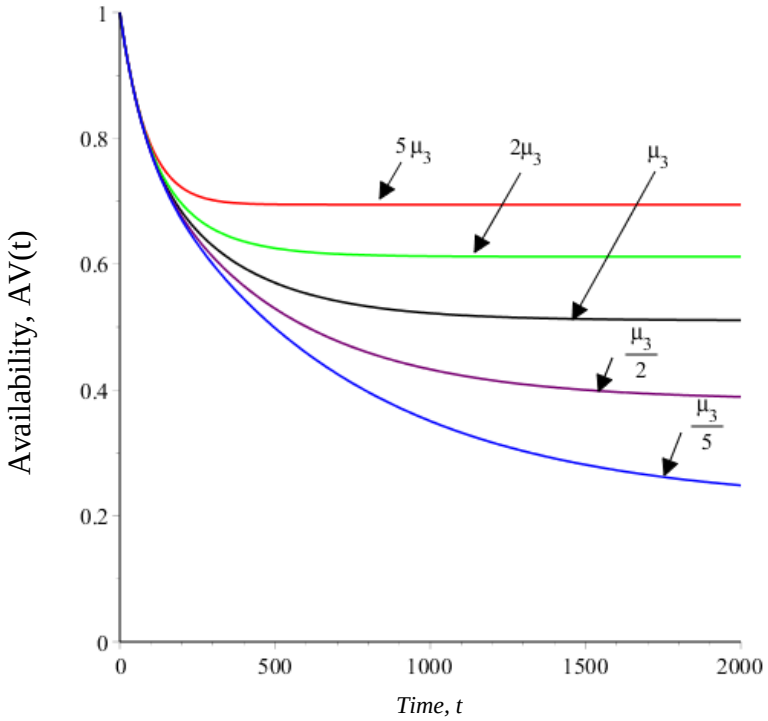

Figure D-10 Availability of single unit system with partially or completely failures at different values of μ_3

D.2 Single Unit Safe and Unsafe Failures of Hardware and Human-Error

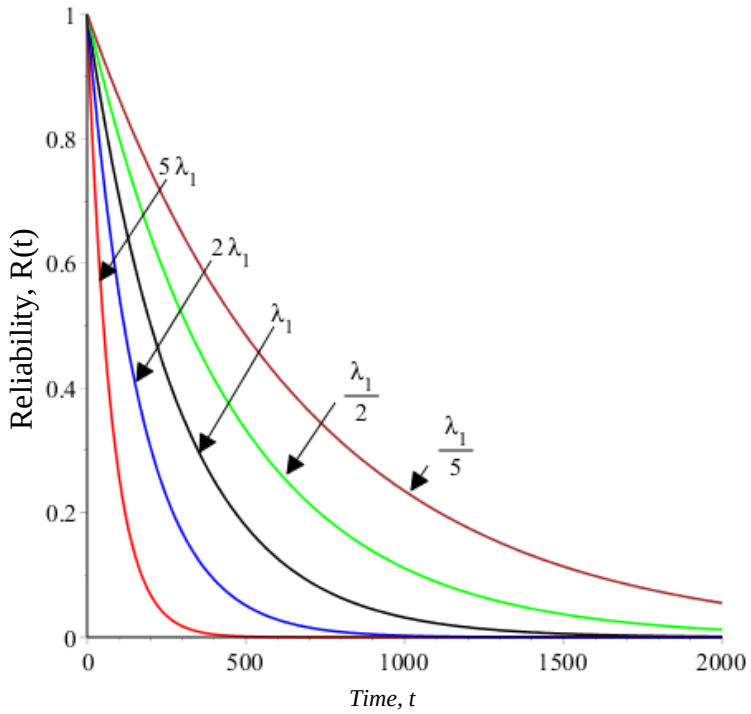

Figure D-11 Reliability of single unit system with safe and unsafe partially failure modes of hardware failure and human-error at different values of λ_1

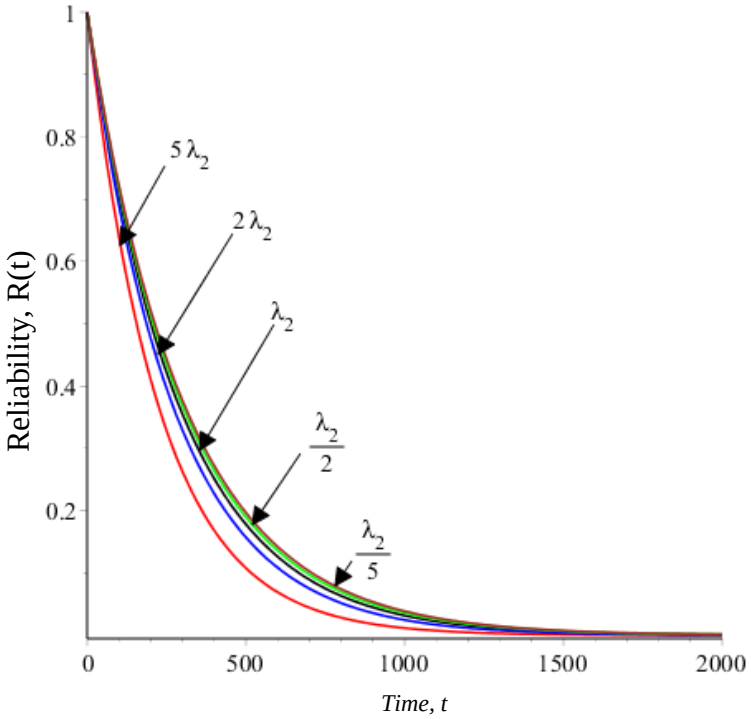

Figure D-12 Reliability of single unit system with safe and unsafe partially failure modes of hardware failure and human-error at different values of λ_2

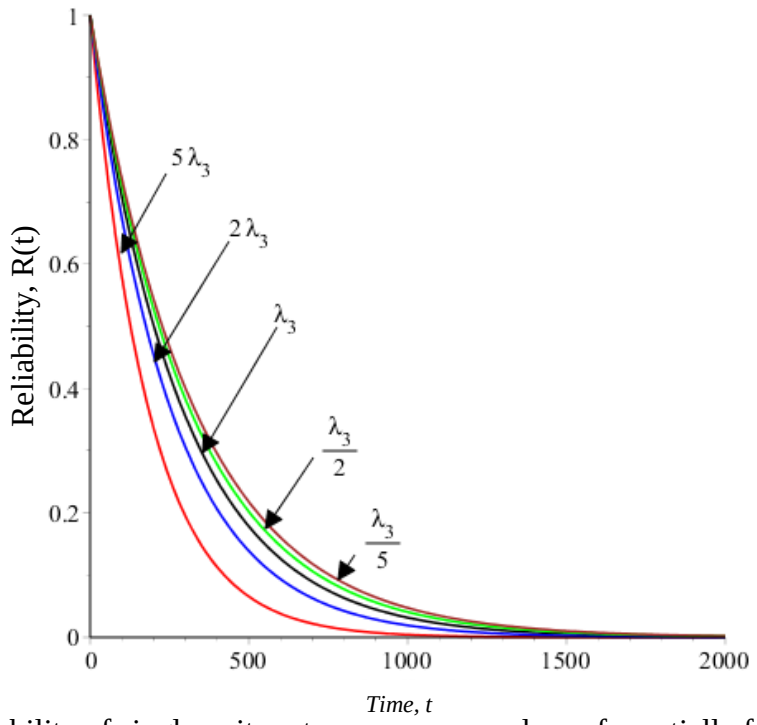

Figure D-13 Reliability of single unit system with safe and unsafe partially failure modes of hardware failure and human-error at different values of λ_3

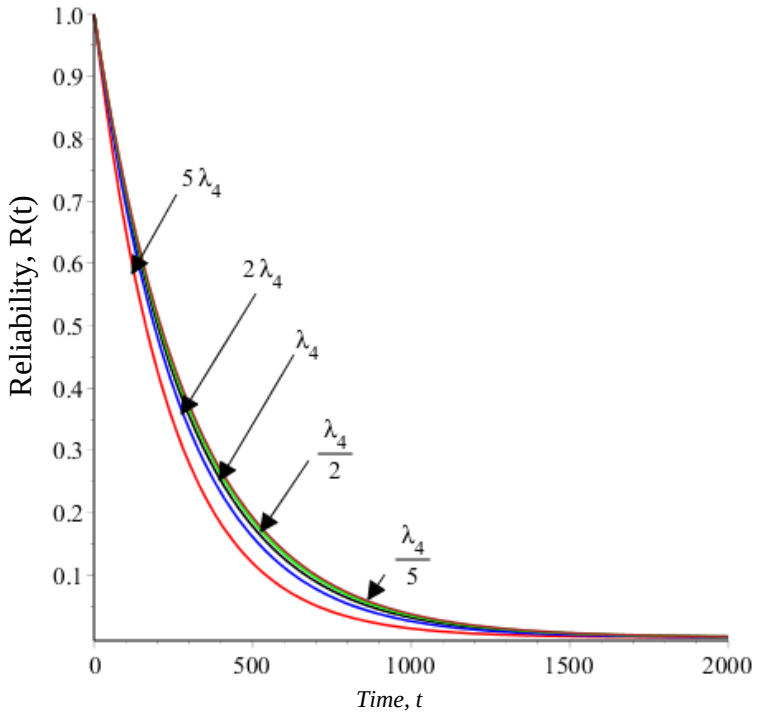

Figure D-14 Reliability of single unit system with safe and unsafe partially failure modes of hardware failure and human-error at different values of λ_4

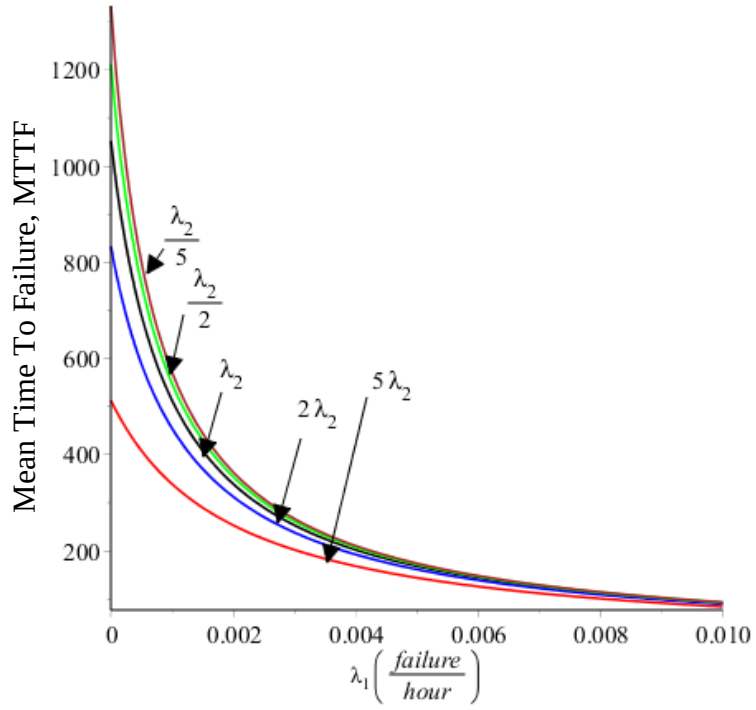

Figure D-15 MTTF of single unit system with safe and unsafe partially failure modes of hardware failure and human-error at different values of λ_2

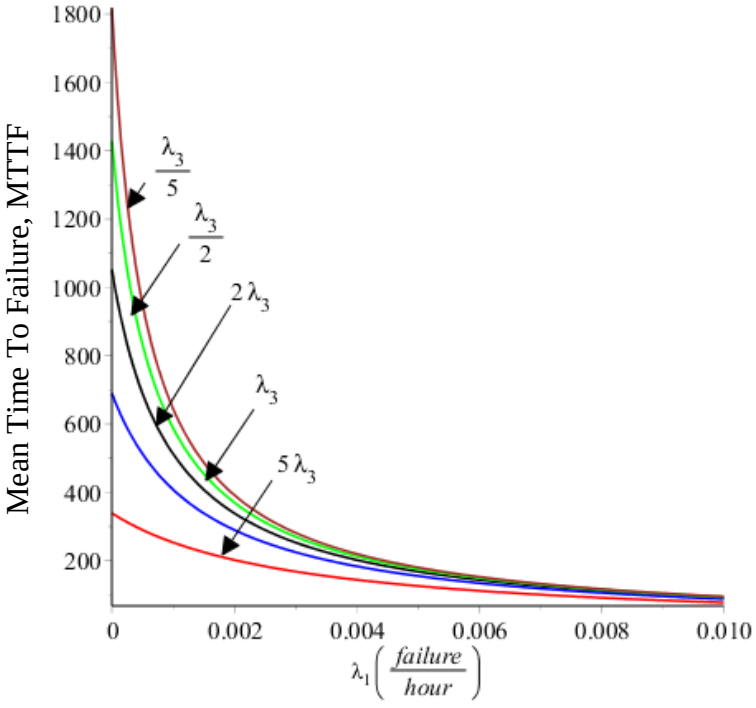

Figure D-16 MTTF of single unit system with safe and unsafe partially failure modes of hardware failure and human-error at different values of λ_3

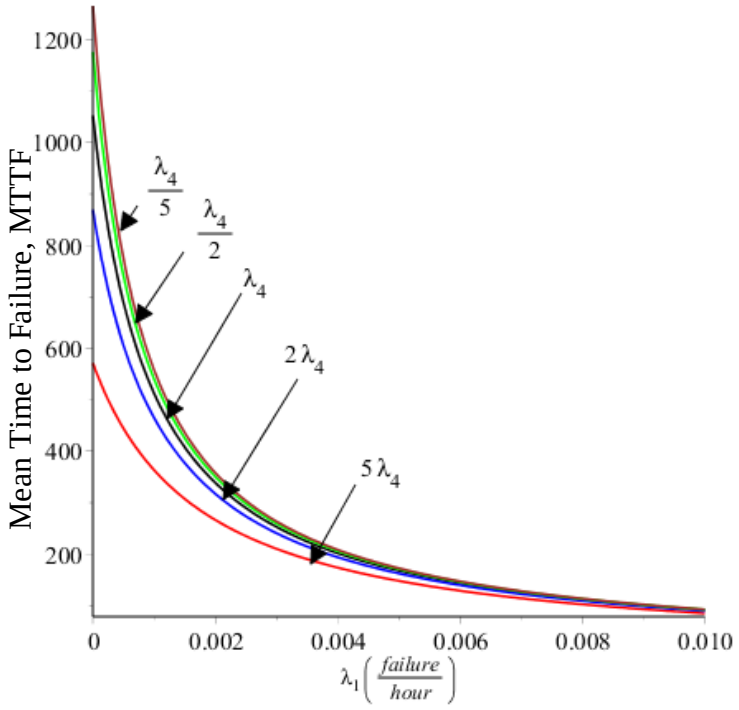

Figure D-17 MTTF of single unit system with safe and unsafe partially failure modes of hardware failure and human-error at different values of λ_4

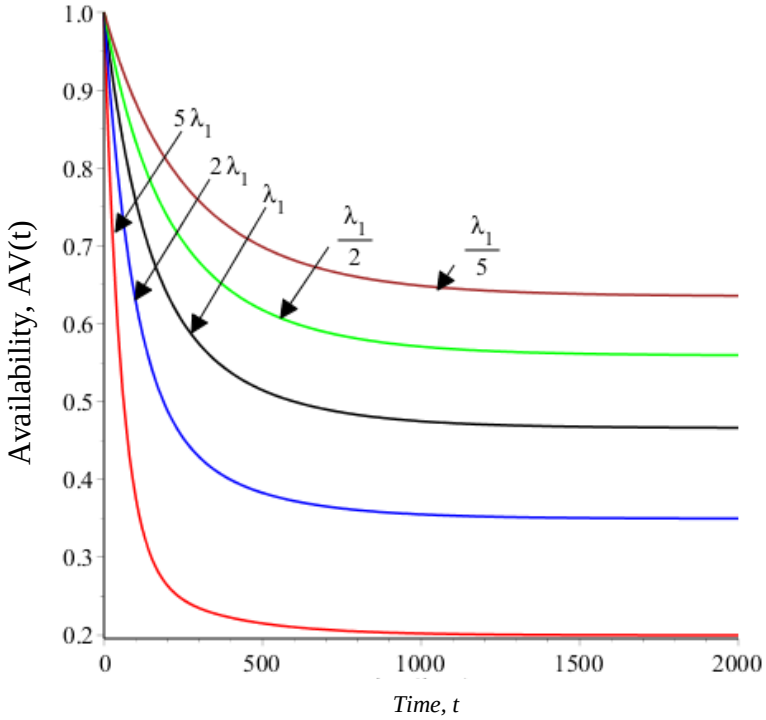

Figure D-18 Availability of single unit system with safe and unsafe partially failure modes of hardware failure and human-error at different values of λ_1

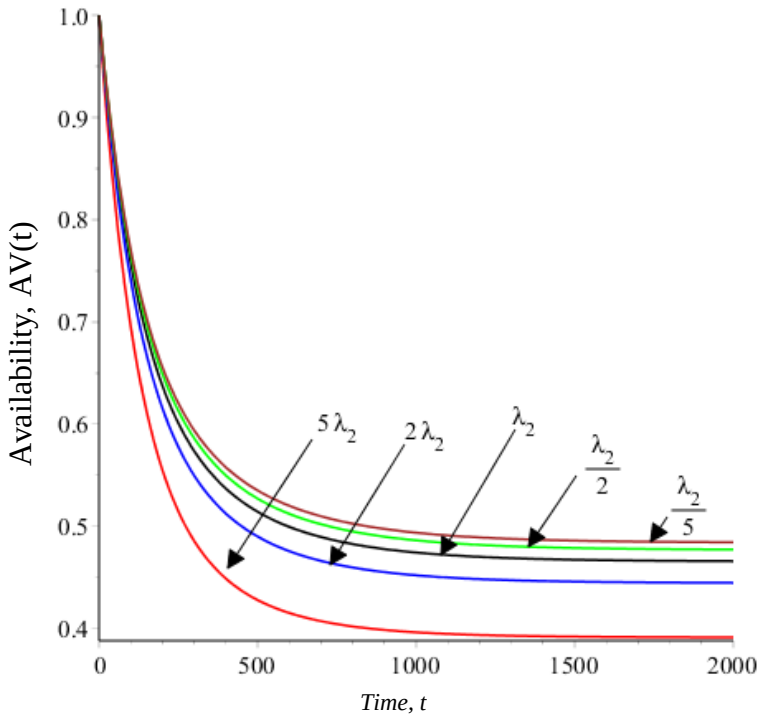

Figure D-19 Availability of single unit system with safe and unsafe partially failure modes of hardware failure and human-error at different values of λ_2

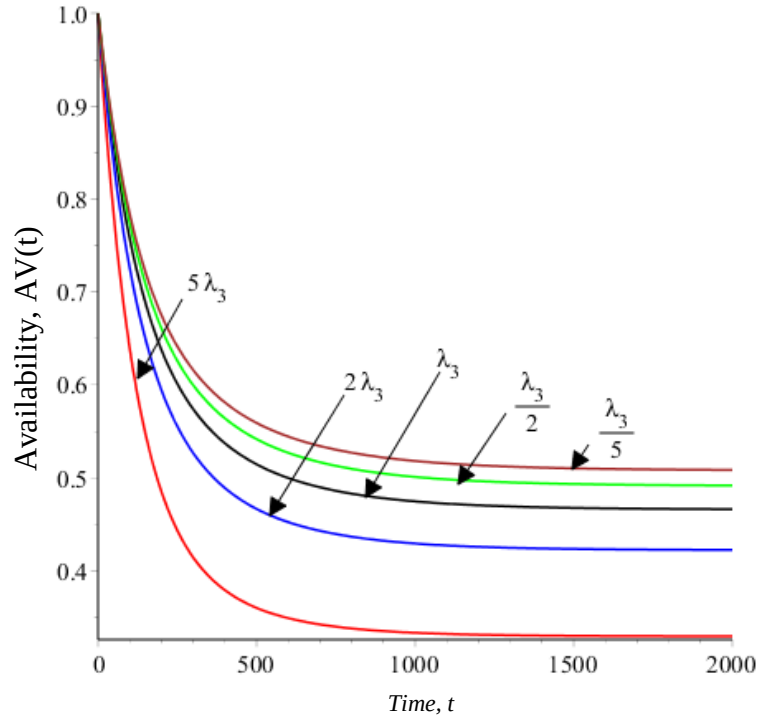

Figure D-20 Availability of single unit system with safe and unsafe partially failure modes of hardware failure and human-error at different values of λ_3

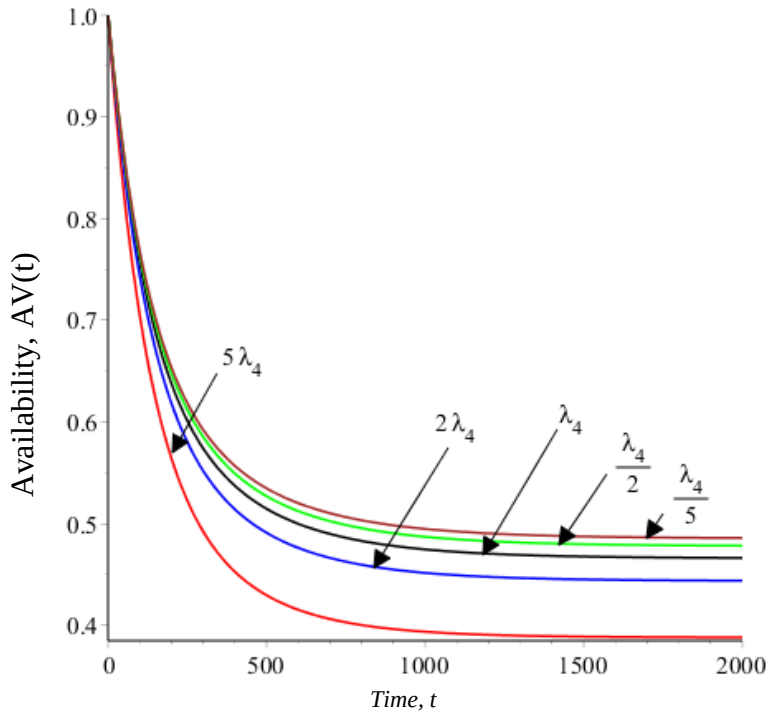

Figure D-21 Availability of single unit system with safe and unsafe partially failure modes of hardware failure and human-error at different values of λ_4

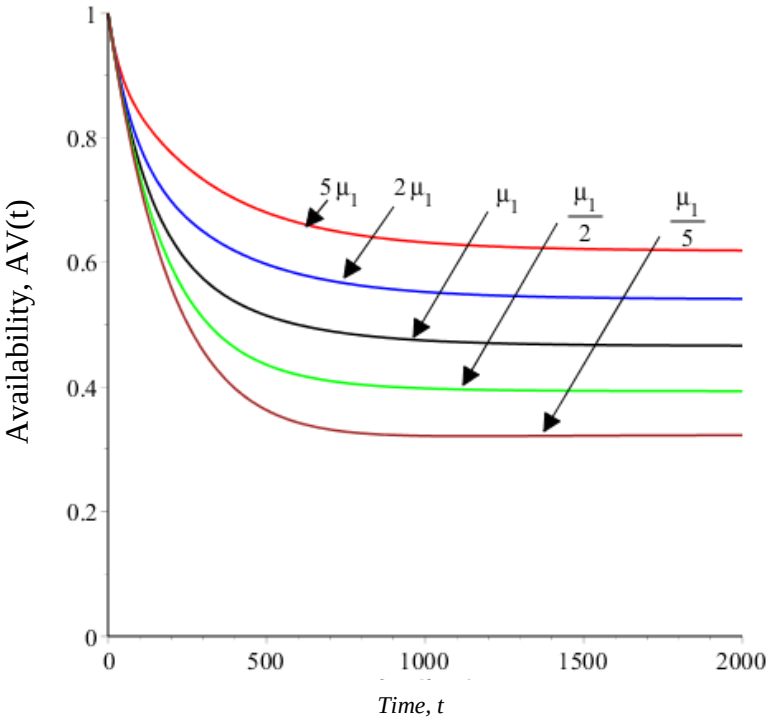

Figure D-22 Availability of single unit system with safe and unsafe partially failure modes of hardware failure and human-error at different values of μ_1

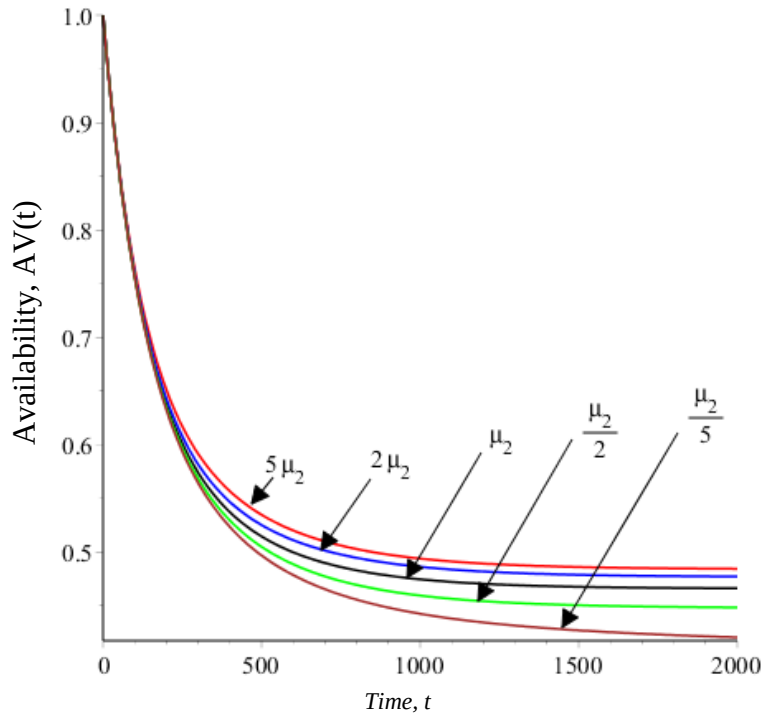

Figure D-23 Availability of single unit system with safe and unsafe partially failure modes of hardware failure and human-error at different values of μ_2

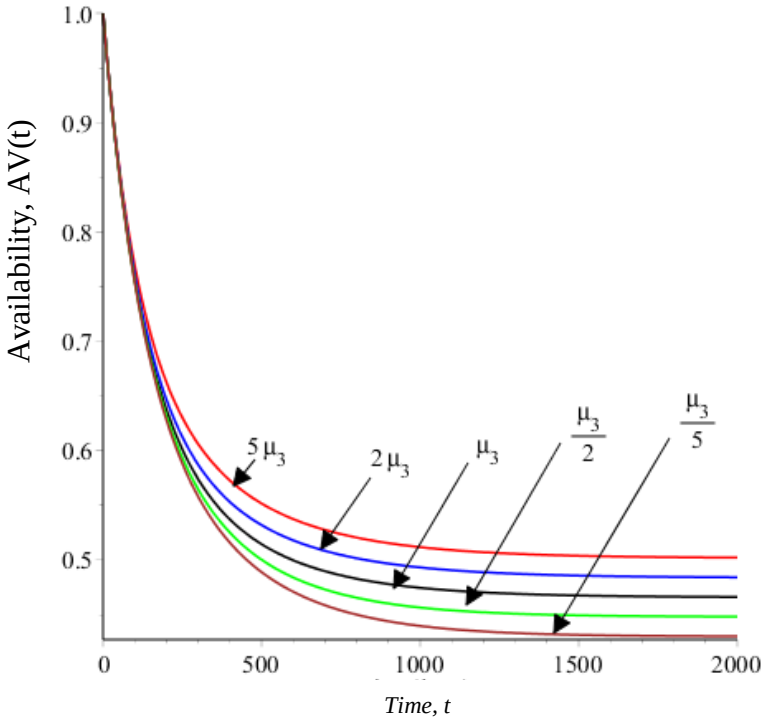

Figure D-24 Availability of single unit system with safe and unsafe partially failure modes of hardware failure and human-error at different values of μ_3

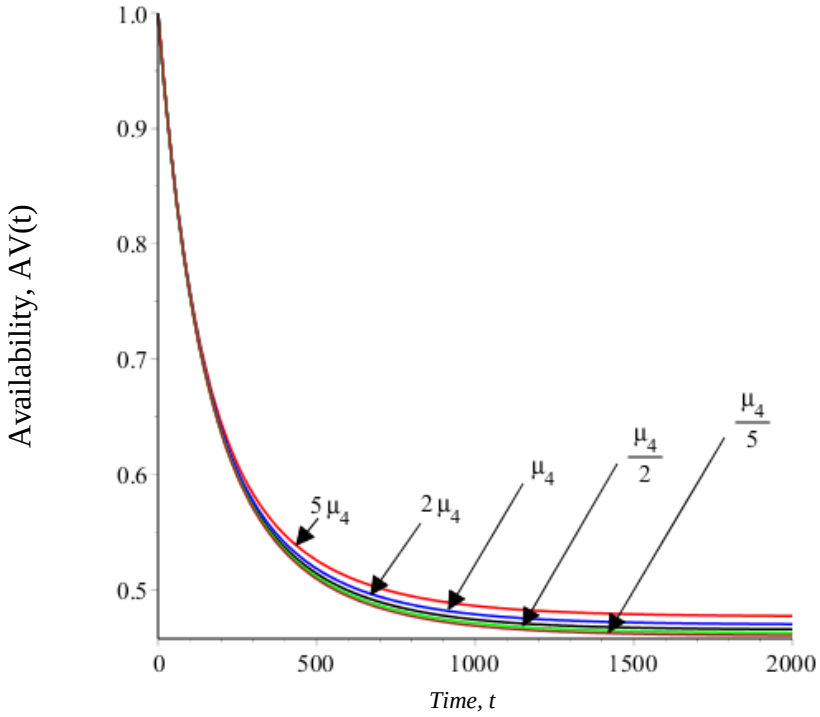

Figure D-25 Availability of single unit system with safe and unsafe partially failure modes of hardware failure and human-error at different values of μ_4

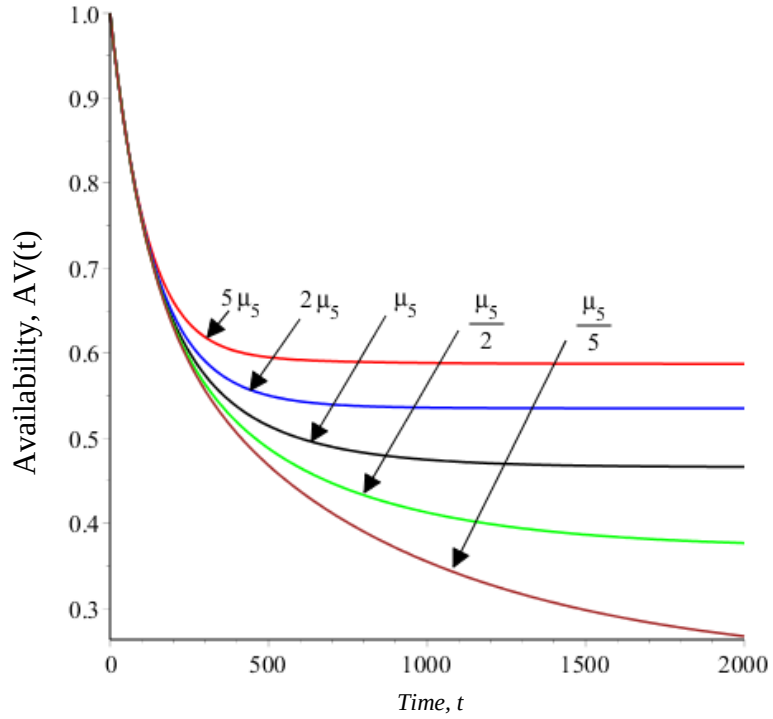

Figure D-26 Availability of single unit system with safe and unsafe partially failure modes of hardware failure and human-error at different values of μ_5

D.3 One-Unit with Three Operational States and One Failure Mode

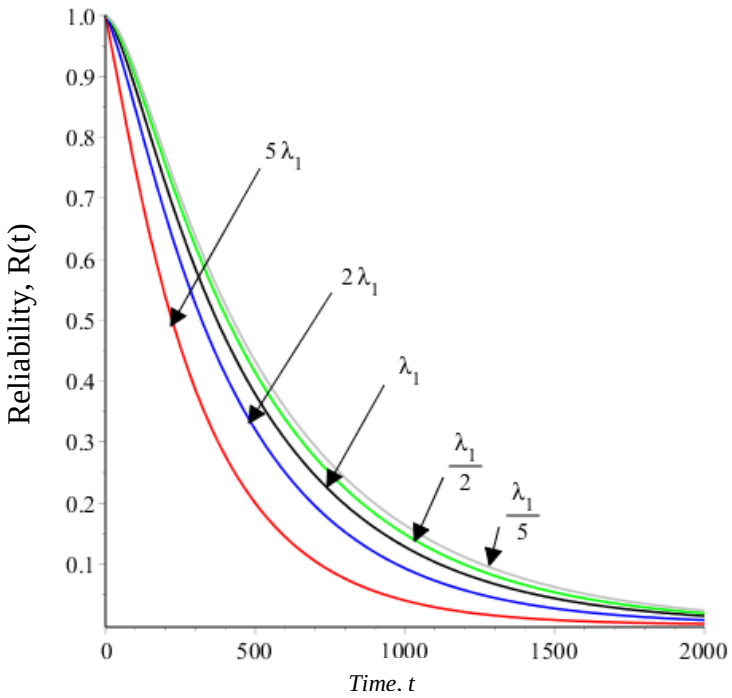

Figure D-27 Reliability plots of single unit system with three operation states at different values of λ_1

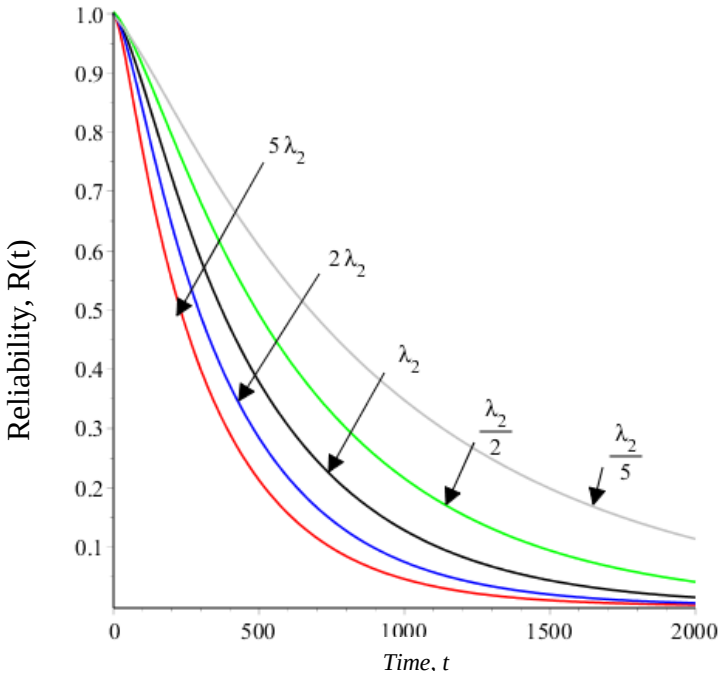

Figure D-28 Reliability plots of single unit system with three operation states at different values of λ_2

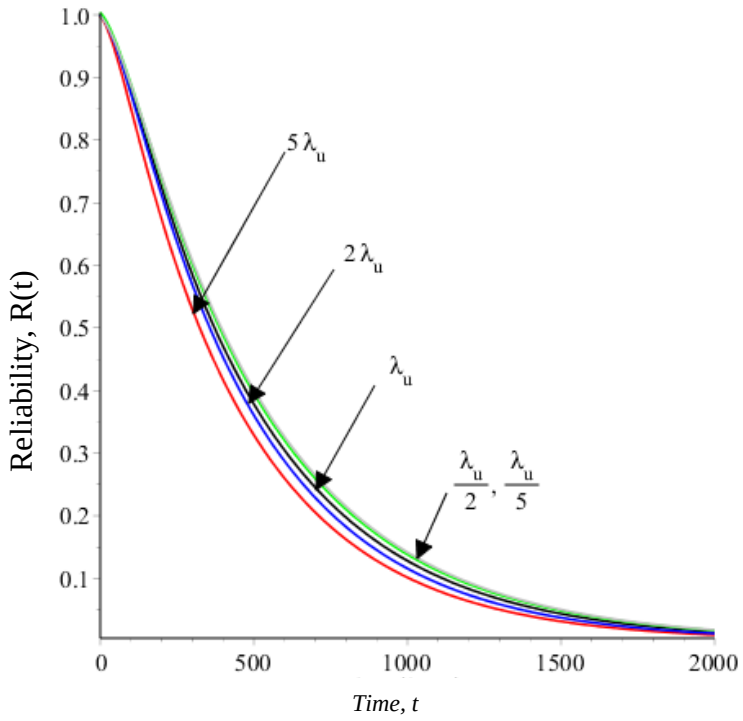

Figure D-29 Reliability plots of single unit system with three operation states at different values of λ_u

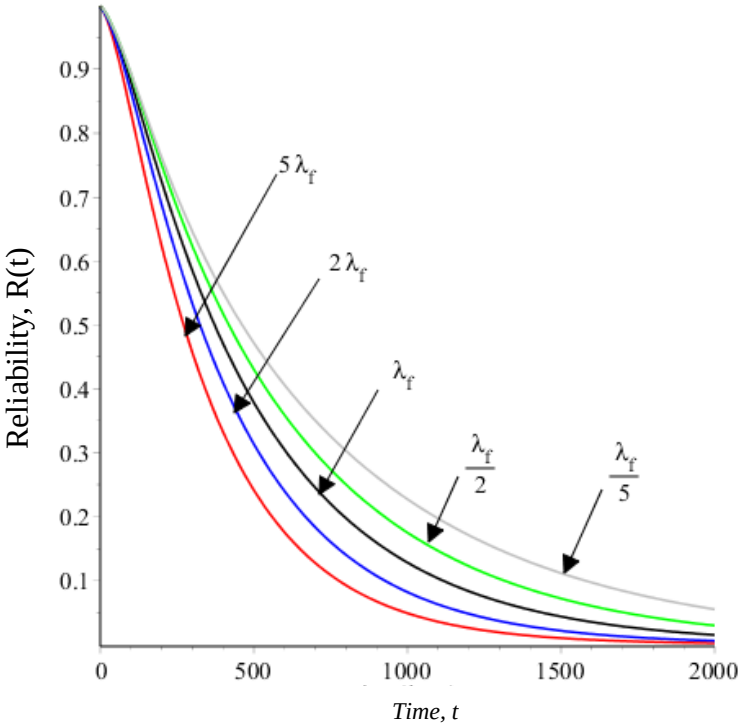

Figure D-30 Reliability plots of single unit system with three operation states at different values of λ_f

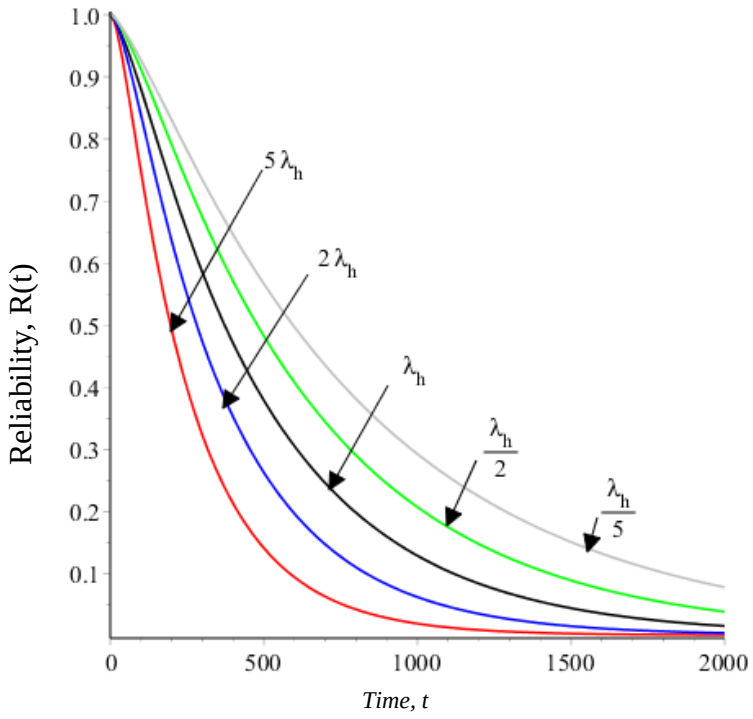

Figure D-31 Reliability plots of single unit system with three operation states at different values of λ_h

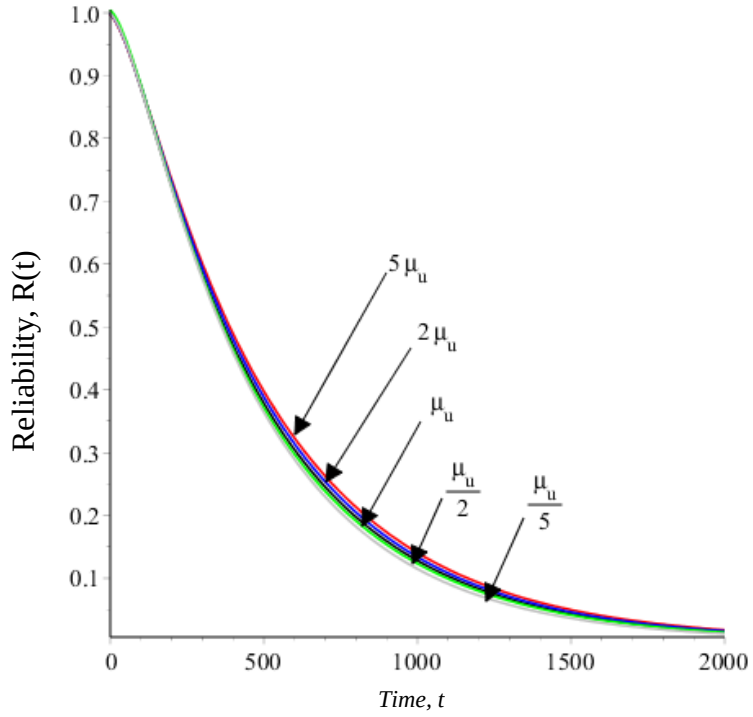

Figure D-32 Reliability plots of single unit system with three operation states at different values of μ_u

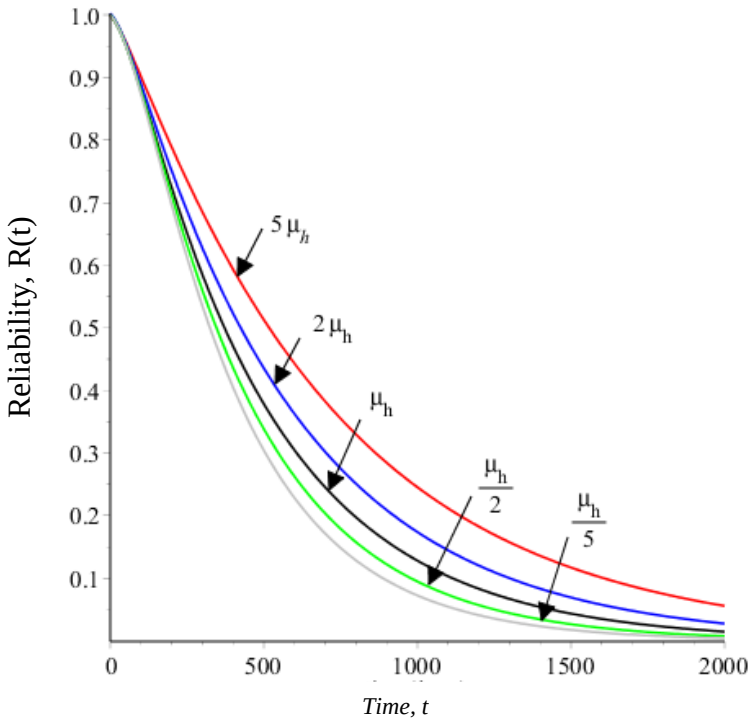

Figure D-33 Reliability plots of single unit system with three operation states at different values of μ_h

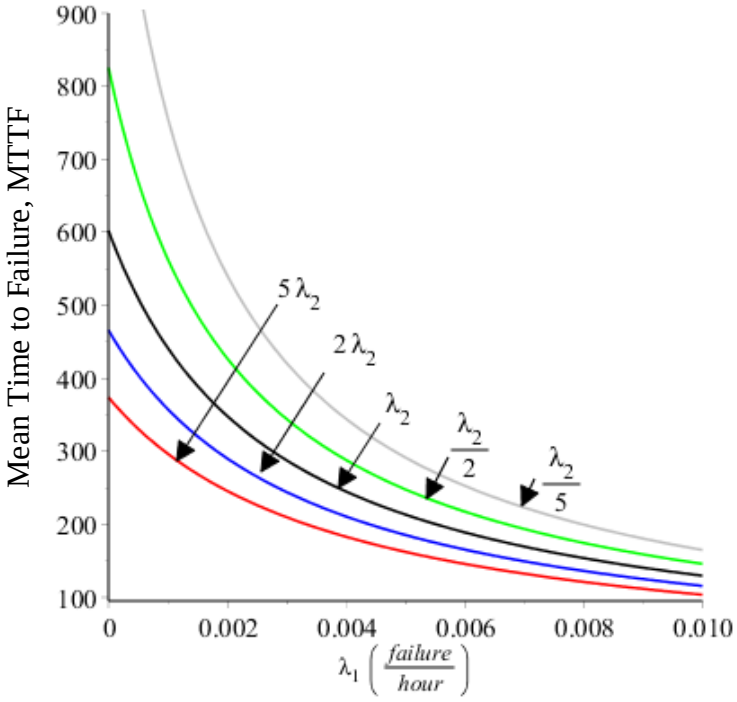

Figure D-34 MTTF Plots of single unit system with three operation states at different values of λ_2

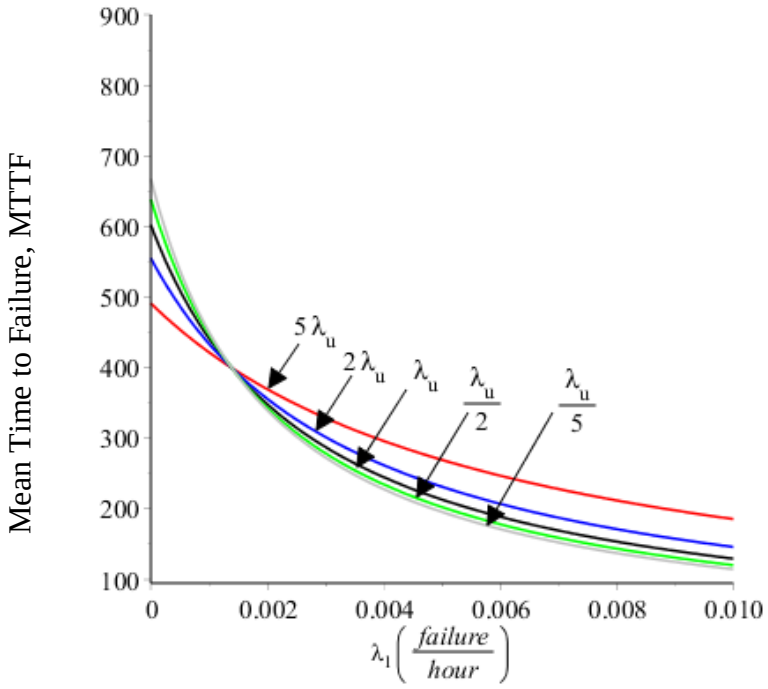

Figure D-35 MTTF plots of single unit system with three operation states at different values of λ_u

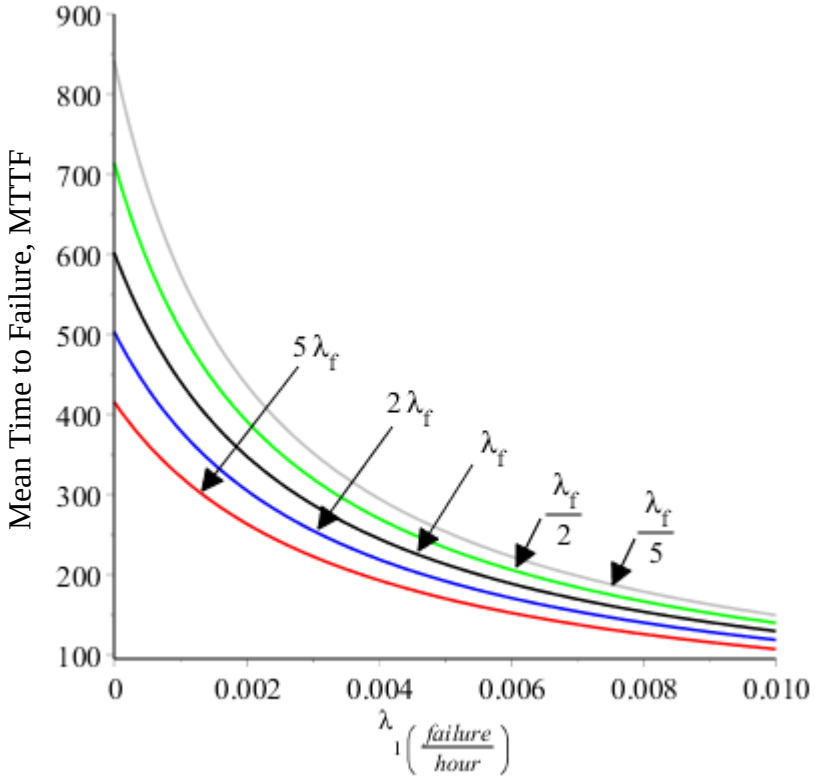

Figure D-36 MTTF plots of single unit system with three operation states at different values of λ_f

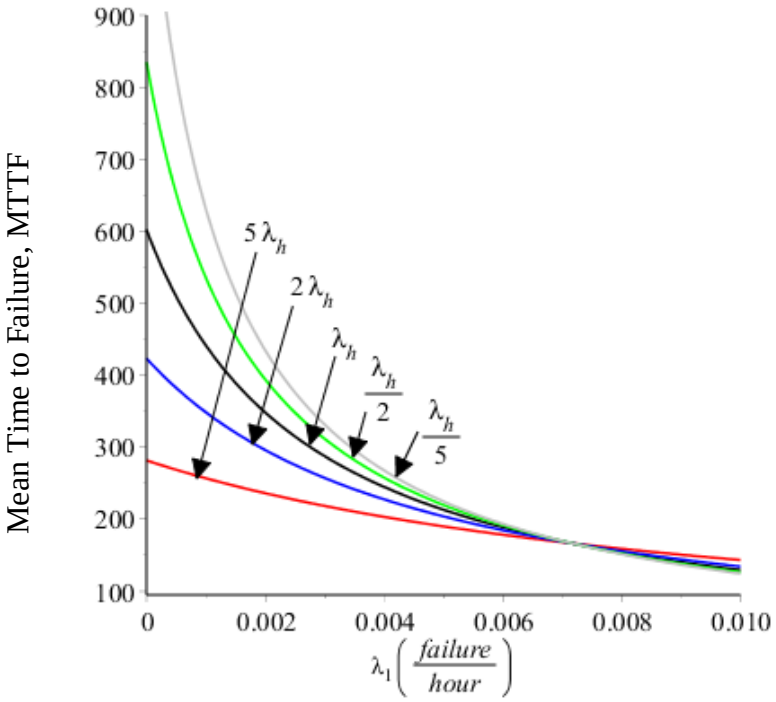

Figure D-37 MTTF plots of single unit system with three operation states at different values of λ_h

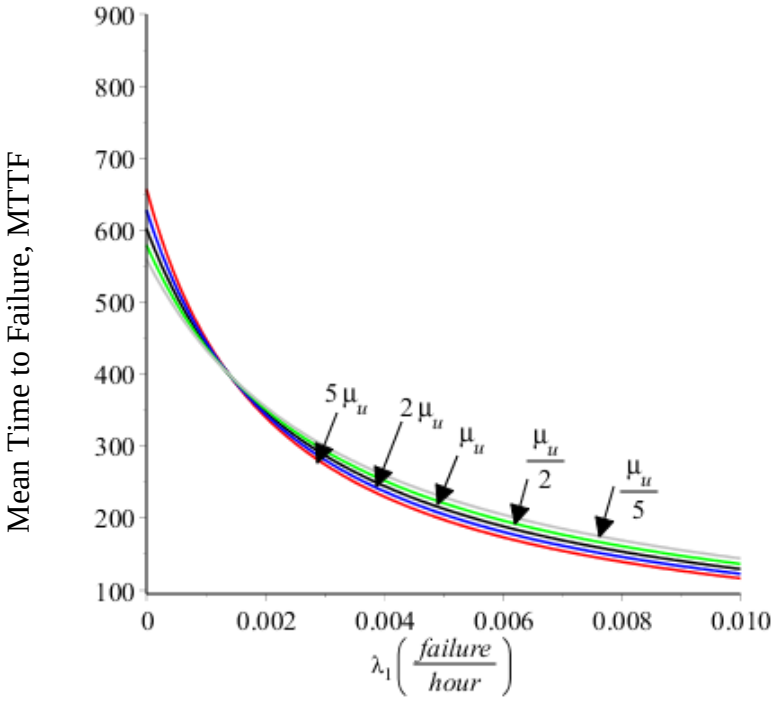

Figure D-38 MTTF plots of single unit system with three operation states at different values of μ_u

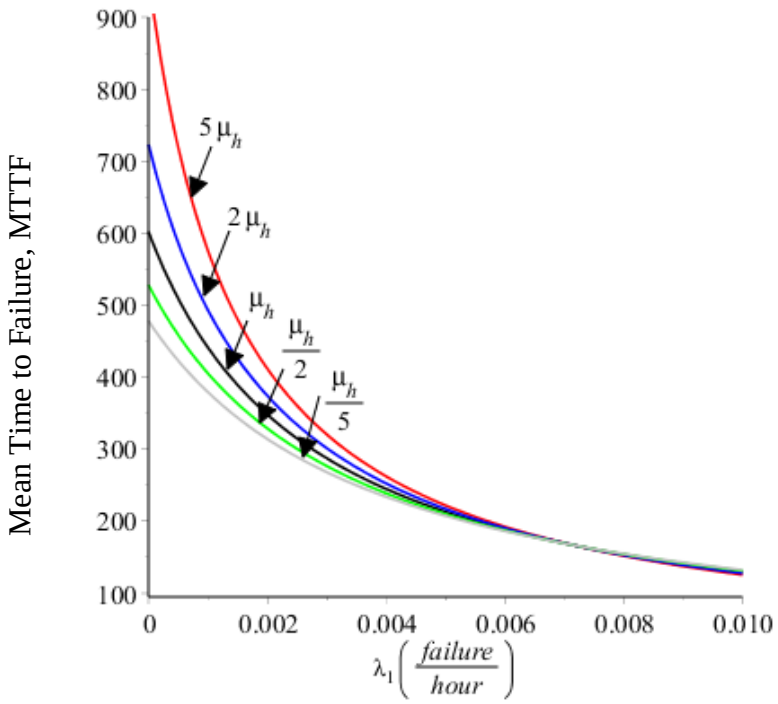

Figure D-39 MTTF plots of single unit system with three operation states at different values of μ_u

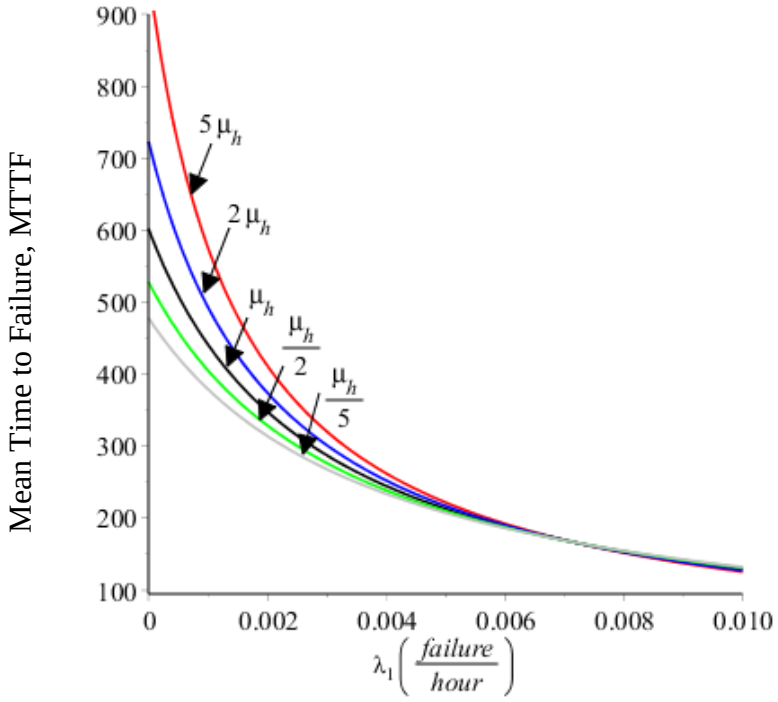

Figure D-40 MTTF plots of single unit system with three operation states at different values of μ_u

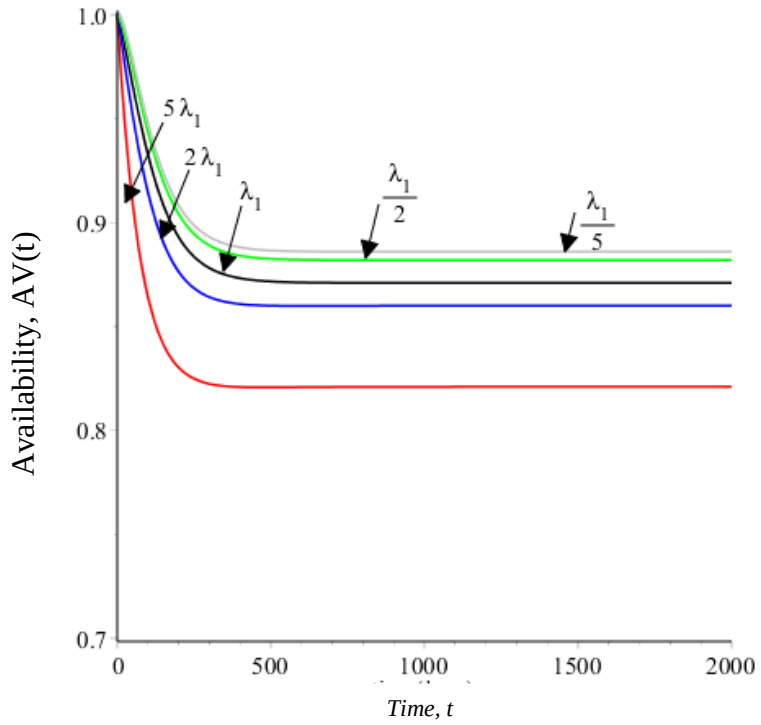

Figure D-41 Availability plots of single system unit with three operation states at different values of λ_1

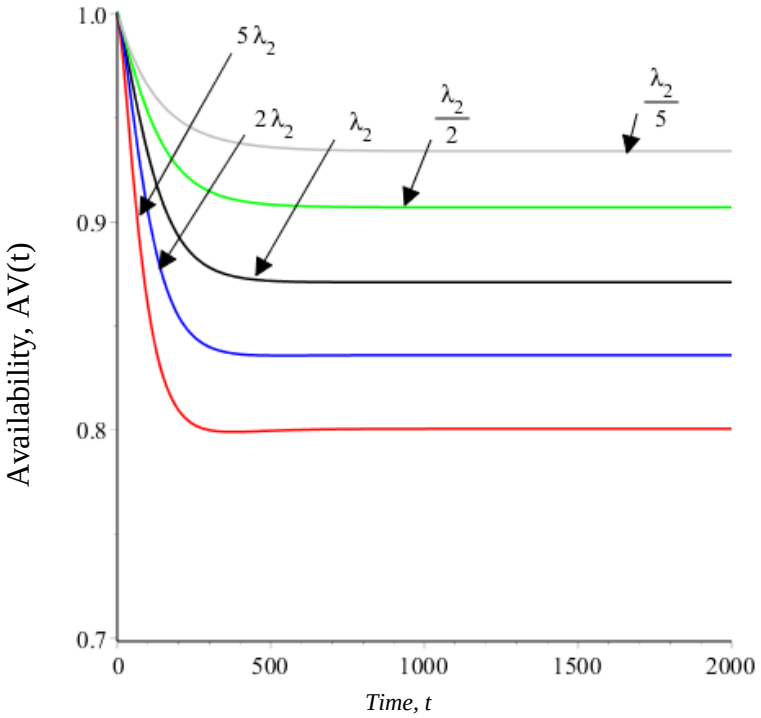

Figure D- Availability plots of single unit system with three operation states at different values of λ_2

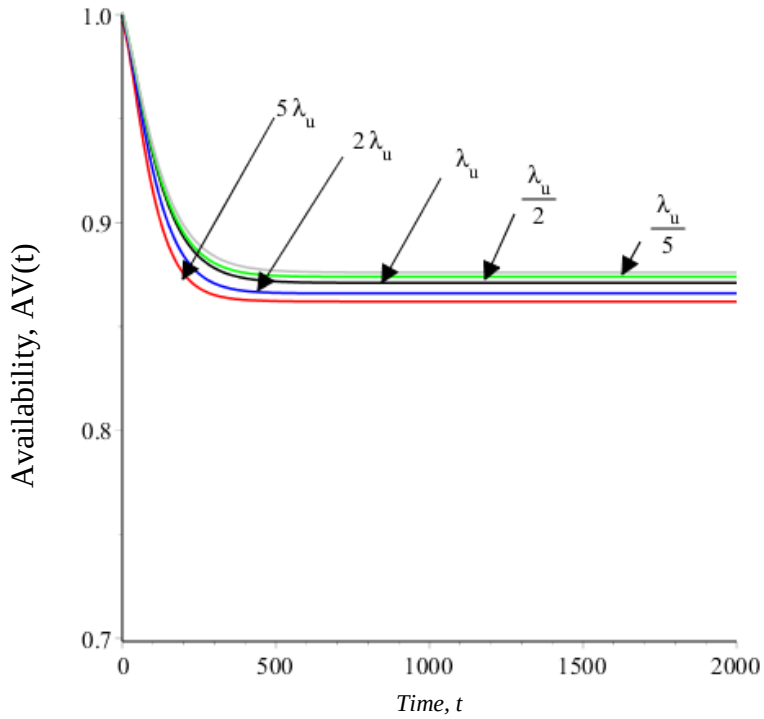

Figure D-42 Availability plots of single unit system with three operation states at different values of λ_u

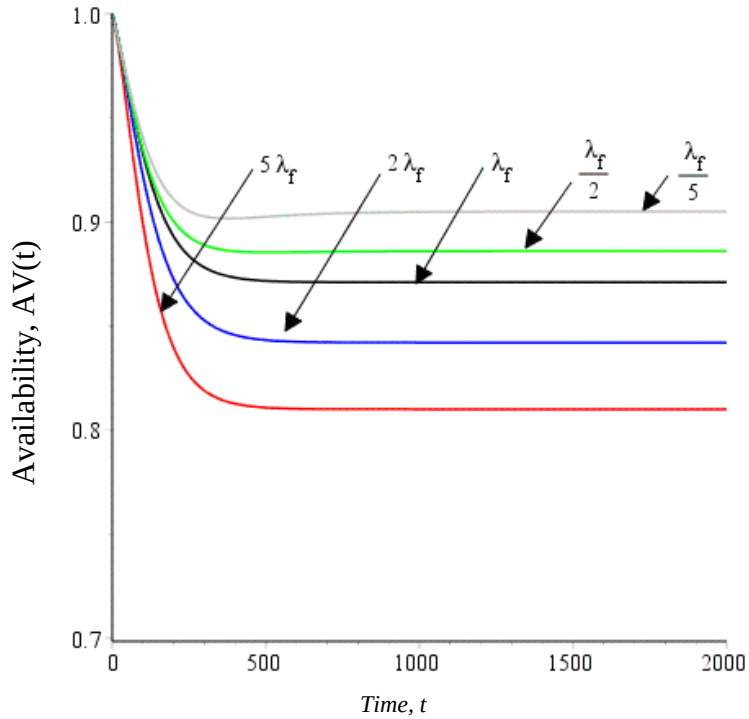

Figure D-43 Availability plots of single unit system with three operation states at different values of λ_f

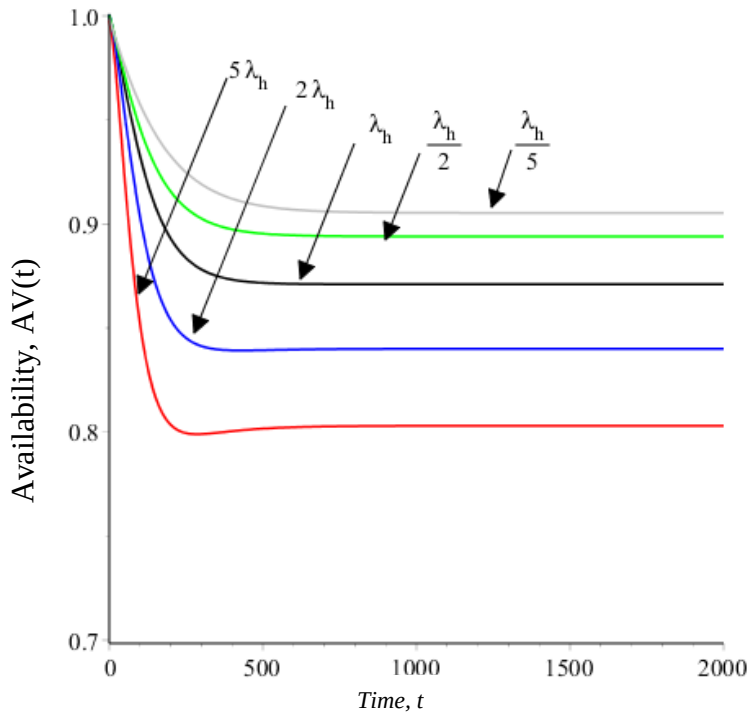

Figure D-44 Availability plots of single unit system with three operation states at different values of λ_h

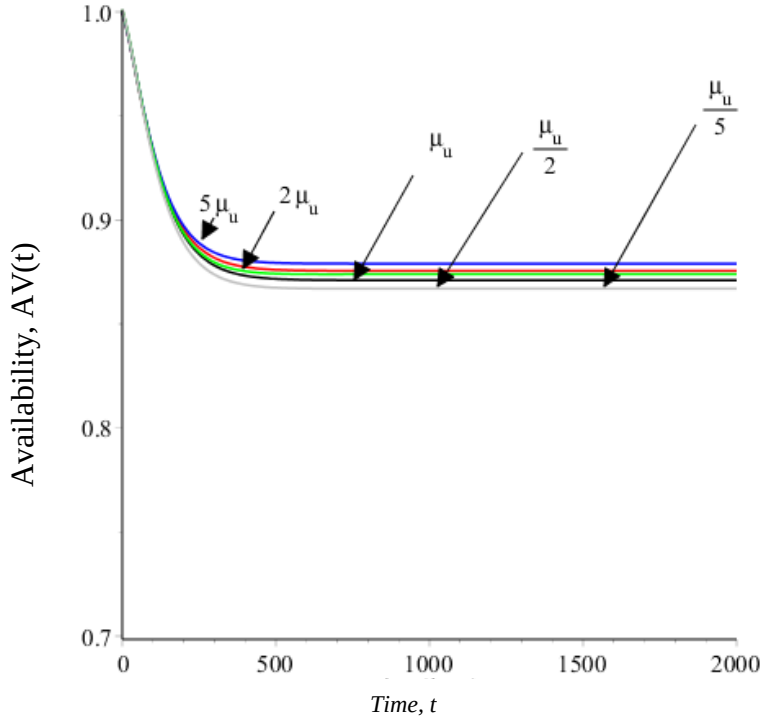

Figure D-45 Availability plots of single unit system with three operation states at different values of μ_u

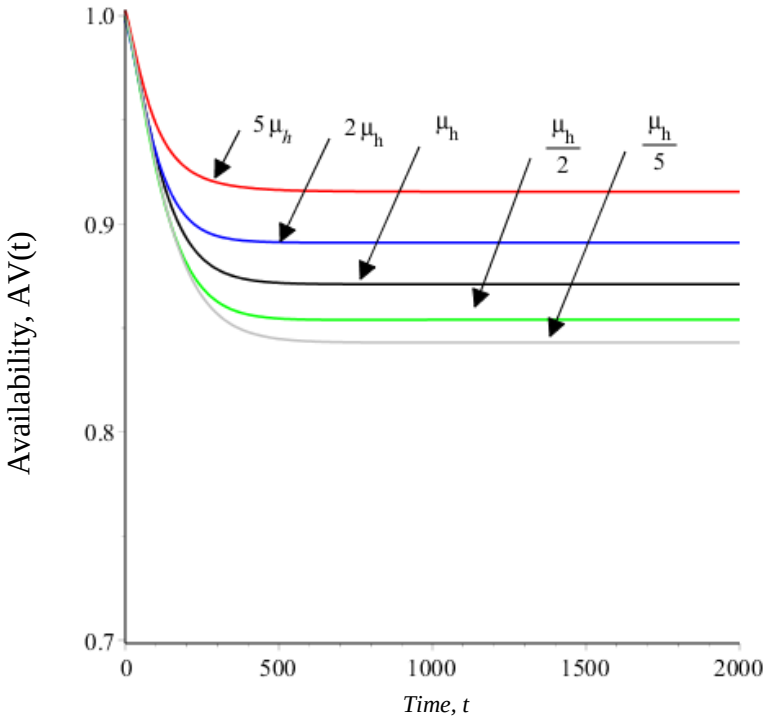

Figure D-46 Availability plots of single unit system with three operation states at different values of μ_h

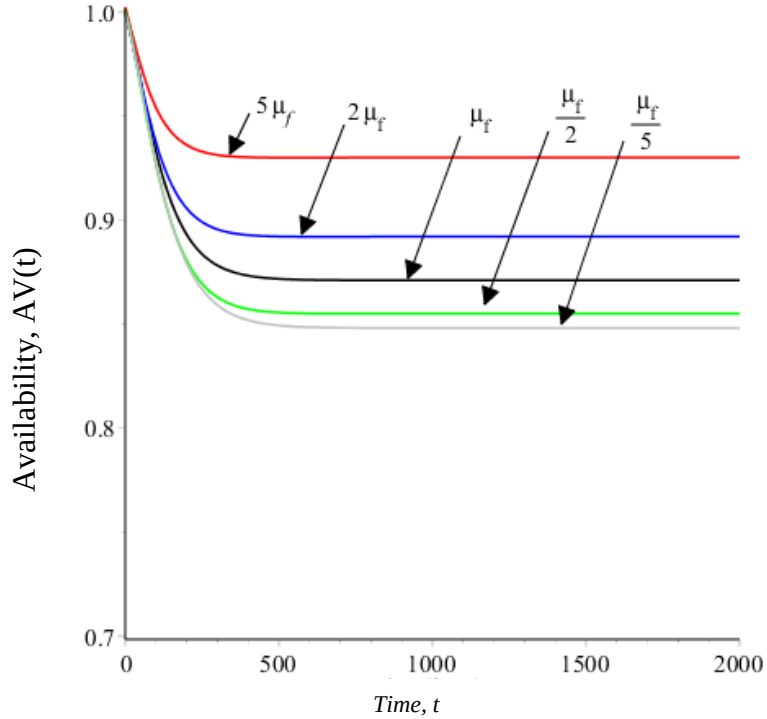

Figure D-47 Availability plots of single unit system with three operation states at different values of μ_f

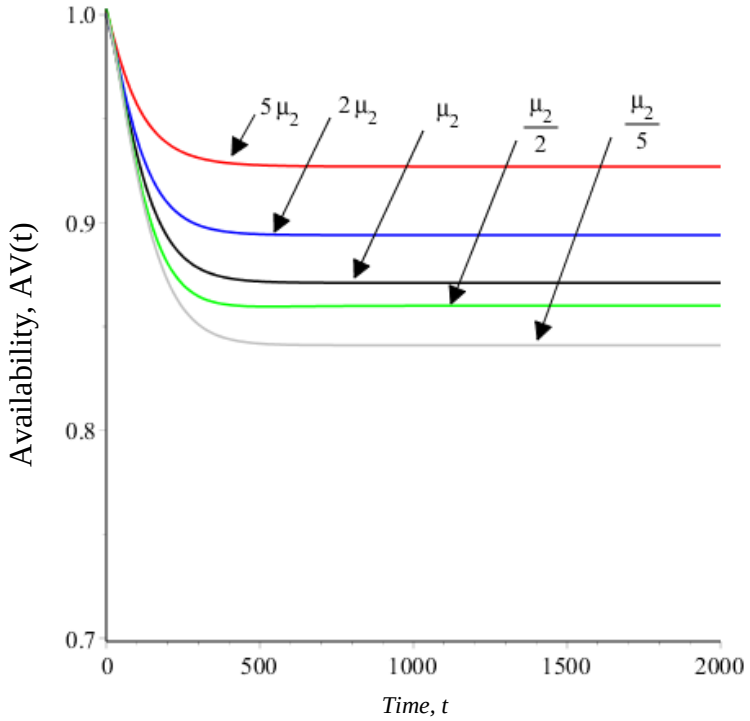

Figure D-48 Availability plots of single unit system with three operation states at different values of μ_2

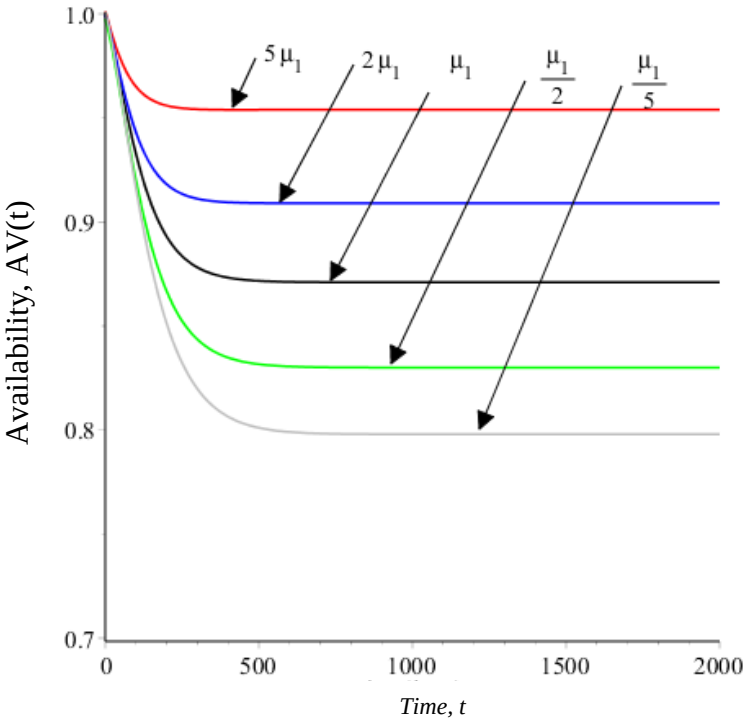

Figure D-49 Availability plots of single unit system with three operation states at different values of μ_2

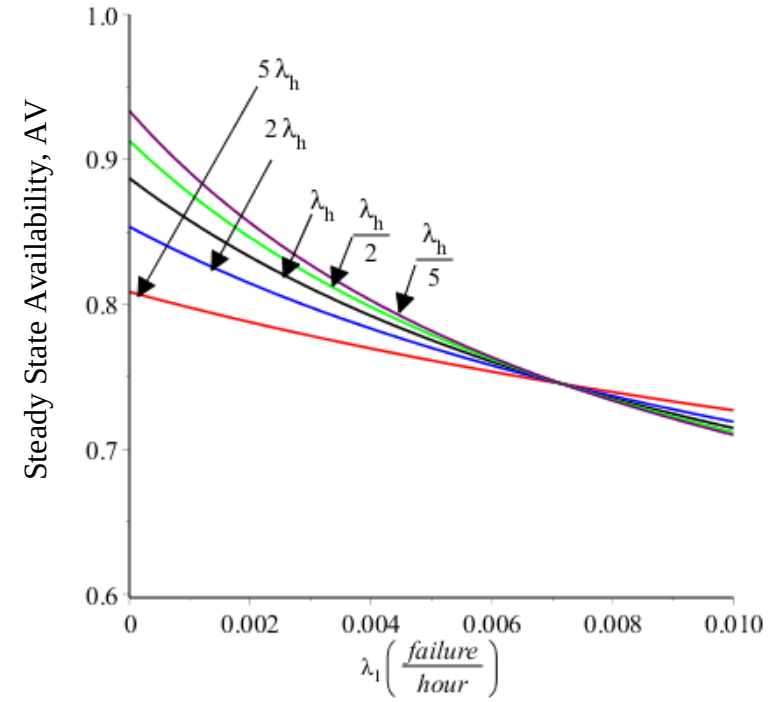

Figure D-50 Steady state availability plots of single unit system with three operation states at different values of λ_h

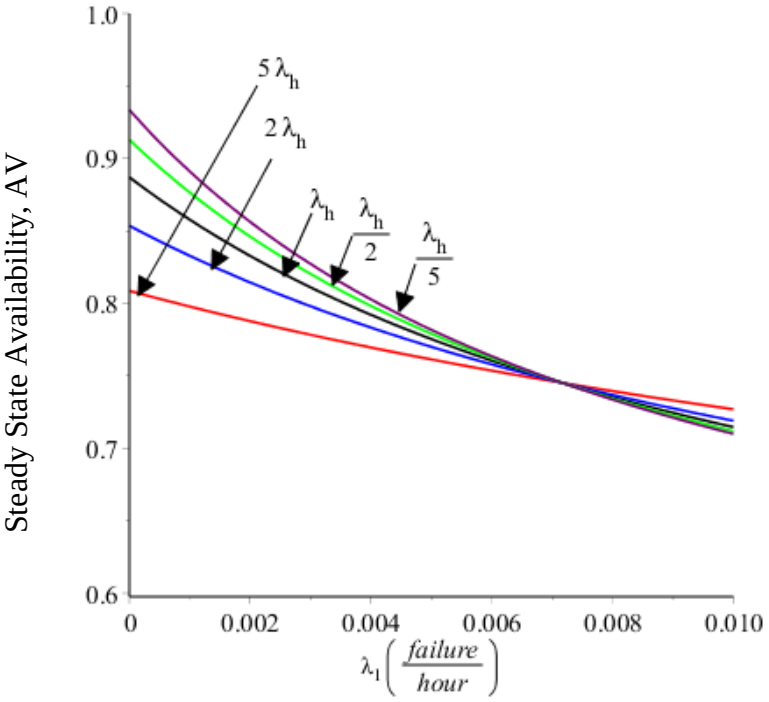

Figure D-51 Steady state availability plots of single unit system with three operation states at different values of λ_h

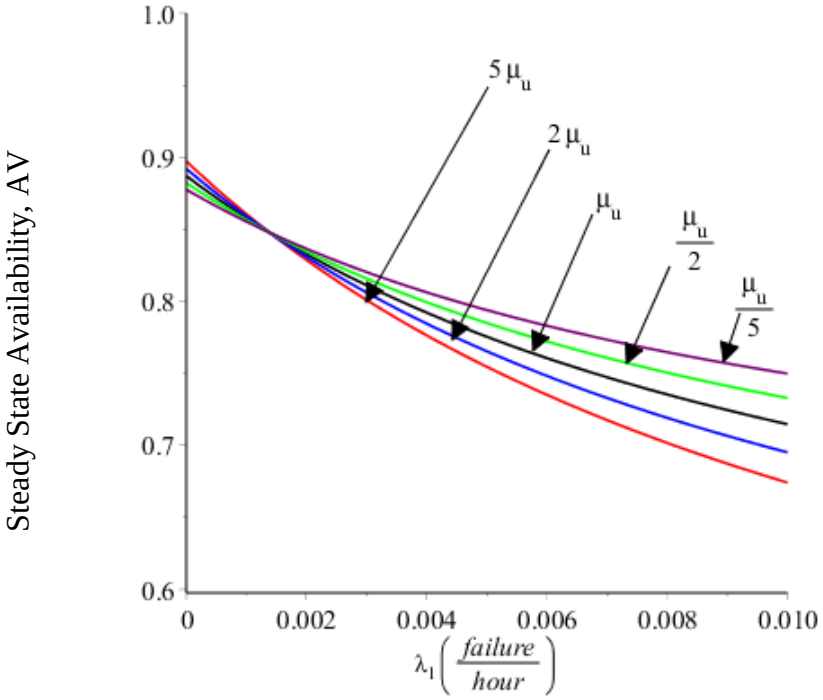

Figure D-52 Steady state availability plots of single unit system with three operation states at different values of μ_u

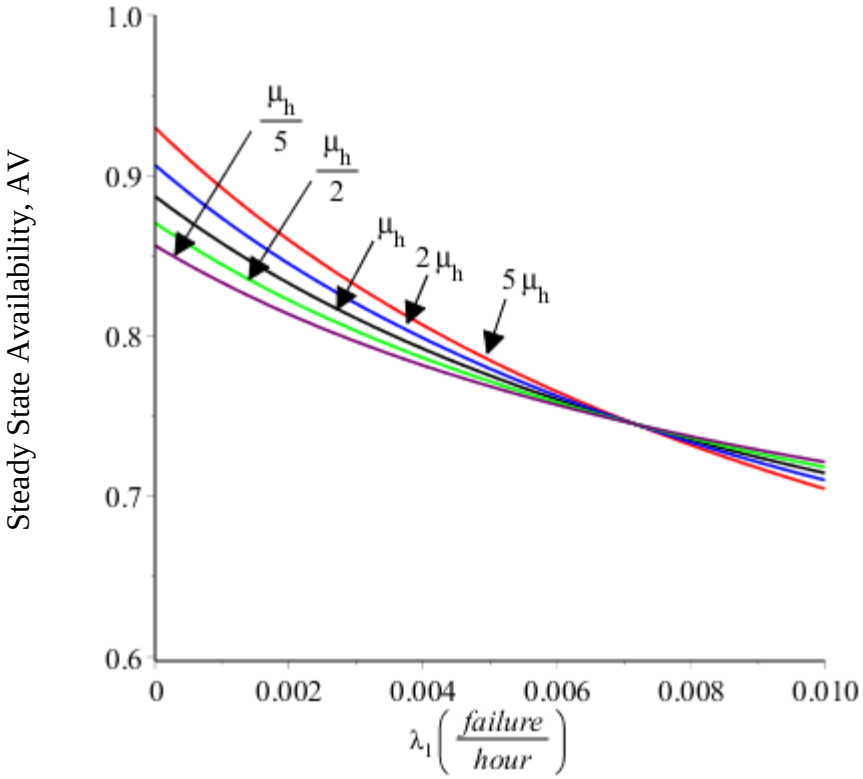

Figure D-53 Steady state availability plots of single unit system with three operation states at different values of μ_h

Appendix E: Reliability Parameter Plots of Chapter 5

E.1 Worker Performance with Critical and Non-Critical Human-Error

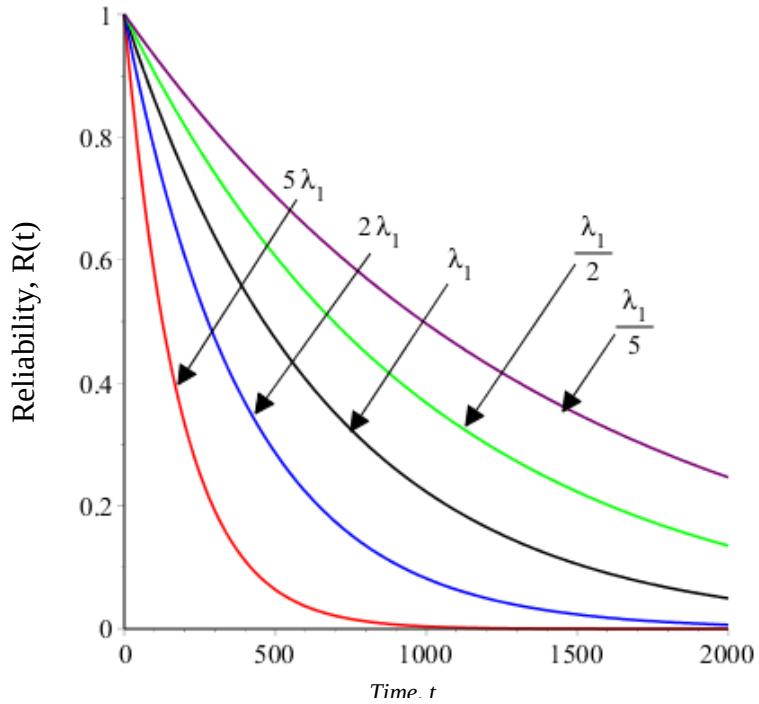

Figure E-1 Reliability of task performance at different values of λ_1

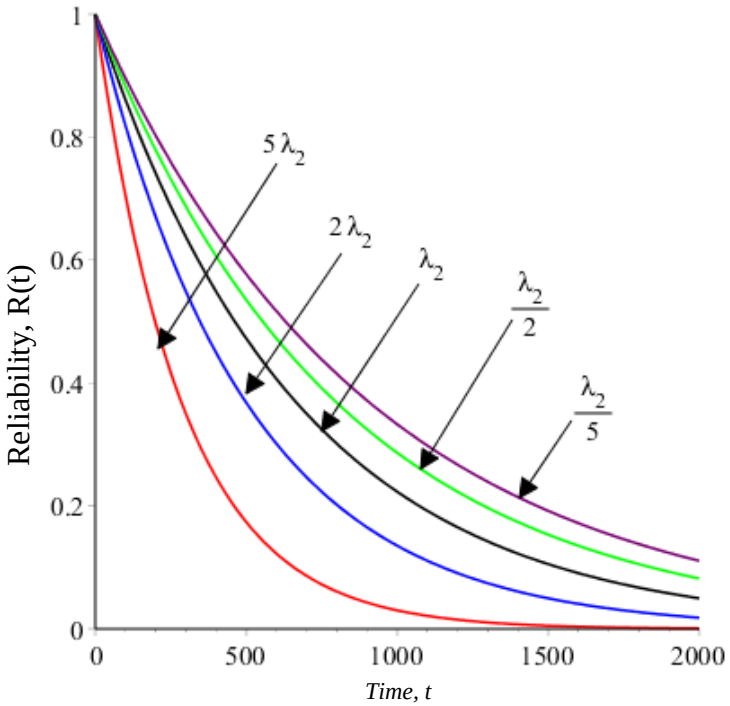

Figure E-2 Reliability of task performance at different values of λ_2

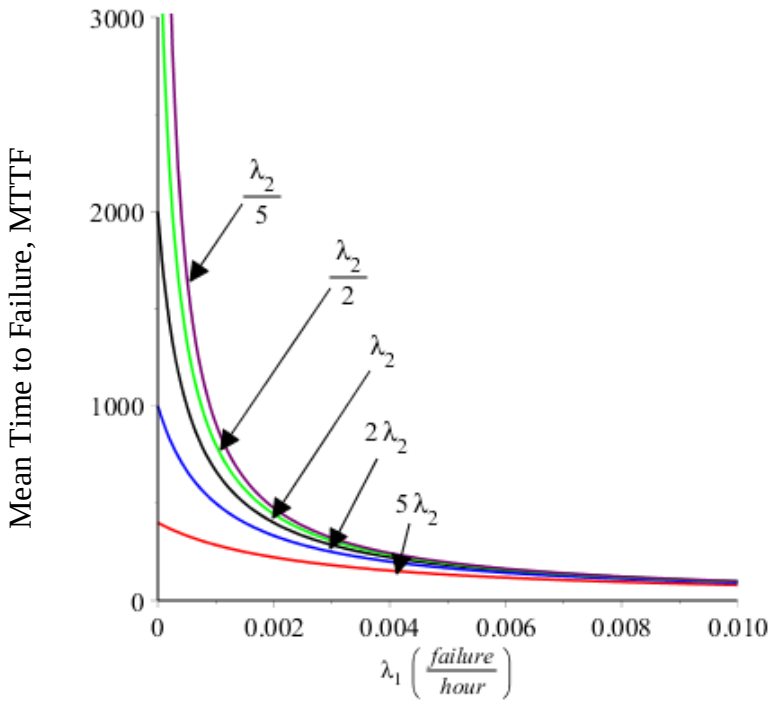

Figure E-3 MTTF of task performance at different values of λ_2

E.2 Worker Performance under Different level of Stress

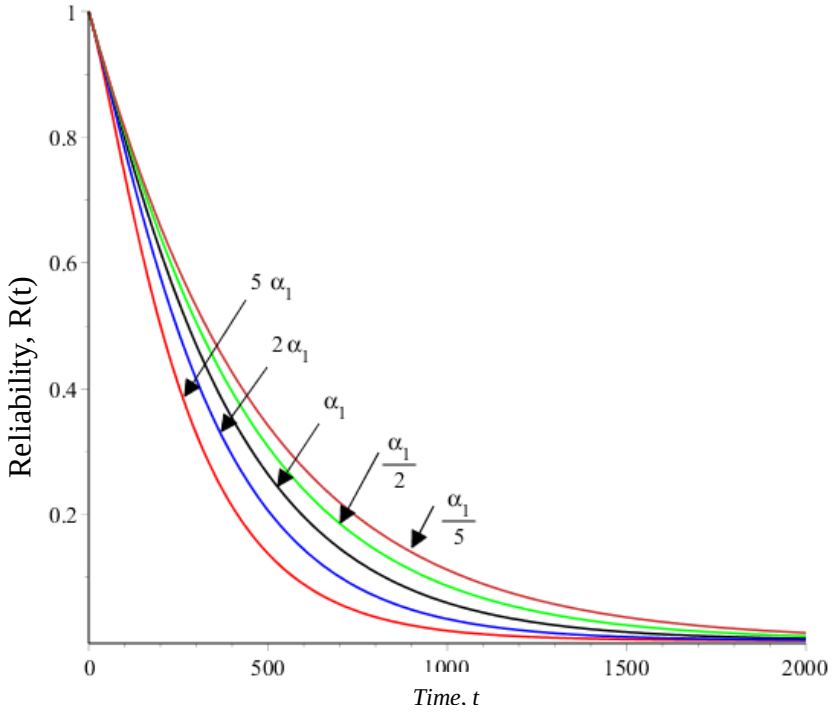

Figure E-4 Reliability plots of task performance under environment effect at different values of α_1

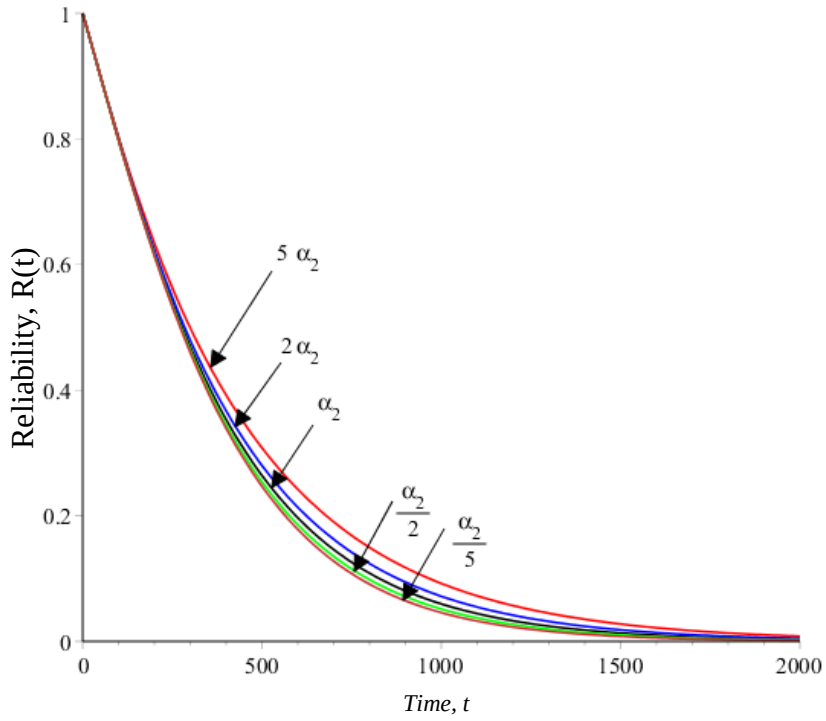

Figure E-5 Reliability plots of task performance under environment effect at different values of α_2

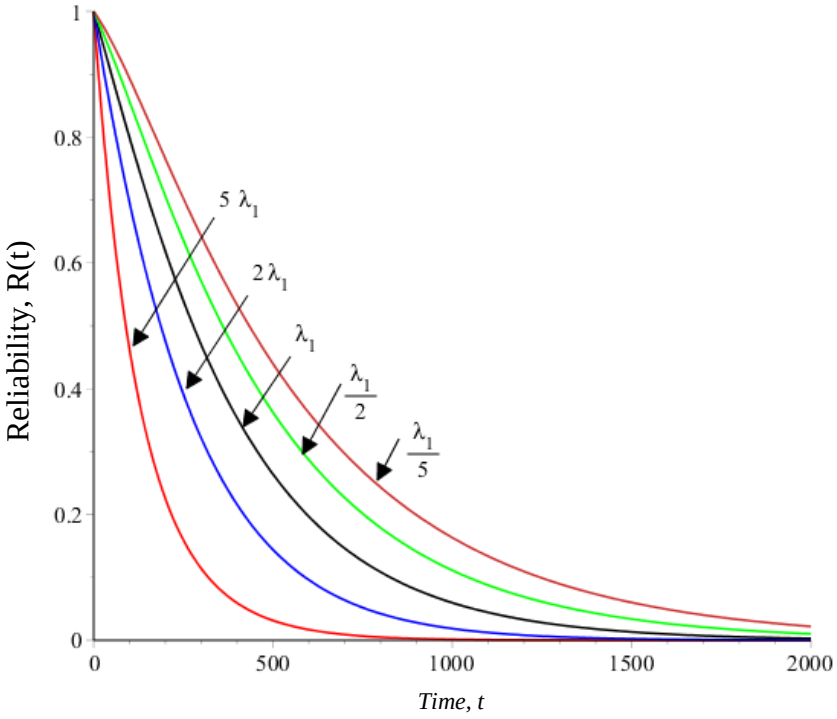

Figure E-6 Reliability plots of task performance under environment effect at different values of λ_1

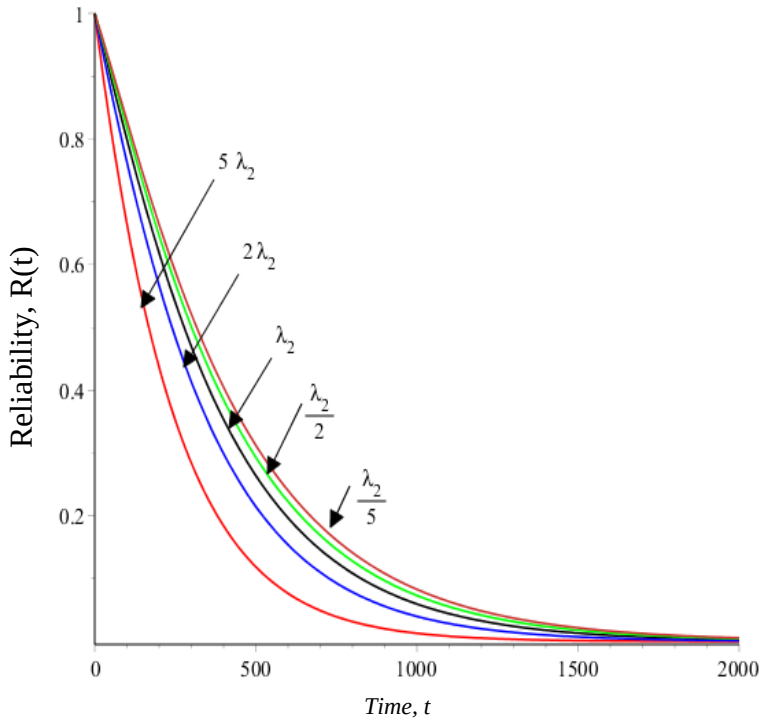

Figure E-7 Reliability plots of task performance under environment effect at different values of λ_2

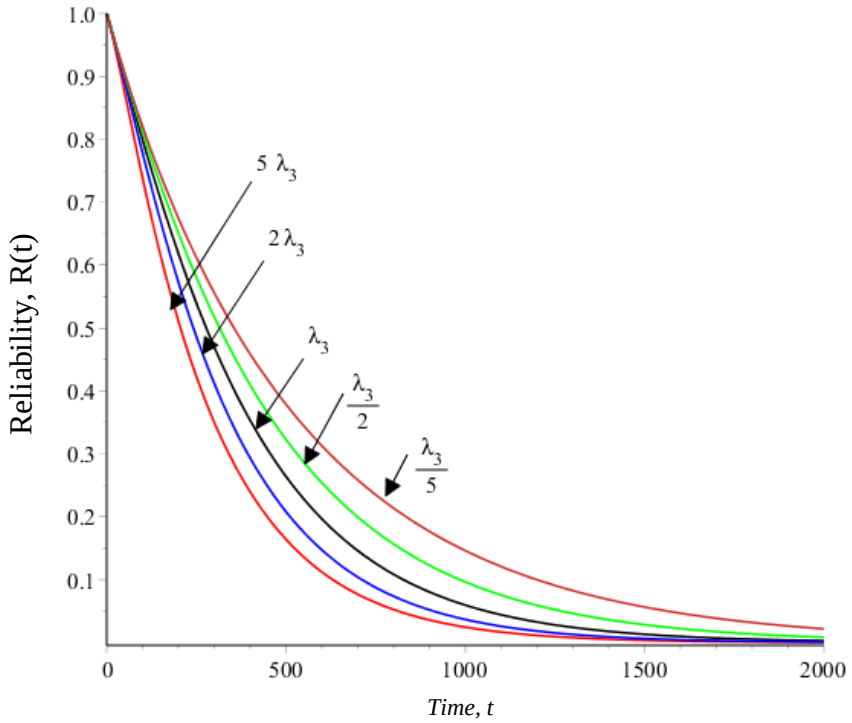

Figure E-8 Reliability plots of task performance under environment effect at different values of λ_3

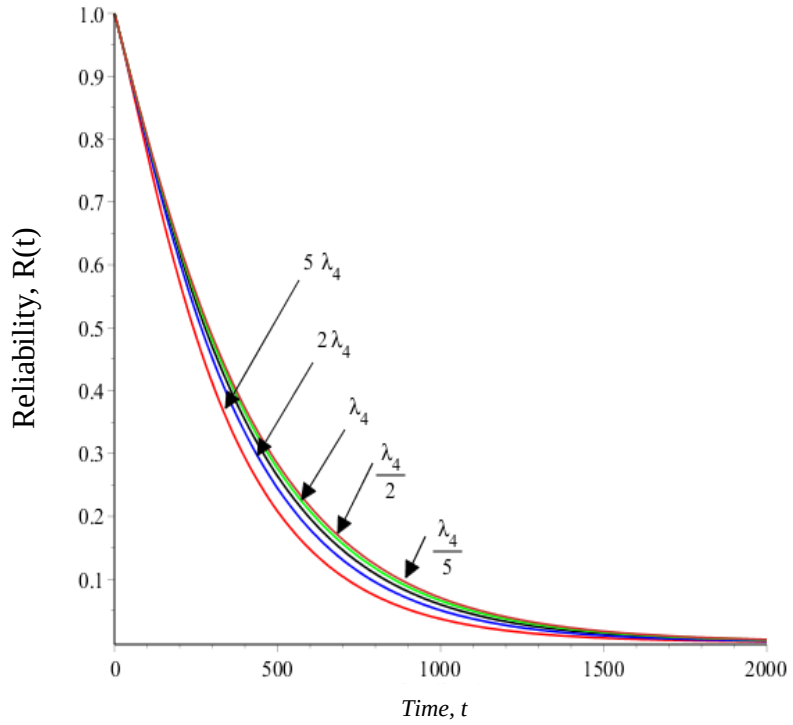

Figure E-9 Reliability plots of task performance under environment effect at different values of λ_4

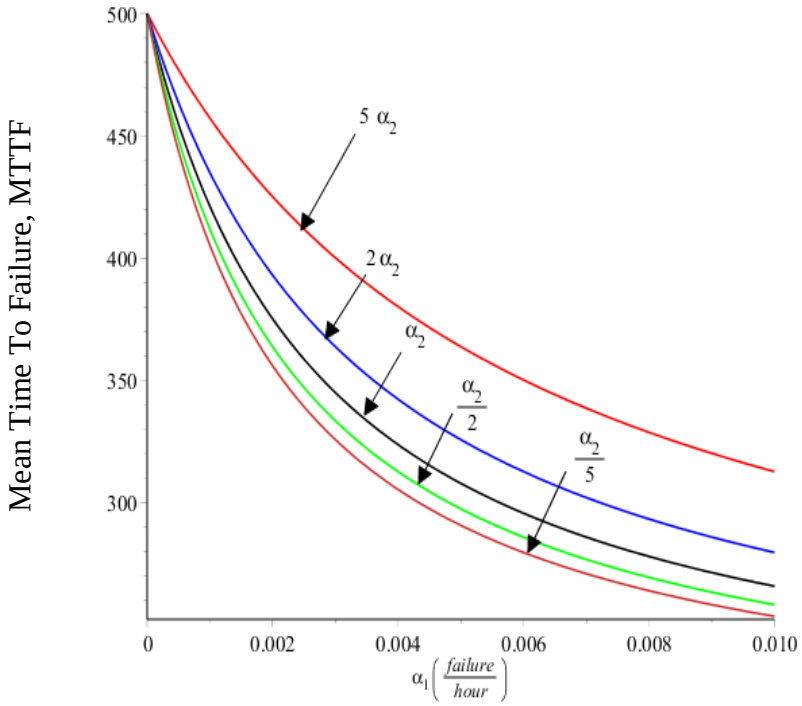

Figure E-10 MTTF plots of task performance under environment effect at different values of α_2

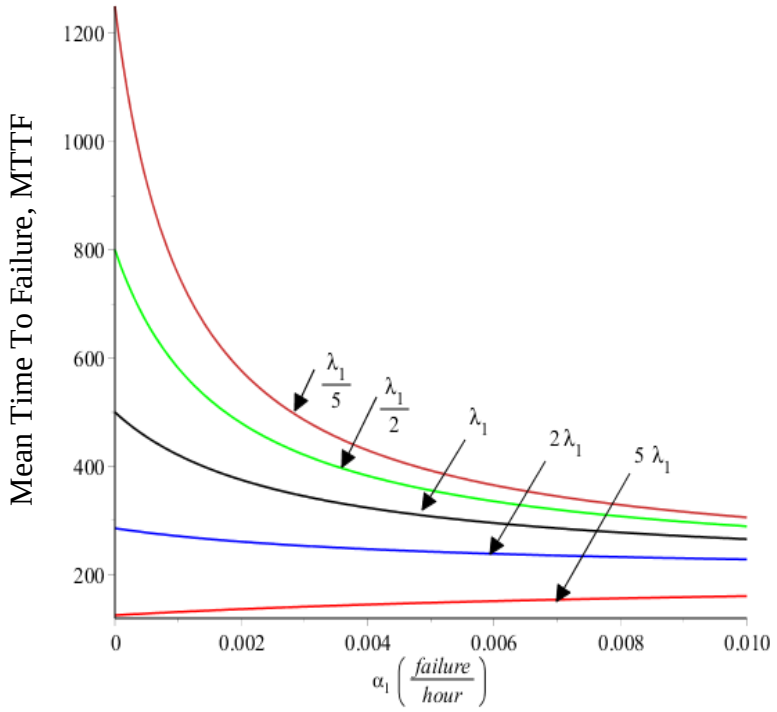

Figure E-11 Task performance MTTF considering the environment at different values of λ_1

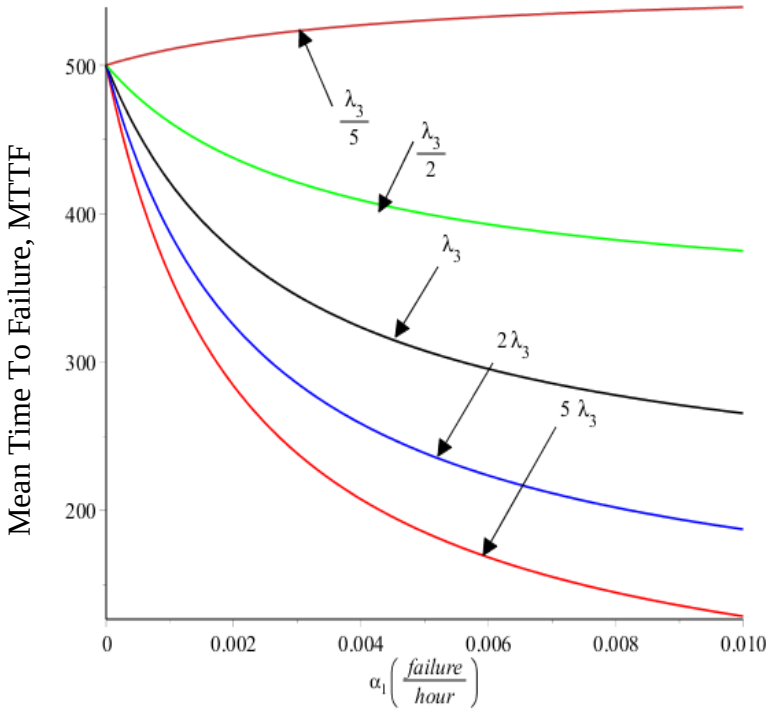

Figure E-12 Task performance MTTF considering the environment different values of $\lambda 3$

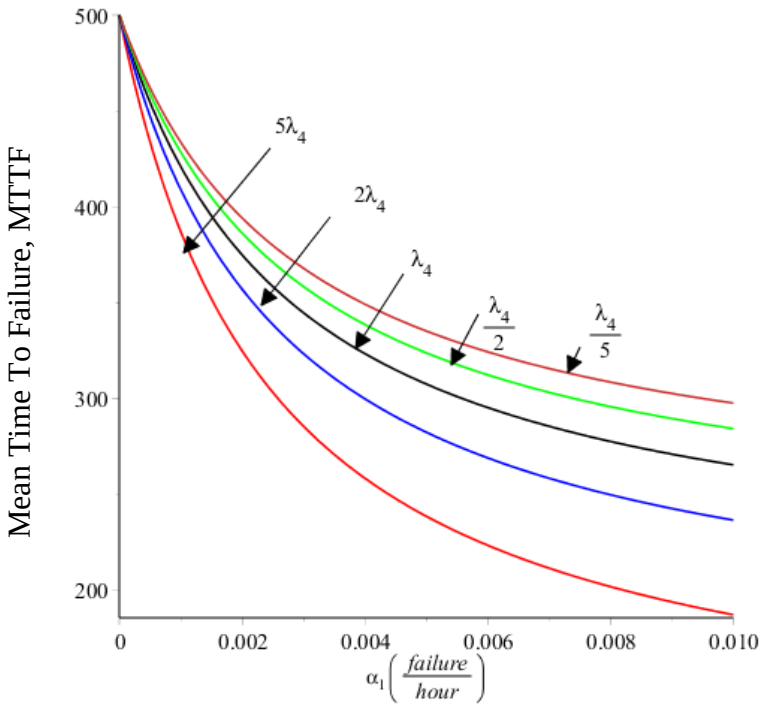

Figure E-13 Task performance MTTF considering the environment at different values of λ_4